University of New Hampshire

University of New Hampshire Scholars' Repository

Winter 1993

Coordination chemistry of polyphosphoxane rings

Xiaoyong Sun
University of New Hampshire, Durham

Follow this and additional works at: https://scholars.unh.edu/dissertation

INFORMATION TO USERS

This manuscript has been reproduced from the microfilm master. UMI films the text directly from the original or copy submitted. Thus, some thesis and dissertation copies are in typewriter face, while others may be from any type of computer printer.

The quality of this reproduction is dependent upon the quality of the copy submitted. Broken or indistinct print, colored or poor quality illustrations and photographs, print bleedthrough, substandard margins, and improper alignment can adversely affect reproduction.

In the unlikely event that the author did not send UMI a complete manuscript and there are missing pages, these will be noted. Also, if unauthorized copyright material had to be removed, a note will indicate the deletion.

Oversize materials (e.g., maps, drawings, charts) are reproduced by sectioning the original, beginning at the upper left-hand corner and continuing from left to right in equal sections with small overlaps. Each original is also photographed in one exposure and is included in reduced form at the back of the book.

Photographs included in the original manuscript have been reproduced xerographically in this copy. Higher quality 6" x 9" black and white photographic prints are available for any photographs or illustrations appearing in this copy for an additional charge. Contact UMI directly to order.

Order Number 9420567

Coordination chemistry of polyphosphoxane rings

Sun, Xiaoyong, Ph.D.

University of New Hampshire, 1993

U·M·I
300 N. Zeeb Rd.
Ann Arbor, MI 48106

COORDINATION CHEMISTRY OF POLYPHOSPHOXANE RINGS

BY

XIAOYONG SUN
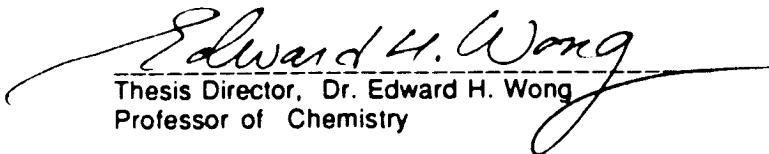
B.S., ZHENGZHOU UNIVERSITY, 1982
M.S., ZHENGZHOU UNIVERSITY, 1985

DISSERTATION

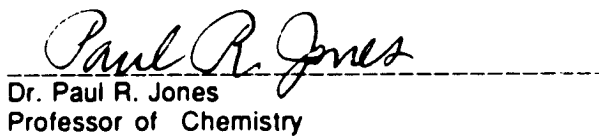Submitted to the University of New Hampshire
in Partial Fulfillment of
the Requirements for the Degree of
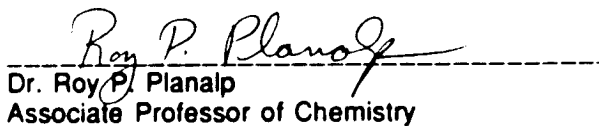
Doctor of Philosophy

in

Chemistry
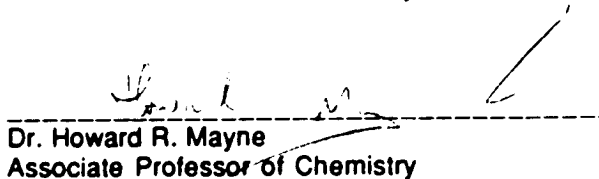
DECEMBER, 1993

This dissertation has been examined and approved.
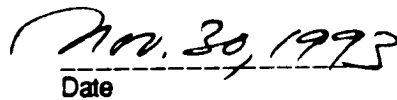
_____
Thesis Director, Dr. Edward H. Wong
Professor of Chemistry

_____
Dr. Paul R. Jones
Professor of Chemistry

_____
Dr. Roy P. Planalp
Associate Professor of Chemistry

_____
Dr. Howard R. Mayne
Associate Professor of Chemistry

_____
Dr. Russell Carr
Professor of Chemical Engineering

Nov. 30, 1993
_____
Date

DEDICATION

TO MY PARENTS, MY WIFE AND MY SON

iii

ACKNOWLEDGMENTS

I thank my research advisor, Dr. Edward H. Wong, for his guidance and encouragement to my thesis research.

I thank the staff in Instrumentation Center, especially Kathy Gallagher for her expertise in NMR, Dee Cardin and Nancy Cherim for their help with the elemental analysis.

I thank the co-workers in my group, professors and other graduate students in the department to create a good working environment.

I thank the University of New Hampshire and Chemistry Department for the financial support during my research work.

TABLE OF CONTENTS

vi

LIST OF TABLES

viii

ix

x

LIST OF SCHEMES

xi

ABSTRACT

COORDINATION CHEMISTRY OF POLYPHOSPHOXANE RINGS

BY

XIAOYONG SUN

University of New Hampshire, December, 1993

Substitution of triphosphoxane rings on metal complexes containing labile ligands, $M(CO)_4NBD$ and MX_2L_2 [X=Cl, Br, I; L=DME, THF, NBD] and thermal reactions of bis(dialkylamino)phosphine oxides with metal hexacarbonyls yielded the tri-, tetra-, and pentaphosphoxane ring complexes cis-$M(CO)_4[R_2NPO]_3$, cis-$M(CO)_4[R_2NPO]_4$, cis-$M_2(CO)_8[R_2NPO]_4$, cis-$M_2(CO)_7[R_2NPO]_5$, cis-$MX_2[R_2NPO]_4$, and cis-$MX_2[R_2NPO]_5$ as the isolated products. The P_4O_4 rings in metal tetraphosphoxane complexes appear in six coordination modes including the 1,3-chelating, 1,5-chelating boat-boat, boat-chair conformation, 1,3,5,7-chelating boat-boat cage mode, twist-boat mode, and 1,3,5-tridentate mode bridging two metals. A novel Ni(0)-cage complex $Ni_2(CO)_4[Cy_2NPO]_4$ was synthesized serendipitously from thermal reaction of $Fe_2(CO)_9$ with $NiBr_2[Cy_2NPO]_4$ in toluene. Several bimetallic complexes were synthesized from the reaction of monometallic polyphosphoxane complexes with suitable metal precursors.

Some side reactions accompanied the above reactions giving metal complexes with new ring skeletons, $Fe(CO)_4\{^iPr_2NP[OP(O)^iPr_2N]_2PN^iPr_2\}$, and a tungsten complex $W(CO)_3[R_2NPO]_4W(CO)_3$. The novel hexaphosphoxane $Cr_2P_6O_6$ complex was produced by a stepwise addition of R-P=O units in the thermal reaction of $Cr_2(CO)_7[DMP-PO]_5$ with bis(dimethylpiperidino)phosphine oxide.

INTRODUCTION

Cyclophosphoxanes with the general formula $[RPO]_n$ are cyclic compounds in which oxygen and trivalent phosphorus occupy alternating positions in the ring skeleton. The phosphorus atoms are tricoordinate with exo-substituents connected by P-N, P-O, or P-C bonds. Since the chelating and bridging ligands of the diphosphoxane P-O-P unit have long been used to coordinate a variety of transition metals,[1] these trivalent phosphorus atoms in the cyclophosphoxane ring system can also provide multiple donor sites that can potentially coordinate one or more metals and form polycyclic and cage complexes.

Previously, only three well-characterized P(III)-O rings have been described: $[^iPr_2NPO]_3$,[2] $[BHT-PO]_2$ and $[BHT-PO]_3$ (BHT=2,6-di-tert-butyl-4-methyl-phenoxy).[3] Earlier Russian workers reported the synthesis of similar heterocycles by the hydrolysis of dichloroalkylphosphines, though the products were only characterized by molecular weight determination.[4] No higher congeners like tetraphosphoxanes $[RPO]_4$, pentaphosphoxanes $[RPO]_5$, or hexaphosphoxane $[RPO]_6$ have been described except for the 1983 serendipitous synthesis in Wong's group of a cage complex $Mo_2(CO)_8[^iPr_2NPO]_4$ which contains the novel $[^iPr_2NPO]_4$ heterocycle functioning as a bis-chelating ligand.[5] Since then, further metal polyphosphoxane complexes have been reported.[6-12] Points of interest including their coordination modes, steric or electronic ligand influence on metal centers, and, conversely, the effect of metal binding on ring oligomeric equilibria and ring conformations are opened in this area. As partial research work in this group, this thesis research can be considered as following points.

1

1. <u>Thermal Reactions of Phosphine Oxides with Metal Carbonyls and the Effect of Metal Binding on Ring Oligomeric Equilibria and Ring Conformations</u>

There are two previously described methods for the synthesis of transition metal polyphosphoxane complexes. One is the synthesis of $Mo_2(CO)_8[R_2NPO]_4$ [R = ^iPr, Cy] by thermal reactions of bis(diisopropylamino)phosphine oxide and bis(dicyclohexyl-amino)phosphine oxide with molybdenum hexacarbonyl resulting in elimination of amine from the coordinated phosphine oxide (equation 1). Another is the synthesis of phenyl-substituted analogues by nucleophilic attack of cis-$Mo(CO)_4[PhPO_2]_2^{4-}$ on cis-$Mo(CO)_4[PhPCl_2]_2$ (equation 2).[7]

$$2Mo(CO)_6 + 4(^iPr_2N)_2P(O)H \longrightarrow Mo_2(CO)_8[^iPr_2NPO]_4 + 4^iPr_2NH + 4CO \quad (1)$$

$$Mo(CO)_4[PhPO_2]_2^{4-} + cis\text{-}Mo(CO)_4[PhPCl_2]_2 \longrightarrow 4Cl^- + Mo_2(CO)_8[PhPO]_4 \quad (2)$$

In the first method, the polyphosphoxane rings formed can be regarded as cyclic head-to-tail oligomers of the unknown phosphinidene oxide R-P=O monomer.[13] There could exist an oligomeric equilibrium due to the effect of metal binding (figure 1). This is illustrated by the thermal reaction of bis(diisopropylamino)phosphine oxide with metal hexacarbonyls. All three Group VI metal hexacarbonyls reacted with the bis(diisopropylamino)phosphine oxide upon heating in toluene to give complexes wherein carbonyls were replaced by cyclic trimeric, tetrameric, or pentameric phosphinidene oxide $[^iPr_2NPO]_n$ ligands.[6,7,8] A molybdenum triphosphoxane complex was also isolated from the thermal reaction of this phosphine oxide with molybdenum hexacarbonyl under mild reaction conditions. This triphosphoxane complex is easily transformed to the cage tetraphosphoxane complex upon further activation.[6] One goal of this thesis work is to understand the effect of metal binding on the polyphosphoxane configuration, oligomeric equilibria, as well as supra-structure of cyclophosphoxane

2

rings. For example, Mo(0) can form the triphosphoxane ring while Cr(0) and W(0) forms only tetraphosphoxane complexes.[8] Will other metal centers, such as Fe(0), Ni(II), Pd(II) and Pt(II) behave like Mo(0) to form both tri- and tetraphosphoxane complexes? What are the reaction difference and metal influence of +2 oxidation state vs zero-valent for metal? Is there any relationship between reaction temperature or sterically bulky substituent on phosphorus and poly-phosphoxane ring size? What is the influence of other substituents on metal? So, thermal reaction of phosphine oxide with metal hexacarbonyl is still adopted for the synthesis of polyphosphoxane metal complexes.

Figure 1.
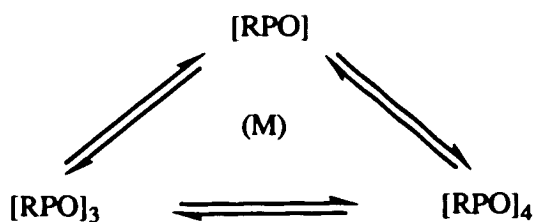
2. Influence of Substituents on Phosphorus Atoms (i.e. Steric and Electronic Ligand Influence on Metal Centers)

Substituents on phosphorus have a significant influence on the reactivities of cyclopolyphosphines. For example, the steric bulk of the diisopropylamino groups in tetrakis(diisopropylamino)cyclotetraphosphine reduces its chemical reactivity relative to other cyclotetraphosphines.[14] Thus, $(^iPr_2N)_4P_4$ is unreactive toward oxygen, carbon disulfide, even potassium metal, and various metal carbonyls [e.g. $Cr(CO)_6$, $Mo(CO)_6$, and $Fe_2(CO)_9$] under conditions where other cyclotetraphosphines like Ph_4P_4, Et_4P_4 reacted. This influence should exist in the coordination chemistry of

3

cycloaminophosphoxane rings also. As mentioned above, changing substituents from an amino group to a phenyl group required a totally different synthetic method for forming the metal tetraphosphoxane complex.[7] The former products gave rise to a rich derivative chemistry while the latter gave only unstable products. Therefore, using different substituents in the phosphoxane ring system could produce alternative results under the same conditions. These could include formation of different sized rings and different coordination modes.

Using phosphine oxides with different substituents as starting materials to investigate this influence is another purpose of this thesis. It is well known that the thermal reaction of bis(diisopropylamino)phosphine oxide with metal carbonyls gives metal polyphosphoxane complexes. The polyphosphoxane rings are built up by elimination of a sterically bulky diisopropylamine from phosphine oxide. Related groups are dicyclohexylamino, cyclohexylisopropylamino, and 2,6-dimethylpiperidino groups. It is expected that the thermal reaction of these phosphine oxides with metal hexacarbonyls should also give metal polyphosphoxane complexes, but, with the less bulky groups, the conformation and ring size of the resulting complexes could well differ.

Other substituents used in addition to analogues of the diisopropylamino group are less bulky with nitrogen bonded to primary carbons, such as bis(diethylamino)-phosphine oxide $(Et_2N)_2P(O)H$, bis(piperidino)phosphine oxide $(PIP)_2P(O)H$, and phosphoroamidite with mixed amino group and phenoxy group bonded to the same phosphorus, $(^iPr_2N)(PhO)P(O)H$. Generally, less bulky groups should afford larger ring sizes. Thus using smaller amino groups might be a way to assemble larger polyphosphoxane ring complexes. Use of mixed amino and phenoxy groups might introduce O-substituents into polyphosphoxane ring complexes after elimination of

4

amine from the coordinated phosphoroamidite since a P-O bond is much stronger than a P-N bond. During thermal reaction with metal hexacarbonyls, the breaking of a P-N bond to eliminate amine might be more favored than cleavage of a P-O bond to eliminate phenol. Thus, various substituted phenoxy groups with varying steric bulks could be suitable starting materials.

3. Build-up higher Congeners of Cyclophosphoxane

The synthesis and interconversion of P(III)-O heterocycles should be of fundamental interest in inorganic as well as heterocyclic chemistry. Cyclophosphazenes[15] are important inorganic materials which are known all the way up to P_8N_8 rings and cyclophosphates[16] have long been studied. Can higher congeners of cyclophosphoxane like $[RPO]_5$, and $[RPO]_6$ be made? Before this thesis work, P_3O_3 and P_4O_4 rings had been reported to build up around Mo, Cr, and W centers, as well as a $Cr_2P_5O_5$ complex, $Cr_2(CO)_7[^iPr_2NPO]_5$, produced in low yield (5%) from the thermal reaction of bis-(diisopropylamino)phosphine oxide with chromium hexacarbonyl.[6-8] Thus, the search for a synthetic method to build up novel larger polyphosphoxane ring complexes is an important goal of this thesis work. Changing substituents at phosphorus could give not only tri-, tetra- or pentaphosphoxane ring complexes and may increase the yield of P_5O_5 ring complexes, but could extend ring coordination to other metal centers having different coordination geometries. If the P_5O_5 ring complexes could be produced in higher yield, they might serve as starting materials to build up novel P_6O_6 ring complexes by reaction with excess phosphine oxide (equation 3).

$$M_2(CO)_7[R_2NPO]_5 + (R_2N)_2P(O)H \longrightarrow M_2(CO)_6[R_2NPO]_6 + R_2NH \qquad (3)$$

5
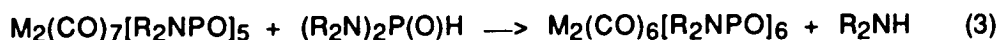
From the molecular structure of the $Cr_2P_5O_5$ complex,[9] the cyclopentaphosphoxane ring coordinated to one cis-$Cr(CO)_4$ and one fac-$Cr(CO)_3$ moiety (Figure 2). It may be possible to add another R-P=O unit into the P_5O_5 ring to build a P_6O_6 ring complex with the hexaphosphoxane ring coordinated to two fac-$Cr(CO)_3$ centers (Figure 2).

Figure 2.

$$Cr_2P_5O_5 \xrightarrow{\ -CO\ } Cr_2P_6O_6$$
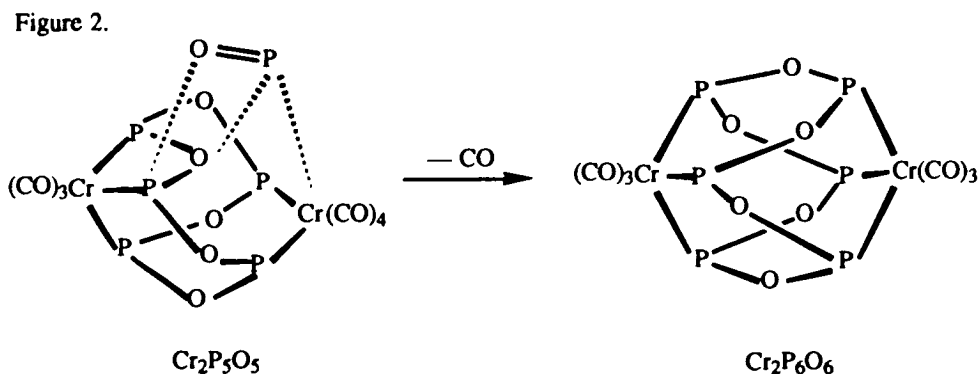
4. Direct Substitution Reactions of Triphosphoxane Ring with Metal Complexes

The thermal reaction with phosphine oxides is applicable for the syntheses of various metal polyphosphoxane complexes with different amino groups, but, this is limited to zero-valent metal complexes. Another problem is the need for thermal activation to achieve amine elimination and ligand substitution which prohibits use of heat-sensitive metal precursors. Thus, another concern of this thesis research is to discover a new synthetic method to extend the synthesis to cationic metal complexes.

Triphosphoxane rings with sterically bulky substituents like amines with secondary carbons, such as $^iPr_2N$, synthesized by controlled hydrolysis of dichloroamino-phosphines and are stable under certain conditions. Direct substitution by this tri-phosphoxane [$^iPr_2PO]_3$ ring at metal centers containing labile ligands could be a new,

6

generally useful approach to polyphosphoxane metal complexes. Since this substitution involves simple replacement of labile ligands at metal centers, divalent metal complexes, such as $NiBr_2 \cdot DME$, $PdCl_2 \cdot 2PhCN$, etc., could be suitable precursors in addition to metal (0) complexes. Several metal complexes will be used as starting materials in the thesis work, $Fe_2(CO)_9$, NiX_2L (X=Cl, Br, I; L=DME) (dimethoxyethane), (L=THF) (tetrahydrofuran), $PdX_2(PhCN)_2$ (X=Cl, Br), $PtCl_2NBD$ (NBD=norbornadiene), $Cu(CH_3CN)_4BF_4$, $Ni(CO)_2(PPh_3)_2$, $Ru(DMSO)_4Cl_2$ (DMSO= dimethylsulfoxide) and, of course, $M(CO)_6$ (M=Cr, Mo, W).

5. Coordination Modes of Polyphosphoxane Rings

A further point of interest is the different coordination modes of polyphosphoxane rings compared to other trivalent phosphorus heterocycles. The cyclophosphazanes[17] and triphosphasiloxanes[18] heterocycles have been known to serve as multidentate ligands where most of the phosphorus sites are used. Three phosphoruses in the cyclo-phosphazane P_4N_4 ring are found to coordinate a single metal (equation 4) while all three phosphoruses in the triphosphasiloxane P_3Si_3 ring are used in coordination (equation 5). In both cases, coordination did not change the original ring size or conformation. The cyclotriphosphoxane rings may have a similar coordination ability toward transition metals. In addition, the P_3O_3 ring itself could be retained or, unlike the above trivalent phosphorus heterocycles, new polyphosphoxane rings may also form via templating at metal centers (equation 6). For example, coordination at Ni (II) could be octahedral with four-coordinate phosphorus or four-coordinate with two-coordinate phosphorus, as well as tetrahedral and square-planar to allow the build-up of new P_nO_n rings. In contrast, Pd (II) could only be four-coordinate with a square-planar geometry in a P_nO_n ring complex. These possibilities will be investigated.

7

$[CH_3PNCH_3]_4$ + $Mo(CO)_6$ $\xrightarrow[\Delta]{\text{toluene}}$

(structure of molybdenum tetraphosphoxane cage complex) (4)

(cyclic phosphasilane structure) $\xrightarrow[-3CH_3CN]{M(CO)_3(CH_3CN)_3}$ (metal complex structure) (5)
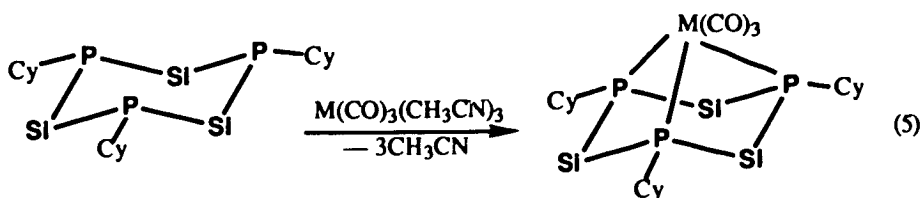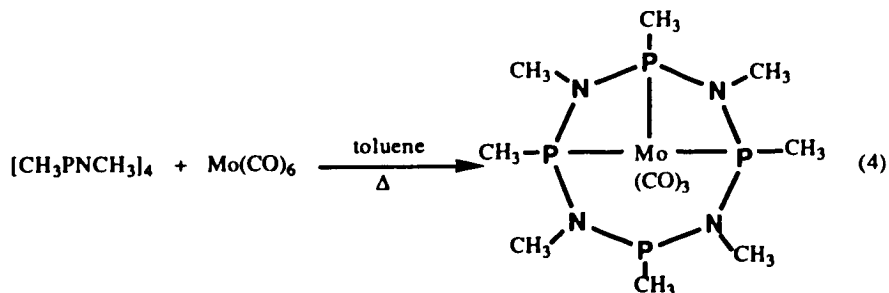
Si= SiHMesitylene,   M= Mo, Cr

$n/3[RPO]_3$ + $MX_2 \cdot L$ $\longrightarrow$ $MX_2 \cdot [RPO]_n$ + L   (6)
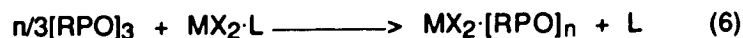
(n= 3,4, 5 ;   M= Ni, Pd, Pt ;   X= Cl, Br, I ;   L=DME, NBD, 2THF, 2PhCN)

To date, the tetraphosphoxane heterocycle has been found in a variety of conformations (i.e. chair-chair, boat-boat, and chair-boat in figure 3) in metal coordination modes in rigid polycyclic and cage or polymetallic complexes (figure 4). For example, the molybdenum cage complex is in the 1,3,5,7-chelating mode (figure 4a). Other molybdenum, chromium and tungsten tetraphosphoxane complexes contain 1,5-chelate boat-boat (Figure 4b) and boat-chair modes (Figure 4c).[6-8] Other metal polyphosphoxane complexes can adopt all these coordination modes or just one or two of them. One question is the possibility of other coordination modes such as a 1,3-chelate (Figure 4d) in addition to the above mentioned. Different metal centers could

8

well influence these results.

Figure 3.

boat-boat   chair-chair   chair-boat

Figure 4.

1,3,5,7-chelating   (a)

1,5-chelating chair-chair   (b)

1,5-chelating boat-chair   (c)

1,3-chelating   (d)
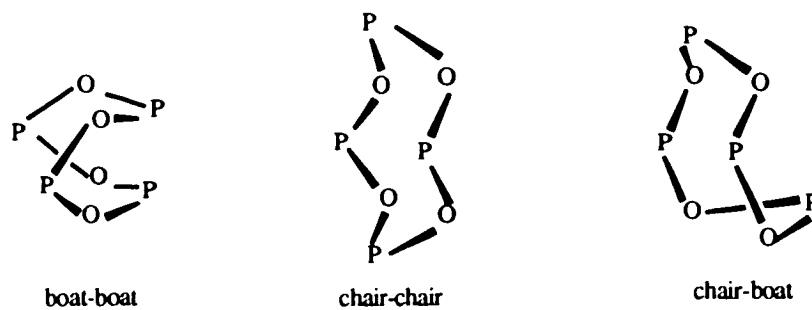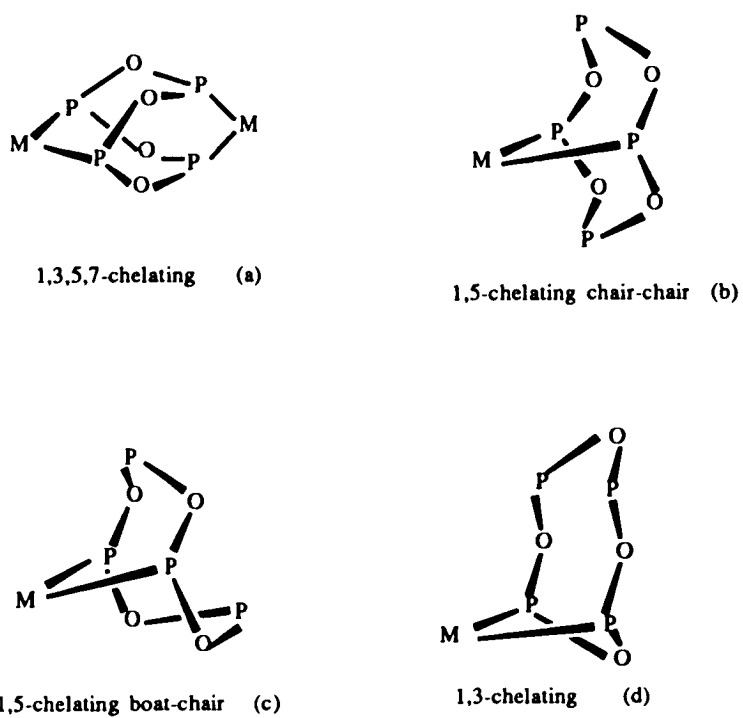
Novel P(III)-O heterocycles isolated as coordination complexes could be precursors

9

to the unknown rings. These P_nO_n rings could be liberated by substitution of suitable nucleophiles at metal P_nO_n ring complexes (equation 7). If the ring could be released from complexes and be stable under certain conditions, it might serve as precursor toward new metal complexes and new ring assemblies. The search for suitable parent metal complexes and nucleophiles to release such P_nO_n rings is another concern of this work.

$$MX_2[R_2NPO]_n + L' \longrightarrow MX_2L' + [R_2NPO]_n \quad (7)$$
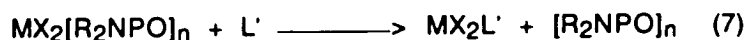
6. <u>Formation of Heterobimetallic Polyphosphoxane Complexes</u>

It is also anticipated that many of the monometallic polyphosphoxane complexes can serve as precursors to bi- or polymetallic products using the available free P sites. Other homo- or hetero-bimetallic complexes could be produced from monometallic complexes (equation 8). Finding suitable precursors, both monometallic poly-phosphoxane complexes and metal centers with labile ligands, to build up homo- or hetero-bimetallic polyphosphoxane complexes is another one of our research goals. The possibilities for homo- and hetero-bimetallic complexes include combinations of M(0)-M'(0), M(0)-M'(II) and M(II)-M'(II).

$$MX_2[R_2NPO]_n + M(CO)_4L \longrightarrow MX_2[R_2NPO]_nM(CO)_4 + L \quad (8)$$

Thus the work presented here is the further study of coordination reactions based on polyphosphoxanes with metal complexes. The substitution reactions of tri-phosphoxane rings and thermal reaction of phosphine oxides with metal complexes, along with selected chemistry of products, are detailed in the following two chapters.

10

CHAPTER 1

COORDINATION CHEMISTRY OF TRIPHOSPHOXANES [R$_2$NPO]$_3$ WITH METAL COMPLEXES

The triphosphoxane rings were synthesized by hydrolysis of dichloroaminophosphines in the presence of triethylamine according to the literature.[3,4] Optimization of reaction conditions here ensured completion of the hydrolysis reaction, and increased the yield and purity of the rings produced.

Theoretically, a substitution reaction involves incoming ligands replacing labile coordinated ligands at the metal center[19] with the ligand structure remaining basically unchanged. In practice, the substitution reactions of our triphosphoxane rings with metal complexes are typically accompanied by a template effect around the metal center to generate metal polyphosphoxane complexes with different ring size and structures. Only for (norbornadiene)molybdenum tetracarbonyl reaction was the parent P$_3$O$_3$ ring structure retained, giving the relatively unstable 1:1 complexes cis-Mo(CO)$_4$[R$_2$NPO]$_3$ (R=^{i}Pr, Cy). More usually, the triphosphoxanes build up to tetra- and pentaphosphoxane rings around metal centers. Typically, monometallic poly-phosphoxane complexes are obtained except for the molybdenum cage complex and its cage-like isomer, Mo$_2$(CO)$_8$[R$_2$NPO]$_4$. Metal tetraphosphoxane complexes alone show six coordination modes (Figure 1-1), including 1,3-chelate, 1,5-chelate in a boat-boat, boat-chair, and chair-chair conformation, as well as 1,3,7-μ-bimetallic structure shown in Figure 1-1F.

Under certain conditions, the coordinated polyphosphoxane ring can be released

11

through replacement by suitable ligands. Furthermore, the uncoordinated phosphoruses on monometallic polyphosphoxane complexes can also be used to coordinate another electron-rich metal center to form bimetallic poly-phosphoxane complexes. In addition, we also found polyphosphoxane ring transfers between two different metal centers. In all these studies, solution ^{31}P NMR spectroscopy served as the primary method for structural analysis.

1,3-chelating mode (A)

1,5-chelating chair-chair mode (B)

1,5-chelating boat-chair mode (C)

cage, boat-boat mode (D)

twist boat-twist boat mode (E)

(F)
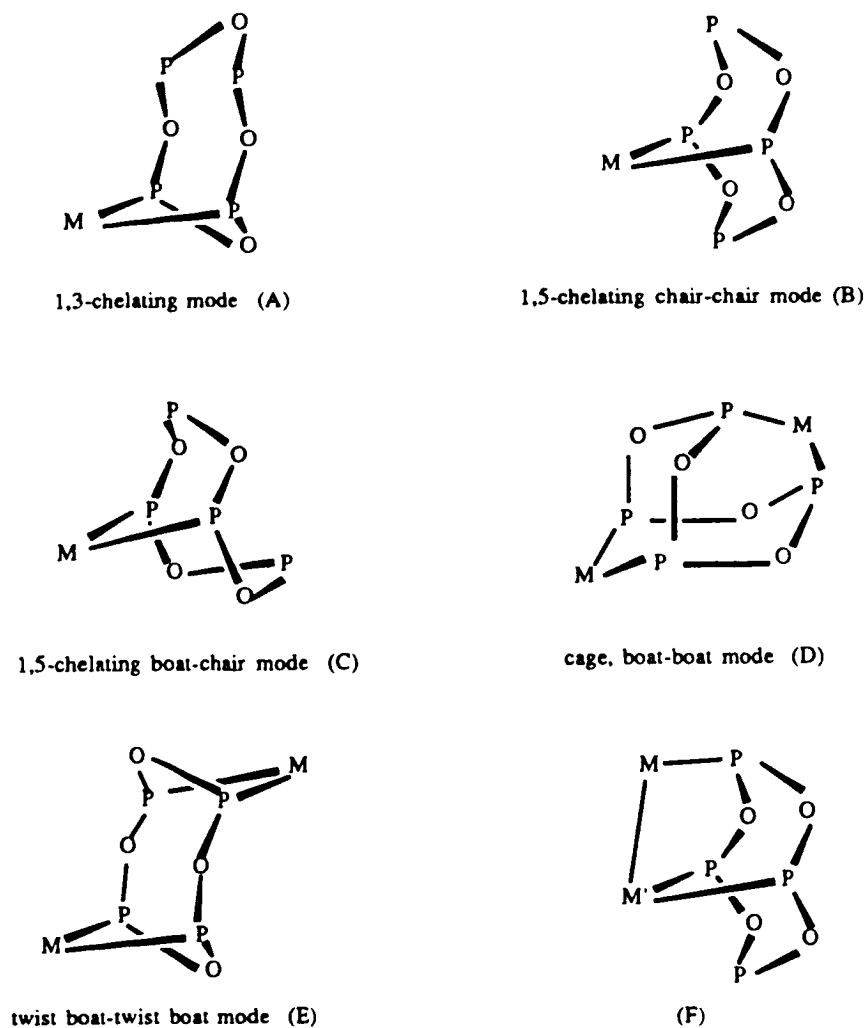
Figure 1-1: Six coordination modes of the P_4O_4 ring (P = R$_2$N-P)

12

RESULTS

1. Synthesis of Cyclotriphosphoxanes:

The syntheses of cyclotriphosphoxanes were performed as shown in equations (9,10):

$$2R_2NH + PCl_3 \xrightarrow[-78°C]{CH_2Cl_2} R_2NPCl_2 + R_2NH_2Cl \qquad (9)$$

$$R_2NPCl_2 + H_2O + Et_3N \xrightarrow[0°C]{THF} 1/3[R_2NPO]_3 + Et_3NHCl \qquad (10)$$
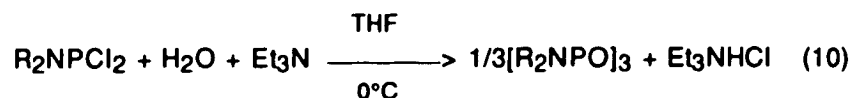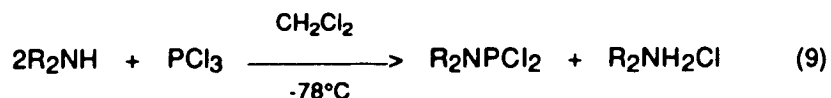
The dichloroalkylaminophosphines were synthesized by reaction of phosphorus trichloride with 2 equivalents of amines in CH_2Cl_2 at -78°C for 2 h. Products were isolated by filtering off the amine hydrochloride and evaporating off the methylene chloride after warming to room temperature. Pure liquid products, Et_2NPCl_2, $C_5H_{10}NPCl_2$, $^iPr_2NPCl_2$, $^sBu_2NPCl_2$, and $(^iPr)(Cy)NPCl_2$, were obtained by vacuum distillation. Pure solid Cy_2NPCl_2 was obtained by reprecipitation from hexanes. However, Ph_2NPCl_2 was a brown liquid which decomposed under vacuum distillation. It was used without further purification. The yields of dichloroaminophosphines were around 60%. ^{31}P NMR spectra of the compounds typically showed singlets from 149 ppm to 170 ppm. Table 1-1 lists the synthesized dichloroaminophosphines and their ^{31}P NMR data.

Table 1-1. ^{31}P NMR Data of the Dichloroaminophosphines

Compound	Chemical shift δ in ppm	
Et_2NPCl_2	singlet	154.0
$C_5H_{10}NPCl_2$,(piperidino-)	singlet	156.6
$^iPr_2NPCl_2$	singlet	168.9
Cy_2NPCl_2	singlet	168.9
$^sBu_2NPCl_2$	singlet	169.1
$(^iPr)(Cy)NPCl_2$	singlet	168.8
Ph_2NPCl_2	singlet	149.0
$^iPrPhNPCl_2$	singlet	152.3

All spectra were run in $CDCl_3$

13

The cyclotriphosphoxanes were produced by the controlled hydrolysis of dichloro-aminophosphines with the stoichiometric amount of water in the presence of triethyl-amine in THF at 0°C. Vigorous stirring and slow addition of the mixture of water and THF into the solution of dichloroaminophosphine and triethylamine were important for reducing side products. Reaction progress was monitored by ^{31}P NMR spectroscopy. The AB_2 splitting pattern of triplets and doublets of the P_3O_3 ring served as evidence for the formation of P_3O_3 rings in the boat conformation. The products were isolated by filtering off the triethylamine hydrochloride and evaporation of the THF. Only the solid products $[^iPr_2NPO]_3$ and $[Cy_2NPO]_3$ were further purified by two reprecipitations from hot hexanes and characterized by IR, NMR, and CHN analysis. Other rings were thick, high boiling point liquids and were used without further purification. Figure 1-2 shows the boat conformation of these synthesized P_3O_3 rings.

R=R'=^{i}Pr	Ring 1
Cy	Ring 2
^{s}Bu	Ring 3
Ph	Ring 4
R=^{i}Pr, R'=Cy	Ring 5
R=^{i}Pr, R'=Ph	Ring 6
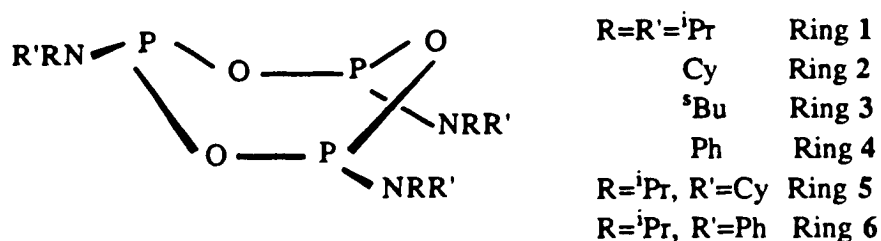
Figure 1-2: The boat conformational structure of rings 1-6

Generally, incomplete hydrolysis or poor stirring produced many side products which showed up in the ^{31}P NMR spectra as several minor singlet resonances and multiplets at -9 ppm to 125 ppm. All these side products could be reacted with extra dichloroaminophosphines in solution to transform to triphosphoxane rings completely by refluxing in THF for about 1 hr. The ^{31}P NMR spectra would eventually show only the AB_2 splitting pattern of product rings. So, optimization of reaction conditions can complete the reaction and increase the yield and purity of products. From this procedure, two solid cyclotriphosphoxanes, $[^iPr_2NPO]_3$ and $[Cy_2NPO]_3$, and the liquids

14

[iPrCyNPO]3, [Ph2NPO]3 and [sBu2NPO]3, have been isolated. The ^{31}P NMR spectra of these compounds showed triplets ranging from 127 ppm to 140 ppm and doublets ranging from 122 ppm to 131 ppm with P-O-P coupling constants typically of 9 Hz to 13 Hz. These products were unstable to air and moisture, particularly when trace amounts of acid were present. Table 1-2 lists the ^{31}P NMR data of these synthesized cyclotriphosphoxanes with a typical ^{31}P NMR spectrum shown in Figure 1-3. Rings with less sterically-bulky amino groups such as [Et2NPO]3 and [C5H10NPO]3 (piperidinophosphoxane) could not be synthesized using above reactions.

Table 1-2. ^{31}P NMR data of the cyclotriphosphoxanes

Compounds	splitting pattern (δ, ppm) (J, Hz)
[iPr2NPO]3	AB2 (δ_A=139.4 δ_B=130.2, J$_{AB}$=13.1)
[Cy2NPO]3	AB2 (δ_A=140.5 δ_B=131.0, J$_{AB}$=14.1)
[Ph2NPO]3	AB2 (δ_A=127.4 δ_B=122.9, J$_{AB}$=11.2)
[iPrCyNPO]3	AB2 (δ_A=139.6 δ_B=130.1, J$_{AB}$=13.2)
[sBu2NPO]3	ABB' (δ_A=138.5 δ_B=130.6, multiplets)
[iPrPhNPO]3	AB2 (δ_A=131.4 δ_B=123.6, J$_{AB}$=9.7)

All spectra were run in CDCl3

Figure 1-3: ^{31}P {^{1}H} NMR spectrum of [Cy2NPO]3

15

2. Ring Coordination Reactions of NiX$_2$·L   (X=Cl, Br, I;   L = DME, 2THF):

$$\text{NiX}_2\text{·L} \;+\; 4/3[^i\text{Pr}_2\text{NPO}]_3 \quad \xrightarrow[\text{RT or } \Delta]{\text{hexanes}} \quad \text{NiX}_2\text{·}[^i\text{Pr}_2\text{NPO}]_4 \;+\; \text{L} \qquad (11)$$

$$\text{NiX}_2\text{·L} \;+\; 4/3[\text{Cy}_2\text{NPO}]_3 \quad \xrightarrow[\text{RT or } \Delta]{\text{hexanes}} \quad \text{NiX}_2\text{·}[\text{Cy}_2\text{NPO}]_4 \;+\; \text{L} \qquad (12)$$

$$\text{NiCl}_2\text{·DME} \;+\; 5/3[\text{Cy}_2\text{NPO}]_3 \quad \xrightarrow[\text{RT}]{\text{hexanes}} \quad \text{NiCl}_2\text{·}[\text{Cy}_2\text{NPO}]_5 \;+\; \text{DME} \qquad (13)$$
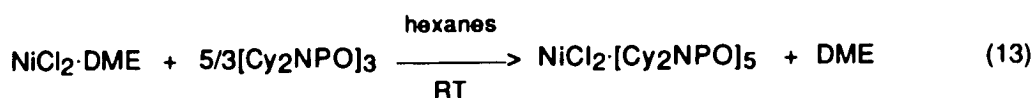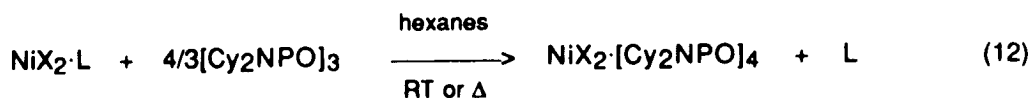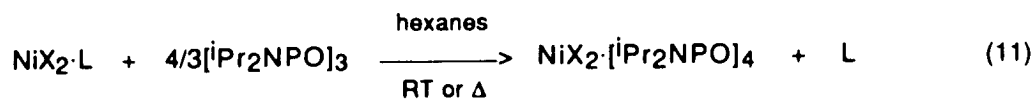
The reagents NiBr$_2$·DME, NiCl$_2$·DME, and NiI$_2$·2THF were stirred as suspensions in hexane or toluene solutions of [R$_2$NPO]$_3$ (R=^{i}Pr, Cy) at room temperature or reflux for about 12 h.   The products were typically square-planar 1,3-coordinated cis-NiX$_2$·[^{i}Pr$_2$NPO]$_4$ compounds with Ring 1, [^{i}Pr$_2$NPO]$_3$. The reactions of NiBr$_2$·DME and NiI$_2$·2THF with Ring 2, [Cy$_2$NPO]$_3$, gave similar cis-NiX$_2$·[Cy$_2$NPO]$_4$ products. However, the reaction of NiCl$_2$·DME with Ring 2 was different.   While the 1,3-coordinated cis-NiCl$_2$·[Cy$_2$NPO]$_4$ compound was obtained when reaction was run in hot toluene, the 1,5-coordinated cis-NiCl$_2$·[Cy$_2$NPO]$_5$ complex was obtained when the reaction was at room temperature or in refluxing hexanes. A mixture of nickel (II) chloride P$_4$O$_4$ and P$_5$O$_5$ complexes were obtained when reaction was run in toluene at room temperature. Figure 1-4 shows the proposed structures of these P$_4$O$_4$ and P$_5$O$_5$ complexes.

These nickel halide cyclopolyphosphoxane complexes were isolated in about 50-60% yields.   The cis-NiCl$_2$·[R$_2$NPO]$_4$ (R=^{i}Pr, Cy) complexes were isolated as brown, unstable solids, while cis-NiBr$_2$·[R$_2$NPO]$_4$ (R=^{i}Pr, Cy) complexes were stable red-orange solids, and cis-NiI$_2$·[Cy$_2$NPO]$_4$ was an unstable purple solid. Their solution ^{31}P NMR spectra exhibit AA'XX' patterns with chemical shifts of the two coordinated

16

phosphoruses (XX') around 54-75 ppm and two uncoordinated phosphoruses (AA') around 142-144 ppm with the large coupling of 50 Hz between A and A', X and X'; the coupling of 20 Hz between A and X, A' and X'; as well as very small coupling of 1 Hz between A and X', A' and X, confirming a unique 1,3-coordination mode (Figure 1-1, A) for the tetraphosphoxane ring. The cis-NiCl$_2$-[Cy2NPO]$_5$ complex was isolated as a stable yellow solid with an AA'MXX' pattern in its solution ^{31}P NMR spectrum with chemical shifts of the two coordinated phosphoruses (XX') at 92 ppm and three uncoordinated phosphoruses at 124 ppm (M) and 143 ppm (AA'), suggestive of a 1,5-coordination mode. Table 1-3 presents these ^{31}P NMR spectra data. Figure 1-5 shows the ^{31}P NMR spectra of these P$_4$O$_4$ and P$_5$O$_5$ complexes.

R=^{i}Pr, X=Cl (I)
X=Br (II)
R=Cy, X=Cl (III)
X=Br (IV)
X=I (V)
1,3-chelated cis-NiX$_2$[R$_2$NPO]$_4$

R=Cy (VI)

1,5-chelated cis-NiCl$_2$[Cy2NPO]$_5$
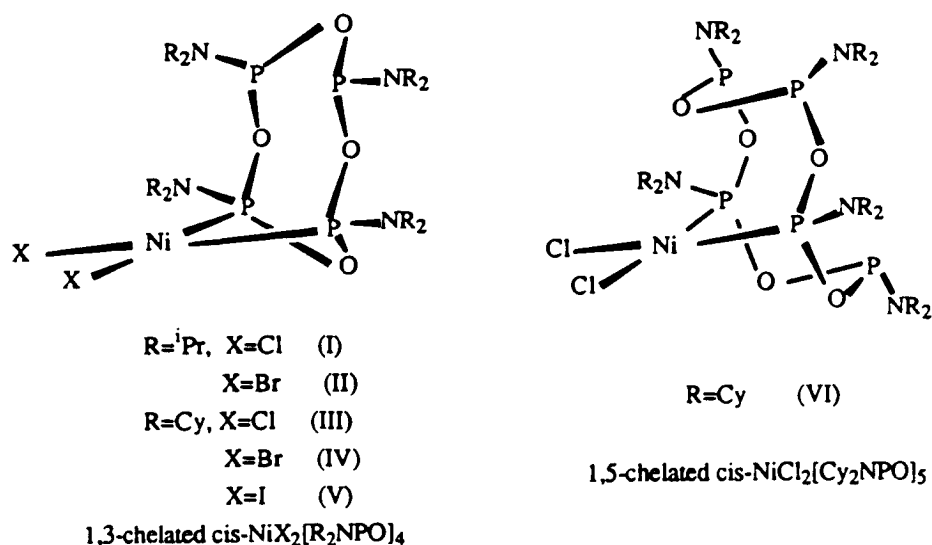
Figure 1-4: Proposed structures of the P$_4$O$_4$ and P$_5$O$_5$ Ni (II) complexes

17
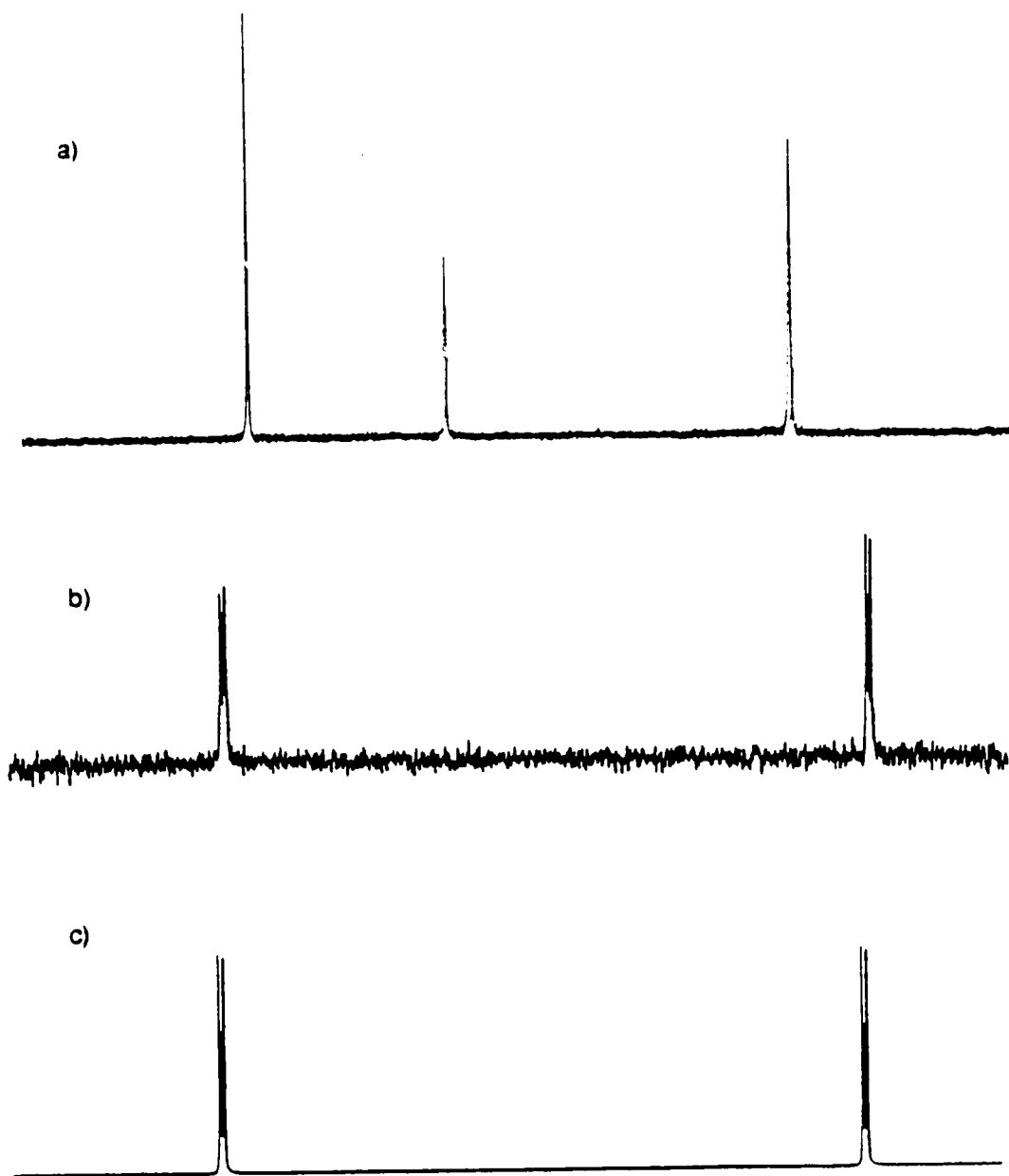
Figure 1-5: a) ^{31}P {^1H} NMR spectrum of $NiCl_2[Cy_2NPO]_5$ at -10°C.
b) ^{31}P {^1H} NMR spectrum of $NiBr_2[{}^iPr_2NPO]_4$.
c) Simulation of the AA'XX' pattern with $\delta_A=\delta_{A'}=144.6$ ppm and
$\delta_X=\delta_{X'}=63.1$ ppm; $^2J_{AA'}={}^2J_{XX'}=50$, $^2J_{AX}={}^2J_{A'X'}=20$
$^4J_{AX'}={}^4J_{A'X}=1$ Hz

18

3. Ring Coordination Reactions of PdX₂·2PhCN (X=Cl, Br):

$$PdX_2 \cdot 2PhCN + 4/3[^iPr_2NPO]_3 \xrightarrow[\text{RT or } \Delta]{\text{hexanes}} PdX_2 \cdot [^iPr_2NPO]_4 + 2PhCN \qquad (14)$$

$$PdX_2 \cdot 2PhCN + 4/3[Cy_2NPO]_3 \xrightarrow[4^\circ C]{\text{hexanes}} PdX_2 \cdot [Cy_2NPO]_4 + 2PhCN \qquad (15)$$

$$PdX_2 \cdot 2PhCN + 5/3[Cy_2NPO]_3 \xrightarrow[\Delta]{\text{hexanes}} PdX_2 \cdot [Cy_2NPO]_5 + 2PhCN \qquad (16)$$
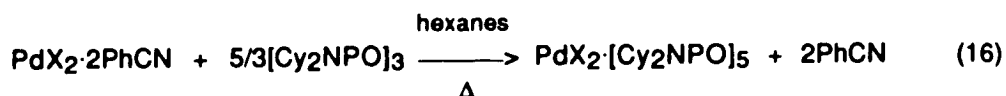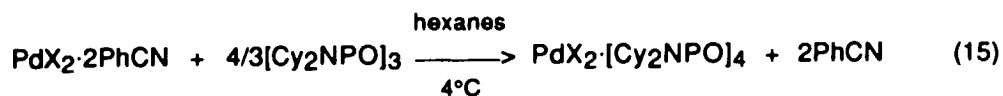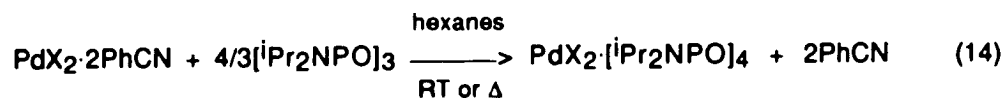
The palladium (II) chloride and bromide were suspended in hexane or toluene solutions of $[R_2NPO]_3$ (R = ^iPr, Cy) at room temperature or at reflux for about 12 h. The products were generally the square-planar 1,5-coordinated cis-$PdX_2 \cdot [^iPr_2NPO]_4$ compounds with Ring 1, $[^iPr_2NPO]_3$. The reactions of palladium (II) halides with Ring 2, $[Cy_2NPO]_3$, gave different results depending upon reaction conditions. At a temperature of 4°C, square-planar 1,5-coordinated cis-$PdX_2 \cdot [Cy_2NPO]_4$ compounds were obtained. In refluxing hexanes, the square-planar 1,5-coordinated cis-$PdX_2 \cdot [Cy_2NPO]_5$ complexes were obtained. At room temperature, a mixture of palladium halide P_4O_4 and P_5O_5 products were obtained with the latter predominant. In refluxing toluene, $PdBr_2 \cdot [Cy_2NPO]_5$ partially rearranged to a conformational isomer (XIII). Figure 1-6 shows the proposed structures of these P_4O_4 and P_5O_5 complexes.

19
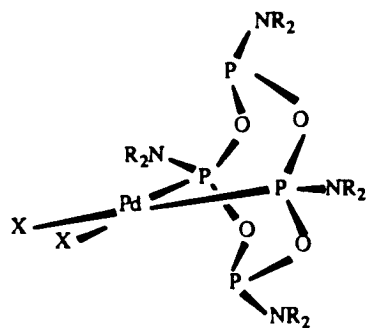
R=ⁱPr, X=Cl (VII)
X=Br (VIII)
R=Cy, X=Cl (IX)
X=Br (X)

1,5-chelated cis-PdX$_2$[R$_2$NPO]$_4$
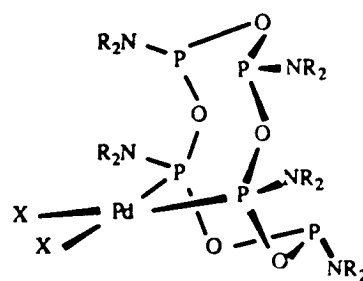
R=Cy, X=Cl (XI)
X=Br (XII). isomer A

1,5-chelated cis-PdX$_2$[R$_2$NPO]$_5$
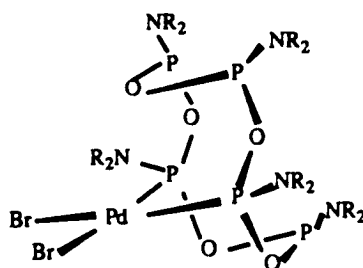
R=Cy, isomer B (XIII)

Figure 1-6: Proposed structures of palladium (II) P$_4$O$_4$ and P$_5$O$_5$ complexes

The palladium halide cyclopolyphosphoxane complexes were isolated typically in 70-80% yields. The cis-PdX$_2$·[^{i}Pr$_2$NPO]$_4$ (X = Cl, Br) products were isolated as white stable solids, cis-PdX$_2$·[Cy$_2$NPO]$_4$ (X = Cl, Br) were unstable white solids. Their solution ^{31}P NMR spectra are obviously different with that of the 1,3-coordinated cis-NiX$_2$·[Cy$_2$NPO]$_4$ in exhibiting A$_2$X$_2$ splitting patterns with chemical shifts of

20

coordinated phosphoruses (X_2) at 88 ppm and uncoordinated phosphoruses (A_2) around 141-146 ppm as well as large $^2J_{P-O-P}$ couplings of over 80 Hz from chair-chair conformation, suggesting a distinct 1,5-coordination mode (Figure 1-1, 3) for the tetraphosphoxane ring. The cis-PdX_2·[Cy2NPO]5 (X = Cl, Br) complexes were isolated as stable pale-yellow solids. Their AA'MXX' patterns in their solution ^{31}P NMR spectra are similar to that of 1,7-coordinated cis-$NiCl_2$·[Cy2NPO]5 (VI) but with $^2J_{AX}=^2J_{AX'}=^2J_{AM'}=^2J_{AM}$ couplings of 15-19 Hz and $^2J_{MX}=^2J_{MX'}$ couplings of about 2 Hz. Isomer B of palladium bromide pentaphosphoxane complex (XIII) can be easily identified by its solution ^{31}P NMR spectrum showing different couplings from isomer A with a very large coupling of over 60 Hz between one uncoordinated phosphoruses (M) and two coordinated P's (XX') and a very small $^2J_{AX'}$ coupling of 2 Hz, as well as $^2J_{AM}=0$ Hz. Table 1-3 lists these ^{31}P NMR spectral data. Figure 1-7 displays the ^{31}P NMR spectra of both kinds of complexes.

Single-crystal X-ray quality crystals of complex (VII) were obtained from slow evaporation of an NMR solution $CDCl_3$. Figure 1-8 shows the molecular structure of complex (VII) along with selected bond length and angle data.

a)

21
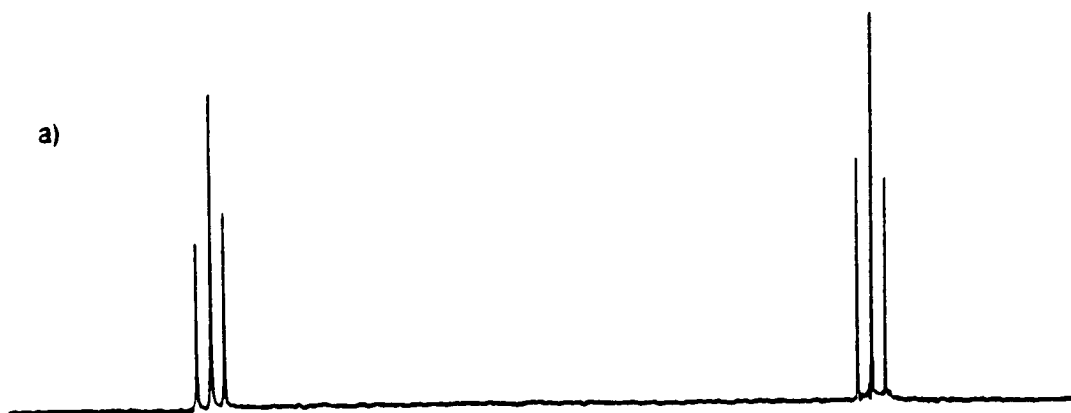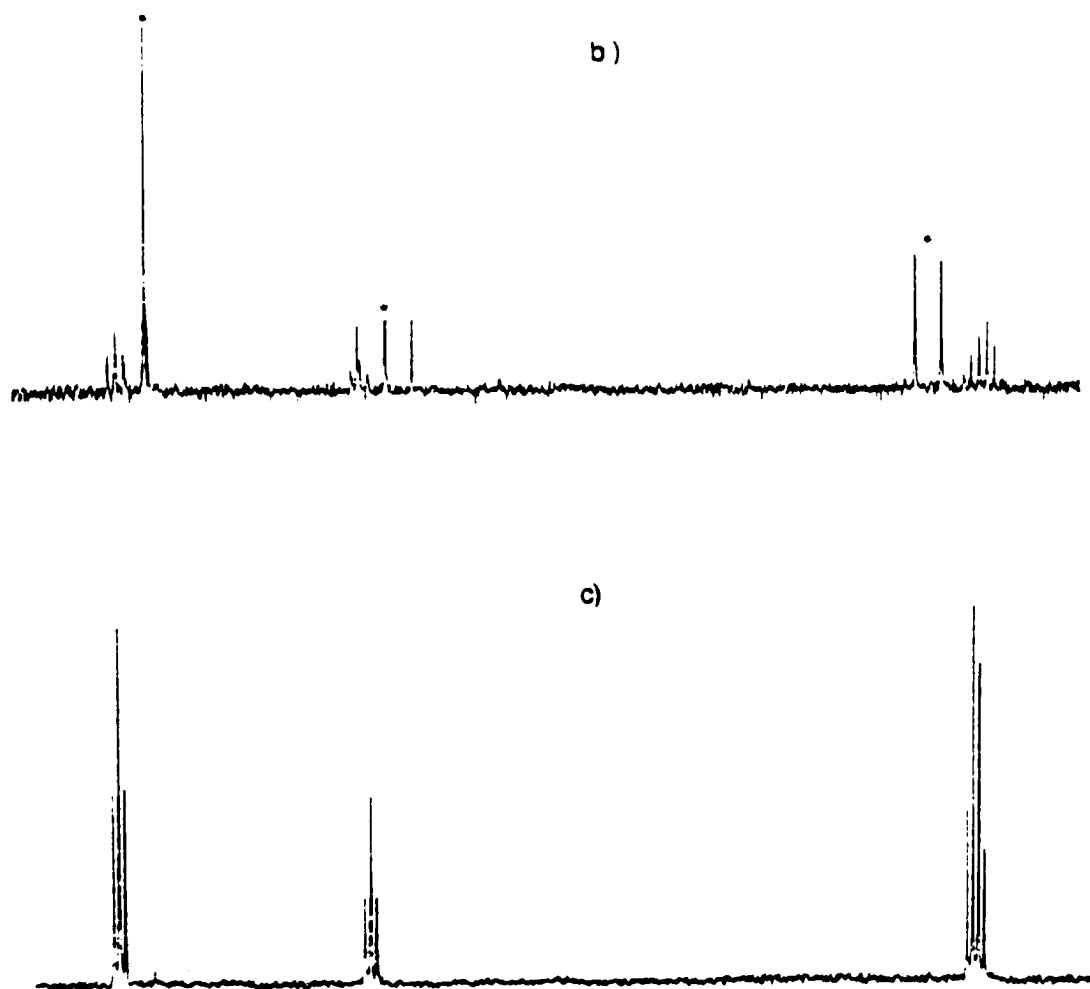
Figure 1-7: a) ^{31}P {^1H} NMR spectrum of cis-PdCl$_2$·[$^iPr_2NPO$]$_4$.

b) ^{31}P {^1H} NMR spectrum of cis-PdBr$_2$·[Cy$_2$NPO]$_5$ and isomer B (XIII), with * marks.

c) ^{31}P {^1H} NMR spectrum of cis-PdBr$_2$·[Cy$_2$NPO]$_5$.

22

X-ray crystal structure of complex (VII)

23

Selected bond distances and bond angles for cis-PdCl$_2$·[^{i}Pr$_2$NPO]$_4$ (VII) in angstroms and degrees.

Pd-Cl	2.3457(17)	Pd-Cla	2.3457(17)
Pd-P(1)	2.2483(15)	Pd-P(1)a	2.2483(15)
P(1)-O(1)	1.617(4)	P(1)-O(2)	1.592(4)
P(1)-N(1)	1.621(5)	P(2)-O(1)	1.663(4)
P(2)-O(2)a	1.686(4)	P(2)-N(2)	1.630(4)
O(2)-P(2)a	1.686(4)		

Cl-Pd-Cla	89.69(8)	Cl-Pd-P(1)	93.04(6)
Cl-Pd-P(1)a	175.80(7)	Cla-Pd-P(1)	175.80(7)
Cla-Pd-P(1)a	93.04(6)	P(1)-Pd-P(1)a	84.41(6)
Pd-P(1)-O(1)	107.88(16)	Pd-P(1)-O(2)	111.16(14)

Pd-P(1)-N(1)	124.74(19)	O(1)-P(1)-O(2)	102.72(21)
O(2)-P(2)a	1.686(4)	O(1)-P(1)-N(1)	105.41(23)
O(2)-P(1)-N(1)	102.76(24)	O(1)-P(2)-O(2)a	96.24(20)
O(1)-P(1)-N(2)	99.84(23)	O(2)a-P(2)-N(2)	99.54(20)
P(1)-O(1)-P(2)	128.59(24)	P(1)-O(2)-P(2)a	124.47(23)
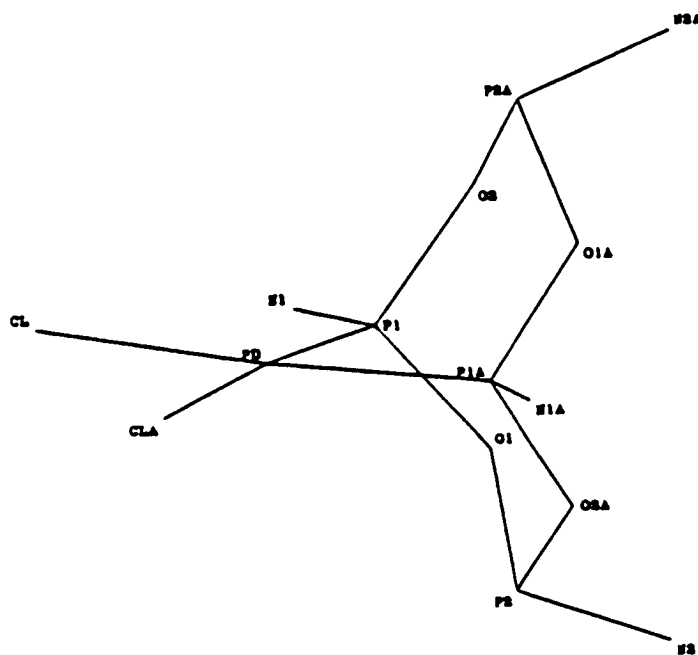
Figure 1-8: X-ray crystal structure of complex (VII).

24

4. Ring Coordination Reactions of PtCl₂·NBD:

The course of substitution reactions of $PtCl_2 \cdot NBD$ with cyclotriphosphoxanes are mostly similar to that of palladium halides and are shown in following equations:

$$PtCl_2 \cdot NBD \ + \ 4/3[^iPr_2NPO]_3 \ \xrightarrow[\text{RT or } \Delta]{\text{hexanes}} \ PtCl_2 \cdot [^iPr_2NPO]_4 \ + \ NBD \qquad (17)$$

$$PtCl_2 \cdot NBD \ + \ 4/3[Cy_2NPO]_3 \ \xrightarrow[\text{4°C}]{\text{hexanes}} \ PtCl_2 \cdot [Cy_2NPO]_4 \ + \ NBD \qquad (18)$$

$$PtCl_2 \cdot NBD \ + \ 5/3[Cy_2NPO]_3 \ \xrightarrow[\Delta]{\text{hexanes}} \ PtCl_2 \cdot [Cy_2NPO]_5 \ + \ NBD \qquad (19)$$
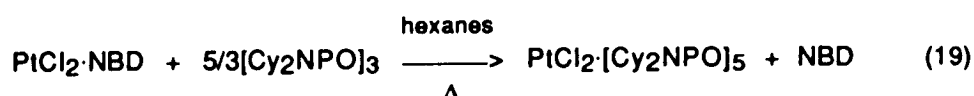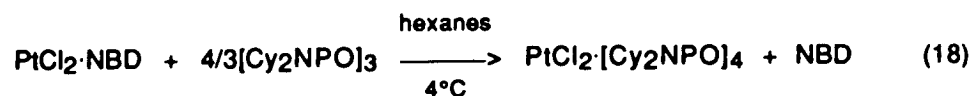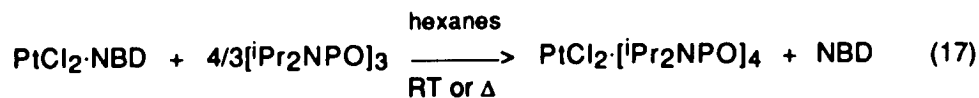
The platinum (II) chloride complex was suspended and stirred in hexane or toluene solutions of $[Cy_2NPO]_3$ at room temperature or at reflux for about 12 h. The product was the square-planar 1,5-coordinated cis-$PtCl_2 \cdot [^iPr_2NPO]_4$ complex (**XIV**) with Ring 1, $[iPr_2NPO]_3$. Reactions of platinum (II) chloride complex with Ring 2, $[Cy_2NPO]_3$, gave several results dependent upon reaction conditions. At 4°C, reaction of platinum chloride with Ring 2 gave a similar product as that of Ring 1, the square-planar 1,5-coordinated cis-$PtCl_2 \cdot [Cy_2NPO]_4$. In refluxing hexanes, the square-planar 1,5-coordinated cis-$PtCl_2 \cdot [Cy_2NPO]_5$ (**XV**) with a similar solution ^{31}P NMR spectrum to complex (**VI**) of the palladium P_5O_5 analogue was obtained instead. At room temperature, a mixture of platinum chloride P_4O_4 and P_5O_5 complexes were obtained with the P_4O_4 product predominant.

There are two isomers of cis-$PtCl_2 \cdot [Cy_2NPO]_4$ as shown by a 2D ^{31}P NMR COSY spectrum. At 4°C, the major product is isomer A (**XVI**), whose solution ^{31}P NMR spectrum showed an ABXX' splitting pattern (triplet at 140.1 ppm, J=43.5 Hz; triplet at 134.4 ppm, J=13.1 Hz; and doublet of doublets at 58.1 ppm, J=43.5, 13.1 Hz), suggesting a 1,5-chelate chair-boat conformation (Figure 1-1, C). At room

25

temperature, isomer B (XVII) was predominant with a solution ^{31}P NMR spectrum showing an A_2X_2 pattern which is consistent with that of complex (VII), suggesting a distinct 1,5-chelate chair-chair conformation (Figure 1-1, B). These two isomers were separately isolated at different temperatures. Figure 1-9 shows the proposed structure of isomer A and the 2D ^{31}P NMR COSY spectrum of an P_4O_4 isomer mixture.

Platinum chloride cyclopolyphosphoxane complexes were obtained in 45-55% yields. The cis-PtCl$_2$·[^{i}Pr$_2$NPO]$_4$ complex was isolated as a stable white solid. Its solution ^{31}P NMR spectrum is the same as that of 1,5-coordinated cis-PdX$_2$·[Cy2NPO]$_4$ exhibiting an A_2X_2 splitting pattern with chemical shifts of uncoordinated P's around 142 ppm and coordinated P's at 59 ppm, as well as a large coupling between ^{195}Pt (nuclear spin =1/2, 38% natural abundance) and phosphorus of 4825 Hz, consistent with a 1,5-coordination mode for the tetraphosphoxane ring. Isomers of cis-PtCl$_2$·[Cy2NPO]$_4$ were unstable white solids. The cis-PtCl$_2$·[Cy2NPO]$_5$ was isolated as a stable white solid, whose AA'MXX' splitting pattern in the solution ^{31}P NMR spectrum has chemical shifts of coordinated P's (XX') at 60 ppm and uncoordinated P's at 142 ppm (AA') and 127 ppm (M) respectively with large satellite coupling between platinum and phosphorus of around 5141 Hz, again suggesting a 1,5-coordination mode. Table 1-3 lists these ^{31}P NMR spectral data.

We further noted a decomposition reaction of the platinum chloride P_5O_5 complex forming the P_4O_4 complex during attempted recrystallization.

$$\text{cis-PtCl}_2\text{·[Cy2NPO]}_5 \xrightarrow[\text{RT}]{\text{CH}_2\text{Cl}_2\text{/hexanes}} \text{cis-PtCl}_2\text{·[Cy2NPO]}_4 + \text{[Cy2NPO]} \quad (20)$$
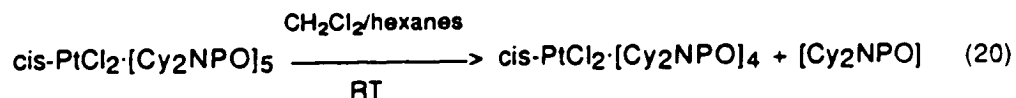
When cis-PtCl$_2$·[Cy2NPO]$_5$ was recrystallized in a mixture of methylene chloride and hexane, single crystals of cis-PtCl$_2$·[Cy2NPO]$_4$ grew instead. Figure 1-10 shows

26

the X-ray molecular structure of this complex (XVII).

a)
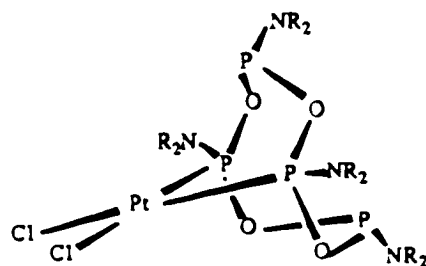
R=Cy. isomer A   (XVI)
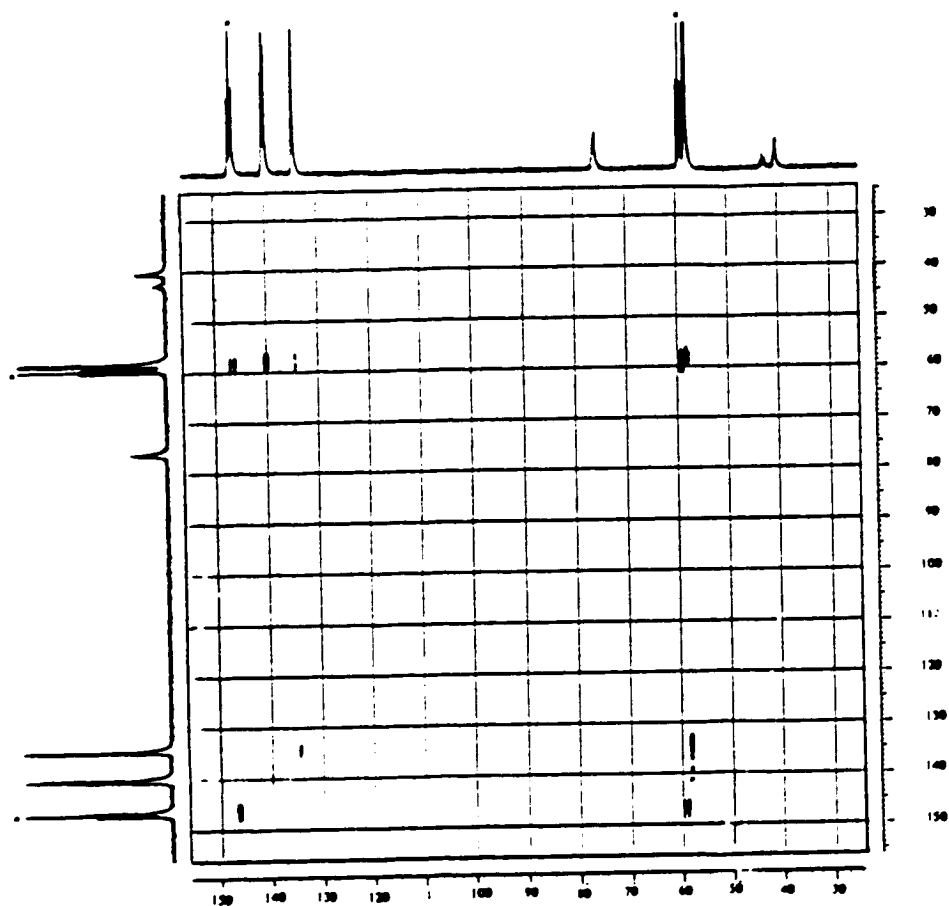
Figure 1-9: a) Proposed structure of isomer A.
b) 2D ^{31}P NMR COSY spectrum of isomer A and B with * marks at 25°C

27
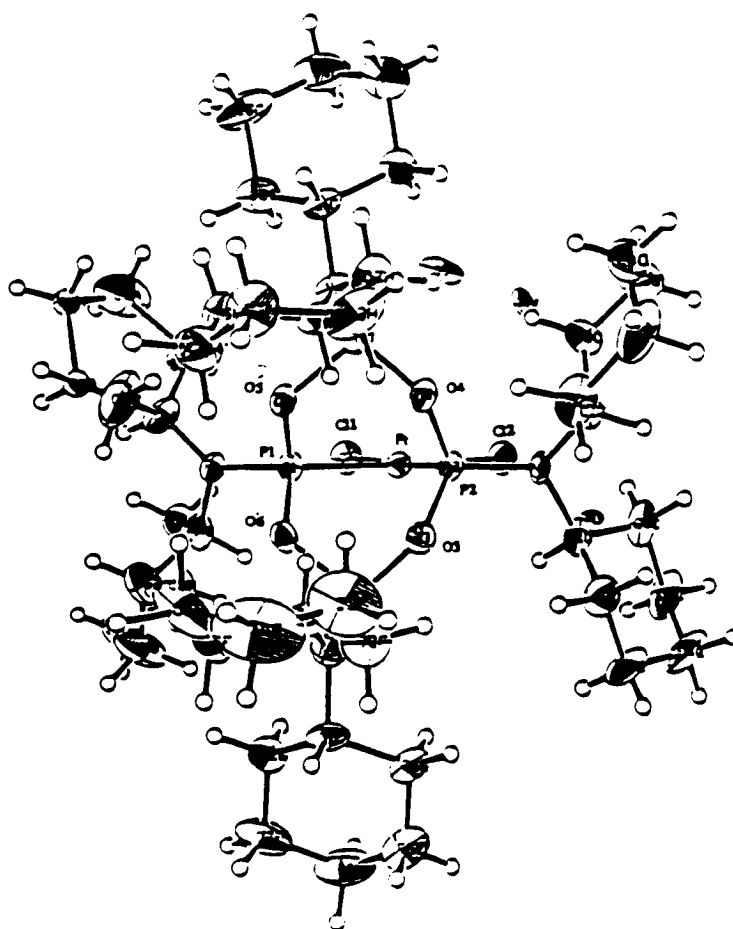
Selected bond distances and bond angles for cis-PtCl$_2$·[Cy$_2$NPO]$_4$ (XVII) complex in angstroms and degrees.

Pt-Cl2	2.344(4)	Pt-P1	2.225(4)	Pt-P2	2.220(4)
P1-O1	1.614(9)	P1-O2	1.583(9)	P1-N1	1.61(1)
P2-O3	1.62(1)	P2-O4	1.603(9)	P2-N2	1.62(1)
P3-O1	1.69(1)	P3-O3	1.69(1)	P3-N3	1.64(1)
P4-O2	1.73(1)	P4O4	1.68(1)	P4-N4	1.63(1)

Cl1-Pt1-Cl2	87.5(1)	Cl1-Pt1-O1	176.9(2)
Cl1-Pt1-P2	93.4(1)	P1-Pt1-P2	85.7(1)
Pt1-P1-O1	109.6(4)	Pt1-P1-O2	110.1(4)
Pt1-P1-N1	124.8(5)	O1-P1-O2	102.6(5)
O1-P1-N1	103.6(6)	Pt1-P2-O3	109.2(4)
Pt1-P2-O4	109.0(4)	Pt1-P2-N2	125.6(5)
O3-P2-O4	104.2(5)	O3-P2-N2	103.7(6)
O1-P3-O3	95.0(5)	P2-O3-P3	121.3(6)

Figure 1-10: X-ray crystal structure of complex (XVII)

28

5. Ring Coordination Reactions of M(CO)$_4$·NBD (M=Cr, Mo, W):

$$Mo(CO)_4 \cdot NBD + [R_2NPO]_3 \xrightarrow[\text{RT, } (R=^iPr, Cy)]{\text{hexanes}} Mo(CO)_4 \cdot [R_2NPO]_3 + NBD \quad (21)$$

$$2Mo(CO)_4 \cdot [R_2NPO]_3 \xrightarrow[\Delta, (R=^iPr, Cy)]{\text{hexanes}} Mo_2(CO)_8 \cdot [R_2NPO]_4 + 2 [R_2NPO] \quad (22)$$

$$Cr(CO)_4 \cdot NBD + 4/3[Cy_2NPO]_3 \xrightarrow[\Delta]{\text{hexanes}} Cr(CO)_4 \cdot [Cy_2NPO]_4 + NBD \quad (23)$$
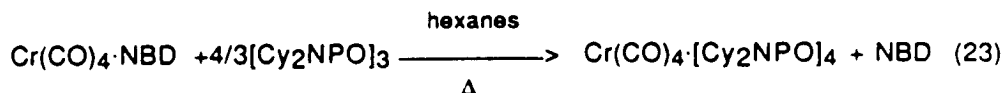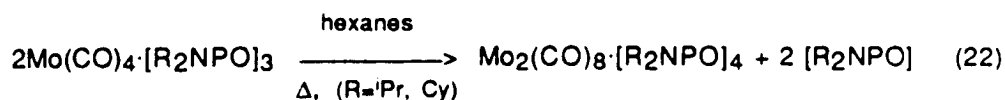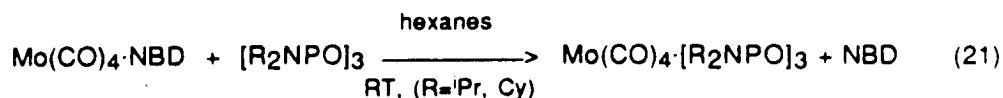
Substitutions by the triphosphoxane rings, [$^iPr_2NPO]_3$ and [$Cy_2NPO]_3$ with Mo(CO)$_4$·NBD in hexanes at room temperature gave the relatively unstable 1:1 complexes (XVIII, XIX) as white precipitates in about 40-90% yield. The A$_2$X splitting patterns of their solution ^{31}P NMR spectra confirm retention of the parent P$_3$O$_3$ rings in these products. These white solids slowly transformed to the molybdenum cage complexes, Mo$_2$(CO)$_8$·[R$_2$NPO]$_4$ (R=^{i}Pr, Cy) (XX, XXI), upon standing at room temperature in the solid state or warming up in solution, according to equation (22). Isomers of molybdenum cage, Mo$_2$(CO)$_8$·[R$_2$NPO]$_4$ (R=^{i}Pr, Cy) (XXII, XXIII) with the coordination mode (Figure 1-1, E), whose solution ^{31}P NMR spectrum show singlets at 135 ppm (XXII) and 137 ppm (XXIII), were obtained as stable pale-yellow crystals in warm reaction conditions at about 30°C in 25% yield. Figure 1-11 shows the proposed structure of complexes (XVIII) and (XIX), as well as the ^{31}P NMR spectrum of complex (XIX).

a)

R=^{i}Pr	(XVIII)
R=Cy	(XIX)

29

b)
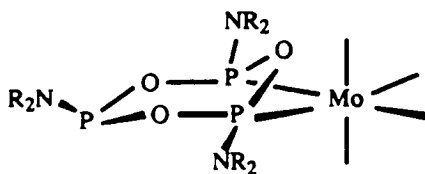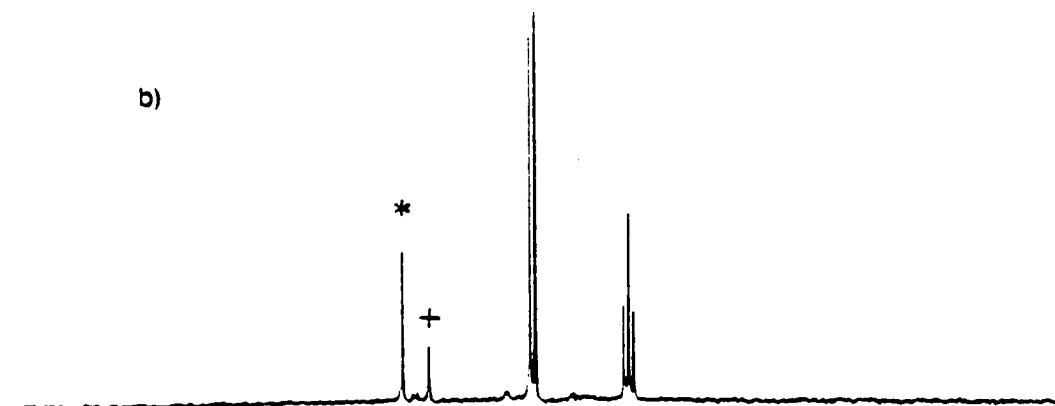
Figure 1-11: a) Proposed structure of Mo(CO)$_4$·[R$_2$NPO]$_3$ (R=^{i}Pr, Cy)

b) ^{31}P {^{1}H} NMR spectrum of Mo(CO)$_4$·[Cy$_2$NPO]$_3$ with '*' marking the cage and '+' the cage isomer.

Reaction of Cr(CO)$_4$·NBD with Ring 2 in refluxing hexanes for prolonged periods yielded the 1,5-coordinated cis-Cr(CO)$_4$·[Cy$_2$NPO]$_4$ (XXIV) as a white solid in about 34% yield. The solution ^{31}P NMR spectrum of this product exhibits an A$_2$MX splitting pattern with two coordinated P's at 177 ppm (A$_2$) and two uncoordinated P's at 123 ppm (M) and 129 ppm (X) respectively, suggesting a 1,5-coordination mode (Figure 1-1, C) for the tetraphosphoxane ring. Table 3 lists the ^{31}P NMR data of these compounds. No reaction occurred, however, when W(CO)$_4$·NBD and Ring 1 or Ring 2 were mixed together in refluxing hexanes even after prolonged periods. Figure 1-12 shows the ^{31}P NMR spectrum of complex (XXIV).

Figure 1-12: ^{31}P {^{1}H} NMR spectrum of cis-Cr(CO)$_4$·[Cy$_2$NPO]$_4$ (XXIV).

30

6. Ring Coordination Reactions of Diiron Nonacarbonyl, $Fe_2(CO)_9$:

$$Fe_2(CO)_9 + [Cy_2NPO]_3 \xrightarrow[\Delta]{toluene} Fe(CO)_3 \cdot [Cy_2NPO]_4 + Fe(CO)_5 + CO \quad (24)$$

$$Fe_2(CO)_9 + [^iPr_2NPO]_3 \xrightarrow[\Delta]{toluene} Fe(CO)_3 \cdot [^iPr_2NPO]_4 + {}^\cdot Fe(CO)_4 \cdot [^iPr_2NPO]_4{}^\cdot + CO \quad (25)$$
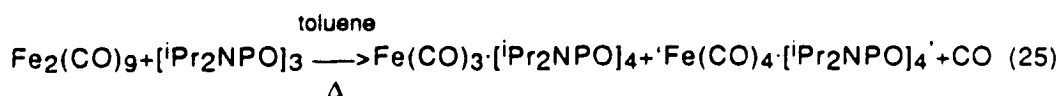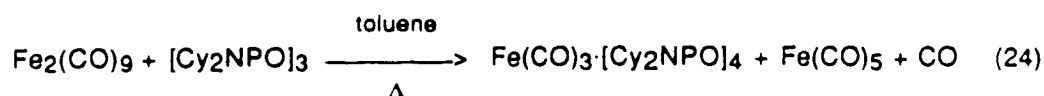
The coordination reaction of $Fe_2(CO)_9$ with $[Cy_2NPO]_3$ in refluxing toluene produced $Fe(CO)_3 \cdot [Cy_2NPO]_4$ (XXV) as a stable pale-yellow solid in about 12% yield. Its solution ^{31}P NMR spectrum shows a similar A_2MX splitting pattern to that of 1,5-coordinated cis-$Cr(CO)_4 \cdot [Cy_2NPO]_4$ (XXIV), with a chair-boat 1,5-coordination mode (Figure 1-1, C) for the tetraphosphoxane ring. The signal of two coordinated P's (A_2) appears at 163 ppm and uncoordinated P's at 125 ppm (M) and 131 ppm (X) respectively. The ^{13}C NMR spectrum in the CO region gives a multiplet at 218 ppm. The IR spectrum shows three CO stretching bands at 1995, 1926, and 1899 cm^{-1}.

The coordination reaction of $Fe_2(CO)_9$ with $[^iPr_2NPO]_3$ in refluxing toluene produced a 60:40 mixture of complexes, $Fe(CO)_3 \cdot [^iPr_2NPO]_4$ (XXVI) and $^\cdot Fe(CO)_4 \cdot [^iPr_2NPO]_4{}^\cdot$ (XXVII), as stable pale-yellow solids in about 20% combined yield. The two complexes could be separated by recrystallization from hot hexanes. The solution ^{31}P NMR spectrum of $Fe(CO)_3 \cdot [^iPr_2NPO]_4$ shows a similar A_2X_2 splitting pattern to that of 1,5-coordinate cis-$PdCl_2 \cdot [Cy_2NPO]_4$ with chemical shifts of two coordinated P's (A_2) at 160 ppm and two uncoordinated P's (X_2) at 145 ppm, suggesting a boat-boat 1,5-coordination mode (Figure 1-1, B) for the tetraphosphoxane ring. The ^{13}C NMR spectrum in the CO region contains a multiplet at 218 ppm. The IR spectrum shows three CO stretching bands at 1999, 1936, and 1908 cm^{-1}. The solution ^{31}P NMR spectrum of $^\cdot Fe(CO)_4 \cdot [^iPr_2NPO]_4{}^\cdot$ (XXVII) exhibits a distinctive AX_2Y splitting pattern, different from any previously known tetraphosphoxane complex.

31

Chemical shift of one coordinated P is at 152 ppm and two uncoordinated P's at 24 ppm, typical of phosphoryl P=O groups, and one uncoordinated P at 6 ppm. Most interestingly, a very large J_{XY} of 187 Hz is diagnostic of a direct P-P single bond coupling rather than a $^2J_{POP}$. Its ^{13}C NMR spectrum in the CO region gives one large doublet at 215.8 ppm ($^2J_{PC}$=15 Hz) and a small doublet at 215.0 ppm with $^2J_{PC}$=15 Hz. The IR spectrum shows four CO stretching bands at 2049, 1984, 1947, and 1933 cm^{-1}. Its X-ray crystal structure has been solved and will be discussed below. The solution ^{31}P NMR spectral data of all iron polyphosphoxane complexes are listed in Table 3. Figure 1-13 gives the solution ^{31}P NMR spectrum of (XXVII) and Figure 1-14 shows its unexpected X-ray crystal structure which turns out to be Fe(CO)$_4${$^iPr_2NP[OP(O)^iPr_2N]_2PN^iPr_2$}.

The coordinated P$_4$O$_4$ ring in iron complex (XXVII) is novel compared to the P$_4$O$_4$ rings in other metal tetraphosphoxane complexes. There is only one phosphorus coordinated to iron. Two phosphoruses (P2 and P4) have rearranged to P=O double bonds while one phosphorus (P3) now has two P-P bonds. The bond distances of Fe-P (2.18 Å), P-O (1.6 Å), P=O (1.45 Å), P-P (2.22 Å) and bond angles of OPO (98.3°), OPN (100.3°) are typical value by comparison with literature data.[20,21] Coordination geometry around Fe is pseudo-trigonal bipyramidal with a compressed P-Fe-C4 (axial) angle of 161.3°. This axial carbonyl is bent away from the PO ring. The bond angles of this carbon with other equatorial carbonyls are 97.1°, 87.3°, 88.9°. Bond angles (C-Fe-C) around the three equatorial carbonyls are 110.2°, 144.5°, and 105.3°. Spectroscopic data on this compound are in complete agreement with the structure. The proton-decoupled ^{31}P NMR spectrum exhibits an AX$_2$Y splitting pattern with the coordinated P at 152.2 ppm and uncoordinated P's at 24.5 ppm and 6.6 ppm respectively. Its IR spectrum exhibits strong CO stretching bands at 2049, 1984, and 1947 cm^{-1}.

32
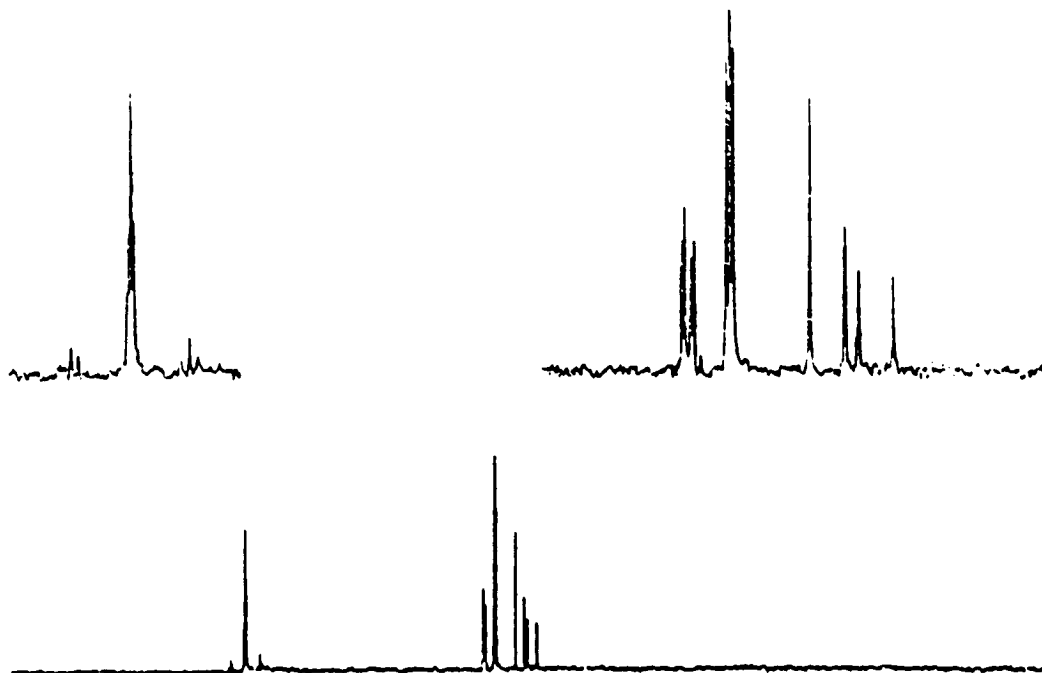
Figure 1-13: ^{31}P {^1H} NMR spectrum of 'Fe(CO)$_4$·[^{i}Pr$_2$NPO]$_4$' (XXVII)

7. Reactions to form Bimetallic Compounds:

$$Mo(CO)_4 \cdot NBD + NiBr_2 \cdot [R_2NPO]_4 \xrightarrow[90°C, (R=^iPr, Cy)]{toluene} Mo(CO)_4 \cdot [R_2NPO]_4 \cdot NiBr_2 + NBD \quad (26)$$

$$Mo(CO)_4 \cdot NBD + PdCl_2 \cdot [Cy_2NPO]_5 \xrightarrow[\Delta]{toluene} Mo(CO)_3 \cdot [Cy_2NPO]_5 \cdot PdCl_2 + CO + NBD \quad (27)$$

$$Mo(CO)_3 \cdot CHT + PdCl_2 \cdot [Cy_2NPO]_5 \xrightarrow[\Delta]{toluene} Mo(CO)_3 \cdot [Cy_2NPO]_5 \cdot PdCl_2 + CHT \quad (28)$$

$$Mo(CO)_4 \cdot NBD + Fe(CO)_3 \cdot [^iPr_2NPO]_4 \xrightarrow[\Delta]{hexanes} Mo(CO)_4 \cdot [^iPr_2NPO]_4 \cdot Fe(CO)_3 + NBD \quad (29)$$
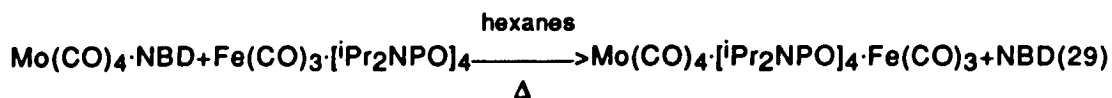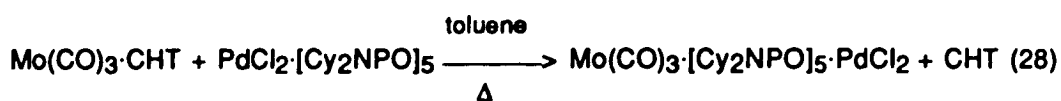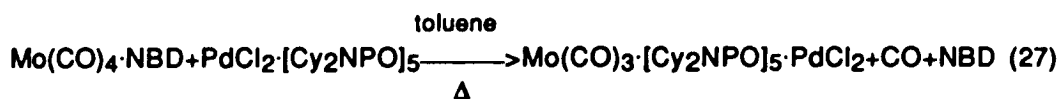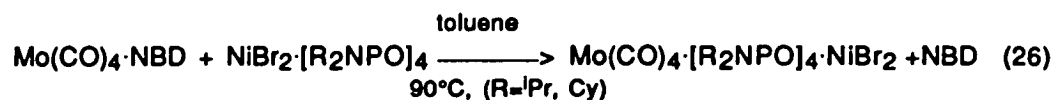
All bimetallic compounds were formed by combination of monometallic poly-phosphoxane complexes with molybdenum tetracarbonyl or tricarbonyl precursors. The reactions of Mo(CO)$_4$·NBD with NiBr$_2$·[Cy$_2$NPO]$_4$ in toluene at 90°C for about 3 h produced the bimetallic compound Mo(CO)$_4$·[Cy$_2$NPO]$_4$·NiBr$_2$ (XXVIII). The product

33
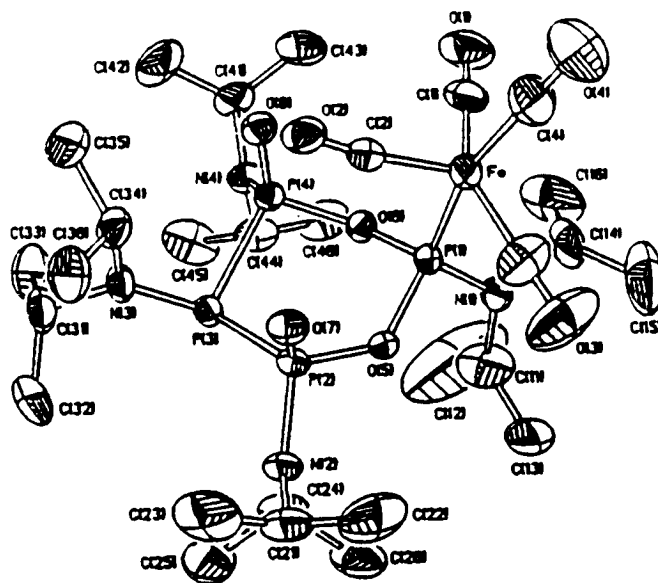
Selected bond distances and bond angles of $Fe(CO)_4\{^iPr_2NP[OP(O)^iPr_2N]_2PN^iPr_2\}$ (**XXVII**) in angstroms and degrees.

P1-Fe	2.189	P1-O5	1.627	P1-O6	1.635
P1-N1	1.644	P2-P3	2.234	P2-O5	1.641
P2-O7	1.451	P2-N2	1.640	P3-P4	2.227
P3-N3	1.673	P4-O6	1.628	P4-O8	1.456

P4-N4	1.640	Fe-C1	1.775	Fe-C2	1.821
Fe-C3	1.776	Fe-C4	1.763	C1-O1	1.145
C2-O2	1.131	C3-O3	1.139	C4-O4	1.150

P1-O5-Fe	118.0	P1-O6-Fe	115.9	P1-N1-O5	100.6
P1-N1-Fe	117.3	P1-O6-O5	98.3	P1-N1-O6	103.7
P2-O5-P3	102.2	P2-O7-P3	116.7	P2-N2-P3	106.6
P2-O7-O5	112.6	P2-N2-O5	104.3	P2-N2-O7	113.0

P3-P4-P2	99.3	P3-N3-P2	104.6	P3-N3-P4	104.8
P4-O6-P3	101.1	P4-O8-P3	116.5	C1-O1-Fe	179.1
C2-O2-Fe	172.1	C3-O3-Fe	179.3	C4-O4-Fe	179.5
P4-N4-P3	106.4				

Figure 1-14: X-ray crystal structure of $Fe(CO)_4 \cdot [^iPr_2NPO]_4$ (**XXVII**)

actually $Fe(CO)_4\{^iPr_2NP[OP(O)^iPr_2N]_2PN^iPr_2\}$

34

was isolated by eluting with 2.5% ethyl acetate/hexanes on an alumina column and precipitated from hot hexanes as a red solid in about 50% yield. The solution ^{31}P NMR spectrum of **XXVIII** (Figure 1-15) exhibits an AA'XX' splitting pattern with two doublets of doublets at 137.8 ppm and 60.71 ppm, respectively, (J=12 and 15 Hz). The ^{13}C NMR spectrum in the CO region contains a doublet of doublets at 215.6 ppm and two triplets at 208.7 and 207.7 ppm with coupling constant J=12 Hz. The IR spectrum shows CO stretching bands at 2022, 1945, 1928, and 1909 cm^{-1}. This compound decomposed upon heating or standing in solution over several days.
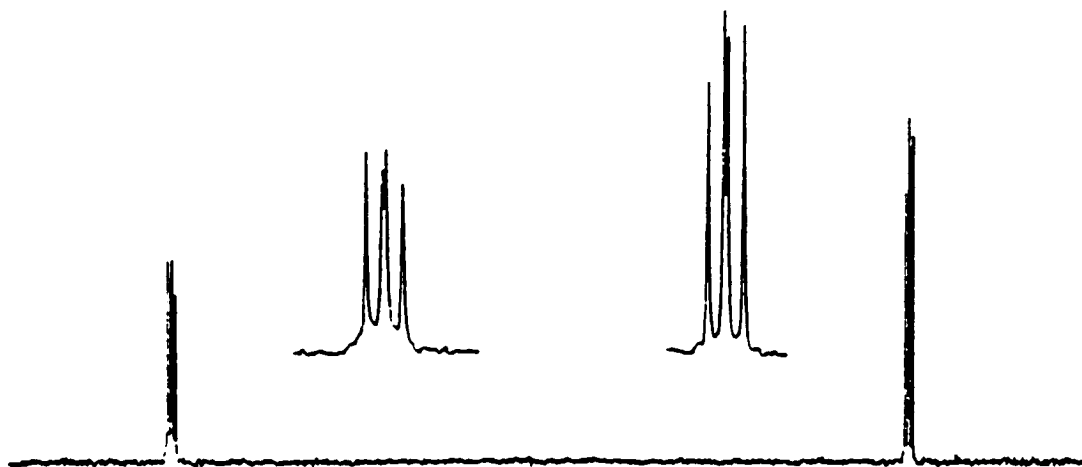
Figure 1-15: ^{31}P {^1H} NMR spectrum of Mo(CO)$_4$·[Cy$_2$NPO]$_4$·NiBr$_2$ (**XXVIII**)

The reaction of Mo(CO)$_4$·NBD with PdCl$_2$·[Cy$_2$NPO]$_5$ in refluxing toluene for 10 h produced the bimetallic compound Mo(CO)$_3$·[Cy$_2$NPO]$_5$·PdCl$_2$ (**XXIX**) with lost of CO from Mo(CO)$_4$. This product was isolated by eluting with 2.5% ethyl acetate/hexanes on an alumina column and precipitating from hot hexanes to give a brown solid in about 40% yield. The reaction of Mo(CO)$_3$·CHT with PdCl$_2$·[Cy$_2$NPO]$_5$ in refluxing toluene for about 10 h produced the same compound, which confirms fac-P$_3$ coordination at molybdenum. This compound was completely characterized by spectral analysis. Its solution ^{31}P NMR spectrum (Figure 1-16) exhibits an AA'MXX' pattern, suggesting retention of the original P$_5$O$_5$ ring. The ^{13}C NMR spectrum in the CO region gives two

35

doublet of triplets at 218.9 and 216.4 ppm with coupling constants J=39, and 12 Hz. The IR spectrum shows CO stretching bonds at 1979, 1912, and 1890 cm^{-1} indicative of the fac-Mo(CO)$_3$ moiety. Its proposed structure is shown in figure 1-17.

Figure 1-16: ^{31}P {^{1}H} NMR spectrum of Mo(CO)$_3$·[Cy$_2$NPO]$_5$·PdCl$_2$ (XXIX)
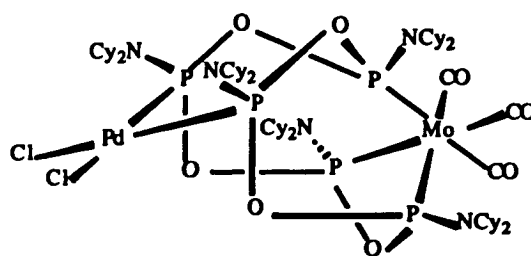
(XXIX)

Figure 1-17: Proposed structure of Mo(CO)$_3$·[Cy$_2$NPO]$_5$·PdCl$_2$ (XXIX)

The reaction of Mo(CO)$_4$·NBD with Fe(CO)$_3$·[^{i}Pr$_2$NPO]$_4$ in refluxing hexanes for 5 h

36

produced another bimetallic compound $Mo(CO)_4 \cdot [^iPr_2NPO]_4 \cdot Fe(CO)_3$ (**XXX**). This product was isolated by eluting with 0.5% ethyl acetate/hexanes through an alumina column and recrystallized from hot hexanes to give a pale-yellow crystalline solid in about 80% yield. Its solution ^{31}P NMR spectrum (Figure 1-18) exhibits an AB_2X splitting pattern. The ^{13}C NMR spectrum in the CO region gives five peaks at 219.2 (triplet, J=6 Hz), 218.8 (doublet, J=9 Hz), 216.7 (doublet, J=54 Hz), 211.0 (doublet of doublets, J=3, 9 Hz), and 207.5 ppm (quartet, J=9 Hz). The IR spectrum shows numerous CO stretching bonds at 2021, 1999, 1962, 1944, 1922, 1912, 1899, 1877, and 1869 cm^{-1}. X-ray quality crystals of this compound were obtained by recrystallization from hot hexane. The X-ray crystal structure is shown in Figure 1-19. Solution ^{31}P NMR spectra data of all bimetallic compounds are listed in Table 1-3.

The structure of bimetallic complex (**XXX**) was determined by a single-crystal X-ray study. The precursor to iron complex (**XXVII**) has the 1,5-chelate chair-chair conformation (mode B) with two uncoordinated P's bent toward iron. After reaction with $Mo(CO)_4 \cdot NBD$, only one phosphorus has coordinated with Mo. The iron center changed from five coordination to six coordination by forming a dative Fe->Mo bond with two P's in equatorial positions trans to two CO's and one CO trans to Mo in axial position. Molybdenum is still six-coordinate with the formation of these Mo-P and Mo-Fe bonds. The P-O distances of 1.66 Å and 1.62 Å, OPO bond angles of 96.1° and 99.9°, and POP bond angles of 127.0° and 119.5° are close to our other structural data (complexes VII and XVII). The Mo-P distance of 2.47Å is slightly shorter than Mo-P distance of 2.50 Å in the Mo cage structure.[5] The Fe-P distance of 2.25 Å, and Mo-Fe distance of 3.03 Å are in the normal range.[22] The coordination geometry around Mo is pseudo-octahedral with the Fe-Mo-C3 bond angle of 174.7°, Fe-Mo-P angle of 72.9°. The three carbonyls trans to P in equatorial position are tilted from the ring with cis C-Mo-C angles of

37

85.9° and 86.8°. The coordination geometry around Fe is also pseudo-octahedral with the C-Fe-Mo bond angle of 166.2° in an axial position. The two carbonyl trans to P's are twisted with Mo-Fe-C5 angle of 73.7°. The spectroscopic data are in agreement with this structure. The proton-decoupled ^{31}P NMR spectrum exhibits an AB_2X pattern with the three coordinated P's at 163.5 ppm and 160.5 ppm, uncoordinated P at 137.4 ppm. Its ^1H NMR spectrum show the expected three isopropyl methine peaks at 4.03 ppm, 3.87 ppm, and 3.63 ppm.

Figure 1-18: ^{31}P {^1H} NMR spectrum of $Mo(CO)_4 \cdot [^iPr_2NPO]_4 \cdot Fe(CO)_3$ (XXX)

8. Miscellaneous Reactions:

(a) $NiBr_2 \cdot [^iPr_2NPO]_4$ + 2 pyridine $\xrightarrow[\text{-20°C}]{\text{CDCl}_3}$ $NiBr_2 \cdot 2pyridine$ + $[^iPr_2NPO]_4$ (30)

$3/4[^iPr_2NPO]_4 \xrightarrow[\text{RT}]{\text{CDCl}_3} [^iPr_2NPO]_3$ (31)
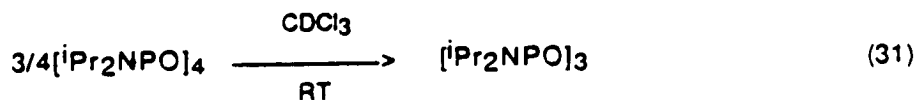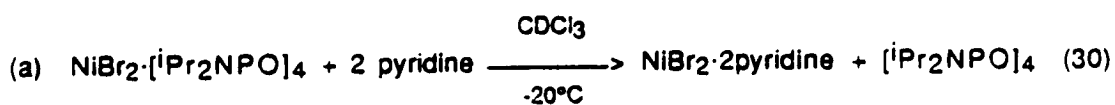
The coordinated tetraphosphoxane ring $[^iPr_2NPO]_4$ has been released by displacement with 2 equivalents of pyridine on the nickel bromide cyclotetra-phosphoxane complex $NiBr_2 \cdot [^iPr_2NPO]_4$ at -20°C in d-chloroform. The displacement was performed in a 10 mm NMR tube and monitored by ^{31}P NMR spectroscopy. The

38

Selected bond distances and bond angles of $Mo(CO)_4\cdot[^iPr_2NPO]_4\cdot Fe(CO)_3$ (**XXX**) in angstroms and degrees.

Mo-Fe	3.034(2)	Mo-C(1)	1.984(6)	Mo-C(3)	1.946(8)
Mo-C(2)	2.057(8)	Mo-C(4)	2.036(8)	Mo-P(1)	2.473(2)
Fe-P(2)	2.225(2)	Fe-P(4)	2.218(2)	Fe-C(5)	1.796(7)
Fe-C(6)	1.798(7)	Fe-C(7)	1.792(7)	P(1)-O(8)	1.663(4)

P(1)-O(11)	1.669(5)	P(1)-N(1)	1.604(4)	P(1)-N(1)	1.604(4)
P(2)-O(8)	1.621(4)	P(2)-O(9)	1.621(5)	P(2)-N(2)	1.645(5)
P(3)-O(9)	1.675(6)	P(3)-O(10)	1.658(4)	P(3)-N(3)	1.637(5)
P(4)-O(10)	1.621(5)	P(4)-O(11)	1.622(4)	P(4)-N(4)	1.651(5)

Fe-Mo-P(1)	72.9(1)	Fe-Mo-C(1)	94.8(2)
Fe-Mo-C(2)	97.5(3)	Fe-Mo-C(3)	174.7(2)
Fe-Mo-C(4)	95.0(3)	P(1)-Mo-C(1)	167.6(2)
P(1)-Mo-C(2)	96.0(2)	P(1)-Mo-C(3)	102.1(2)

P(1)-Mo-C(4)	93.7(2)	C(1)-Mo-C(2)	86.8(3)
C(1)-Mo-C(3)	90.1(3)	C(2)-Mo-C(3)	84.5(3)
C(2)-Mo-C(4)	166.0(4)	C(3)-Mo-C(4)	83.6(3)
Mo-Fe-P(2)	89.8(1)	Mo-Fe-P(4)	90.4(1)

Mo-Fe-C(5)	73.7(2)	Mo-Fe-C(6)	71.8(3)
Mo-Fe-C(7)	166.2(2)	P(2)-Fe-P(4)	83.0(1)
P(2)-Fe-C(5)	91.9(2)	P(4)-Fe-C(6)	90.6(2)
P(2)-Fe-C(6)	160.5(2)	P(4)-Fe-C(6)	90.6(2)
C(5)-Fe-C(6)	89.0(3)	P(2)-Fe-C(7)	100.0(2)
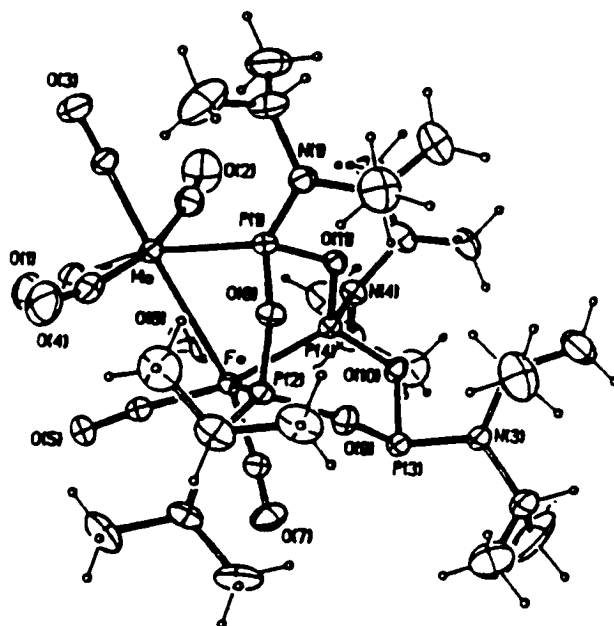
Figure 1-19: X-ray crystal structure of $Mo(CO)_4\cdot[^iPr_2NPO]_4\cdot Fe(CO)_3$ (**XXX**)

39

AA'XX' pattern at 144 and 55 ppm due to $NiBr_2 \cdot [^iPr_2NPO]_4$ disappeared and a singlet at 130.7 ppm due to free ligand $[^iPr_2NPO]_4$ appeared, suggesting either a static or averaged C_{4v} geometry for the uncomplexed ring $[^iPr_2NPO]_4$. This compound is stable at low temperature but irreversibly converts to the triphosphoxane heterocycle upon warming to room temperature. ^{31}P NMR monitoring showed the disappearance of this singlet at 130.7 ppm due to ring $[^iPr_2NPO]_4$ and emergence of an AB_2 pattern (139 ppm and 130 ppm) due to the $[^iPr_2NPO]_3$ ring.

$$\text{(b)} \quad NiBr_2 \cdot [Cy_2NPO]_4 + Fe_2(CO)_9 \xrightarrow[\text{90°C (R=}^iPr, Cy)]{\text{toluene}} Ni_2(CO)_4 \cdot [Cy_2NPO]_4 + FeBr_3 \quad (32)$$

$$NiBr_2 \cdot [Cy_2NPO]_4 + Fe(CO)_5 \xrightarrow[\text{90°C (R=}^iPr, Cy)]{\text{toluene}} Ni_2(CO)_4 \cdot [Cy_2NPO]_4 + FeBr_3 \quad (33)$$
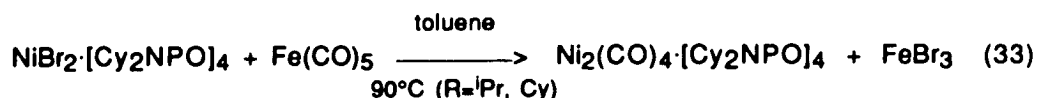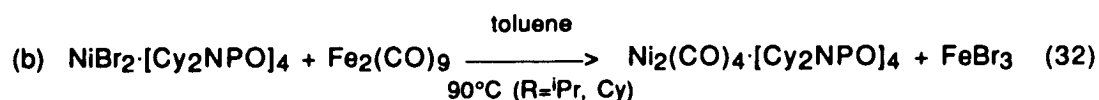
Reactions of the nickel bromide cyclotetraphosphoxane complex with diiron nona-carbonyl or iron pentacarbonyl in toluene at 90°C produced dinickel tetracarbonyl cyclotetraphosphoxane cage compounds (**XXXI**). The product was isolated by eluting with 2.5% ethyl acetate/hexanes through an alumina column which was evaperated to give a white solid in about 17% yield. Solution ^{31}P NMR spectrum of **XXXI** shows a singlet at 133.8 ppm. Its ^{13}C NMR spectrum in the CO region gives a triplet at 198 ppm with J=2 Hz and other ^{13}C peaks in methine and methylene regions consistent with that of the known molybdenum cage.[5] Its ^1H NMR spectrum shows a broad peak at 3.38 for methine protons and multiplet for methylene protons. The IR spectrum shows two CO stretching bands at 2000 and 1947 cm^{-1}. The proposed structure is shown in Figure 1-20. This cage complex decomposed slightly upon standing for several weeks.

40

R=Cy.   (XXXI)
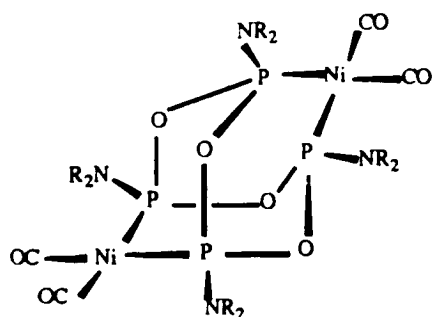
Figure 1-20: Proposed structure of nickel cage (XXXI)

(c) $NiBr_2 \cdot [Cy_2NPO]_4 + PdBr_2 \cdot 2PhCN \xrightarrow[4°C]{toluene} PdBr_2 \cdot [Cy_2NPO]_4 + NiBr_2 \cdot 2PhCN$ (34)

$NiBr_2 \cdot [Cy_2NPO]_4 + PdBr_2 \cdot 2PhCN \xrightarrow[90°C]{toluene} PdBr_2 \cdot [Cy_2NPO]_5 + NiBr_2 \cdot 2PhCN$ (35)
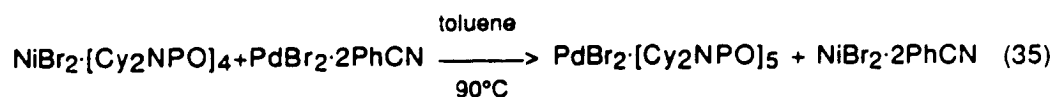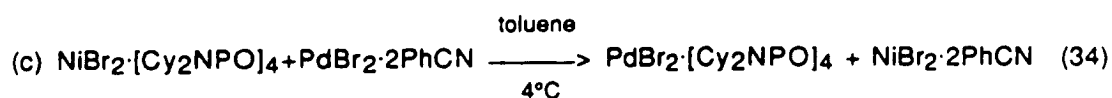
A polyphosphoxane ring transfer reaction occurred when the nickel bromide tetra-phosphoxane complex was mixed with palladium bromide containing labile ligands in toluene.   At 4°C after 2 days, the tetraphosphoxane ring has transferred from nickel to palladium. The AA'XX' pattern of the ^{31}P NMR spectrum at 144 ppm and 55 ppm due to $NiBr_2 \cdot [Cy_2NPO]_4$ disappeared and the A_2X_2 pattern at 144 ppm and 88 ppm due to $PdBr_2 \cdot [Cy_2NPO]_4$ had emerged. At 90°C after 8 hrs, the nickel complex had lost its tetraphosphoxane ring while palladium bromide has coordinated the built up penta-phosphoxane ring. An AA'MXX' pattern at 143 ppm, 127 ppm and 87 ppm due to $PdBr_2 \cdot [Cy_2NPO]_5$ emerged.

(d) $NiBr_2 \cdot [Cy_2NPO]_4 + PtCl_2 \cdot NBD \xrightarrow[4°C]{toluene} PtCl_2 \cdot [Cy_2NPO]_4 + NiBr_2 + NBD$ (36)

$NiBr_2 \cdot [Cy_2NPO]_4 + PtCl_2 \cdot NBD \xrightarrow[90°C]{toluene} PtCl_2 \cdot [Cy_2NPO]_5 + NiBr_2 + NBD$ (37)

41
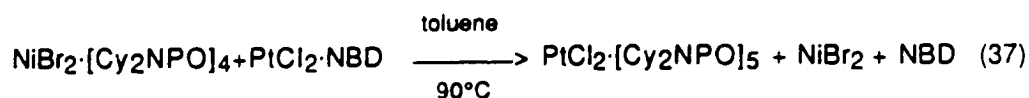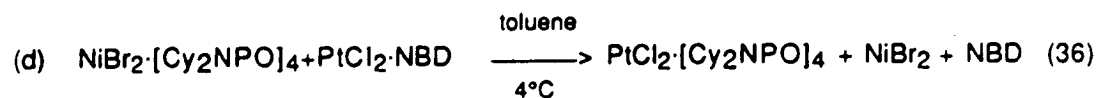
The reaction of nickel bromide tetraphosphoxane with platinum chloride containing labile ligands in toluene at high temperature produced the same results as that of the palladium compound forming the platinum chloride pentaphosphoxane complex. Its solution ^{31}P NMR spectrum exhibited an AA'MXX' pattern for the 1,7-coordinated P_5O_5 ring. At room temperature, the 1,5-coordinated platinum P_4O_4 ring complex was formed with a A_2X_2 pattern at 144 ppm and 88 ppm for 1,5-coordinated $PtCl_2 \cdot [Cy2NPO]_4$. Both are identical to previously described direct substitution products by triphosphoxane rings at a Pt metal center. At low temperatures, however, the 1,3-coordinated platinum P_4O_4 complex was formed. Its AA'XX' pattern (Figure 1-21) at 142.6 ppm for uncoordinated P_A's and 24.6 ppm for coordinated P_X's with $\delta_{AX}=24.4$ Hz, $\delta_{A'X'}=29.3$ Hz and $J_{Pt-P}=4995$ Hz was due to a 1,3-coordinated $PtCl_2 \cdot [Cy2NPO]_4$ (Figure 1-1, A). This complex was too unstable to be isolated and was only detected by solution ^{31}P NMR spectroscopy. It seems that this complex was the result of direct metal ion exchange from Ni(II) to Pt(II) without changing P_4O_4 ring skeleton or coordination mode.
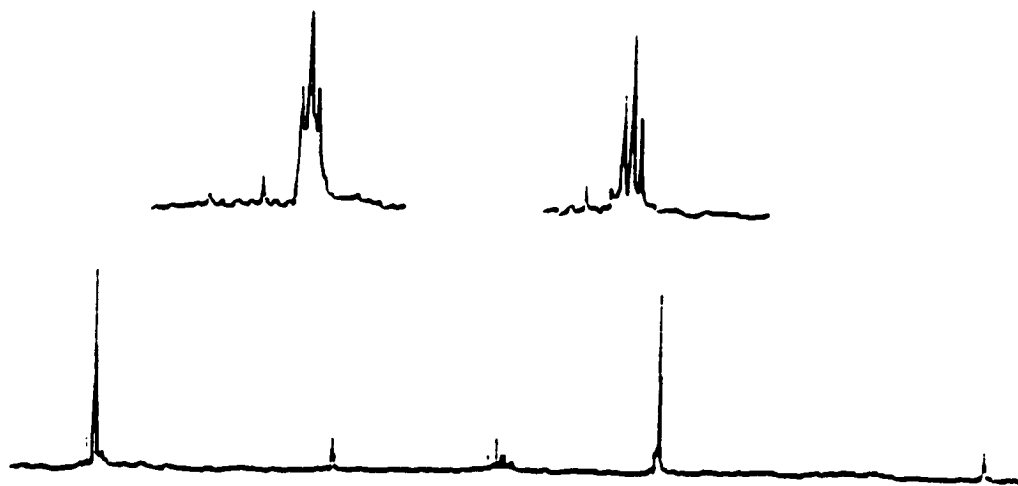
Figure 1-21: ^{31}P {^1H} NMR spectrum of 1,3-chelated $PtCl_2 \cdot [Cy2NPO]_4$

42

(e) $PdCl_2 \cdot [Cy_2NPO]_5 + NiBr_2 \cdot DME \xrightarrow[90°C]{\text{toluene}} PdClBr \cdot [Cy_2NPO]_5 + NiClBr \cdot DME$ (38)
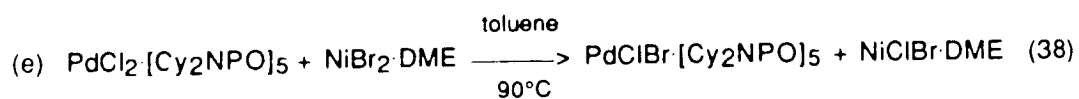
The reaction of $PdCl_2 \cdot [Cy_2NPO]_5$ with $NiBr_2 \cdot DME$ in toluene at 90°C for 12 h produced the only mixed palladium chloride bromide pentaphosphoxane complex (**XXXII**) isolated. The halides transferred between the two metal centers and the product was isolated as a pale-yellow solid in about 52% yield. Its solution ^{31}P NMR spectrum shows an AA'MXX' splitting pattern at 143ppm, 127ppm and 88ppm (figure 1-22).
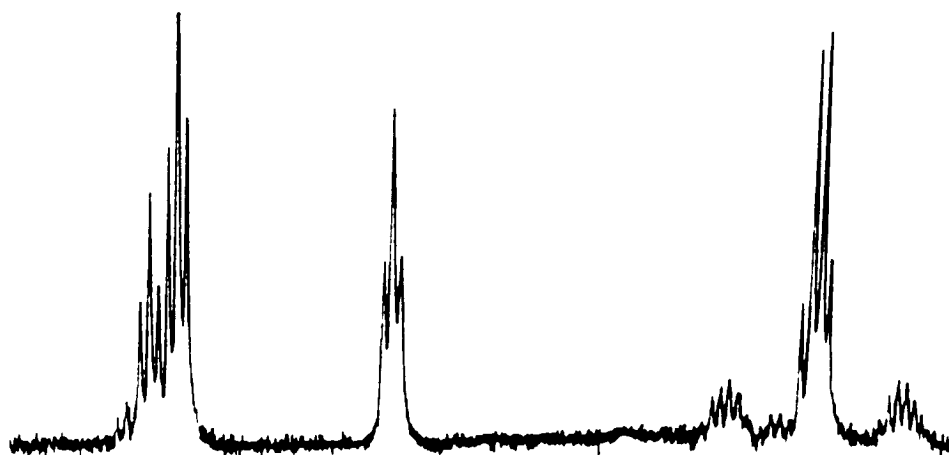
Figure 1-22: ^{31}P {^1H} NMR spectrum of PdClBr·[Cy$_2$NPO]$_5$ (**XXXII**).

(f) $[^sBu_2NPO]_3 + PdBr_2 \cdot 2PhCN \xrightarrow[\Delta]{\text{hexanes}} PdBr_2 \cdot [^sBu_2NPO]_4 + 2PhCN$ (39)

$[(^iPr)(Cy)NPO]_3 + PdBr_2 \cdot 2PhCN \xrightarrow[\Delta]{\text{hexanes}} PdBr_2 \cdot [(^iPr)(Cy)NPO]_4 + 2PhCN$ (40)

$[Ph_2NPO]_3 + NiBr_2 \cdot DME \xrightarrow[\Delta]{\text{hexanes}} NiBr_2 \cdot [Ph_2NPO]_5 + DME$ (41)
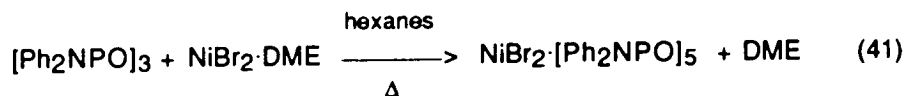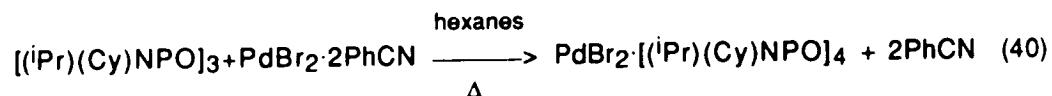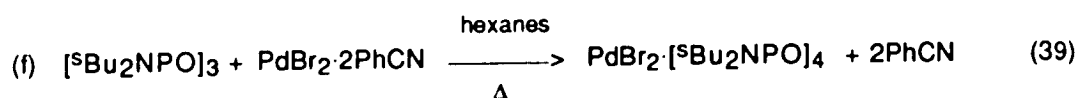
Reactions of other triphosphoxane rings with metal complexes have been tried as shown in equations (39), (40) and (41). The 1,5-coordinated cis-PdBr$_2 \cdot [^sBu_2NPO]_4$

43

(XXXIII) was produced by reaction of Ring 3 [$^sBu_2NPO]_3$ with palladium bromide in refluxing hexanes or at room temperature for 8 hrs. The product was isolated as an unstable pale-yellow solid in about 51% yield. Its solution ^{31}P NMR spectrum exhibits an AA'XX' pattern with chemical shifts for the two coordinated P's at 145.9 ppm and two uncoordinated P's at 87.7 ppm. Another reaction of Ring 5 [($^iPr)(Cy)NPO]_3$ with palladium bromide in refluxing hexanes or at room temperature for 8 hrs gave a similar result. The 1,5-coordinated cis-PdBr$_2\cdot$[($^iPr)(Cy)NPO]_4$ (XXXIV) was also isolated as an unstable white solid in about 35% yield. It has an A_2X_2 pattern in its solution ^{31}P NMR spectrum with chemical shifts for the two coordinated P's at 144.5 ppm and two uncoordinated P's at 88.1 ppm (J=58 Hz) similar to that of complexes (VIII) and (X). The reaction of Ring 4, [Ph$_2$NPO]$_3$, with NiBr$_2\cdot$DME as in equation (33) in a hot mixture of toluene and hexane for 2 hrs gave complex (XXXV), NiBr$_2\cdot$[Ph$_2$NPO]$_5$, as a red unstable solid in about 40% yield. Its ^{31}P NMR spectrum at room temperature exhibits a AA'MXX' splitting pattern with a broad peak at 124 ppm for two uncoordinated P_A's, a sharp singlet at 114 ppm for another uncoordinated P_M, and a broad peak at 84 ppm for two coordinated P_X's similar to that of complex (VI). This compound decomposed during purification.

(g)   [Cy$_2$NPO]$_3$ + (excess) S $\xrightarrow[\text{RT}]{\text{hexanes}}$ [Cy$_2$NPO]$_3$S$_2$ (42)
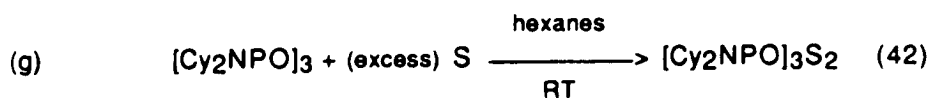
The triphosphoxane ring can be easily sulfurized by excess elemental sulfur in hexanes at room temperature. The product cyclotriphosphoxane disulfide (XXXVI) was isolated as an unstable and foul-smelling white solid in about 80% yield. Its solution ^{31}P NMR spectrum exhibits a second-order splitting pattern with a P=S resonance shifted upfield to 50.2 ppm. Its proposed structure and 31P NMR spectrum are in

44

Figure 1-23. The solution ^{31}P NMR spectral data of all products from the miscellaneous reactions are also listed in Table 1-3.

a)

(XXXVI)

b)
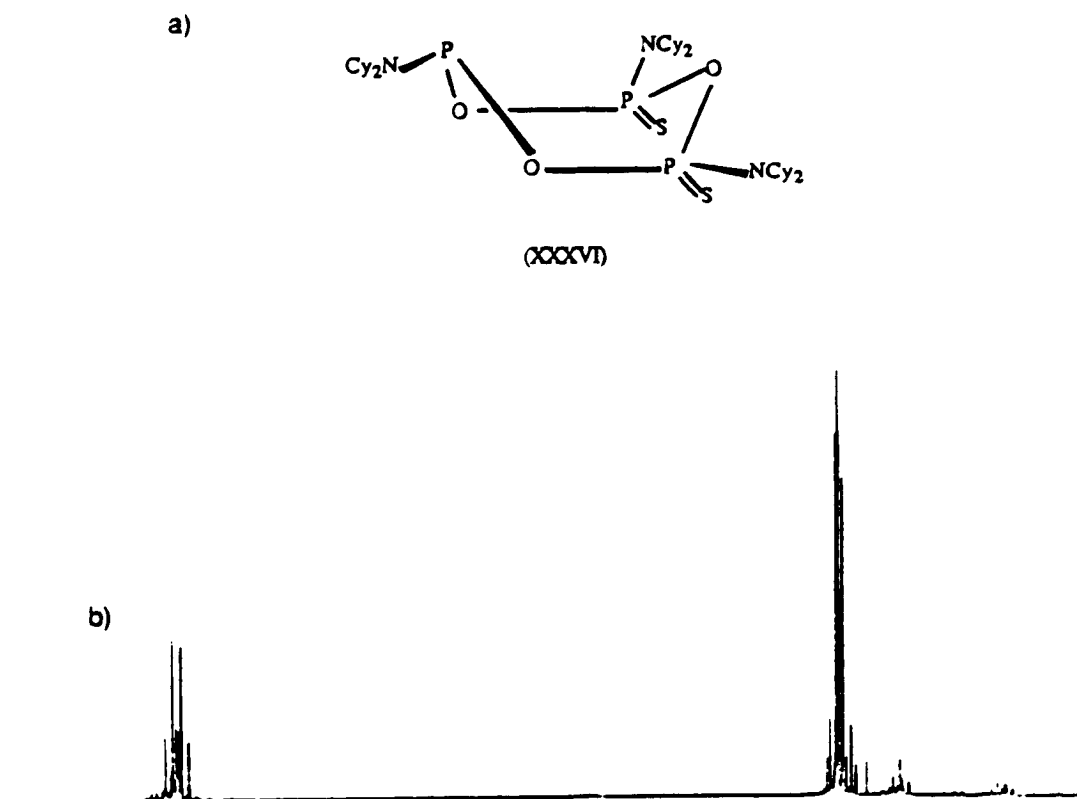
Figure 1-23: a) Proposed structure of compound (XXXVI).
b) ^{31}P (^{1}H) NMR spectrum of this compound.

Numerous other reactions have also been attempted. No reaction occurred when NiBr$_2$·[Cy$_2$NPO]$_4$ was mixed with NiBr$_2$·DME or NiCl$_2$·DME, or when PdCl$_2$·[Cy$_2$NPO]$_5$ was mixed with NiCl$_2$·DME or PdCl$_2$·2PhCN in hexanes or toluene at room temperature or refluxing solvents. The reactions of other metal complexes, such as Ni(CO)$_2$(PPh$_3$)$_2$, Cu[CH$_3$CN]$_4$BF$_4$ and Ru(DMSO)$_4$Cl$_2$, with triphosphoxane rings gave only unstable and ill-characterized products.

45

DISCUSSION:

(A) NMR and IR Spectra:

The single most useful method for structural analyses of the complexes described in this work is proton-decoupled ^{31}P NMR spectroscopy. The large chemical shift range, reduced number of resonances, and sensitivity of both chemical shift and coupling constant to structural changes, as compared with ^1H NMR, often allow direct structure determination.

In the ^{31}P NMR spectra of all our metal polyphosphoxane complexes, the chemical shifts and coupling constants vary depanding on metal coordination, as well as lone pair orientations of uncoordinated P's. Chemical shifts of uncoordinated phosphoruses of parent rings range from 122 ppm to 140 ppm (Table 1-2). In polyphosphoxane complexes, chemical shifts of coordinated phosphoruses changed predictably with new ring sizes, coordinated metals, and ancillary ligands. By contrast, the chemical shifts of uncoordinated phosphoruses stay almost unchanged. Generally, divalent metal ion coordination produces upfield shifts ranging up to 54 ppm in the Ni complex (III) and to 91 ppm in the Pd complex (XIII). Zero-valent metals, by contrast, give down-field coordination shifts down to 136 ppm in the Mo complex (XIX) and to 177 ppm in the Cr complex (XXIV). Slight changes of chemical shifts also appear in complexes with same metal ion but with different halide or P_nO_n ring sizes. For example, chemical shift of the coordinated phosphoruses in NiP_4O_4 chloride complex (III) is 54 ppm, changing to 62 ppm in the bromide complex (IV) and 75 ppm in the iodide complex (V). A shift to 91 ppm was observed in the P_5O_5 Ni chloride complex (VI).

The unique splitting patterns and coupling constants between phosphoruses also give a wealth of information for structural assignment. Generally, P's with lone pairs

46

pointing away from metal centers have only a small up-field shift with decreased $^2J_{POP}$ coupling constants with the coordinated P's. On the other hand, uncoordinated P's with lone pairs pointing toward the metal center have down-field shifts and large couplings with coordinated P's. For example, the A_2X_2 splitting pattern with a large coupling constant of from 39 Hz to 88 Hz can be assigned to the 1,5-chelate chair-chair coordination mode (Figure 1-1, B) with lone pairs of two uncoordinated P's pointed toward the metal. The A_2MX splitting pattern with a large coupling between A and M (lone pair of M toward metal) and a small coupling between M and X, as well as A and X (lone pair of X away from metal) can be assigned to the chair (large coupling)-boat (small coupling) coordination mode (Figure 1-1, C). An AA'XX' splitting pattern with $J_{AX} \neq J_{AX'}$ for the Ni complexes (I) to (V) can be assigned to a 1,3-chelate mode (Figure 1-1, A) with lone pairs of AA' toward the metal.

The AA'MXX" splitting pattern with a large J_{AX} and a small J_{MX}, J_{AM} as seen in the complexes (XI), (XII), (XV), and (XXXII) can be assigned to a P_5O_5 ring complex. In these structures, the P_M's bent away from metal with lone pairs pointed away and have upfield shifts of around 127 ppm, while P_A's have lone pairs pointed toward the metal with a downfield shift of around 142 ppm. The chemical shift of coordinated P_X's vary depanding upon the metal. For example, P_X in NiP_5O_5 is at 91 ppm, PdP_5O_5 at 87 ppm, while PtP_5O_5 at 60 ppm. The complex (XIII) [isomer B] displayed an AA'MXX' splitting pattern also, but with significantly different J_{PP}'s. Only slight chemical shift changes compared to complex (XII) [isomer A] indicate that the coordination mode and the ring size are similar. The large coupling of 63 Hz between M and X indicates that the lone pair of M should point toward the metal opposite to that in isomer A. However, the very small J_{AM} and J_{AX} show that the lone pairs of the two A's may point away from the metal in a boat form. From this analysis, this complex may be assigned the proposed structure of complex (XIII) in Figure 1-6. In the platinum complexes, coupling between ^{195}Pt

47

(natural abundance=33.8%, spin=1/2) and coordinated P's also appeared. This coupling gives satellite peaks symmetrically distributed about the main signal. These coupling constants are around 5000 Hz, typical of platinum (II) phosphine complexes.[22]

In bimetallic complex (XXX), the coordinated phosphoruses shifts remain unchanged but the chemical shifts of uncoordinated P's in (XI) at 143 ppm and 127 ppm are now shifted down-field to 157 ppm and 137 ppm due to coordination to $Mo(CO)_4$. The AM_2X_2 splitting pattern shows large $^2J_{PMoP}$ couplings between the three P's coordinated with Mo and small $^2J_{P-O-P}$ between A and X due to A being bent away from Pd in the boat form. In addition, the almost zero coupling between M and X is due to the M's bending away from Pd.

The AXY splitting pattern in the P_3O_3 disulfide compound (XXXVI) has two multiplets due to the twisted asymmetric P_3O_3 ring backbone. The multiplet at 134 ppm is due to the unreacted phosphorus which is in the bow position of the original ring. The other multiplets at 50 ppm and 49 ppm are due to the two sulfurized P's which were equivalent in the original ring. These chemical shifts are in the normal range for phosphorus sulfides.[23]

Complexes (XVIII) and (XIX) both displayed A_2X spectra consistent with proposed structures featuring a symmetrically-coordinated P_3O_3 ring in either the boat or chair conformation. A coordination shift of only +7 ppm is consistent with the upfield ring contribution due to the formation of a four-membered chelate ring.[24] The chair form is likely since the upfield shift of the free P_X from 140 ppm to 130 ppm upon coordination can be a result of the P_3O_3 ring flipping into a chair conformation. This will relieve the postulated transannular P-O interaction in the boat form of the parent heterocycle, causing an upfield shift for this nucleus.[2]

48

Proton NMR spectra of the complexes with diisopropylamino-groups displayed the isopropyl methine groups as septets or broad peaks in the 3.5-4.2 ppm region and methyl groups as doublets in the 1.1-1.4 ppm region with $^3J_{H-H}$ couplings of 6-7 Hz. Complexes with dicyclohexylamino groups displayed the cyclohexyl methine groups as broad resonances in the 2.7-4.1 ppm region and methylene groups as multiplets in the 0.7-2.2 ppm region.

The ^{13}C NMR data of complexes with diisopropylamino groups have the isopropyl methyl carbons in the 19-26 ppm region and methine carbons in the 45-56 ppm region. Complexes with dicyclohexylamino groups displayed cyclohexyl methylene carbons in the 21-38 ppm and methine carbons in the 52-59 ppm region. The methine carbons typically have $^2J_{C-P}$ couplings of 6-9 Hz.

These methine proton and methine carbon NMR spectra are useful in assisting structural assignments. For example, the methine proton and carbon NMR spectra of the P_4O_4 complexes with A_2X_2 or $AA'XX'$ splitting patterns in their ^{31}P NMR spectra exhibit two sets of peaks each, consistent with two different kinds of phosphoruses. The P_5O_5 complexes displayed methine proton and carbon NMR spectra having three sets of peaks consistent with the presence of three different kinds of phosphoruses.

The ^{13}C NMR spectra of complex (XXVII) exhibited two broad peaks in the methine ^{13}C region and two other broad peaks in the methyl region at room temperature which sharpened and resolved into doublets at lower temperature (-10°C) (Figure 1-24). These ^{13}C resonances have been assigned to methine carbons C11 and C14 and methyl carbons C12, C13, C15, and C16 of the diisopropylamino group on the same phosphorus coordinated to iron tetracarbonyl (Figure 1-25). Sharp resonances could be caused by inhibition of the P-N bond rotation. At low temperature (-10°C), all groups are rigid.

49

Rotation about the P-N bond is inhibited by the bulky iron tetracarbonyl unit. C11 and C14 give rise to two sharp doublets at $\delta=44.6$ ppm ($^2J_{PNC}=26.9$ Hz) and $\delta=56.9$ ppm ($^2J_{PNC}=10.5$ Hz). For the same reason, C12 and C13 will also give a sharp doublet at $\delta=26.4$ ppm ($^3J_{PNCC}=10.5$ Hz), and C15 and C16 give a sharp peak at $\delta=22.9$ ppm. At room temperature, the slow exchange between those carbons occured through slow P-N bond rotation to give broad ^{13}C peaks.

25°C

*

*

*

*

- 10°C

*

*

*

*

*

| 58 | 54 | 50 | 46 | 42 | 38 | 34 | 30 | 26 | 22 |
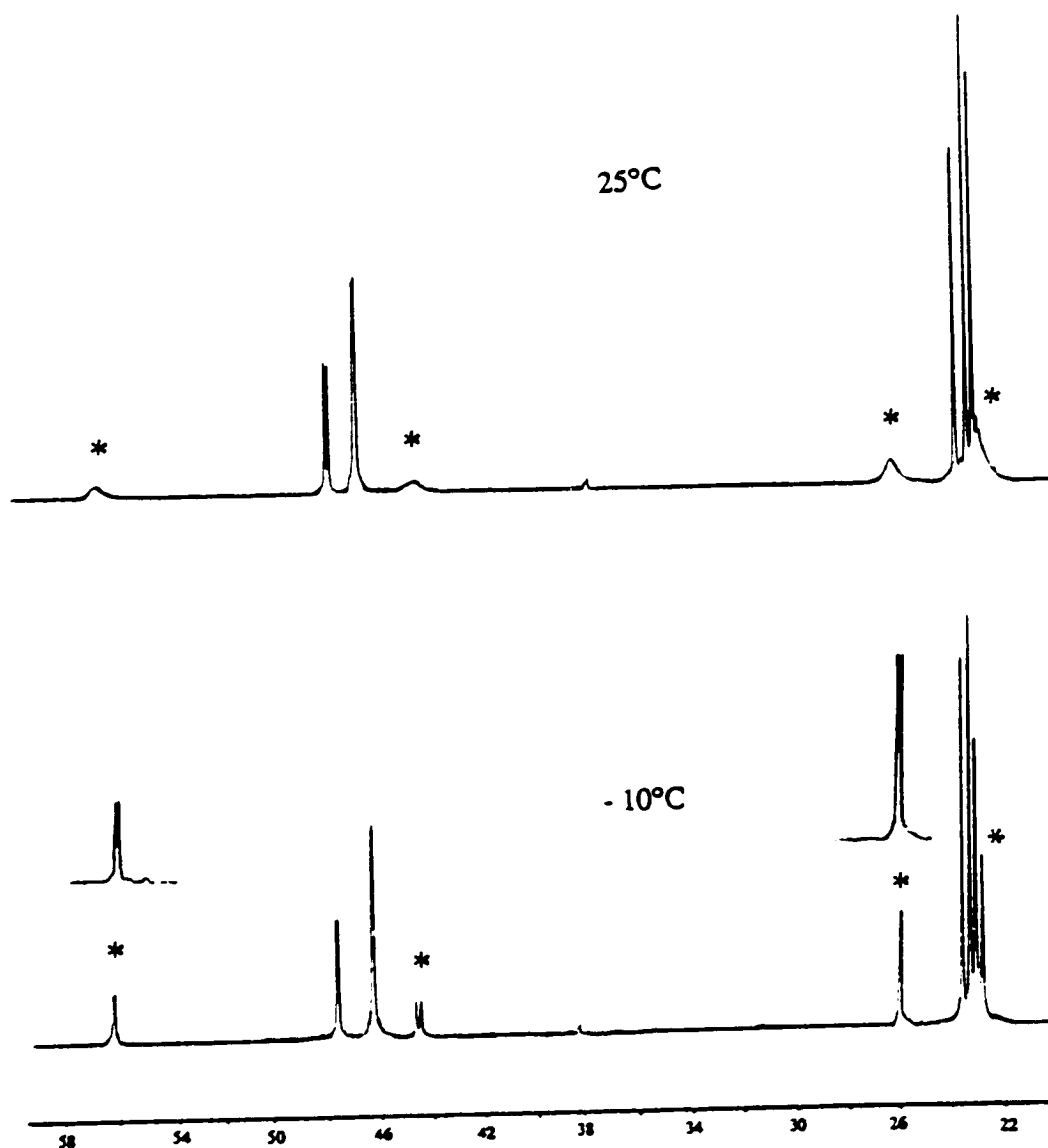
Figure 1-24: ^{13}C (^1H) NMR spectra of complex (XXVII) at different temperature.

50
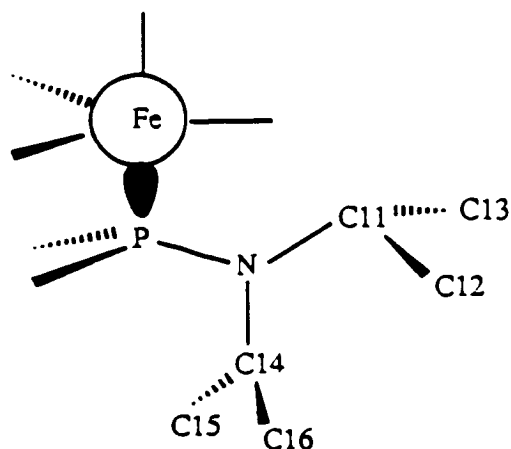
Figure 1-25: Illustration of rotation barrier of P-N bond.

Carbonyl ^{13}C NMR spectra are also useful in assigning coordination structure. For example, complex (XXIV) displayed carbonyl triplets at 226.0 ppm, 219.4 ppm, and 219.0 ppm with $^2J_{C-P}$ couplings of 20 Hz. The first triplet can be readily assigned to the two CO groups trans to the P ligands, and other two are axial CO's, one to the P in boat position and another to a P in chair position. In complex (XXX), carbonyl NMR exhibits two doublet of triplets at 218.9 ppm and 216.4 ppm with $^2J_{C-P}$ couplings of 39 and 13 Hz. The large doublet of triplets is due to two CO groups in equatorial positions trans to the two P's and cis to one P. The small doublet of triplets is the CO group in axial position trans to one P ligand and cis to two P's. Figure 1-26 shows the carbonyl carbon NMR spectra of complexes (XXIV) and (XXIX).

a)

51

b)
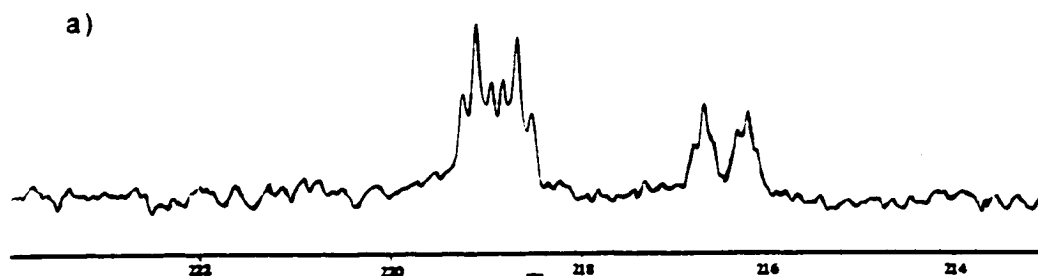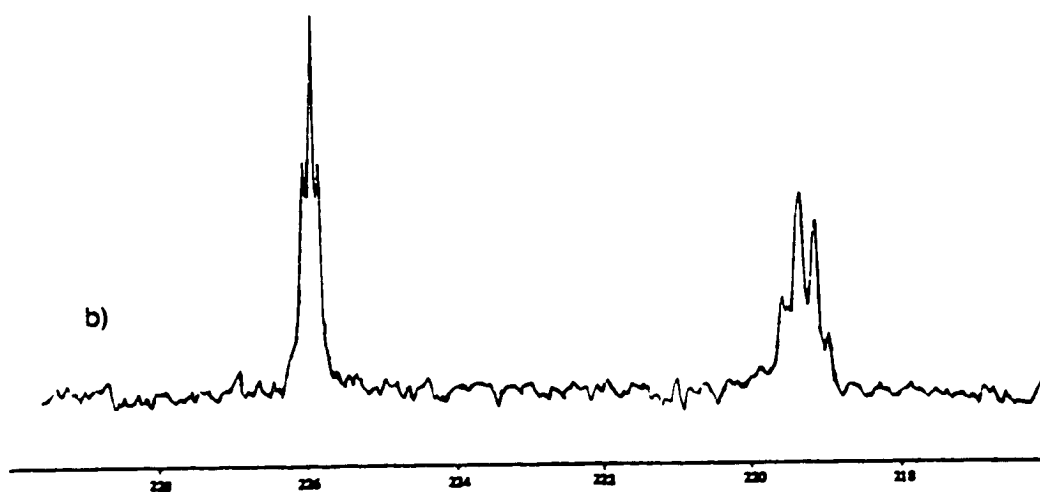
Figure 1-26: a) Carbonyl ^{13}C NMR spectrum of Mo(CO)$_3$[Cy$_2$NPO]$_5$PdCl$_2$ (**XXIX**)

b) Carbonyl ^{13}C NMR spectrum of Cr(CO)$_4$[Cy$_2$NPO]$_4$ (**XXIV**)

The infrared spectra of complexes provide different P-O-P stretching bands among different coordination modes of P$_4$O$_4$ rings and P$_5$O$_5$ rings. Generally, P$_4$O$_4$ ring complexes show strong P-O-P bond stretching around 900 cm^{-1}, and P$_5$O$_5$ ring complexes show strong P-O-P bond stretching around 869 cm^{-1}. The different P-O-P stretching in different ring complexes is shown in Figure 1-27. The carbonyl stretching in complexes containing metal carbonyls are most useful in the determination of molecular symmetry. They are observed in a region free of most other bands and are very intense absorptions. For consideration of complex (**XXV**), there are two possibilities of iron coordination, which can have either C$_{2v}$ or C$_S$ symmetry. With C$_{2v}$ symmetry, two coordinated P's occupy the equatorial positions. There should be two allowed CO stretching bands (see Scheme 1). In C$_S$ symmetry, the two P's occupy inequivalent sites. One is equatorial, the other axial. There should then be three stretching bands. Only the C$_S$ symmetry is consistent with the experimental spectrum. The Mo center in complex (**XXVIII**) has C$_{2v}$ symmetry. The expected four CO stretching bands are in accordance with experimental results. Complex (**XXX**) contains a six-

52

coordinated molybdenum with three fac-P's and three fac-CO groups can be a symmetrical structure with C_{3v} symmetry or unsymmetrical structure with C_s symmetry. The former predicts two CO stretching bands and the latter three. Most likely, the structure is near C_{3v} symmetry as the fine-structure in the 1912-1890 cm^{-1} region may be due to the intrermolecular vibrational coupling or pressure-

a) P-O-P stretching bands in $NiBr_2[^iPr_2NPO]_4$ (II)
b) P-O-P stretching bands in $PdBr_2[^iPr_2NPO]_4$ (VII)
c) P-O-P stretching bands in $PdBr_2[Cy_2NPO]_5$ (XII)
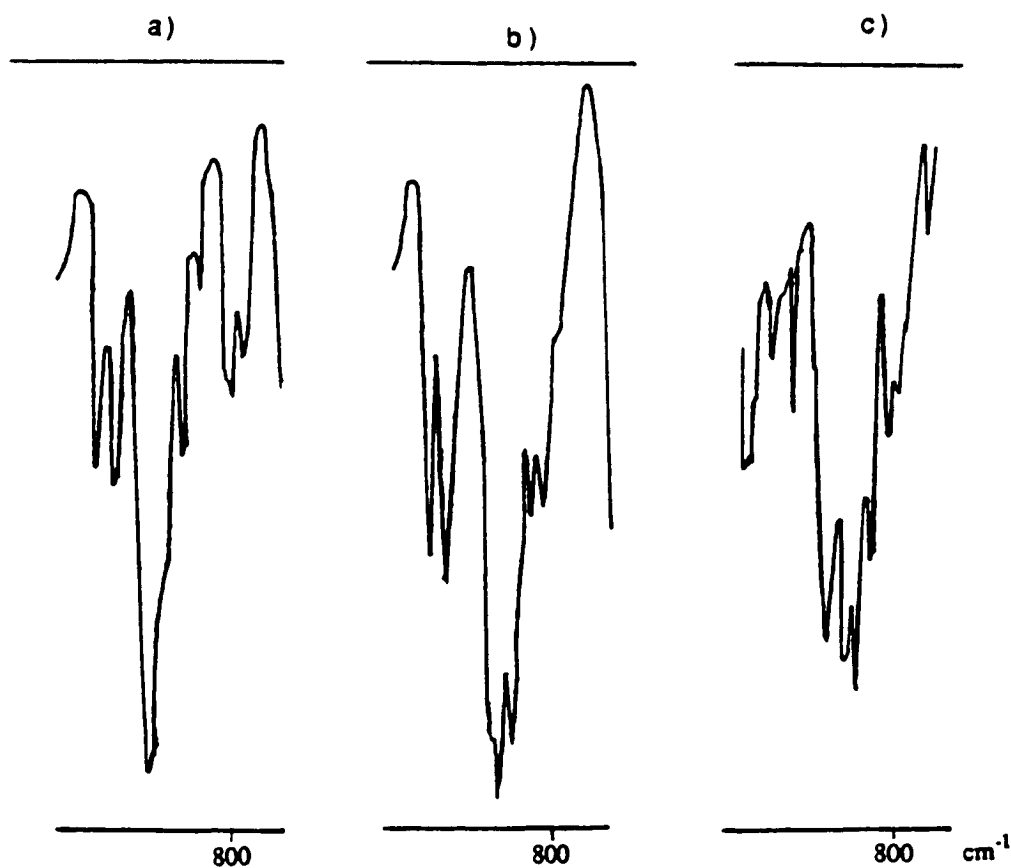
Figure 1-27: IR spectra of $NiBr_2[^iPr_2NPO]_4$ (II), $PdBr_2[^iPr_2NPO]_4$ (VII) $PdBr_2[Cy_2NPO]_5$ (XII) in P-O-P stretching region.

53

SCHEME 1

a) C_{2v}
two bands
expected

a_1 b_1

C_s
three bands
expected

$a'_{(1)}$ $a'_{(2)}$ a''
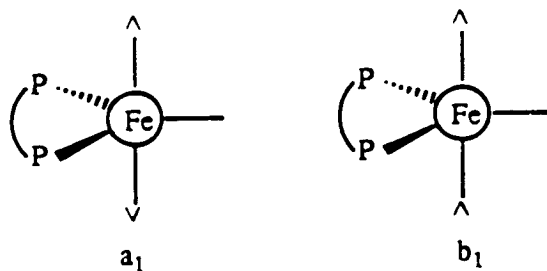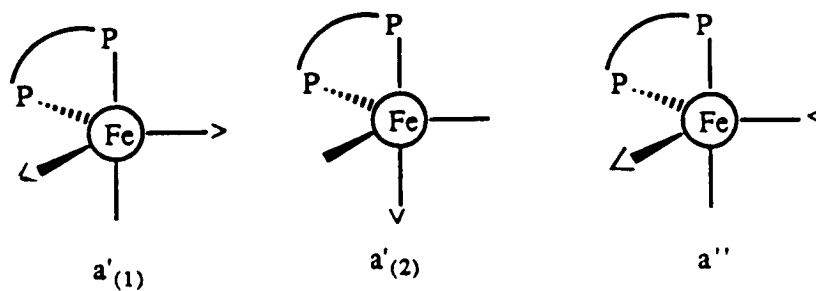
b) C_{2v}
four bands
expected

$a_{1\,(1)}$ $a_{1\,(2)}$

b_1 b_2

54
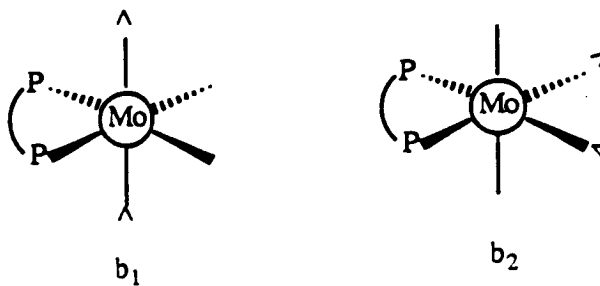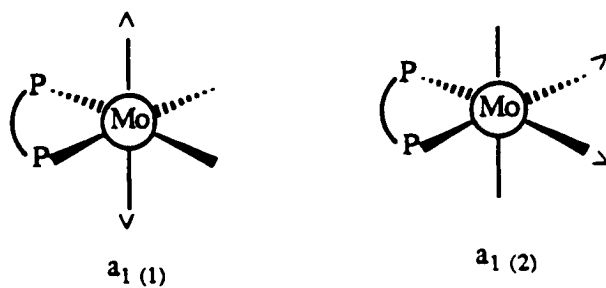
SCHEME 1 (continued)

c) C_{3v}
two bands
expected

a_1

e

C_s
three bands
expected

a''

$a'_{(1)}$

$a'_{(2)}$

55
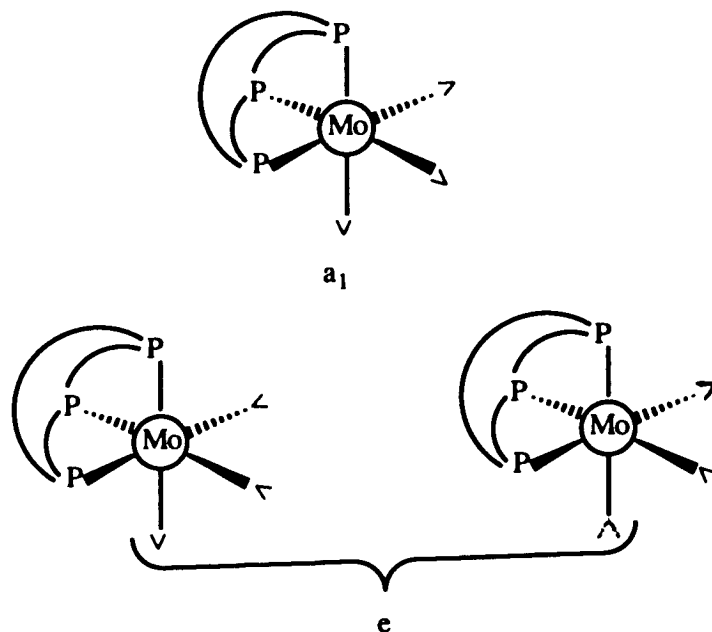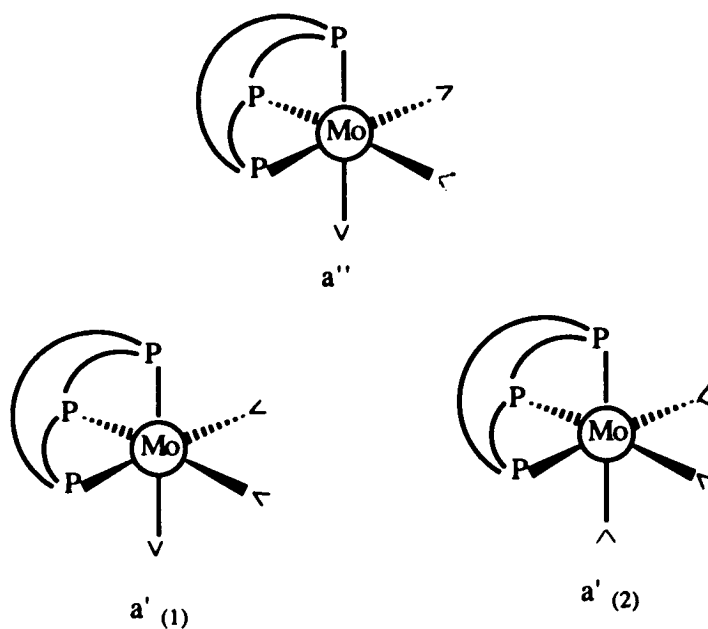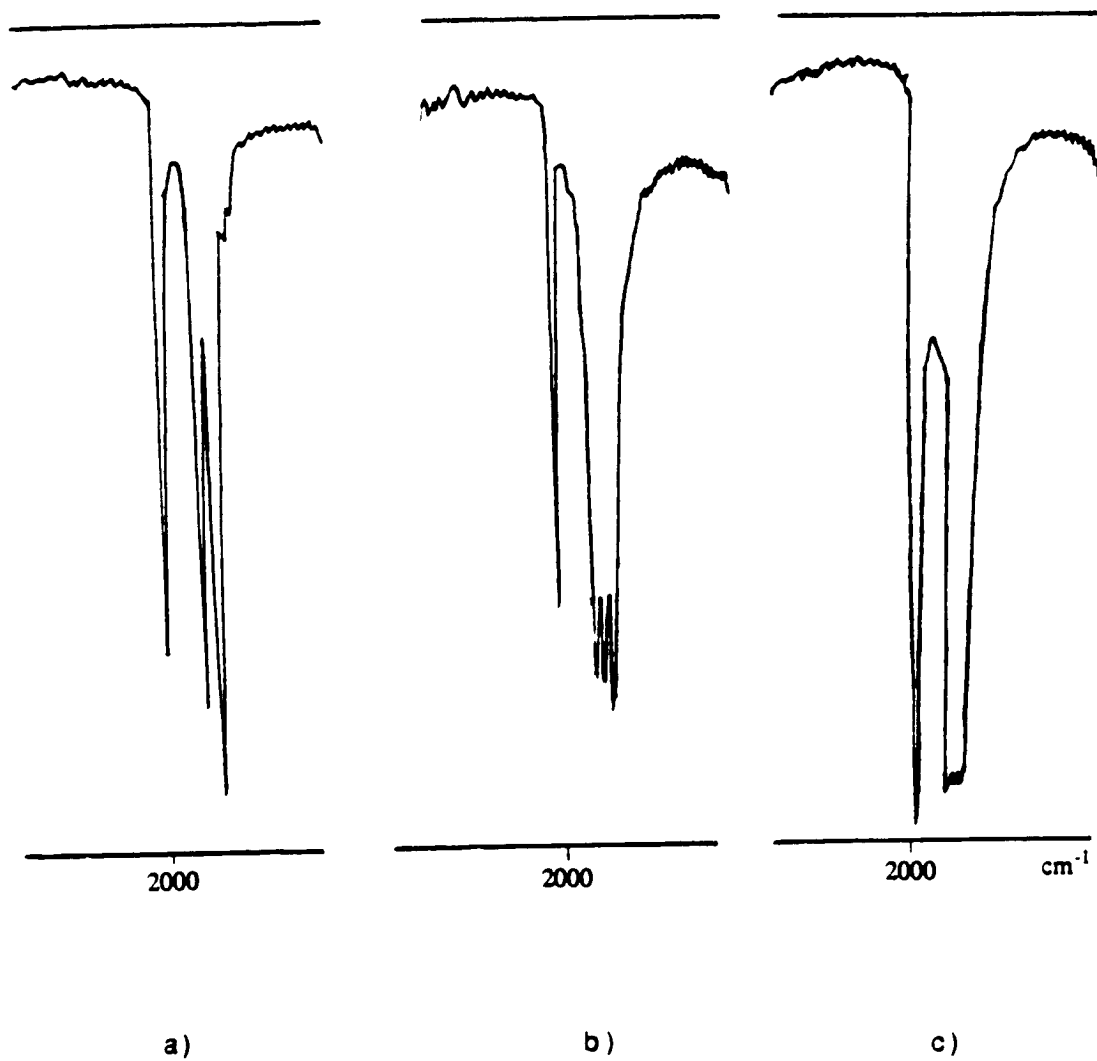
Figure 1-28: IR spectra of Fe(CO)$_3$[^{i}Pr$_2$NPO]$_4$ (**XXV**) (a)

NiBr$_2$[^{i}Pr$_2$NPO]$_4$Mo(CO)$_4$ (**XXVIII**) (b)

PdCl$_2$[Cy$_2$NPO]$_5$Mo(CO)$_3$ (**XXX**) in the CO stretching region (c)

56

induced molecular distortion in the solid KBr phase. Scheme 1 gives the CO vibrational modes in the above geometries and figure 1-28 shows infrared CO stretching bands of these complexes.

The spectroscopic data of Ni cage compound (XXXIII) can be compared with the molybdenum cage (XX) of D_{2d} symmetry. In the molybdenum cage, each metal is six-coordinate with two cis-phosphoruses and four CO ligands. The IR spectrum of this indeed show four CO stretching bands. In the nickel cage, each metal is four-coordinate with two phosphoruses and other CO ligands. The IR spectrum of this does show two CO stretching bands at 2000, and 1947 cm^{-1}. Because of the highly symmetrical geometry of this cage structure, its four phosphoruses are magnetically equivalent appearing as a singlet at 135 ppm in the ^{31}P NMR spectrum. This chemical shift is reasonable for nickel (0) phosphine compounds.[26] The ^{1}H NMR spectrum gives a broad singlet at 3.38 ppm in the methine region consistent with ^{31}P NMR and as for the molybdenum cage.

Cyclodiisopropylaminotriphosphoxane, $[^{i}Pr_2NPO]_3$, is a compound well characterized by E. Niecke in 1980.[2] The six-membered ring of P_3O_3 is in the boat conformation according to its X-ray crystal structure. The ^{31}P {^{1}H}-NMR spectrum shows two different types of phosphorus atoms (δ=140.3 ppm, δ=131.3 ppm, J=13.5 Hz). In accord with these results, the ^{1}H-NMR spectrum shows two (areas 2:1) multiplets each for the methyl and methine protons: δ=1.21 ppm (J=6.8 Hz), δ=1.24 ppm (J=6.8 Hz), δ=3.59 ppm (J=10.8 Hz); δ=3.83 ppm (J=11.5 Hz). The other synthesized cyclotri-phosphoxanes have similar typical ^{31}P NMR spectra (Table 1-2). The ^{1}H NMR spectrum of cyclo(dicyclohexylamino)triphosphoxane, $[Cy_2NPO]_3$, shows the two multiplets, for the methine-protons at δ=3.18 ppm and δ=3.15 ppm. Methylene-protons are at δ=0.86-1.18 ppm. By analogy, these rings, $[Cy_2NPO]_3$, $[^{i}PrCyNPO]_3$, $[Ph_2NPO]_3$ and $[^{s}Bu_2NPO]_3$, should exist in the same boat conformation as $[^{i}Pr_2NPO]_3$.

57

(B) Mechanism of Ring Formation:

A mechanism for the formation of cyclotriphosphoxane by hydrolysis of dichloro-aryloxyphosphines have been proposed (Scheme 2).[3] An alternative mechanism has been suggested by the following observations and is shown in Scheme 3. When 1 equivalent of water was gradually added to dichloroaminophosphines in THF in the presence of 2 equivalents of triethylamine at 0°C with the reaction monitored by solution ^{31}P NMR spectroscopy, the signal at 168 ppm due to A decreased, while the characteristic doublet and triplet, attributed to D began to grow. Other signals at 152, 95, and 3.3 ppm appeared upon stirring after addition of all the water as the signal at

SCHEME 2

TBA=tributylamine
TEA=triethylamine
THF=tetrahydrofuran
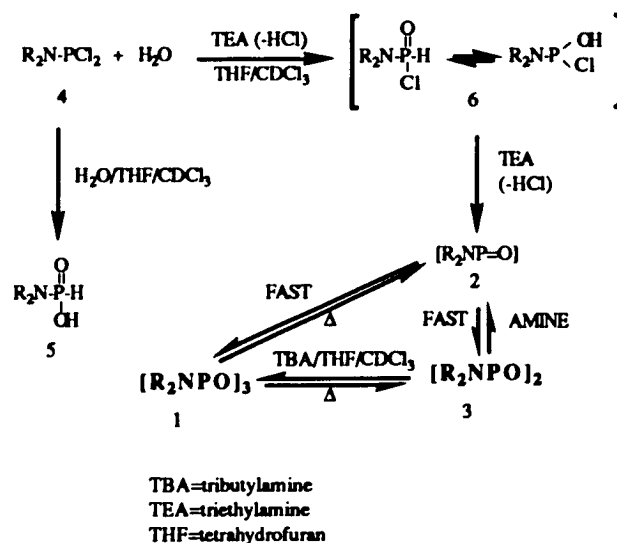
152 ppm disappeared. This resonance is probably due to B, while the other absorptions may be from the mixture E. Actually, there are several possibilities for the formation

58

of side products dependent on reaction conditions. The reaction of B with itself and triethylamine in a stepwise fashion would afford D. On the other hand, TEA could promote the internal β-elimination of HCl from B to give C. C would have a fleeting existence and should undergo head-to-tail [2+2] cycloadditions to form D. Poor stirring and fast addition of water gave rise to several side products as indicated in mixture E. By refluxing such a THF suspension, this mixture E could undergo further disproportionation and elimination reactions or with unhydrolyzed dichloroamino-phosphines with the help of triethylamine to form the ring product. This was evidenced

SCHEME 3

$$R_2N\text{-}PCl_2 + H_2O \xrightarrow[0°C]{TEA (-HCl)} \left[\; R_2N\overset{O}{\underset{Cl}{\overset{\|}{P}}}\text{-}H \rightleftarrows R_2N\text{-}P\overset{OH}{\underset{Cl}{\diagdown}} \right]$$

(A) (B)

TEA
(-HCl)

$$\left[\begin{array}{c} R_2N\overset{O}{\underset{OH}{\overset{\|}{P}}}\text{-}H \rightleftarrows R_2N\text{-}P\overset{OH}{\underset{OH}{\diagdown}} \\[6pt] R_2N\text{-}P\overset{Cl\;\; Cl}{\underset{O}{\diagdown\!\diagup}}P\text{-}NR_2 \end{array}\right]$$

(mixture E)

TEA
Δ (-HCl)

TEA
(-HCl)

$$[R_2NPO]_3 \longleftarrow [R_2NP{=}O]$$

(D) (C)
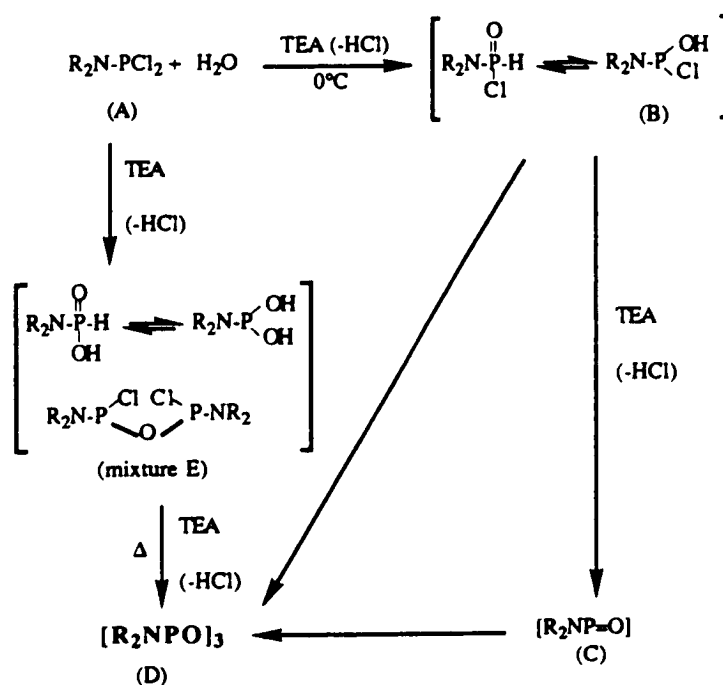
by the disappearance of other phosphorus peaks and appearance of the AB_2 pattern of the P_3O_3 ring in the ^{31}P NMR spectrum of the reaction mixture after a 2 hr reflux. Such

59

examples of disproportionation of phosphorus halides have been found in previous literature.[25]

(C) Coordination Geometry of the Nickel Group Complexes:

Four-coordinate d^8 nickel (II) complexes can be tetrahedral or square-planar in structure. Generally, the tetrahedral complexes are favored by weak-field, like Cl^-, Br^-I^- and sterically bulky ligands , as found in $NiCl_4^{2-}$, $NiBr_4^{2-}$, and NiI_4^{2-}. The square-planar geometry is favored by strong-field such as alkyl-phosphines and less bulky ligands . In transition metal-phosphine complexes, d_π-d_π bonding occurs and this may be compared to the situation in corresponding carbonyl monoxide complexes as illustrated in Scheme 4.

As the groups attached to phosphorus become more electronegative (nitrogen and oxygen), the phosphorus d orbitals become lower in energy and contract radially so as to overlap better with a metal orbital of π symmetry such as d_{xy} in the square-planar complexes. In contrast to tetrahedral complexes, metal-to-ligand π bonding can better stabilize the square-planar complexes.

For the vast majority of four-coordinate nickel (II) complexes, planar geometry is prefered. This is a natural consequence of the d^8 configuration, since the planar ligand set causes one of the metal d orbitals ($d_{x^2-y^2}$) to be uniquely high in energy and the eight electrons can occupy the other four d-orbitals, leaving this strongly antibonding one vacant. In tetrahedral coordination, on the other hand, occupation of antibonding orbitals is unavoidable. With the congeneric d^8 systems Pd (II) and Pt (II) this factor becomes so important that no tetrahedral complex is formed. Through σ-bonding between phosphorus and nickel and π-backbonding from a nickel d-orbital to phosphorus

60

SCHEME 4

M d_π (d_{xy}) - - ➤ P d_π

M d_π - - ➤ CO π^*
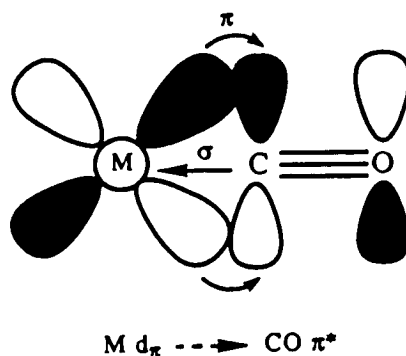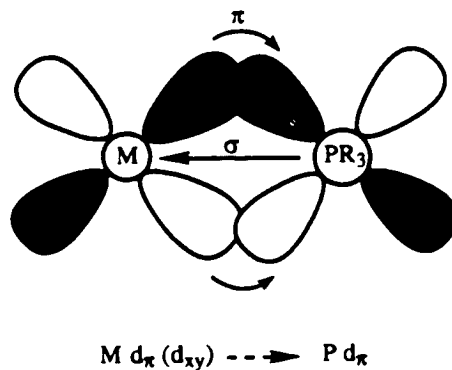
d-orbital, all nickel(II) halide polyphosphoxane complexes are formed in square-planar geometry as are the Pd (II) and Pt (II) polyphosphoxane analogues. Because these eight d-electrons of each metal (II) ion are paired, the resulting diamagnetic complexes give useful ^{31}P NMR spectra.

Chelate effect of polyphosphoxane ligands helps to stabilize the metal complexes while the metal template helps to increase the ring size. Palladium (II) halide tetraphosphoxane complexes and some platinum chloride tetra-phosphoxane complexes are in a 1,5-chelating mode (Figure 1-1, B) with the chair-chair conformation. This structure is readily recognized by solution ^{31}P NMR spectra and, of course, by X-ray

61

crystal diffraction. The A_2X_2 splitting pattern of these ^{31}P NMR spectra show coordinated phosphorus shifts downfield around 88 ppm and uncoordinated phosphorus shifts upfield at 144 ppm (J_{AX}=40-80 Hz). The unstable platinum complex (XVI) with a 1,5-chelate boat-chair mode (Figure 1-1, C) was also identified by its distinctive ^{31}P NMR spectrum. The relatively large sizes of Pd (II) and Pt(II) ions probably favor the 6-membered ring in M-P-O-P-O-P.

The $NiCl_2$, $NiBr_2$, and NiI_2 products (complexes I to V) are also 1:1 complexes of tetraphosphoxane in addition to nickel halide pentaphosphoxanes (complexes VI and XXXV). There are several possibilities of coordination. Choices include a 1,3-chelate mode (Figure 1-1, B), a 1,5-chelate mode (Figure 1-1, C), and a 1,5-chelate boat-boat conformation as found for the structure of Mo tetraphosphoxane cage. However, their ^{31}P NMR spectra were clearly AA'XX' instead of A_2X_2 and their structure can be unambiguously assigned as in the 1,3-chelating mode, suggesting that smaller nickel (II) ion may prefer the four-membered chelate ring of Ni-P-O-P.

The proton-decoupled ^{31}P NMR spectra of NiP_5O_5 complex (VI) are interesting with a broad peak at 91.7 ppm from two coordinated P_X's, another broad peak at 143.9 ppm from two uncoordinated P_A's, and a sharp resonance at 124.6 ppm from another uncoordinated P_M. These two broad peaks sharpened at lower temperature (-10°C) and disappeared at higher temperature (50°C) (Figure 1-30). This behavior might be due to the existence of two NiP_5O_5 isomers as found in the palladium analogue (Figure 1-29). Two P_A's in the complex may twist toward or away from the Ni metal at room temperature. This motion can slightly change the chemical shift for both P_A's and P_X's without affecting P_M. At higher temperature (50°C), these exchanges are rapid enough that signals due to P_A's and P_X's were too broad to appear in the spectra. At lower temperature (-10°C), the isomeric exchange was frozen out and though one isomer

62

dominated (> 99%) and the minor isomer was not observed.
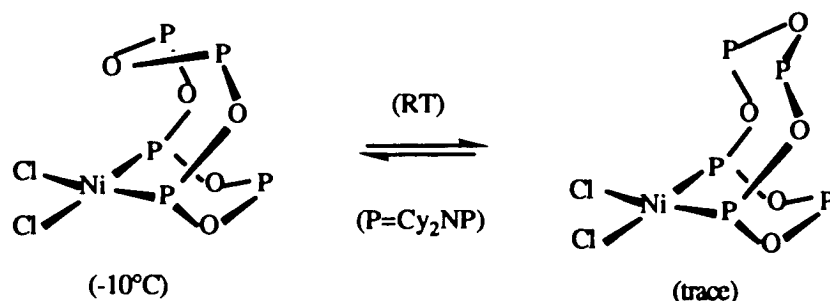
Figure 1-29: Geometry exchange between two isomers

D) Substituent Influence on Metal Polyphosphoxane Complexes:

Different R groups on phosphorus in the original trimer exhibit a significant influence on the coordinated ring size. Rings with diisopropylamino, disecbutylamino, and isopropylcyclohexylamino groups on phosphorus gave the tetraphosphoxane (P_4O_4) complexes after coordination with Ni family metals. However, rings with dicyclohexyl-amino, and diphenylamino on the phosphorus can also form pentaphosphoxane (P_5O_5) complexes under suitable conditions. Apparently, less bulky substituents lead to larger rings. The cone angle has long been used as the parameter to describe the steric bulk of phosphine ligands. The larger the cone angle, the more bulky the ligand. From previous data, the cone angles of two phosphines, $^iPr_3P$ and Cy_3P, are 160° and 170°[26] respectively. It seems that the cyclohexyl group is more bulky than a isopropyl group. However, there are no direct cone angle data on dicyclohexylamino and diisopropylamino groups. The ^{s}-butylamino group is obviously more bulky. Only formation of metal tetraphosphoxane complexes were observed. The diphenylamino group is less bulky since the formation of nickel (II) bromide pentaphosphoxane complex (XXXV) with the

63

-10°C

25°C

50°C
in d8-toluene

| 155.0 | 140.0 | 125.0 | 110.0 | 95.0 |
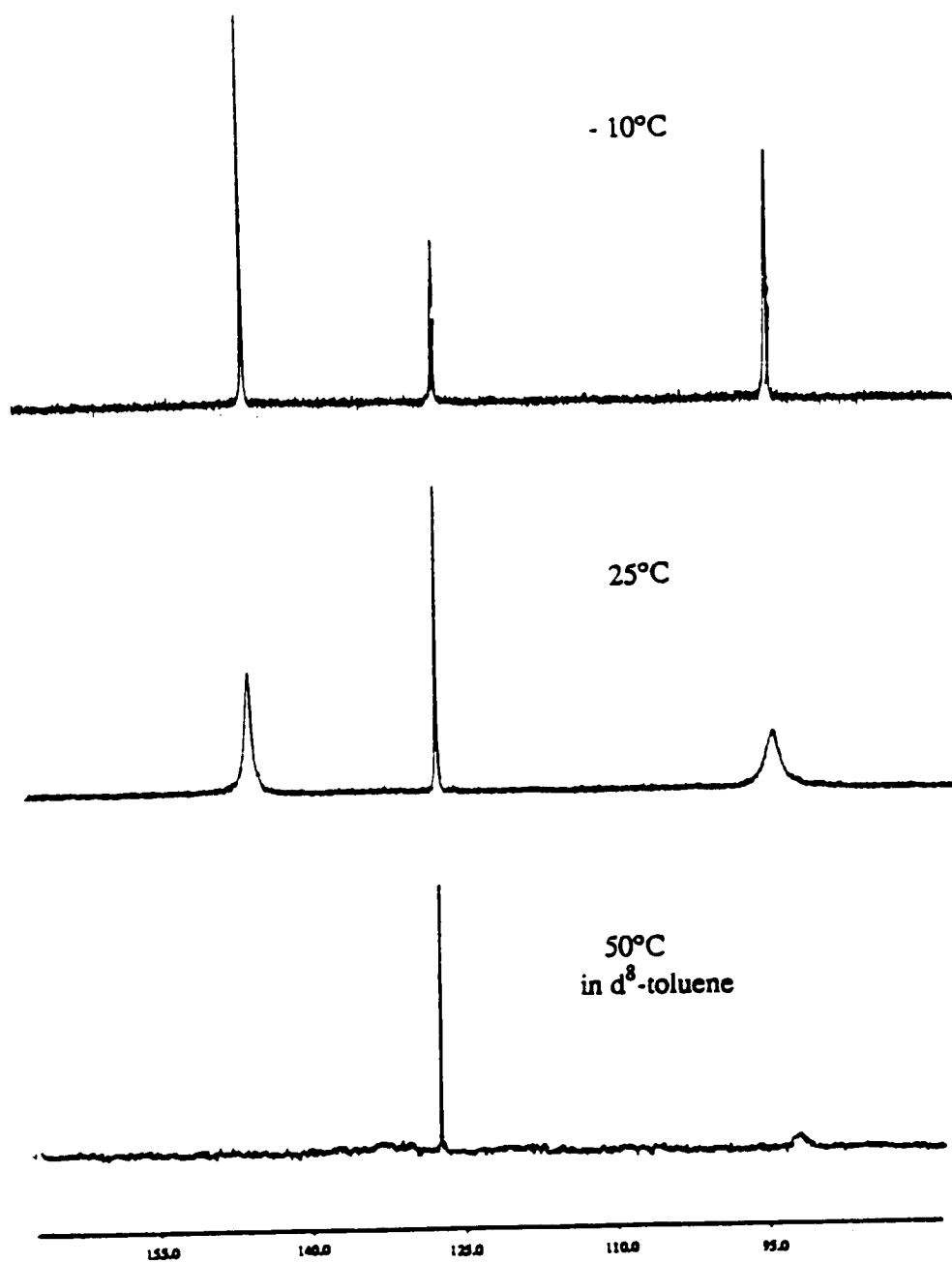
Figure 1-30: Variable-temperature ^{31}P {^1H} NMR spectra of complex (VI)

64

diphenylamino group is possible. However, the sterical difference between diisopropyl-amino and dicyclohexylamino groups is not obvious.

From the X-ray crystal structures of complexes (VII) and (XVI) (Figure 1-8, 10), the bond distances between phosphorus and metal are Pd-P of 2.24 Å and Pt-P of 2.22 Å. The metal chlorine bonds are both about 2.34 Å. The bond distances between P and O, P and N are all around 1.6 Å. These bond distances and angles are typical of cis-dichloropalladium and cis-dichloroplatinum diphosphine complexes.[28] Slight difference appears in the relative ring flattening. In the diisopropylamino P_4O_4 ring, the two uncoordinated P's are out of the O (1), O(1A), O(2), O(2A) plane by only 0.01Å. The P-O-P bond angle is about 129°. In the dicyclohexylamino ring, the P-O-P bond angle is only 122° (figure 1-31). This means that its two uncoordinated P's are a little bit more bent toward the metal than in the Pd complex. It seems that the dicyclohexylamino group may be slightly bulkier. But this slight difference makes steric arguments overly speculative.
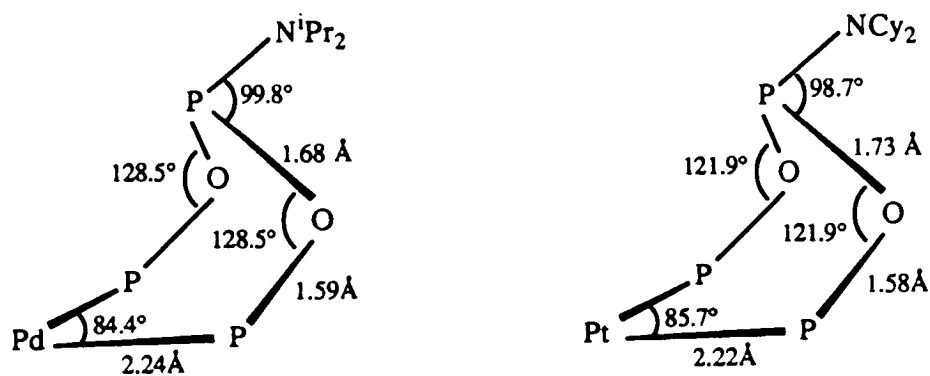
Figure 1-31: Structural comparison of the rings in boat chelate complexes (VII) and (XVI)

65

Different R-P groups also appear to influence the conformational preferences of metal complexes. This influence appears in the reaction of diiron nonacarbonyls. The reaction of Ring 1 gave a tetraphosphoxane complex with a chair-chair conformation (complex XXVI) in addition to complex XXVII. Reaction of Ring 2 gave only the tetraphosphoxane complex with a boat-chair conformation (complex XXV). These two conformational isomers do not interconvert as indicated by the VT ^{31}P NMR of complex (XXVI) in d^8-toluene solution (Figure 1-32). The A_2X_2 splitting pattern of the boat-boat conformation remained unchanged to 100°C. Hence, the conformational isomer formed depends on the different R group on the phosphorus.

The different anions on nickel (II) also influence the relative stability of nickel halide tetraphosphoxane and pentaphosphoxane complexes. The stability can be predicted from hard-soft acids-base theory. Hard acids prefer to bind to hard bases and soft acids prefer to bind to soft bases. Chloride is a hard or borderline base, I⁻ is a soft base, Br⁻ is in between. The Ni (II) ion is considered a borderline acid. Thus nickel bromide should give a stable complex while the other nickel halides should give less stable complexes. This prediction is consistent with our experimental results. Only nickel bromide tetra-phosphoxane complexes can be isolated and fully characterized as stable compounds, while the nickel chloride and iodide tetraphosphoxane complexes are all unstable and gradually decomposed during attempts at isolation and purification.

The different size of the halide anions can be an additional factor influencing phosphoxane ring sizes upon coordination with nickel. From Ring 1 and Ring 2 reactions, nickel halide tetraphosphoxane complexes were produced for nickel bromide and nickel iodide. Nickel chloride, however, can form the pentaphosphoxane complex (VI) with Ring 2. The difference appears when the sizes of the anions are compared. The relatively smaller ionic radius of Cl⁻ (1.67 Å) compared to Br⁻ (1.82 Å) and I⁻

(2.06 Å) may provide a less congested environment and an opportunity for formation of the stable P_5O_5 complex.

100°C

75°C

25°C
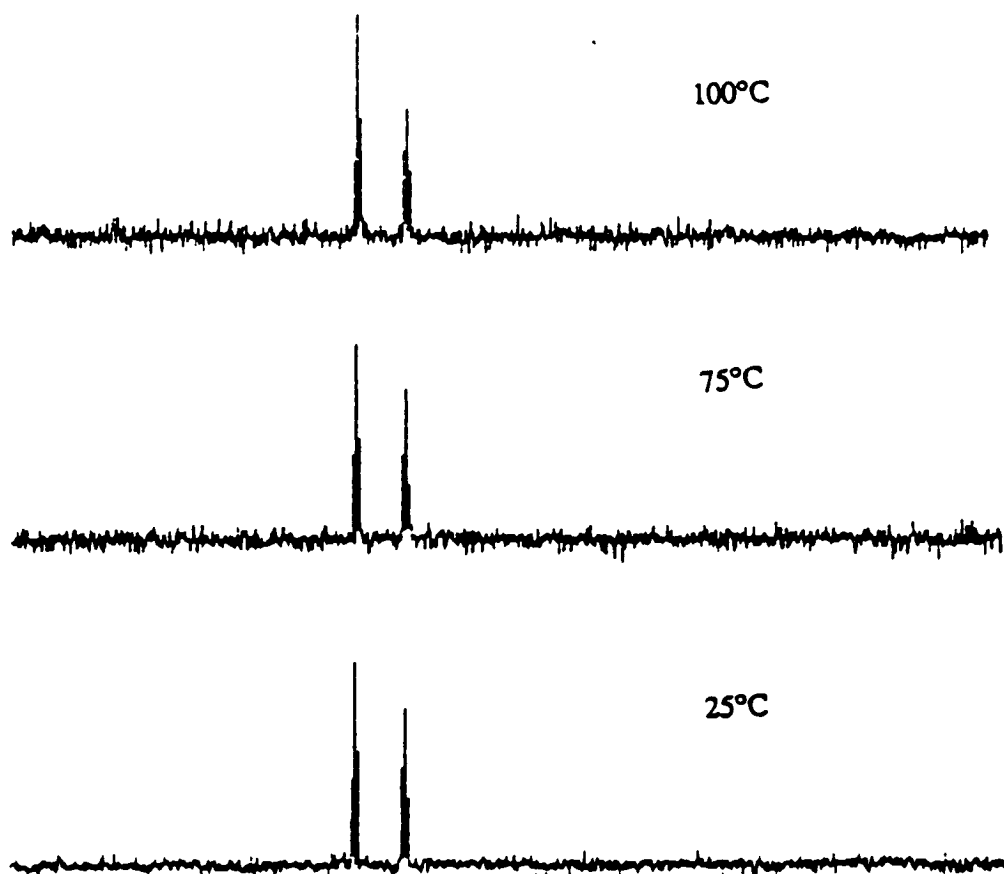
Figure 1-32: Variable temperature ^{31}P {^{1}H} NMR spectra of complex (XXVI) $Fe(CO)_3[^iPr_2NPO]_4$ in chair-chair conformation

F) Formation of Bimetallic Polyphosphoxane Complexes:

The phosphine ligand can be compared with carbon monoxide both of which exhibit σ-donor and π-accepter properties. The σ-donor and π-accepter ability of a phosphine ligand is influenced by its substituents. As more electronegative groups (nitrogen, oxygen or fluorine) are attached, the energies of both the HOMO and LUMO are lowered.

67

The ligand σ-donor ability will decrease and π-acceptor ability will increase. The reactions of metal compounds with PO rings produce only monometallic polyphosphoxane complexes regardless of molar ratio of reactants used and reaction conditions. This is because the divalent metals are electron-deficient compared with zero-valent metal compounds, such as molybdenum hexacarbonyl and (norbornadiene)molybdenum tetracarbonyl, exhibiting good σ-acceptor and weak π-donor abilities. Coordination of divalent metal in monometallic polyphosphoxane complexes is thus mainly through the strong σ-bonding from phosphorus to metal ion and weak π-bonding from divalent metal ion to phosphorus. It is possible that the uncoordinated phosphoruses may also be influenced by coordinated phosphoruses via the P-O-P linkage and exhibit weaker σ-donor and good π-acceptor abilities. They can therefore no longer coordinate additional divalent metal cations so that monometallic polyphosphoxane complexes are the only products formed.

In ligand transfer reactions (equation 36 and 37), the tetraphosphoxane ring is released from nickel to palladium and platinum to form new complexes. Palladium (II), platinum (II), and phosphorus all belong to the soft family of acids and base. Their complexes are prefered to that of nickel with phosphorus. The result of these reactions are ligand transfers without formation of bimetallic complexes. The reaction of palladium chloride pentaphosphoxane with nickel bromide(DME) gave a palladium mixed halide pentaphosphoxane complex without ring transfer. Electron-rich metals exhibit a good π-donor ability to form strong π-back bonding from metal to phosphorus. Coordination of such complexes with free phosphoruses in monometallic polyphosphoxane complexes can occur under certain conditions. Successful examples are the bimetallic compounds (XXVIII), (XXIX), (XXX), and molybdenum cage. These bimetallic complexes are formed between low valent metal ion and zero-valent metal, as well as two zero valent metals.

68

The proposed structure of the bimetallic complexes (**XXVIII**) as cages (Figure 1-1, E) is in agreement with its spectroscopic data. Its proton-decoupled ^{31}P NMR spectrum has a resonance at 60.7 ppm for the P's coordinated to Ni (II), and a resonance at 137.9 ppm for the P's coordinated with Mo. This signal is shifted upfield with the coordination of cage-like structure compared to the 142 ppm in the Ni precursor (**IV**). The ^{13}C NMR spectrum of the complex in the CO region consists of a doublet of doublets at 215.6 ppm due to two equatorial CO's coupled to two trans-coordinated P's, and two triplets at 208.7 ppm and 207.7 ppm due to two axial CO's and coupled to two cis-P's. Its IR spectrum has been discussed. The spectroscopic data of complex (**XXIX**) are also in agreement with its proposed structure (see Figure 1-17). Since the uncoordinated phosphoruses in the proposed structure of both the Ni and Pd precursors (Figure 1-4, 1-6) are bent toward the metal in a chair form, formation of bimetallic complexes requires converting all these phosphoruses to the boat form.

F) Mechanism of Formation of Metal Polyphosphoxane Complexes:

The formation of such complexes like $PdCl_2[R_2NPO]_4$ (R=iPr, Cy) from P_3O_3 requires incorporation of an additional phosphinidene oxide unit as well as a phosphorus inversion at one of the original ring phosphorus atoms. One can speculate that coordination of the P_3O_3 ring to the metal occurs initially. The reaction of Ring **2** with sulfur gave the disulfide ring compound (**XXXVI**). The two equivalent phosphoruses on the ring are readily sulfided. This means that the two equivalent phosphoruses on the original ring are more reactive. Coordination through these phosphoruses is the possible first step. Assuming a small but finite concentration of phosphinidene oxide monomer in equilibrium with the trimer, this can insert in a head-to-tail manner at a P-O ring bond. The insertion must occur at a coordinated ring phosphorus. From this consideration, the complex with the boat-chair conformation is produced as an

69

intermediate. Considering the mild reaction conditions, the P inversion step can only be feasible if an original ring [R_2N-P=O] unit eliminates and subsequently readds from a new orientation (Scheme 5).

SCHEME 5:

$$[R_2NPO]_3 \rightleftharpoons 3 [R_2NPO]$$

$$MX_2L_2 + [R_2NPO]_3 \longrightarrow \left[\begin{array}{c} X_2M \end{array} \right]$$

$$\xrightarrow{[R_2NPO]} \left[\begin{array}{c} X_2M \end{array} \right] \longrightarrow$$
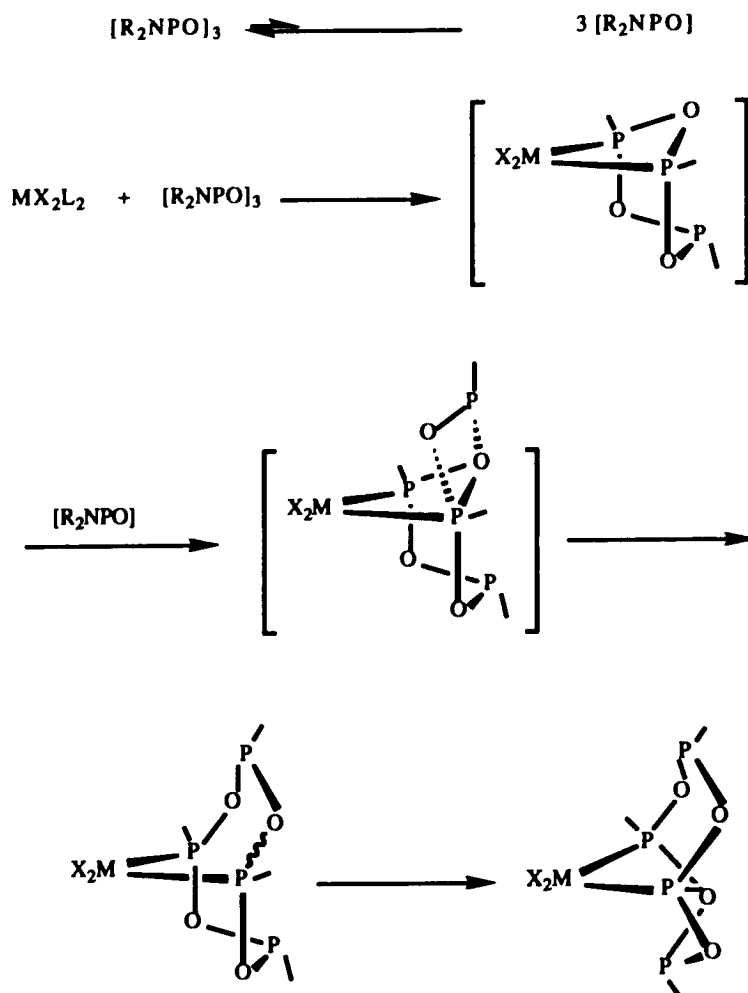
The nickel cage compounds were synthesized serendipitously in our attempt to prepare the nickel-iron bimetallic compound. When nickel bromide tetraphosphoxane was mixed with diiron nonacarbonyl, the nickel cage (XXXIII) is the only isolated and

70

product obtained in a low yield with no formation of the desired nickel-iron bimetallic complex. Formation of this compound requires reduction of nickel (II) to nickel (0) and ligand exchange between iron and nickel, as well as the original P_4O_4 ring breaking up and reassembling. A redox reaction should occur between iron(0) and nickel(II) according to the redox potentials ($E^\circ_{Fe^{2+}/Fe^0}$ = -0.48, $E^\circ_{Ni^{2+}/Ni^0}$ = -0.28). A highly speculative reaction sequence is shown in Scheme 6. The labile CO groups on iron can be replaced by a bridging bromide on nickel in a facile inner-sphere substitution process. The electrons can be transferred across the bridging group. At the same time, nickel binds two CO groups released from iron. The two uncoordinated phosphoruses are released from the P_4O_4 ring to form $Ni(CO)_2[R_2NPO]_2$ as a intermediate. Dimerization of this together produces the cage product. The other possibilities may be the bridging between iron and nickel through Br^- and CO at the same time with six coordinated nickel, because CO is the good bridging ligand too.

Reaction of iron nonacarbonyl with Ring 1, $[^iPr_2NPO]_3$, gave two different ring complexes. Complex (XXV), cis-$Fe(CO)_3[^iPr_2NPO]_4$, with a chair-chair conformation probably formed in the similar procedure as its palladium analogue discussed above. Formation of complex (XXVI), $Fe(CO)_4\{^iPr_2NP[OP(O)^iPr_2N]_2PN^iPr_2\}$, should be a different process (Scheme 7). Coordination to Fe metal could still be the first step. Since triphosphoxane is in boat form, coordination through two equivalent phosphoruses gave the possibility to form complex (XXV), while another possibility was coordination through only one phosphorus in boat site. After coordination, the R-P=O unit from the same consideration as PdP_4O_4 formation can insert in a head-to-tail manner at a P-O ring bond. But, this insertion must occur at one of the two uncoordinated phosphoruses to form an unstable P_4O_4 intermediate. Because the P_4O_4 ring only exists at low temperature (-20°) and coordination through one phosphorus in the end of the ring could not stabilize the P_4O_4 ring at a higher temperature and this P_4O_4 intermediate

71

should quickly undergo a P-O-P -> P-P(O) rearrangement to the final product under the reaction condition.

SCHEME 6:

NiBr$_2$[Cy$_2$NPO]$_4$ + Fe$_2$(CO)$_9$ $\xrightarrow[\text{- CO}]{\text{- Fe(CO)}_5}$

$$\left[-Fe \overset{Br}{\underset{Br}{\diagdown\diagup}} Ni \cdots \overset{P}{\underset{P}{\diagup}} \right]$$

$\xrightarrow[\text{+ 2 CO}]{\text{- FeBr}_2}$

$$\left[\text{structure with OC—Ni and P, O atoms} \right]$$

$\xrightarrow{\text{— 2 [RPO]}}$

$$\left[(CO)_2Ni \overset{P}{\underset{P}{\diagup\diagdown}} \overset{O}{\underset{O}{}} \right] \xrightarrow{2 \text{ x}} (CO)_2Ni \cdots \text{Ni(CO)}_2$$

72

SCHEME 7:

$Fe_2(CO)_9$ + $['Pr_2NPO]_3$ $\xrightarrow[- Fe(CO)_5]{}$

$\xrightarrow{+ ['Pr_2NPO]}$

73
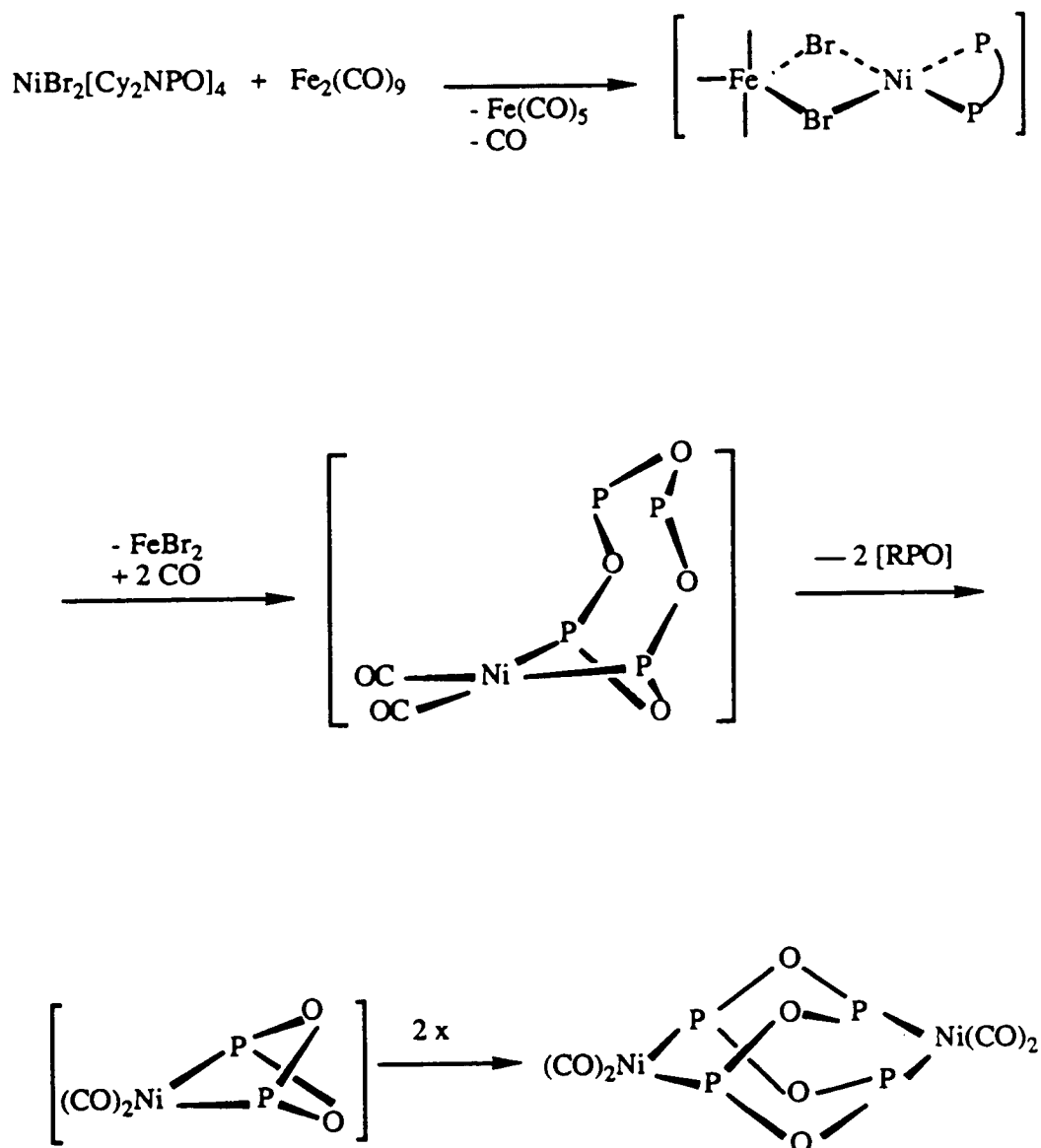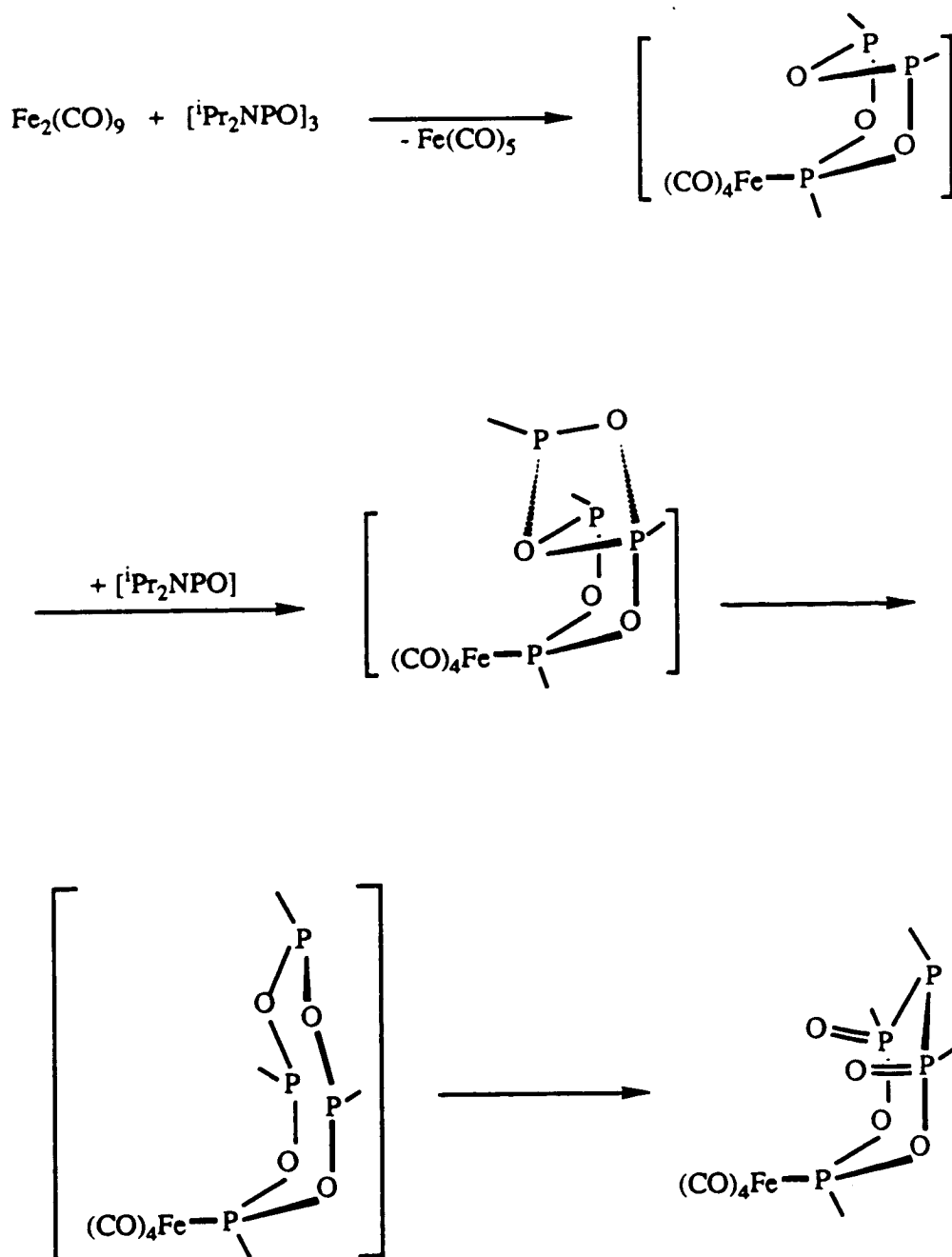
Table 1-3: ^{31}P {^1H} NMR Spectral Data of the Polyphosphoxane Complexes

Compound	(Chem. shift δ in ppm)
$NiCl_2 \cdot [^iPr_2NPO]_4$ (I)	AA'XX' ($\delta_A = \delta_{A'} = 144.2$, $\delta_X = \delta_{X'} = 55.7$) ($J_{AA'} = J_{XX'} = 50$, $J_{AX} = J_{A'X'} = 20$, $J_{AX'} = J_{A'X} = 1$ Hz)
$NiBr_2 \cdot [^iPr_2NPO]_4$ (II)	AA'XX' ($\delta_A = \delta_{A'} = 144.4$, $\delta_X = \delta_{X'} = 63.4$) ($J_{AA'} = J_{XX'} = 50$, $J_{AX} = J_{A'X'} = 20$, $J_{AX'} = J_{A'X} = 1$ Hz)
$NiCl_2 \cdot [Cy_2NPO]_4$ (III)	AA'XX' ($\delta_A = \delta_{A'} = 142.3$, $\delta_X = \delta_{X'} = 54.0$) ($J_{AA'} = J_{XX'} = 50$, $J_{AX} = J_{A'X'} = 20$, $J_{AX'} = J_{A'X} = 1$ Hz)
$NiBr_2 \cdot [Cy_2NPO]_4$ (IV)	AA'XX' ($\delta_A = \delta_{A'} = 142.4$, $\delta_X = \delta_{X'} = 62.3$) ($J_{AA'} = J_{XX'} = 50$, $J_{AX} = J_{A'X'} = 20$, $J_{AX'} = J_{A'X} = 1$ Hz)
$NiI_2 \cdot [Cy_2NPO]_4$ (V)	AA'XX' ($\delta_A = \delta_{A'} = 142.4$, $\delta_X = \delta_{X'} = 75.4$) ($J_{AA'} = J_{XX'} = 50$, $J_{AX} = J_{A'X'} = 20$, $J_{AX'} = J_{A'X} = 1$ Hz)
$NiCl_2 \cdot [Cy_2NPO]_5$ (VI)	AA'MXX' ($\delta_A = \delta_{A'} = 143.9$, $\delta_M = 124.6$, $\delta_X = \delta_{X'} = 91.7$) ($J_{AX} = J_{A'X'} = J_{AX'} = J_{A'X} = 0$, $J_{A'M} = J_{AM} = 0$ $J_{MX'} = 12.6$, $J_{MX} = 11$ Hz)
$PdCl_2 \cdot [^iPr_2NPO]_4$ (VII)	A_2X_2 ($\delta_A = 147.8$, $\delta_X = 88.3$) ($J_{AX} = 44$ Hz)
$PdBr_2 \cdot [^iPr_2NPO]_4$ (VIII)	A_2X_2 ($\delta_A = 146.1$, $\delta_X = 88.3$) ($J_{AX} = 49$ Hz)
$PdCl_2 \cdot [Cy_2NPO]_4$ (IX)	A_2X_2 ($\delta_A = 143.9$, $\delta_X = 88.9$) ($J_{AX} = 83$ Hz)
$PdBr_2 \cdot [Cy_2NPO]_4$ (X)	A_2X_2 ($\delta_A = 141.9$, $\delta_X = 88.8$) ($J_{AX} = 88$ Hz)
$PdCl_2 \cdot [Cy_2NPO]_5$ (XI)	AA'MXX' ($\delta_A = \delta_{A'} = 143.4$, $\delta_M = 127.5$, $\delta_X = \delta_{X'} = 87.9$) ($J_{AA'} = J_{XX'} = 50$, $J_{AX} = J_{A'X'} = J_{AX'} = J_{A'X} = 15$ $J_{AM} = J_{A'M} = 2.6$ Hz, $J_{MX} = J_{MX'} = 11.5$ Hz)
$PdBr_2 \cdot [Cy_2NPO]_5$ (XII) isomer A	AA'MXX' ($\delta_A = \delta_{A'} = 142.7$, $\delta_M = 127.3$, $\delta_X = \delta_{X'} = 87.4$) ($J_{AA'} = J_{XX'} = 50$, $J_{AX} = J_{A'X'} = J_{AX'} = J_{A'X} =$ $J_{MX'} = J_{MX} = 19$ Hz, $J_{AM} = J_{A'M} = 3$ Hz)

74

Table 1-3 continued.

PdBr$_2$·[Cy$_2$NPO]$_5$ (XIII) isomer B	AA'MXX'($\delta_A=\delta_{A'}=140.9,\delta_M=125.7$, $\delta_X=\delta_{X'}=91.0$) ($J_{AA'}=J_{XX'}=50$, $J_{AX}=J_{A'X'}=J_{AX'}=J_{A'X}=2$ Hz, $J_{A'M}=J_{AM}=0$ Hz, $J_{MX'}=J_{MX}=63$ Hz)
PtCl$_2$·[^{i}Pr$_2$NPO]$_4$ (XIV)	A$_2$X$_2$ ($\delta_A=142.8$, $\delta_X=59.0$) ($J_{AX}=34$ Hz)
PtCl$_2$·[Cy$_2$NPO]$_5$ (XV)	AA'MXX'($\delta_A=\delta_{A'}=141.8,\delta_M=127.5$, $\delta_X=\delta_{X'}=60.1$) ($J_{AX}=J_{A'X'}=J_{AX'}=J_{A'X}=13.8$ Hz $J_{MX'}=J_{MX}=10.7$ Hz, $J_{A'M}=J_{AM}=3.1$ Hz) $J_{Pt-P}=5141.6$ Hz
PtCl$_2$·[Cy$_2$NPO]$_4$ (A) (XVI)	A$_2$X$_2$ ($\delta_A=146.8$, $\delta_X=59.3$) ($J_{AX}=63.5$ Hz) $J_{Pt-P}=4825.5$ Hz
PtCl$_2$·[Cy$_2$NPO]$_4$ (B) (XVII)	ABXX' ($\delta_A=140.1$, $\delta_B=134.4$, $\delta_X=58.1$)($J_{AB}=0$) ($J_{AX}=J_{AX'}=43.5$, $J_{BX}=J_{BX'}=13.1$Hz) $J_{Pt-P}=5205.8$ Hz
Mo(CO)$_4$·[^{i}Pr$_2$NPO]$_3$ (XVIII)	A$_2$X ($\delta_A=138.5$, $\delta_X=130.1$) ($J_{AX}=2$ Hz)
Mo(CO)$_4$·[Cy$_2$NPO]$_3$ (XIX)	A$_2$X ($\delta_A=136.8$, $\delta_X=128.2$) ($J_{AX}=15$ Hz)
Mo$_2$(CO)$_8$·[^{i}Pr$_2$NPO]$_4$ (XX)	singlet ($\delta=150.0$)
Mo$_2$(CO)$_8$·[Cy$_2$NPO]$_4$ (XXI)	singlet ($\delta=149.8$)
Mo$_2$(CO)$_8$·[^{i}Pr$_2$NPO]$_4$ (XXII)	singlet ($\delta=135.0$)
Mo$_2$(CO)$_8$·[Cy$_2$NPO]$_4$ (XXIII)	singlet ($\delta=137.6$)
Cr(CO)$_4$·[Cy$_2$NPO]$_4$ (XXIV)	A$_2$MX ($\delta_A=177.1$, $\delta_M=129.4$, $\delta_X=123.4$) ($J_{AM}=36.7$, $J_{MX}=2.7$, $J_{AX}=9.6$ Hz)
Fe(CO)$_3$·[Cy$_2$NPO]$_4$ (XXV)	A$_2$MX ($\delta_A=163.8$, $\delta_M=131.6$, $\delta_X=125.6$) ($J_{AM}=53.7$, $J_{MX}=0$, $J_{AX}=0.2$ Hz)
Fe(CO)$_3$·[^{i}Pr$_2$NPO]$_3$ (XXVI)	A$_2$X$_2$ ($\delta_A=160.6$, $\delta_X=145.0$) ($J_{AX}=39$ Hz)
·Fe(CO)$_4$·[^{i}Pr$_2$NPO]$_4$· (XXVII)	AX$_2$Y ($\delta_A=152.5$, $\delta_X=24.5$, $\delta_Y=6.6$) ($J_{AX}=14.7$, $J_{XY}=187.0$, $J_{AY}=0$ Hz)
Mo(CO)$_4$·[Cy$_2$NPO]$_4$·NiBr$_2$(XXVIII)	AA'XX' ($\delta_A=\delta_{A'}=137.9$, $\delta_X=\delta_{X'}=60.7$) ($J_{AA'}=J_{XX'}=0$, $J_{AX}=J_{A'X'}=15$, $J_{AX'}=J_{A'X}=12$ Hz)
Mo(CO)$_3$·[Cy$_2$NPO]$_5$·PdCl$_2$ (XXIX)	AM$_2$X$_2$($\delta_A=157.1,\delta_M=137.5,\delta_X=88.9$) ($J_{AM}=28.9$, $J_{AX}=9.5$, $J_{MX}=0$ Hz)
Mo(CO)$_4$·[^{i}Pr$_2$NPO]$_4$·Fe(CO)$_3$(XXX)	AB$_2$X ($\delta_A=163.5$, $\delta_B=160.5$, $\delta_X=137.4$) ($J_{AB}=85$, $J_{AX}=0$, $J_{BX}=5$ Hz)

Table 1-3 continued.

$Ni_2(CO)_4 \cdot [Cy_2NPO]_4$ (XXXI)	singlet ($\delta = 133.8$)
$PdClBr \cdot [Cy_2NPO]_5$ (XXXII)	$AA'MXX'(\delta_A = \delta_{A'} = 143.4, \delta_M = 127.5, \delta_X = \delta_{X'} = 87.9)$ (multiplets)
$PdBr_2 \cdot [^sBu_2NPO]_4$ (XXXIII)	$AA'XX'$ ($\delta_A = \delta_{A'} = 145.9, \delta_X = \delta_{X'} = 88.7$ multiplets)
$PdBr_2 \cdot [^iPrCyNPO]_4$ (XXXIV)	A_2X_2 ($\delta_A = 144.5, \delta_X = 88.1$) ($J_{AX} = 58$ Hz)
$NiBr_2 \cdot [Ph_2NPO]_5$ (XXXV)	$AA'MXX'(\delta_A = \delta_{A'} = 124, \delta_M = 114, \delta_X = \delta_{X'} = 84)$
$[Cy_2NPO]_3S_2$ (XXXVI)	AXY ($\delta_A = 134.8, \delta_X = 50.2, \delta_Y = 49.7$, multiplets)

All spectra were run in $CDCl_3$.

Table 1-4: ^{13}C $\{^1H\}$ NMR Spectral Data of the Polyphosphoxane Complexes

Compound	(Chemical Shifts, δ ppm, J Hz)
II	CH (48.6; 45.1); CH_3 (24.5; 22.9)
IV	CH (58.1; 53.5); CH_2 (33.3; 33.1; 26.7; 26.4; 26.1; 25.5;24.8)
VI	CH (58.1; 53.8; 52.7); CH_2 (33.4; 32.4; 29.3; 27.1; 26.5; 25.6; 25.4; 24.9; 21.5)
VII	CH (47.7, 47.2); CH_3 (23.2, 19.2)
VIII	
XI	CH (58.5; 53.7; 52.7); CH_2 (37.7; 35.7; 35.2; 33.2; 32.5; 31.5; 29.2; 26.9; 26.3; 25.3; 24.7)
XII	CH (58.5; 54.1; 53.0); CH_2 (37.6; 37.3; 33.4; 33.1; 32.7; 32.4; 29.1; 27.1; 26.4; 25.8; 25.6; 25.4; 24.8)
XIII	CH (58.5; 53.6; 53.1); CH_2 (38.2; 35.1; 32.8; 29.3; 27.0; 26.2; 25.6; 24.9)

76

Table 1-4 continued.

XV CH (58.0; 53.8; 53.6; 52.9);   CH$_2$ (37.8; 37.2; 33.1; 32.8;
32.5; 29.3; 27.1; 26.4; 25.8; 25.6; 25.4; 24.8)

XVIII CO (not avail.);   CH   (47.8 triplet, J=6; 44.7; 44.4)
CH$_3$ (24.4; 23.6; 23.2)

XIX CO (not avail.);   CH(57.4 triplet, J=6; 53.7 doublet, J=12)
CH$_2$ (34.9; 33.7; 34.2; 26.9; 26.6; 26.5; 25.4; 25.1)

XXIV CO (226.0 triplet, J=10; 219.4 triplet; 219.0 triplet, J=20)
CH (57.4; 53.2; 52.5);   CH$_2$ (33.7; 33.1; 26.8; 25.6)

XXV CO (218.1 multiplet);
CH (57.8; 53.5 doublet, J=9; 52.5 doublet, J=12)
CH$_2$ (33.5; 33.0; 26.9; 26.8; 26.3; 25.8; 25.7)

XXVI CO (218.0 multiplet);   CH   (47.5; 44.4 doublet, J=15)
CH$_3$ (24.1; 22.8)

XXVII (-10°C) CO (215.8 doublet, J=15; 215. 0 doublet, J=15)
CH (56.9 doublet, J=10.5; 48.0 doublet, J=12; 46.9 doublet,
J=7; 44.6 doublet, J=26.9 Hz);
CH$_3$ (26.4 doublet, J=10.5; 23.9; 23.5; 23.2; 22.9)

XXVIII CO (215.9 doublet, J=12; 215.4 doublet, J=12
208.7 triplet, J=8; 207.7 triplet, J=10)
CH (58.4; 58.2);   CH$_2$ (36.4; 34.2; 33.5; 32.9;
26.4; 25.9; 25.3; 25.1)

XXIX CO (218.9 doublet of triplets, J=39, 13
216.4 doublet of triplets, J=39, 13)
CH (59.3; 58.2; 57.7);   CH$_2$ (35.8; 35.4; 34.7; 33.3; 27.0
26.7; 26.1; 25.4; 25.2; 24.9)

XXX CO(219.2 triplet, J=6; 218.8 doublet, J=9; 216.7 doublet,J=54
211.0 doublet of doublets, J=3, 9; 207.5 quartet, J=9)
CH (49.2; 47.6 doublet, J=9; 44.3 doublet, J=14);
CH$_3$ (23.4; 23.0; 22.4)

XXXI CO (198 triplet, J=2);   CH   (55.4 triplet, J=6)
CH$_2$ (34.2; 26.6; 25.5)

All spectra were run in CDCl$_3$ with chemical shifts referenced to internal TMS standard.

77

Table 1-5: Proton NMR Data of the Polyphosphoxane complexes

Compound	Methine Region	Methyl(a) or Methylene(b) Region
II	4.2 (multiplets)	(a) 1.36; 1.32; 1.31(doublets, J=6.8)
IV	3.8 (broad)	(b) 1.99-0.84; (multiplets)
VI	3.6; 3.1; 2.9 (broad)	(b) 2.14-1.07; (multiplats)
VII	3.74 (multiplets)	(a) 1.36; 1.28; (doublet, J=6.7)
VIII	2.17 (multiplets)	(a) 1.51; 1.37; 1.28 (doublets, J=6.1)
XI	3.52;3.04;2.82(broad)	(b) 2.25-0.88; (multiplets)
XII	3.51;3.17;2.80(broad)	(b) 2.26-0.85; (multiplets)
XIII	3.98;3.54;3.05(broad)	(b) 2.19-0.88; (multiplets)
XV	3.56;3.06;2.79(broad)	(b) 2.19-0.82; (multiplets)
XVIII	3.86(singlet,6.9);3.7(broad)	(a)1.32;1.31;1.26(doublets,6.9)
XIX	3.25 (broad)	(b) 1.70-1.18; (multiplets)
XXIV	3.48 (broad)	(b) 1.76-0.84; (multiplets)
XXV	3.52 (broad)	(b) 1.82-0.84; (multiplets)
XXVI	3.92; 3.79 (broad)	(a) 1.26; (doublet, J=23)
XXVII (-10°C)	4.58; 4.15; 3.50 3.33 (singlets)	(a) 1.35;1.31;1.24;1.19 (doublets, 6)
XXVIII	3.98(multiplet);3.79(broad)	(b)1.95-0.84; (multiplets)
XXXIX	4.11;3.66;2.98(broad)	(b) 2.06-1.00; (multiplets)
XXX	4.03(septets);3.87(singlets,7) 3.63 (broad)	(a)1.44;1.38;1.33;1.18 (doublets,7)
XXXI	3.38 (broad)	(b) 2.18-0.72; (multiplets)

All spectra were run in $CDCl_3$ and shifts referenced to internal TMS standard.

78

Table 1-6: Infrared Data of the Polyphosphoxane Complexes

Compound	CO Stretches (cm^{-1})	P-O-P stretches (cm^{-1})
II		939
IV		932
VI		863
VII		896
VIII		896
IX		880
X		878
XI		868
XII		869
XIII		869
XV		870
XVIII	2014; 1913; 1896; 1886	839
XIX	2000; 1918; 1898; 1885	826
XXIV	2000; 1912; 1896; 1886	829
XXV	1995; 1926; 1899	832
XXVI	1999; 1936; 1908	829
XXVII	2049; 1984; 1947; 1933	873
XXVIII	2022; 1945; 1928; 1909	904
XXIX	1979; 1912; 1902;1890	919
XXX	2021; 1999; 1962; 1944; 1922; 1912; 1899; 1877; 1869	873
XXXI	2000; 1947	870
XXXII		864

KBr pellets.

CHAPTER 2

THERMAL REACTIONS OF AMINOPHOSPHINE OXIDES $(R_2N)_2P(O)H$ AND PHOSPHOROAMIDITES $(^iPr_2N)(RO)P(O)H$ WITH METAL HEXACARBONYLS $M(CO)_6$ [M = Cr, Mo, W]

In the coordination chemistry of bis(dialkylamino)phosphine oxides with metal carbonyls, coordinated tri- and tetraphosphoxanes have been isolated and characterized, apparently formed by metal-assisted amine elimination and oligomerization.[5-8] The latter formed adamantane-like cage complexes of the type $Mo_2(CO)_8[R_2NPO]_4$ ($R=^iPr$, Cy) featuring the P_4O_4 ring in a chair-chair conformation, allowing chelation of two metals in a back-to-back orientation and monometallic complexes, cis-$M(CO)_4[^iPr_2NPO]_4$ (M=Cr, Mo, W), which contained both the chair-boat and the chair-chair configurations of the tetraphosphoxane heterocycle. Even a $Cr_2P_5O_5$ complex, $Cr_2(CO)_7[^iPr_2NPO]_5$ was isolated in a low yield (5%),[8] containing a cyclo-pentaphosphoxane P_5O_5 ring coordinated to one cis-$Cr(CO)_4$ and one fac-$Cr(CO)_3$ moiety.

This thermal reaction should be a good way to prepare zero-valent metal poly-phosphoxane complexes. There are two advantages to this method. One is ready synthesis of starting aminophosphine oxides with different amino groups. A second is that purchased metal hexacarbonyls can be used directly in thermal reactions without further derivatization. In this paper, this kind of reaction is used mainly to study the influence of different phosphorus R groups on coordinated polyphosphoxane ring size. Finally, the novel P_6O_6 ring complex has been selectively synthesized in high yield. Figure 2-1 shows the schematic structure of this dichromium hexacarbonyl hexa-

80

phosphoxane 'cubane' complex.
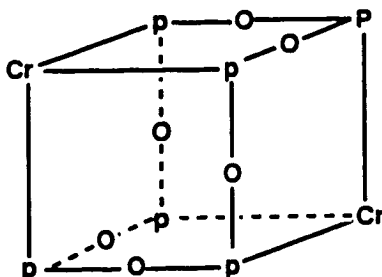
Figure 2-1: The cube structure of the $Cr_2P_6O_6$ complex

Three different types of substituents on phosphorus were used. One consists of diiso-propylamino analogues with methine carbons attached to nitrogen, including dicyclo-hexylamino-, isopropylcyclohexylamino-, and 2,6-dimethylpiperidino groups (**Type 1**). It was anticipated that the reaction of these phosphine oxides will give metal poly-phosphoxane complexes, differing in coordination conformation and ring size.

A second group had less sterically bulky amino groups with methylene carbons attached to nitrogen, including diethylamino and piperidino groups (**Type 2**), possibly leading to form polyphosphoxane metal complexes with larger P_nO_n ring sizes, because of less bulky substituents.

The third group consists of phosphoroamidites $(^iPr_2N)(RO)P(O)H$ (**Type 3**) with mixed amino and phenoxyl groups. The aim was to produce metal polyphosphoxane complexes with O-substituents by elimination of amino groups. Since a P-O bond is much stronger than a P-N bond, under appropriate reaction conditions, a elimination of

81

the amine may be possible compared to cleaving a P-O bond to eliminate phenol as in the equation below. In reality, the last two types of phosphine oxides gave did not lead to formation of metal polyphosphoxane complexes. All results of these thermal reactions will be given and discussed in this chapter.

$$n(^iPr_2N)(RO)P(O)H + xM(CO)6 \longrightarrow M_x(CO)_y[ROPO]_n + n^iPr_2NH + (6x-y)\ CO$$

It is tempting to propose that the synthesis of larger polyphosphoxane rings can be achieved by directly thermal reaction of smaller polyphosphoxane ring complexes with excess phosphine oxide. The reaction of chromium dimethylpiperidino-P_5O_5 complex with bis(dimethylpiperidino)phosphine oxide in hot xylene provides direct support for this hypothesis in leading selectively to the novel $Cr_2P_6O_6$ ring complex.

82

RESULTS:

1. Syntheses of Phosphoroamidites. (^{i}Pr$_2$N)(RO)P(O)H:

$$ROH + PCl_3 + Et_3N \longrightarrow ROPCl_2 + Et_3NHCl \quad (2\text{-}1)$$

$$ROPCl_2 + iPr_2NH + Et_3N \longrightarrow (^iPr_2N)(RO)PCl + Et_3NHCl \quad (2\text{-}2)$$

$$(^iPr_2N)(RO)PCl + H_2O + Et_3N \longrightarrow (^iPr_2N)(RO)P(O)H + Et_3NHCl \quad (2\text{-}3)$$
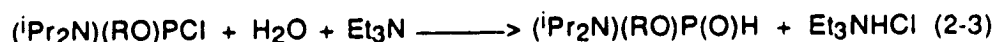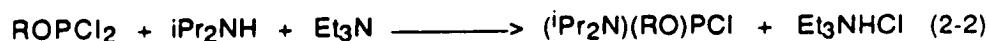
Detailed synthetic conditions for the dichloride products (Equation 2-1) varied according to the alcohol. Thus BHT-PCl$_2$ was synthesized by refluxing a mixture of BHT, PCl$_3$, and Et$_3$N for a short time. DIPP-PCl$_2$ (DIPP=diisopropylphenoxyl) was synthesized by adding DIPP dropwise into a mixture of PCl$_3$ and Et$_3$N at 0°C. ^{t}BuO-PCl$_2$ was synthesized by adding a mixture of ^{t}BuOH and Et$_3$N into a solution of PCl$_3$ in petroleum ether at 0°C. Then, the first two monochlorides (^{i}Pr$_2$N)(RO)PCl were synthesized (Equation 2-2) by adding ^{i}Pr$_2$NH dropwise into a suspension of ROPCl$_2$ and Et$_3$N in CH$_2$Cl$_2$ at -78°C. The (^{i}Pr$_2$N)(^{t}BuO)PCl was obtained by adding ^{i}Pr$_2$NH into a suspension of (^{t}BuO)PCl$_2$ in petroleum ether at 0°C. The last step included hydrolysis (Equation 2-3) of these monochlorides in the presence of Et$_3$N at 0°C.

The product (^{i}Pr$_2$N)(BHT)P(O)H (oxide I) is a white solid, slightly soluble in hexane. (^{i}Pr$_2$N)(DIPP)P(O)H (oxide II) is a thick liquid with a high boiling point. (^{i}Pr$_2$N)(^{t}BuO)P(O)H (oxide III) is a colorless liquid. All these oxides were contaminated with side products which were difficult to remove as these liquids decomposed during vacuum distillation. Their solution proton-decoupled ^{31}P NMR spectra exhibited singlets from -3 ppm to 8 ppm. Their proton-coupled ^{31}P NMR spectra exhibited doublets of triplets with $J_{P\text{-}H}$=640 Hz and $^3J_{P\text{-}H}$ =15 Hz (Table 2-1).

83

Table 2-1: ^{31}P NMR Data for the Phosphoroamidites:

Compound		splitting pattern (δ, ppm) (J, Hz)	
$(^iPr_2N)(BHT)P(O)H$	(oxide I)	$\delta = -3$ [a],	$^1J_{P-H} = 640$, $^3J_{P-H} = 15$ [b]
$(^iPr_2N)(DIPP)P(O)H$	(oxide II)	$\delta = 8$ [a],	$^1J_{P-H} = 640$, $^3J_{P-H} = 15$ [b]
$(^iPr_2N)(^tBuO)P(O)H$	(oxide III)	$\delta = 5$ [a],	$^1J_{P-H} = 640$, $^3J_{P-H} = 15$ [b]

(a). Proton-decoupled

(b). Proton-coupled, (doublet of triplets)

2. Syntheses of Phosphine Oxides, $(R_2N)_2P(O)H$:

$$PCl_3 + Et_3N + R_2NH \xrightarrow[-78°C]{CH_2Cl_2} (R_2N)_2PCl + Et_3NHCl \qquad (2-4)$$

$$(R_2N)_2PCl + Et_3N + H_2O \xrightarrow[0°C]{CH_2Cl_2} (R_2N)_2P(O)H + Et_3NHCl \qquad (2-5)$$
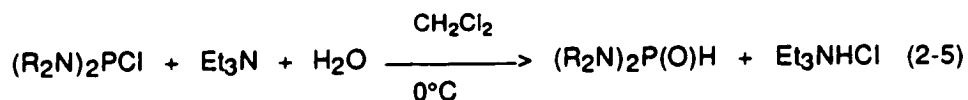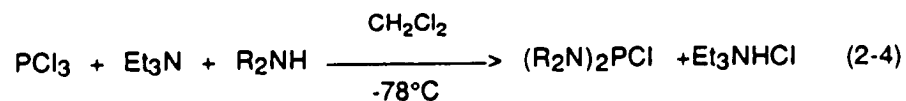
The monochlorides $(R_2N)_2PCl$ were obtained by reaction of phosphorus trichloride and the secondary amine in the presence of triethylamine at -78°C (Equation 2-4). Then, hydrolysis of these mono-chlorophosphines in the presence of triethylamine at 0°C gave the desired phosphine oxides (Equation 2-5).

Bis(diethylamino)phosphine oxide $(Et_2N)_2P(O)H$ (oxide IV) and bis(piperidino)-phosphine oxide $(PIP_2N)_2P(O)H$ (oxide V) are liquids. Their solution proton-decoupled ^{31}P NMR spectra showed singlets at 19.5 ppm and 17.7 ppm respectively. The proton-coupled ^{31}P NMR spectra of both oxides showed doublets of nonets with $J_{P-H} = 585.9$ Hz and $^3J_{P-H} = 14.6$ Hz. Bis(dicyclohexylamino)phosphine oxide $(Cy_2N)_2P(O)H$ (oxide VI) and bis(2,6-dimethylpiperidino)phosphine oxide $(DMP)_2P(O)H$ (oxide

84

VII) were white solids. Bis(isopropylcyclohexylamino)phosphine oxide (^{i}PrCyN)$_2$P(O)H (oxide VIII) is a thick liquid. Their ^{31}P NMR spectral data list in table 2-2.

Table 2-2: ^{31}P NMR Data for the Phosphine Oxides:

Compound	splitting pattern (δ, ppm) (J, Hz)
(Et$_2$N)$_2$P(O)H (oxide IV)	δ=19.5 [a], J$_{P-H}$=585.9, ^{3}J$_{P-H}$=14.6 [b]
(PIP$_2$N)$_2$P(O)H (oxide V)	δ=17.7 [a], J$_{P-H}$=585.9, ^{3}J$_{P-H}$=14.6 [b]
(Cy$_2$N)$_2$P(O)H (oxide VI)	δ=7.6 [a], J$_{P-H}$=571.2, ^{3}J$_{P-H}$=19.5 [b]
(DMP)$_2$P(O)H (oxide VII)	δ=19.7 [a], J$_{P-H}$=566.4, ^{3}J$_{P-H}$=9.7 [b]
(^{i}PrCyN)$_2$P(O)H (oxide VIII)	δ=6.8 [a], J$_{P-H}$=551.7, ^{3}J$_{P-H}$=14.6 [b]

(a). Proton-decoupled
(b). Proton-coupled, (doublet of nonets and doublet of septets).

3. Attempted Complexation Reactions of Phosphoroamidites. (^{i}Pr$_2$N)(RO)P(O)H:

In refluxing toluene, reactions of oxide I and II with Mo(CO)$_6$ gave purple precipitates and oxide III gave a yellow precipitate. These precipitates were difficult to characterize, being only slightly soluble even in polar solvents. In refluxing hexane, reactions of these three oxides with Mo(CO)$_6$ gave pale yellow, unstable, precipitates which were soluble in hexane but quickly decomposed during purification attempts. The decomposed products contained the original oxides and Mo(CO)$_6$ according to the solution ^{31}P NMR and IR spectra. These unstable compounds are most likely the oxygen-coordinated complexes Mo(CO)$_5$·(^{i}Pr$_2$N)(RO)P(O)H. Figure 2-2 shows the proposed structure of these species.

4. Complexation Reactions of bis(diethylamino)phosphine oxide. (Et$_2$N)$_2$P(O)H:

The reaction of oxide IV with metal hexacarbonyls gave a black suspension. The

85

black precipitate was elemental metal from the decomposed metal carbonyls. In the reaction of Cr(CO)$_6$, the solution ^{31}P NMR spectrum showed two major singlets at 174.6 ppm and 162.1 ppm (1:3 ratio). After separation by alumina chromatography,
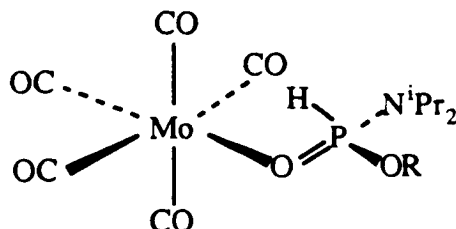
Figure 2-2: Proposed structure of Mo(CO)$_5$·(^{i}Pr$_2$N)(RO)P(O)H.

the compound at 162.1 ppm, identified as the chelate complex Cr(CO)$_4$(Et$_2$N)$_2$POP(Et$_2$N)$_2$ (complex **XXXVII**), was obtained as a pale yellow solid. The minor component was not recovered but was possibly the chromium cage. The ^{13}C NMR spectrum of the isolated complex exhibited two apparent triplets at 228.6 ppm and 221.9 ppm with $^2J_{P-C}$=11.2 Hz, a triplet at 39.5 with $^2J_{P-C}$=5.2 Hz for methylene carbon, and a singlet at 14.2 ppm for the methyl carbon. Its ^{1}H NMR spectrum showed two quartets each overlapping with several other quartets at 3.18 ppm and 3.07 ppm (1:1 ratio) with $^2J_{H-H}$=6.9 Hz for the methylene protons and a triplet at 1.12 ppm with $^2J_{H-H}$=6.9 Hz for the methyl protons. Its IR spectrum gave four CO stretching bands at 1999, 1953, 1886, 1868 cm^{-1}. Elemental analyses are consistent with its formulation as complex **XXXVII**.

In the reaction with Mo(CO)$_6$, the ^{31}P NMR spectrum of the reaction mixture showed two major singlets at 152.1 ppm and 138.6 ppm (1:3 ratio). After separation on an alumina column, the Mo-cage (complex **XXXIX**) with a ^{31}P signal at 152.1 ppm was obtained as pale yellow crystals, and the complex Mo(CO)$_4$(Et$_2$N)$_2$POP(Et$_2$N)$_2$

86

(complex **XXXVIII**) containing a chelating P-O-P phosphoxane ligand with its ^{31}P peak at 138.6 ppm was obtained as a pale yellow solid. The ^{13}C NMR spectrum of the Mo cage (complex **XXXIX**), exhibited two apparent triplets in the CO region at 213.7 ppm and 206.9 ppm with $^2J_{P\text{-}C}=14.5$ Hz and a triplet at 39.2 with $^2J_{P\text{-}C}=6.1$ Hz for the methylene carbon. Its ^{1}H NMR spectrum showed an overlapping quartet at 3.37 ppm with $^2J_{H\text{-}H}=6.9$ Hz for the methylene proton and a triplet at 1.15 ppm with $^2J_{H\text{-}H}=6.9$ Hz for the methyl proton. Its IR spectrum gave four CO stretching bands at 2016, 1909, 1897, 1874 cm^{-1}. The spectroscopic data of Mo(CO)$_4$(Et$_2$N)$_2$POP(Et$_2$N)$_2$ (complex **XXXVIII**) exhibited similar features as the chromium analogue (**XXXVII**), suggesting identical coordination geometry with a chelating P-O-P phosphoxane ligand.

In the reaction with tungsten, after the same separation procedure as above, the chelate complex W(CO)$_4$(Et$_2$N)$_2$POP(Et$_2$N)$_2$ (complex **XL**) was obtained as a stable pale yellow solid in about 32% yield. Its ^{31}P NMR spectrum exhibited a singlet at 110.9 ppm with satellite peaks at 114.6 ppm and 107.0 ppm due to coupling between ^{31}P and ^{183}W (natural abundance 14.4 %, spin=1/2) nuclei with $^1J_{W\text{-}P}=136.7$ Hz. Its ^{13}C NMR spectrum in the CO region exhibited two triplets at 210.94 ppm and 203.15 ppm with $^2J_{P\text{-}C}=10.6$ Hz, each of which had satellite peaks due to coupling with a ^{183}W nucleus with $^1J_{W\text{-}C}=61.3$ Hz and other spectroscopic data are similar to it chromium and molybdenum analogues. Figure 2-3 (a) gives the proposed structure of complex (**XL**) and (b), (c) its NMR spectra.

(a)

87

(b)

(c)
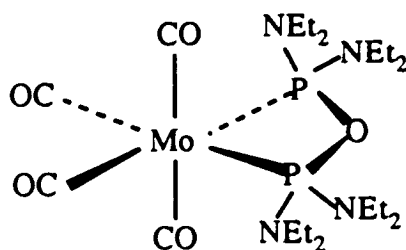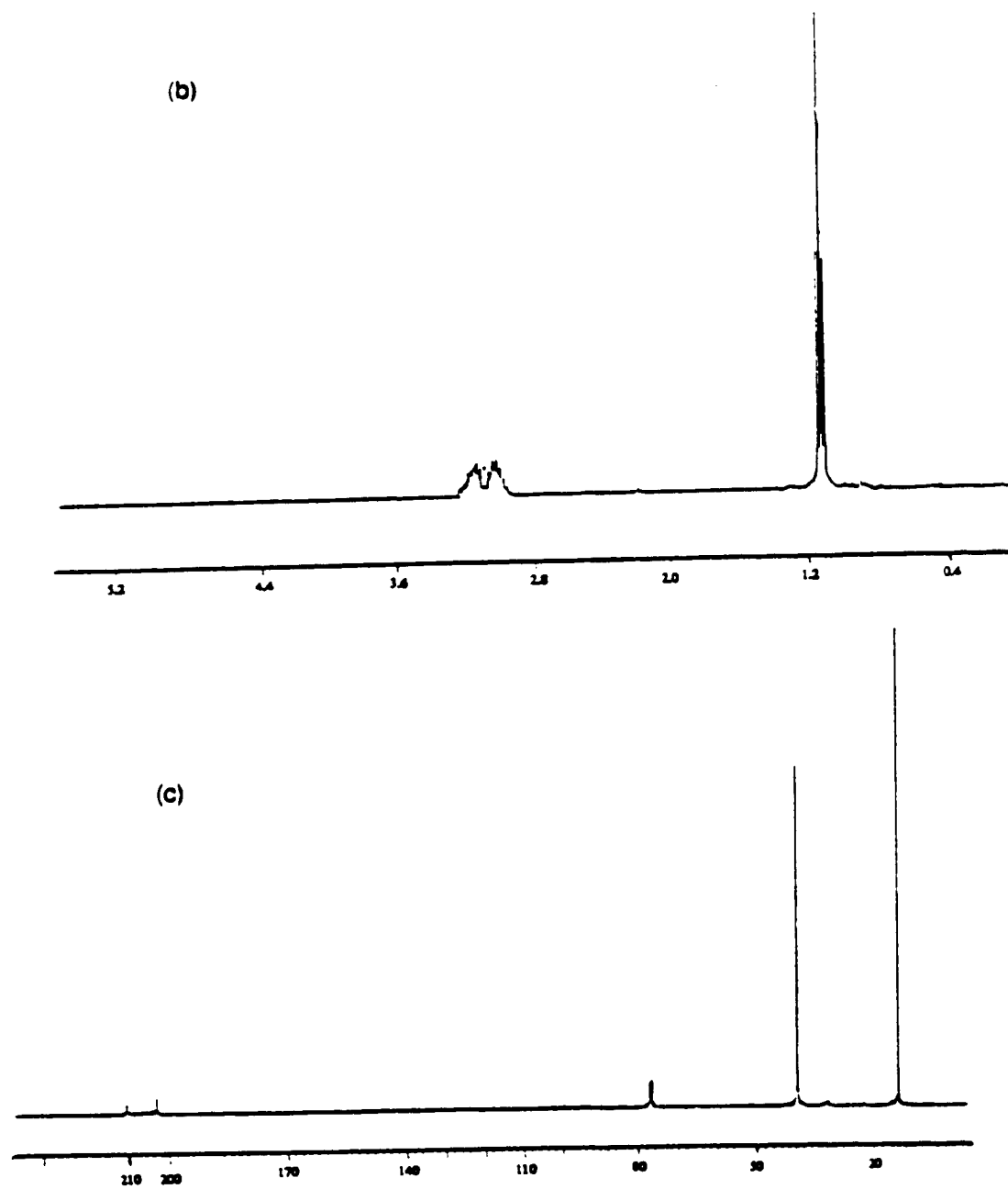
Figure 2-3: (a).Proposed structure of W(CO)$_4$(Et$_2$N)$_2$POP(Et$_2$N)$_2$ (complex XL)

(b).^{1}H NMR spectrum of complex XL

(c).^{13}C {^{1}H} NMR spectrum of complex XL

88

5. Complexation Reactions of Bis(piperidino)phosphine oxide, (PIP)$_2$P(O)H:

The reaction of **oxide V** with metal hexacarbonyls gave a black suspension also. The black precipitate was elemental metal decomposed from the metal carbonyls. In the reaction with Cr(CO)$_6$, after the same separation procedure as described above, the chelate complex (**XLI**), Cr(CO)$_4$(PIP)$_2$POP(PIP)$_2$, was obtained as a pale-yellow solid in about 10% yield. The solution ^{31}P NMR spectrum of this complex showed a singlet at 154.0 ppm. Its ^{13}C NMR spectrum exhibited two apparent triplets in the CO region at 228.1 ppm and 221.9 ppm with $^2J_{P-C}$=15.5 Hz, for methylene carbons a triplet at 45.7 ppm with $^3J_{P-C}$=3.57 Hz, a triplet at 26.3 ppm with $^4J_{P-C}$=2.1 Hz and a singlet at 24.8 ppm. Its ^{1}H NMR spectrum showed two multiplets at 3.11 ppm and 3.05 ppm (1:1 ratio) for the methylene protons on the carbons adjacent to nitrogens and multiplets from 1.58-1.57 ppm for other methylene protons. IR spectrum gave four CO stretching bands at 1999, 1906, 1889, 1878 cm^{-1} and a P-O-P stretching band at 940 cm^{-1}. Because of the similar spectroscopic data to the diethylamino analogues described in reaction 4, this complex should have a similar P-O-P phosphoxane ligand chelate coordination geometry.

In the reaction with tungsten, after the same separation procedure, the chelate complex W(CO)$_4$(PIP)$_2$POP(PIP)$_2$ (**XLII**) was obtained as a stable pale yellow solid. The proton-decoupled solution ^{31}P NMR spectrum of this complex exhibited a singlet at 132.7 ppm with satellite peaks at 137.3 ppm and 128.3 ppm due to coupling between ^{31}P and ^{183}W (spine=1/2) nuclei with $^1J_{W-P}$=166.0 Hz. Other spectroscopic data are similar to the chromium analogue, again suggesting a similar proposed chelate structure.

6. Complexation Reactions of Bis(dicyclohexylamino)phosphine Oxide, (Cy$_2$N)$_2$P(O)H:

The reaction of **oxide VI** with Cr(CO)$_6$ in hot toluene gave several products. Most of

89

these contained tetra- and pentaphosphoxane rings. The products were selectively extracted by different solvents (acetone and hexane). From the solution ^{31}P NMR spectrum of the hexane extract, the P_4O_4 ring complexes can be identified as: $Cr(CO)_4(Cy_2NPO)_4$ (**XLIII**) with a chair-chair conformation (minor product, C_{2V} symmetry, A_2X_2 at 174.0 ppm and 138.7 ppm, J_{AX}= 63.5 Hz), $Cr(CO)_4(Cy_2NPO)_4$ (**XXVII**) with a boat-chair conformation (major product, C_s symmetry, A_2XY at 176.2 ppm, 128.6 ppm, and 124.5 ppm, J_{AX}=39.1 Hz, J_{AY}=9.7 Hz, J_{XY}=2.7 Hz), and $Cr_2(CO)_8(Cy_2NPO)_4$ the cage-isomer (**XLIV**) (minor product, singlet at 157.8 ppm). After recrystallization, complex (**XXVII**) was isolated as small white crystals in about 32% yield. The other spectroscopic data of these compounds can be found in Tables 1-3, 1-4, 1-5 and 1-6.

The acetone extract yielded two products after chromatographic separation. One was a small amount of an unstable white solid, $Cr(CO)_5 \cdot (Cy_2N)_2P(O)H$ (**XLV**), whose proton-decoupled solution ^{31}P NMR spectrum gave a singlet at 94.1 ppm and proton-coupled spectrum exhibited a doublet of quintets with coupling constants of J_{P-H}=366.2 Hz and $^3J_{P-H}$=9.8 Hz. Its ^{13}C NMR spectrum exhibited two doublets in the CO region at 217.5 ppm (high intensity) and 221.8 ppm (lower intensity) with $^2J_{P-C}$=15.5 Hz, two singlets at 58.2 ppm and 58.1 ppm for methine carbons. Its ^{1}H NMR spectrum showed two triplets of triplets at 3.22 ppm and 3.18 ppm with coupling constants of $^2J_{P-H}$=12.1 Hz and $^3J_{P-H}$=3.4 Hz for methine protons. Its IR spectrum contained three CO stretching bands at 2017, 1975, 1927 cm^{-1} and a P=O stretching band at 968 cm^{-1}. These spectral data are in agreement with the proposed structure as indicated for complex XLVII. A major product was the stable white solid $Cr_2(CO)_7(Cy_2NPO)_5$ (**XLVI**). The proton-decoupled solution ^{31}P NMR spectrum of this complex exhibited an A_2MX_2 splitting pattern at 176.1 ppm, 175.1 ppm, and 155.4 ppm with J_{AM}=9 Hz, J_{AX}=0 Hz, and J_{MX}=40 Hz, suggesting a similar structure as its diisopropylamino

90

Cr$_2$P$_5$O$_5$ analogue in the literature.[9] Figure 2-4 shows (a) the proposed structure of complex (XLVI) and, (b) its proton-decoupled solution ^{31}P NMR spectrum.

(a)

P=Cy$_2$NP-

(b)
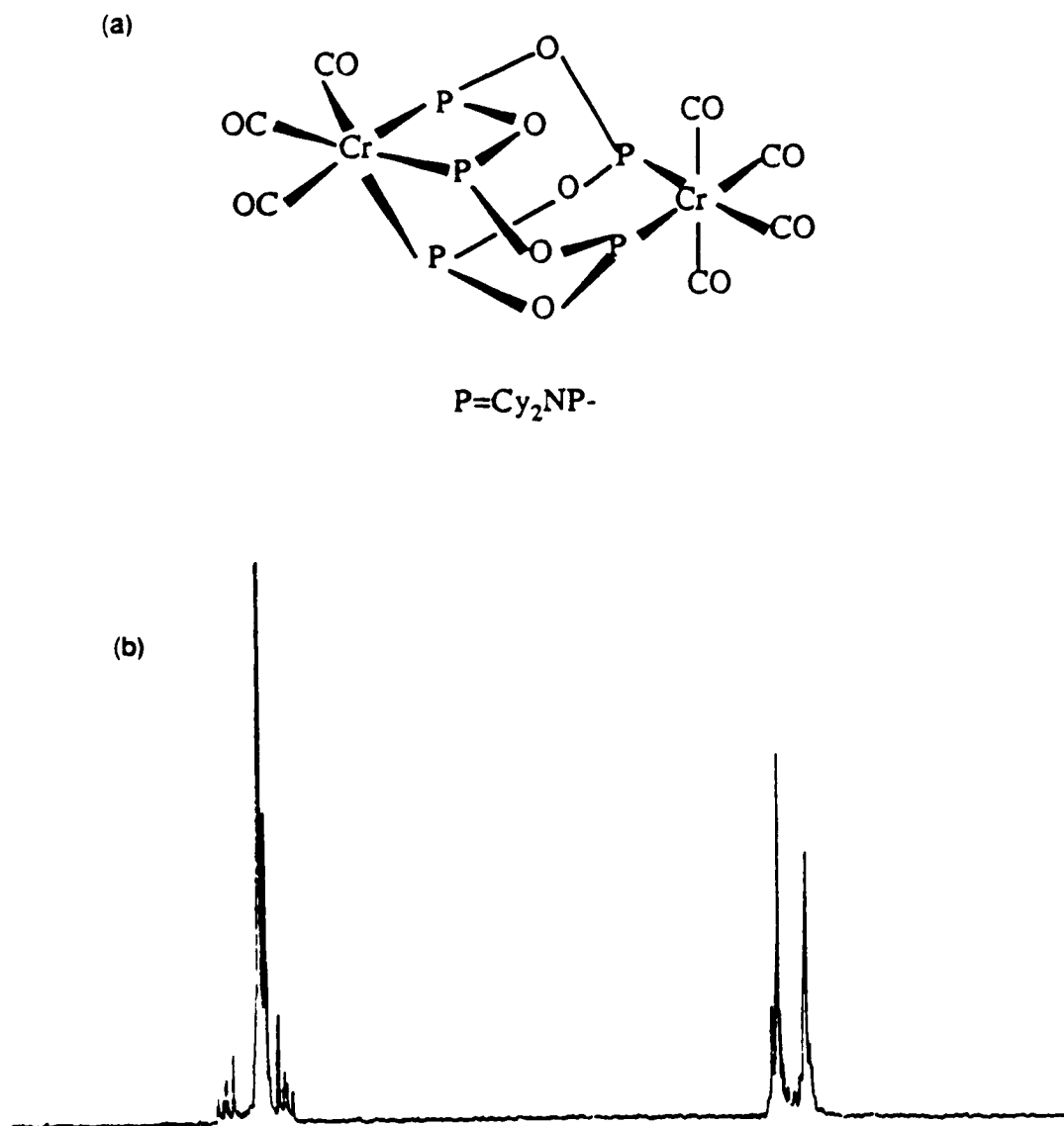
Figure 2-4: (a) Proposed structure of Cr$_2$(CO)$_7$(Cy2NPO)$_5$ (XLVI).

(b) Its ^{31}P {^{1}H} NMR spectrum.

91

The reaction of oxide VI with $W(CO)_6$ in hot toluene also gave a mixture of products. After separation by chromatograghy, two of these were isolated and characterized by spectroscopy. The major product is $W_2(CO)_7(Cy_2NPO)_5$ (XLVII) obtained as an unstable white solid in about 20% yield. The proton-decoupled solution ^{31}P NMR spectrum of this complex exhibited the expected A_2MX_2 splitting pattern at 128.6 ppm, 125.7 ppm, and 99.0 ppm with J_{AM}=1.5 Hz, J_{AX}=0.9 Hz, and J_{MX}=17.0 Hz, each one with the ^{183}W (spin=1/2) satellite peaks ($^1J_{W-P}$=185.5 Hz and 200.1 Hz), also suggesting a $W_2P_5O_5$ complex as the chromium analogue described above. Figure 2-5 shows its proton-decoupled solution ^{31}P NMR spectrum.

Figure 2-5: ^{31}P (^1H) NMR spectrum of $W_2(CO)_7(Cy_2NPO)_5$ (XLVII)

A minor product, $W_2(CO)_6(Cy_2NPO)_4$ (XLVIII), was obtained as a red solid in about 5% yield. Its spectral data are different from all other metal polyphosphoxane complexes. The proton-decoupled solution ^{31}P NMR spectrum of this complex exhibited a doublet of triplets at 267.75 ppm with J=19.8 Hz and 13.2 Hz, a doublet of doublets of doublets at 133.26 ppm with J=138.6, 105.4 and 13.2 Hz, and a doublet of doublets of doublets at 100.17 ppm with J=101.1, 32.9 and 13.2 Hz, a doublet of doublets of doublets at 133.26 ppm with J=138.6 Hz, 32.9 Hz and 19.8 Hz. Its ^{13}C NMR spectrum

92

exhibited multiplets in the CO region at 212.98 ppm, 217.65 ppm, 210.88 ppm, 210.32 ppm, 209.85 ppm, 209.45 ppm, and 206.96 ppm; and doublets at 57.89 ppm (J=9.6 Hz), 57.2 ppm (J=9.2 Hz), and 55.68 ppm (J=7.9 Hz) for methine carbons. Its ^1H NMR spectrum showed three multiplets at 3.41 ppm, 3.30 ppm, and 3.20 ppm for methine protons. IR spectrum of this complex gave CO stretching bands at 2000, 1970, 1932, 1908, 1904, 1875 cm^{-1}, suggesting a unique structure different from any other metal polyphosphoxane complexes. This unique complex will be further discussed later. Figure 2-6 shows its proton-decoupled solution ^{31}P NMR spectrum.
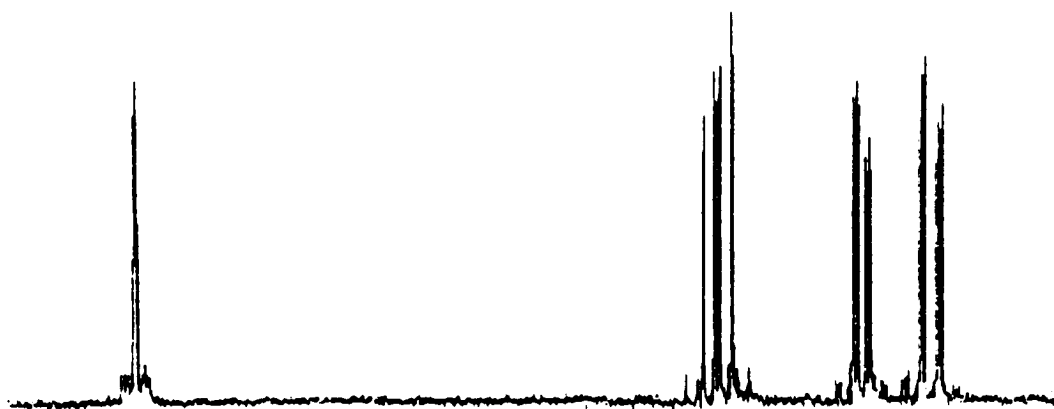
Figure 2-6: ^{31}P {^1H} NMR spectrum of $W_2(CO)_6(Cy_2NPO)_4$ (XLVIII).

The complex $W_2(CO)_7(Cy_2NPO)_5$ (XLVIII) decomposed during recrystallization in hexane to a white solid $W(CO)_4(Cy_2NPO)_3$ (XLIX). The proton-decoupled solution ^{31}P NMR spectrum of this complex exhibited an AA'X splitting pattern at 132.4 ppm and 126.0 ppm. Its ^{13}C NMR spectrum exhibited multiplets in the CO region at 206.5 ppm, 206.2 ppm, 202.4 ppm, and 201.8 ppm. Its ^1H NMR spectrum showed three multiplets at 3.5 ppm, 2.9 ppm, and 2.1 ppm for methine protons. IR spectrum of this complex gave the CO stretching bands at 2002, 1910, 1897, 1884 cm^{-1} and P-O-P stretching band at 869 cm^{-1}, suggesting a similar structure as molybdenum analogues already

93

described (complexes **XVIII, XIX**) in Chapter 1. Figure 2-7 shows its proton-decoupled solution ^{31}P NMR spectrum.
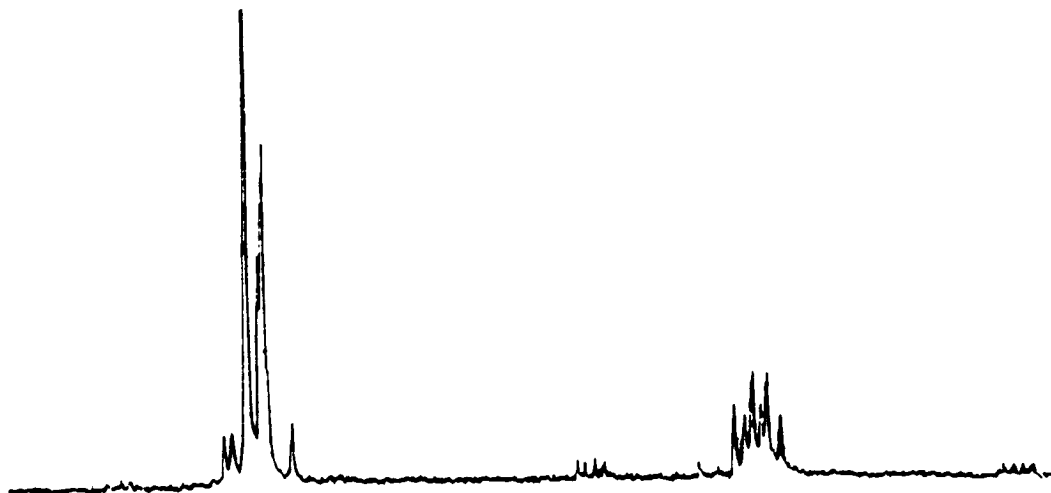
Figure 2-7: ^{31}P {^{1}H} NMR spectrum of W(CO)$_4$(Cy$_2$NPO)$_3$ (XLIX).

7. Complexation Reaction of Bis(isopropylcyclohexylamino)phosphine oxide, ('PrCyN)$_2$P(O)H:

The reaction of oxide (VIII) with Cr(CO)$_6$ in hot toluene gave similar results as above. The products identified by proton-decoupled solution ^{31}P NMR spectrum of the product mixture were Cr$_2$(CO)$_7$(^{i}PrCyNPO)$_5$ with an A$_2$MX$_2$ splitting pattern at 175.6 ppm, 174.5, and 155.7 ppm (J$_{AM}$=9 Hz, J$_{AX}$=0 Hz, J$_{MX}$=40 Hz); and Cr(CO)$_4$(^{i}PrCyNPO)$_4$ with a boat-chair conformation (C$_s$ symmetry, A$_2$XY at 176.6 ppm, 128.8 ppm, and 125.7 ppm, J$_{AX}$=38 Hz, J$_{AY}$=11 Hz, J$_{XY}$=2 Hz).

8. Complexation Reactions of Bis(dimethylpiperidino)phosphine Oxide, (DMP)$_2$P(O)H:

The reaction of oxide VII with Cr(CO)$_6$ in hot toluene also gave several products. After separation by chromatograghy, the products were characterized to be the cage-

94

isomer $Cr_2(CO)_8(DMPPO)_4$ (complex L), cage $Cr_2(CO)_8(DMPPO)_4$ (complex LI), $Cr_2(CO)_7(DMPPO)_5$ (complex LII), and $Cr_2(CO)_6(DMPPO)_6$ (complex LIII).

The minor product cage-isomer complex L was obtained as a stable pale-yellow solid in about 5% yield. The proton-decoupled solution ^{31}P NMR spectrum of the complex gave a singlet at 155.4 ppm. Its ^{13}C NMR spectrum exhibited three multiplets in the CO region at 226.17 ppm, 220.33 ppm, and 219.71 ppm. Its ^{1}H NMR spectrum showed two multiplets at 4.46 ppm and 4.22 ppm for its methine protons. The IR spectrum gave three CO stretching bands at 2006, 1942, 1892 cm^{-1} and one P-O-P stretching band at 819 cm^{-1}. X-ray quality crystals were obtained by recrystallization from hot toluene. The molecular structure of this complex is fully consistent with the spectral data. The structure of the 8-membered tetraphosphoxane ring complex chelating both cis-$Cr(CO)_4$ units is shown in Figure 2-8. There is a mirror plane containing the Cr atoms and O6 and O6a that bisects the P_4O_4 ring. The four-membered chelate rings made up of Cr1, P1, O6, P2 and Cr1a, P1a, O6a, P2a contain a small P-O-P angle of 100.9° as well as an unusually compressed P-Cr-P angle of 66.5°.[10] The other two P-O-P angles of 134.5° in P_4O_4 ring are larger than that in P_4O_4 complexes VII and XVII. The coordination geometry around each Cr is pseudo-octahedral with a compressed P-Cr-P angle of 56.8°. The two axial carbonyls are tilted away from the P_4O_4 ring with a C-Cr-C angle of 85.6°. The axial C1-Cr-C3 angle is only 169.2°, about 11° distorted from linearity. Carbonyls cis to the P-donors have average Cr-C distances of 1.879 Å and C-O distances of 1.146 Å. Corresponding average values for trans-carbonyls are 1.866 Å and 1.142 Å, consistent with known trends in trans-$Cr(CO)_4(PR_3)_2$ and $Cr(CO)_5(PR_3)$ complexes.[11,12] Atoms P1 and P2 in this heterocycles are 2.560 Å apart, only 0.23 Å longer than typical P-P single bond distance. The P-O distances of 1.635 Å and 1.657 Å and P-N distances of 1.627 Å are close to that of other polyphosphoxane rings.

95

Another minor product is the cage complex LI obtained as a pale-yellow solid in about 2% yield. The solution ^{31}P NMR spectrum of the complex consisted of a singlet at 171.1 ppm. Its ^{13}C NMR spectrum exhibited two doublets at 224.1 ppm (J=9.0 Hz), 217.1 ppm (J=19.5 Hz) in CO region. Its ^{1}H NMR spectrum showed a singlet at 4.46 ppm for methine protons. The IR spectrum gave four CO stretching bands at 2004, 1927, 1908, and 1897 cm^{-1} and P-O-P stretching band at 881 cm^{-1}. X-ray quality crystals were obtained by recrystallization from hot toluene. Its molecular structure (Figure 2-9) is similar to that of the molybdenum cage.[5] The P-O distance of 1.631 Å and 1.662 Å, P-N distances of 1.644 Å and 1.632 Å, P-O-P angles of 99.5° are close to the corresponding P-O distances of 1.650 Å and 1.642 Å, P-N bond distance of 1.665 Å, and O-P-O angles of 99.1° respectively in the molybdenum cage. The coordination geometry around each chromium is close to octahedral with a P-Cr-P angle of 80.0°. The four carbonyls are slightly tilted away from the cage with cis-C-Cr-C angles of 88.1°, 88.0°, and 84.5°. The axial C3-Cr-C4 angle of 173.1° is only about 7° distorted from linearity. The Cr-P distances of 2.329 Å, Cr-C distance of 1.879 Å are similar to the above complex (L).

The major product complex LII was obtained as a pale-yellow solid in about 18% yield. The proton-decoupled solution ^{31}P NMR spectrum of this complex exhibited the expected A_2MX_2 splitting pattern at 172.9 ppm, 171.5 ppm, and 152.4 ppm with J_{AM}=9 Hz, J_{AX}=0 Hz, and J_{MX}=40 Hz, confirming the $Cr_2P_5O_5$ structure similar to complex XLVIII and XLIX.

The trace product complex LIII was obtained as pale-yellow needles. This complex was later obtained in high yield (90%) by direct thermal reaction of complex LII with phosphine oxide (VIII) in hot xylene as in Equation 2-6. X-ray quality crystals

96
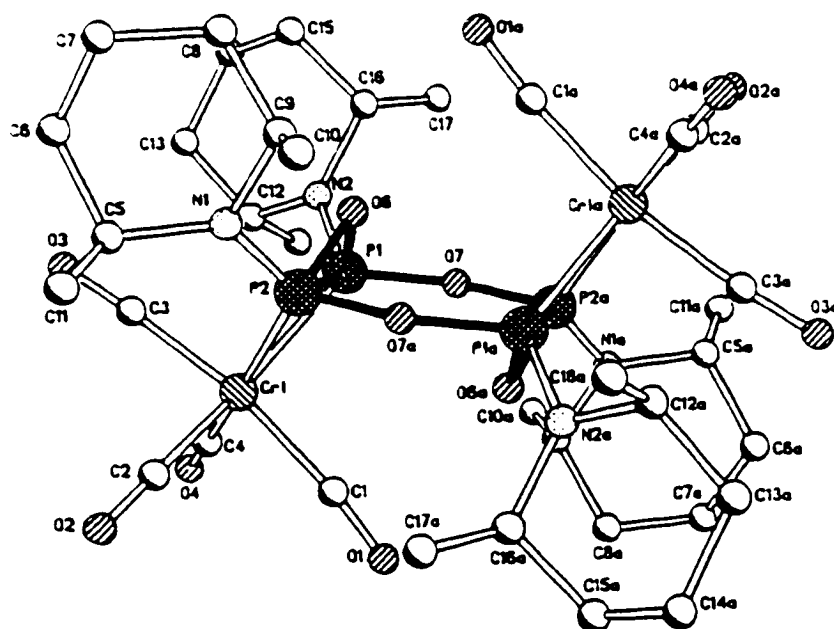
Selected bond distance and bond angles for $Cr_2(CO)_8[DMPPO]_4$ cage-isomer (L) in angstroms and degrees.

P1-Cr1	2.337	P2-N1	1.627	Cr1-C4	1.872
P1-P2	2.560	P2-O6	1.664	N2-C12	1.475
P1-N2	1.633	Cr1-C1	1.884	N2-C16	1.486
P1-O6	1.657	Cr1-C2	1.862		
P1-O7	1.635	Cr1-C3	1.875		

P1-Cr1-P2	56.7	N2-P1-Cr1	12.5	N2-P1-P2	132.5
P1-Cr1-O6	95.5	O6-P1-P2	39.7	O6-P1-N2	105.2
P1-Cr1-O7	125.9	O7-P1-P2	112.8	O7-P1-N2	100.6
P1-O6-O7	98.0	N1-P2-Cr1	127.2	N1-P2-P1	134.1
P2-Cr1-O6	95.5	O6-P2-P1	39.5	O6-P2-N1	105.9

C1-Cr1-P1	97.9	C1-Cr1-P2	98.7	C2-Cr1-P1	162.7
C2-Cr1-P2	96.3	C2-Cr1-C1	85.5	C3-Cr1-P1	89.9
C3-Cr1-P2	91.3	C3-Cr1-C1	169.2	C3-Cr1-C2	89.3
C4-Cr1-P1	100.2	C4-Cr1-P2	166.4	C4-Cr1-C1	85.6

C4-Cr1-C2	96.9	C4-Cr1-C3	85.6	O1-C1-Cr1	173.7
O2-C2-Cr1	177.5	O3-C3-Cr1	175.5	O4-C4-Cr1	178.2
P2-O6-P1	100.9	P1a-O7a-P2	134.5	P2a-O7-P1	134.5

Figure 2-8: The Molecular structure of $Cr_2(CO)_8[DMPPO]_4$ cage-isomer (L).

97
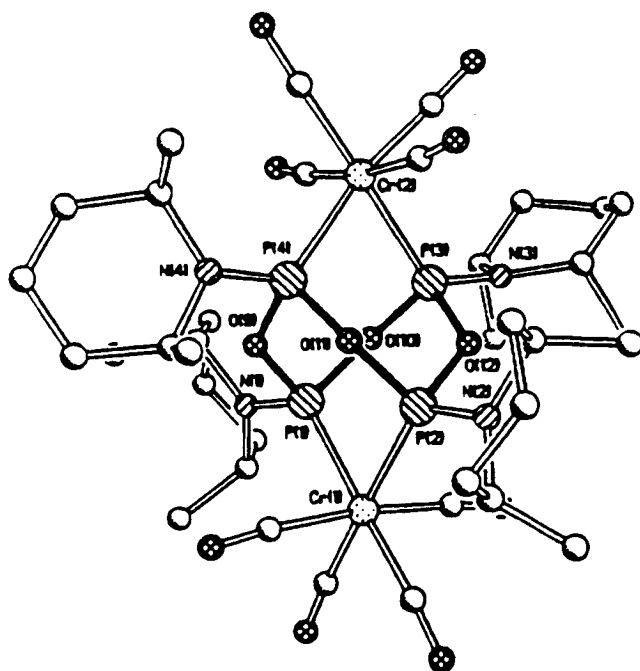
Selected bond distance and bond angles for $Cr_2(CO)_8[DMPPO]_4$ cage (LI) in angstroms and degrees.

CR1-P1	2.329	CR1-P2	2.240	CR1-C1	1.872
CR1-C2	1.852	CR1-C3	1.879	CR1-C4	1.895
P1-N1	1.644	P1-O9	1.631	P1-O10	1.662
P2-N2	1.632	P2-O11	1.656	P2-O12	1.645
P3-CR2	2.323	P3-N3	1.638	P3-O10	1.647

CR1-P2-P1	80.0	CR1-C1-P1	177.3	CR1-C1-P2	97.6
CR1-C2-P1	98.0	CR1-C2-P2	176.1	CR1-C2-C1	84.5
CR1-C3-P1	93.5	CR1-C3-P2	90.7	CR1-C3-C1	87.7
CR1-C3-C2	86.1	CR1-C4-P1	90.9	CR1-C4-P2	95.4

CR1-C4-C1	88.1	CR1-C4-C2	88.0	CR1-C4-C3	173.1
P1-C1-CR1	125.8	P1-O9-CR1	113.1	P1-O9-N1	99.0
P1-O10-CR1	112.6	P1-O10-N1	103.1	P1-O10-O9	99.5
P2-N2-CR1	126.0	P2-O11-CR1	115.1	P2-O11-N1	101.9

P2-O12-CR1	111.0	P2-O12-N2	99.8	P2-O12-O11	98.9
P3-N3-CR2	124.5	P3-O10-CR2	111.0	P3-O10-N3	100.6
P3-O12-CR2	115.6	P3-O12-N3	100.5	P3-O12-O10	101.4

Figure 2-9: The molecular structure of $Cr_2(CO)_8[DMPPO]_4$ cage (LI).

98

$$\text{Cr}_2(\text{CO})_7[\text{DMPPO}]_5 + [\text{DMP}]_2\text{P(O)H} \xrightarrow[\Delta]{\text{xylene}} \text{Cr}_2(\text{CO})_6[\text{DMPPO}]_6 + \text{CO} + \text{DMP} \quad (2\text{-}6)$$
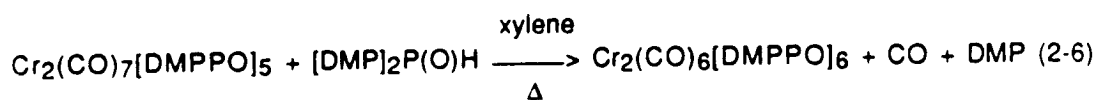
were obtained by recrystallization from hot xylene. The solution ^{31}P NMR spectrum of the complex gave a singlet at 175.5 ppm. Its ^{1}H NMR spectrum showed a multiplet at 4.47 ppm for the methine protons. The IR spectrum gave three CO stretching bands at 1949, 1893, 1876 cm^{-1} and a P-O-P stretching band at 912 cm^{-1}. Because of the poor solubility of the complex, the ^{13}C NMR data were not available. This cubane complex LIII has an overall D_{3d} symmetry. The novel 12-membered hexaphosphoxane ring is set up to complex both fac-Cr(CO)$_3$ units. In this cube structure, two chromium and six phosphoruses occupy the eight corners with six μ-O's along six P-P edges. The P-O distances of 1.652 Å and 1.627 Å, P-N distances of 1.647 Å, and O-P-O angles of 97.1° and 99.0° are close to the data of other chromium polyphosphoxane complexes L and LI. The coordination geometry around each Cr is almost octahedral with cis-C-Cr-C angles of 87.8°, 89.5°, and 90.1°. The axial P-Cr-C angle of 172.6° is about 8° distorted from linearity. The Cr-P distance of 2.335 is close to the data of the above two chromium complexes, but, the Cr-C distance of 1.835 Å with carbonyls cis to the P donors is 0.04 Å shorter. All methyl groups stay in the axial position on the piperidine ring. Figure 2-10 shows this X-ray crystal structure.

Reaction of oxide VII with Mo(CO)$_6$ in hot toluene gave Mo-cage (LIV) as a pale-yellow solid in about 50% yield. The solution ^{31}P NMR spectrum of the complex gave a singlet at 149.6 ppm. Its ^{13}C NMR spectrum in the CO region exhibited two doublets at 213.5 ppm (J=14.6 Hz), 206.9 ppm (J=12.4 Hz), a triplet at 45.6 ppm (J=6.6 Hz) for methine carbons. Its ^{1}H NMR spectrum showed a multiplet at 4.40 ppm for methine protons. The IR spectrum gave four CO stretching bands at 2012, 1928, 1914, and 1898 cm^{-1} and a P-O-P stretching band at 885 cm^{-1}. These similar spectral data again suggest a similar molybdenum cage structure as the diisopropylamino Mo described in

99
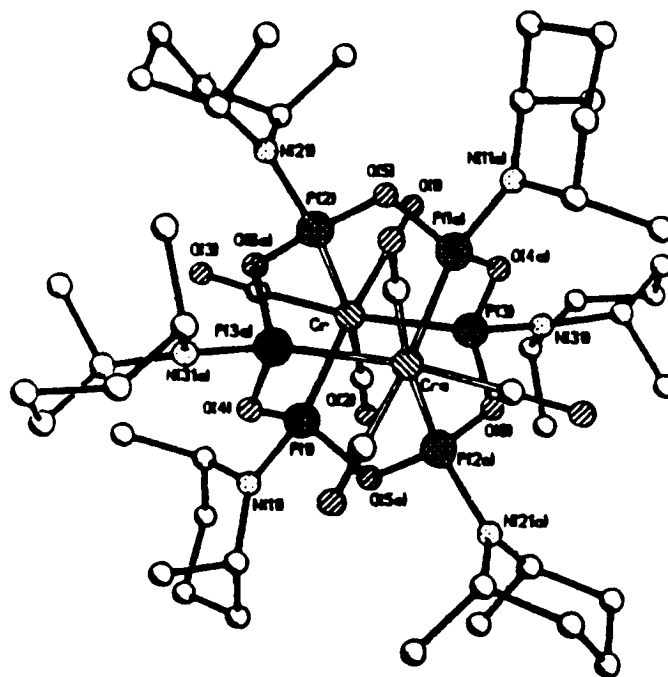
Selected bond distance and bond angles for $Cr_2(CO)_6[DMPPO]_6$ cube (LIII) in angstroms and degrees.

CR-P1	2.335	CR-P2	2.336	CR-P3	2.331
CR-C1	1.835	CR-C2	1.833	CR-C3	1.822
P1-N11	1.647	P1-O4	1.652	P1-O5A	1.627
P2-N21	1.649	P2-O5	1.661	P2-O6A	1.623
P3-O6	1.656	P3-N31	1.650	P3-O4A	1.630

P2-CR-P1	93.1	P3-CR-P1	93.0	P3-CR-P2	92.8
C1-CR-P1	172.3	C1-CR-P2	94.4	C1-CR-P3	85.1
C2-CR-P1	84.9	C2-CR-P2	172.4	C2-CR-P3	94.6
C3-CR-P1	93.1	C3-CR-P2	82.7	C3-CR-P3	172.6

C3-CR-C1	89.5	C3-CR-C2	90.1	O4-P1-CR	118.8
N11-P1-CR	122.3	N11-P1-O4	100.5	O5A-P1-CR	114.7
O5A-P1-O4	97.1	O5A-P1-N11	99.0	O5-P2-CR	119.0
N21-P2-CR	122.6	N21-P2-O5	101.5	O6A-P2-CR	113.7

O6A-P2-O5	97.1	O6A-P2-N21	98.3	O6-P3-CR	118.2
N31-P3-CR	123.3	N31-P3-O6	100.3	O4A-P3-CR	114.2
O4A-P3-O6	97.2	O4A-P3-N31	98.3	P2-CR-P1	93.1
P3-CR-P2	92.8	C1-CR-P1	172.3	C1-CR-P2	94.4
C1-CR-P3	85.1	C2-CR-P1	84.9	C2-CR-P2	172.4

Figure 2-10: The Molecular structure of $Cr_2(CO)_6[DMPPO]_6$ cube (LIII).

100

9. Complexation Reactions of Iron Nonacarbonyl with $R_2P(O)H$, $(R=^iPr_2N, Cy_2N)$:

The thermal reaction of $Fe_2(CO)_9$ with $(^iPr_2N)_2P(O)H$ Bis(diisopropylamino)-phosphine oxide gave a black suspension. This black precipitate was iron metal decomposed from the starting material. No other tractable product was obtained from this reaction. By contrast, thermal reaction of $Fe_2(CO)_9$ with $(Cy_2N)_2P(O)H$ (phosphine oxide VI) gave a brown suspension. After separation by chromatograghy, $Fe(CO)_3[Cy_2NPO]_4$ (XXV), was obtained as a pale yellow solid in about 20% yield. The NMR and IR data of this complex are given in Tables 1-3, 1-4, 1-5 and 1-6.

Table 2-3: ^{31}P $\{^1H\}$ NMR spectral data for the complexes.

Compound	Splitting pattern (δ, ppm) (J, Hz)
$Cr(CO)_4(Et_2N)_2POP(Et_2N)_2$ (XXXVII)	$\delta=162.1$
$Mo(CO)_4(Et_2N)_2POP(Et_2N)_2$ (XXXVIII)	$\delta=138.6$
$Mo_2(CO)_8[Et_2NPO]_4$ (XXXIX)	$\delta=152.1$
$W(CO)_4(Et_2N)_2POP(Et_2N)_2$ (XL)	$\delta=110.9$, $J_{W-P}=136.7$
$Cr(CO)_4(PIP)_2POP(PIP)_2$ (XLI)	$\delta=154.0$
$W(CO)_4(PIP)_2POP(PIP)_2$ (XLII)	$\delta=132.7$, $J_{W-P}=166.0$
$Cr(CO)_4[Cy_2NPO]_4$ (XLIII)	A_2X_2 $(\delta_A=174.0, \delta_X=138.7)(J_{AX}=63.4)$
$Cr_2(CO)_8[Cy_2NPO]_4$ cage-isomer(XLIV)	$\delta=157.8$
$Cr(CO)_5 \cdot (Cy_2N)_2P(O)H$ (XLV)	$\delta=94.1$ $(J=366.2, 9.8)$
$Cr_2(CO)_7[Cy_2NPO]_5$ (XLVI)	$A_2MX_2(\delta_A=176.1, \delta_M=175.1, \delta_X=155.4)$ $(J_{AM}=6.1, J_{AX}=0, J_{MX}=34.2)$
$W_2(CO)_7[Cy_2NPO]_5$ (XLVII)	$A_2MX_2(\delta_A=176.1, \delta_M=175.1, \delta_X=155.4)$ $(J_{AM}=1.5, J_{AX}=0.9, J_{MX}=17)$ $J_{W-P}=185.5$
$W_2(CO)_6[Cy_2NPO]_4$ (XLVIII)	$AXYZ(\delta_A=267.7, \delta_X=133.21, \delta_Y=100.1$ $\delta_Z=84.2)(J_{AX}=J_{AY}=13.1, J_{YZ}=32.8$ $J_{AZ}=19.7, J_{XY}=101.1, J_{XZ}=140.0)$

$$J_{W-P} = 120.0$$

W(CO)₄[Cy₂NPO]₃	(**XLIX**)	AA'X($\delta_A = \delta_{A'} = 132.4, \delta_X = 126.0$)
		($J_{AX} = 6.5$, $J_{A'X} = 10.0$)
Cr₂(CO)₈[DMPPO]₄ cage-isomer(L)		$\delta = 155.4$
Cr₂(CO)₈[DMPPO]₄ cage	(**LI**)	$\delta = 171.1$
Cr₂(CO)₇[DMPPO]₅	(**LII**)	A₂MX₂($\delta_A = 176.1, \delta_M = 175.1, \delta_X = 155.4$)
		($J_{AM} = 6.3$, $J_{AX} = 0$, $J_{MX} = 41.8$)
Cr₂(CO)₆[DMPPO]₆ cube	(**LIII**)	$\delta = 175.5$
Mo₂(CO)₈[DMPPO]₄ cage	(**LIV**)	$\delta = 149.6$

_____

All spectra were run in CDCl₃.

Table 2-4: ^{13}C {^1H} NMR spectral data for the complexes.

_____

Compound	Chemical Shifts, δ, ppm, (J, Hz)
XXXVII	CO: 228.6 (t), 221.9 (t), (J=11.2)
	CH₂: 39.5 (t), J=5.2; CH₃: 14.2
XXXVIII	CO: 219.2 (t), 210.9 (t), (J=10.6)
	CH₂: 39.4 (t), (J=6.2); CH₃: 14.1
XXXIX	CO: 213.7 (t), 209.6 (t), (J=14.5)
	CH₂: 39.2 (t), (J=6.1); CH₃: 14.6
XL	CO: 210.9 (t), 203.1 (t),(J=9.2,J_{W-C}=61.3)
	CH₂: 39.6 CH₃: 14.0
XLI	CO: 228.1 (t), 221.9 (t), (J=15.5)
	CH₂: 45.7(t)(J=3.5), 26.3(t)(J=2.1),24.8
XLII	CO: 200.0 (t), 198.9 (t), (J=10.1)
	CH₂: 45.9 (t) (J=2.5), 26.2, 24.8
XLV	CO: 221.8 (d), 217.5 (d), (J=15.3)
	CH: 58.2, 58.1
	CH₂: 35.1, 28.9, 26.9, 25.6
XLVI	CO:229.9(m),229.1(t)(J=13.5), 224.4(t)
	(J=8.9),219.7(t), 216.7(t), (J=19.5)

102

	CH:	58.5, 58.3, 57.5(d)(J=10)
	CH$_2$:	36.2, 35.9, 35.3, 34.8, 34.3, 27.3, 27.1, 26.9, 26.7, 25.8, 25.6, 25.2
XLVII	CO:	213.5(m),209.8(m),203.6(m), 201.2(m),199.1(m)
	CH:	59.0, 58.7, 58.0(d)(J=14.2)
	CH$_2$:	36.0, 35.4, 35.2, 34.8, 34.3, 27.1, 27.0, 26.9, 26.6, 25.7, 25.5, 25.2, 24.8
XLVIII	CO:	212.9(m),217.6(m), 210.8(m) 210.3(m), 209.8(m), 206.9(m)
	CH:57.8(d)(J=9.5),57.2(d)(J=9.2),57.5(d)(J=7.9)
	CH$_2$:	34.0, 33.9, 33.7, 33.6, 33.4, 31.5, 26.9, 26.6, 26.5, 25.4, 25.3, 24.9, 22.6, 14.1
XLIX	CO:206.5(m),206.2(m),202.4(m),201.8(m)
	CH:	57.7(m), 53.5(m), 52.5(m)
	CH$_2$:	33.7, 33.2, 29.4, 26.6, 25.5, 24.9, 25.0
L	CO:	213.5(m),209.8(m),203.6(m)
	CH:	47.3(t)(J=4.1), 46.1
	CH$_2$:	31.0, 30.1, 13.6
	CH$_3$:	23.3, 21.7
LI	CO:	224.1(t)(J=8.9), 217.1(t)(J=19.4)
	CH:	45.6
	CH$_2$:	30.9, 14.2
	CH$_3$:	23.2
LII	CO:	229.5(m),228.3(m), 226.4(t)(J=10.5) 219.3(t)(J=20.8), 216.2(t)(J=19.6)
	CH:	47.6(t)(J=7.0), 45.8(m), 45.6(m)
	CH$_2$:	31.44, 31.09, 31.89, 30.85, 30.56, 30.49 14.16, 14.10, 13.88
	CH$_3$:	23.36, 23.04, 22.88, 22.86, 22.53, 22.36
LIV	CO:	213.5(t)(J=14.6), 206.9(t)(J=12.4)
	CH:	45.6(t)(J=6.6)
	CH$_2$:	31.0, 14.1
	CH$_3$:	23.0

All spectra were run in CDCl$_3$ with chemical shifts referenced to internal TMS standard.

103

Table 2-5: Proton NMR spectral data for the complexes

Compound	Methine Region	Methyl(a) and/or Methylene(b) Region		
XXXVII		(a):	3.18(m), 3.07(m), (J=6.9)	
		(b):	1.12(t), (J=6.9)	
XVIII		(a):	3.15(m), 3.03(m), (J=7.0)	
		(b):	1.10(t), (J=7.0)	
XXXIX		(a):	3.37(m), (J=7.0)	
		(b):	1.15(t), (J=7.0)	
XL		(a):	3.15(m), 3.03(m), (J=7.0)	
		(b):	1.12(t), (J=6.9)?	
XLI		(a):	3.11(m), 3.05(m), 1.58-1.47(m)	
XLII		(b):	3.25(m), 2.96(m), 1.55(m)	
XLV	3.22(t),3.18(t)(J=12.1,3.4)	(a):0.88-1.19(m)		
XLVI	4.19(m),3.76(m),3.51(m)	(a):0.84-1.98(m)		
XLVII	4.21(m),3.73(m),3.10(m)	(a):0.84-1.92(m)		
XLVIII	3.41(m),3.30(m),3.20(m)	(a):0.84-2.03(m)		
XLIX	3.50(m),2.90(m),2.10(m)	(a):0.84-1.70(m)		
L	4.46(m), 4.22(m)	(a):1.55-1.87(m)		
		(b): 1.35(d), 1.40(d)(J=6.8)		
LI	4.46(s)	(a):1.15-1.18(m)		
		(b): 1.35(d)(J=7.0)		
LII	4.55(m),4.46(m),4.37(m)	(a): 1.55-1.87(m)		
	4.25(m),4.13(m)	(b): 1.41(d),1.37(d),1.32(d)(J=7.0)		
LIII	4.47(m)	(a): 1.51-1.19(m)		
		(b): 1.37(d)(J=7.0)		
LIV	4.40(m)	(a):1.50-1.92(m)		
		(b): 1.31(d)(J=7.1)		

All spectra were run in CDCl$_3$ and shifts referenced to internal TMS standard.

104

Table 2-6: Infrared Data of the Complexes

Compound	CO Stretches (cm^{-1})	P-O-P Stretches(cm^{-1})	
XXXVII	1999, 1953, 1886, 1868		918
XXXVIII	2003, 1909, 1897, 1874		927
XXXIX	2016, 1909, 1897, 1874		934
XL	2000, 1899, 1888, 1864		1005
XLI	1999, 1906, 1889, 1878		940
XLII	2016, 1948, 1905, 1876		912
XLV	2017, 1975, 1927	P=O	968
XLVI	2005, 1961, 1930, 1905, 1892, 1875		900
XLVIII	2002, 1910, 1897, 1884		869
XLIX	2000, 1970, 1932, 1904, 1875		883,834,819
L	2006, 1942, 1892		819
LI	2004, 1927, 1908, 1897		881
LII	2011, 1963, 1933, 1912, 1898, 1969		898
LIII	1949. 1893, 1876		912
LIV	2012, 1928, 1914, 1898		885

KBr pellets

105

DISCUSSION:

a) Formation of the Metal Complexes:

All three Group VI metal hexacarbonyls reacted with the phosphine oxides of type 1 upon heating in toluene or xylene to give complexes wherein carbonyls were replaced by cyclo-tetrameric, pentameric, or hexameric phosphinidene oxide $[R_2NPO]_n$ ligands. Likely intermediates would contain the P-coordinated R_2N-P=O unit, similar to that found in the $Cr(CO)_5[^iPr_2NPO]$ complex reported by Niecke and co-workers.[13] A prime driving force for this and subsequent oligomerization steps must be the elimination of a bulky dialkylamine group from the metal-coordinated phosphinous acid fragment $(R_2N)_2P$-OH. Because the oxygen-coordinated complex **XLIII** was isolated from reaction 6, the first step of the reaction may be the replacement of CO group of $M(CO)_6$ by an oxygen of the phosphine oxide. Then, this unstable compound may rearrange to phosphinous acid coordinated intermediates (Scheme 8). Oligomerization to form the polyphosphoxane ring through elimination of amine and addition of more $[R_2NPO]$ units was confirmed by the formation of Cr-cubane complex **LII** as indicated in Equation 2-6.

The thermal reactions of $Fe_2(CO)_9$ with phosphine oxides clearly showed the subtle influence of different substituents on the products. Reaction of $Fe_2(CO)_9$ with oxide **VI** gave the tetraphosphoxane ring complex (**XXXV**). Simply changing cyclohexyl group to an isopropyl in $(^iPr_2N)_2P(O)H$ gave no tractable product. This influence also appeared in the formation of different polyphosphoxane ring complexes in the reactions of chromium hexacarbonyl. With the dicyclohexylamino group, both monometallic and bimetallic chromium complexes were obtained. Monometallic complexes cis-$Cr(CO)_4(Cy_2NPO)_4$ isomers, featuring the tetraphosphoxane ring as a 1,5-chelating ligand include chair-chair and chair-boat conformations of the P_4O_4 ring. Bimetallic

106

SCHEME 8:

$(R_2N)_2P(O)H + M(CO)_6 \xrightarrow{-CO} (R_2N)_2P\overset{H}{\underset{\underset{M(CO)_5}{\downarrow}}{\diagdown O}} \longrightarrow (R_2N)_2P\text{-OH}\overset{}{\underset{\underset{M(CO)_5}{\downarrow}}{}}$

$\xrightarrow{-R_2NH} R_2N\text{-}P\text{=}O\underset{\underset{M(CO)_5}{\downarrow}}{}$

$\overset{-R_2NH}{\underset{+(R_2N)_2P(O)H}{\nearrow}}$ M$_2$(CO)$_8$[R$_2$NPO]$_4$

M=Cr, Mo

$\overset{+(R_2N)_2P(O)H}{\underset{-R_2NH}{\searrow}}$ M(CO)$_4$[R$_2$NPO]$_4$

+

M$_2$(CO)$_8$[R$_2$NPO]$_4$ cage-isomer

+

M$_2$(CO)$_7$[R$_2$NPO]$_5$

+

M$_2$(CO)$_6$[R$_2$NPO]$_6$

(M=Cr, W)
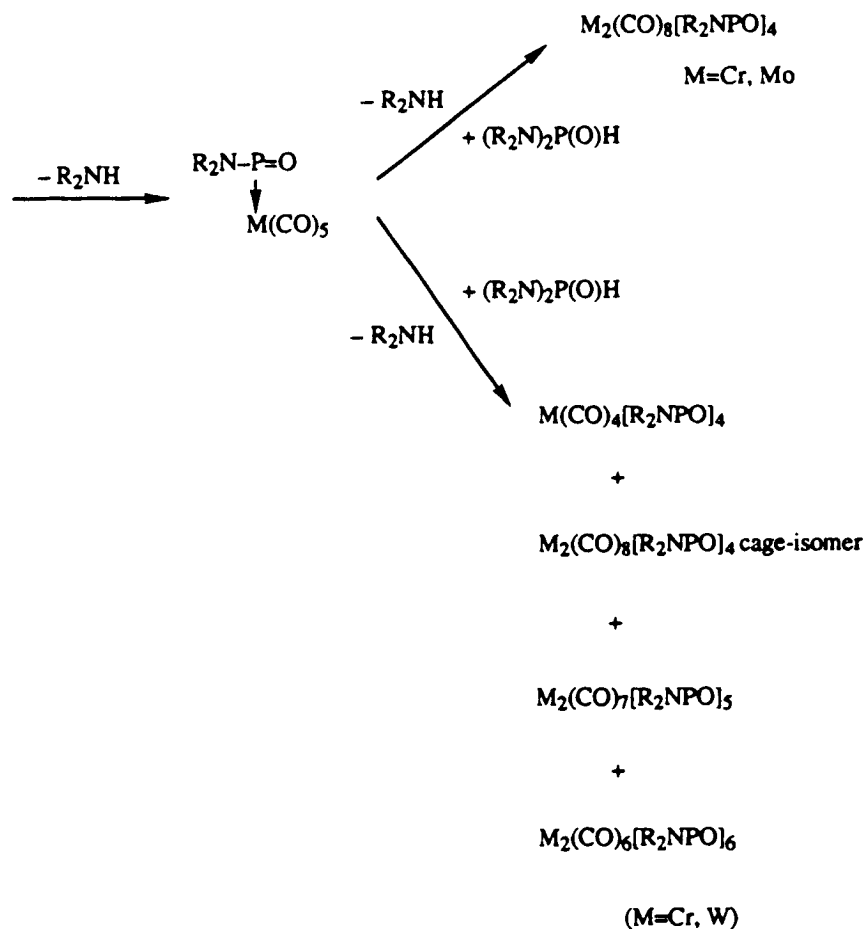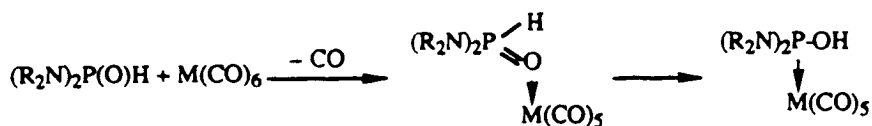
products are mainly dichromium-P$_5$O$_5$ complexes with small amounts of the cage-isomer. With the DMP group, all isolated products are bimetallic complexes. Chromium cage complex LI was also produced in this thermal reaction, as well as trace amounts of the chromium-P$_6$O$_6$ complex LIII. Since this Cr$_2$P$_6$O$_6$ complex can be formed in high

107

yield by direct thermal reaction of the chromium-P_5O_5 complex with excess phosphine oxide, it supports the stepwise build up of these P_nO_n rings around metal templater. Here in the structure of the chromium-P_5O_5 complex, the pentaphosphoxane ring coordinates one cis-$Cr(CO)_4$ and one fac-$Cr(CO)_3$ unit. By adding one $[R_2NPO]$ unit to the P_5O_5 precursor and loss of another CO from the cis-$Cr(CO)_4$ moiety, a symmetrical CrP_6O_6 cage can form. Scheme 9 illustrates this ring expansion.

SCHEME 9:
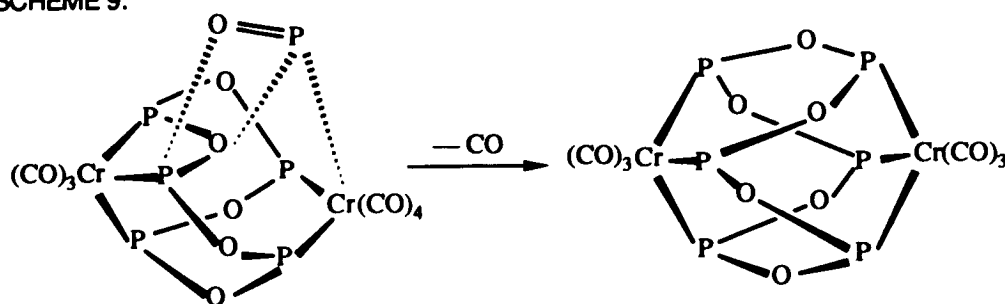
Different metals in the Cr triad also behave differently. Reactions of $Mo(CO)_6$ gave only Mo-cage complexes. Chromium forms both monometallic and bimetallic complexes. Tungsten can also form bimetallic P_5O_5 complexes, though these are unstable and decompose to monometallic P_3O_3 complexes.

Formation of the red tungsten complex **XLVIII** is an interesting phenomenon. According to literature,[11] similar molybdenum diisopropylaminophosphoxane analogues were obtained by nucleophilic attack of the Mo-cage by amines or phosphines. Compound XLVIII may thus be produced by similar carbonyl substitution at an unisolated tungsten-cage precursor with the dicyclohexylamine already eliminated from the phosphine oxide. Dicyclohexylamine is an effective nucleophile with the high boiling point which allows it accumulated in solution to react with any tungsten cage complex formed. Subsequently, one P-O-P intracage linkage was cleaved and oxidatively added to the two tungsten

108

vertices to create a μ_2-PO$^-$ as well as a μ_2-P$^-$ bridge. In addition, an intracage metal-metal bond formed. Further, the dicyclohexylamine was replaced by the free CO lost from $W(CO)_6$ in solution to give the final product (Scheme 10).

SCHEME 10:

$$[\ W_2(CO)_8[Cy_2NPO]_4\ ] \quad + \quad Cy_2NH$$
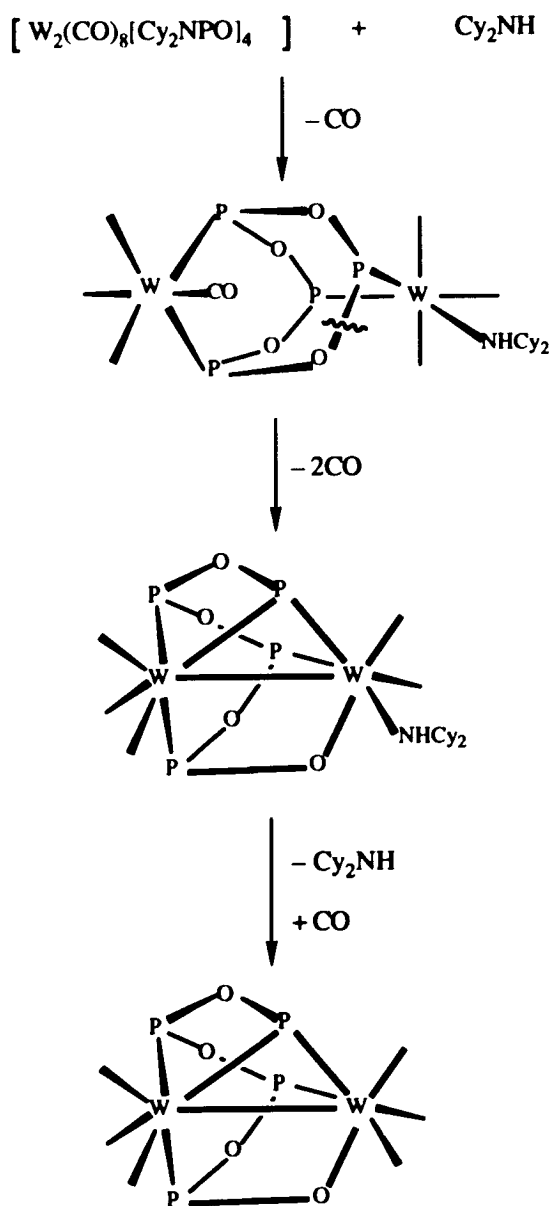
All three Group VI metal hexacarbonyls reacted with the phosphine oxides of **Type 2** upon heating in toluene or xylene to give chelate complexes wherein two carbonyls were replaced by a bidentate phosphoxane $[(R_2N)_2POP(R_2N)_2]$ ligand. Only a small amount of Mo-cage complex was isolated. According to Scheme I, in order to form cyclopoly-phosphoxane ring complexes, likely intermediates may contain the P-coordinated R_2N-$P=O$ unit. Since diethylamino and piperidino groups are less sterically bulky compared to diisopropylamino, dicyclohexylamino, and DMP groups, they may not provide sufficient driving force for amine elimination. Therefore, the opportunity of forming these intermediates is much diminished by changing phosphine oxide from **Type 1** to **Type 2**. On the other hand, the intermediates containing cis-coordinated phosphinous acid fragments $(R_2N)_2P\text{-}OH$ could be formed. The elimination of water from these intermediates to form complexes with diphosphoxane can then occur (Scheme 11). Because of the chelate effect, a complex with such a bidentate ligand should more stable than a comparable complex with monodentate ligands only.

SCHEME 11:

$$(R'_2N)_2P(O)H + M(CO)_6 \xrightarrow{-2CO}$$

$$\xrightarrow{-H_2O} \quad (M=Cr, Mo, W)$$
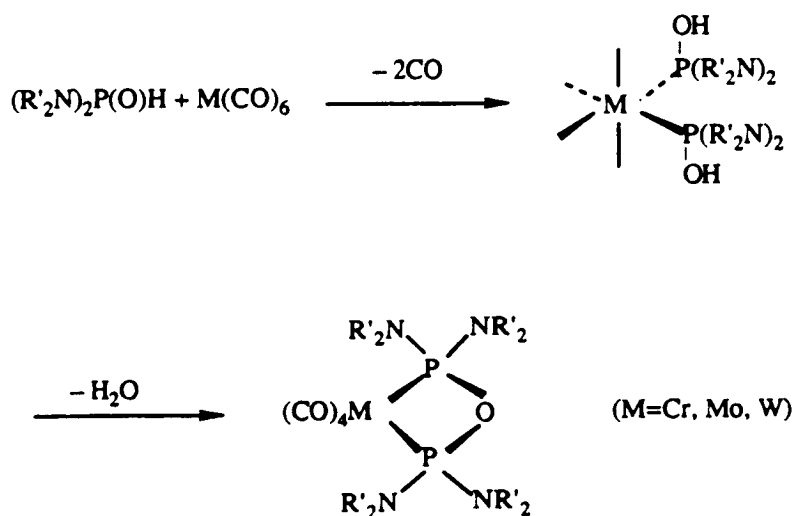
The oxides of **Type 3** yielded product mixtures that were unstable and hard to purify. Because of the tendency of certain trivalent phosphorus compounds to redistribute groups linked to phosphorus, every step of the formation of phosphine monochloride produced mixtures of disproportionation, $P(OR)_3$, $P(OR)_2Cl$, and $P(OR)_2(NR2)$, as well as $P(OR)(NR2)_2$. Starting from phosphorus trichloride, the better literature synthetic procedure requires first formation of $(RO)PCl_2$ and subsequent preparation of $(RO)(NR_2)PCl$.[27] Since the reaction of amines with phosphorus chloride is straightforward and more easily controlled than the formation of P-O bonds from attack of phenol on phosphorus trichloride, the chance of forming sideproducts is reduced by delaying the amine reaction till the second step. Purification by distillation was unsuccessful due to thermal decomposition of the product mixtures.

b) NMR and IR spectra:

Proton-decoupled ^{31}P NMR spectroscopy typically provides firm structural assignments for many of the products. Observed coordinated P chemical shifts at 154 ppm-175 ppm, 138 ppm-152 ppm, 110 ppm-133 ppm for Cr, Mo, and W, respectively, are in the expected shift ranges for phosphine complexes of this triad.[28] The $^1J_{PW}$ coupling constants of 136 Hz-166 Hz are also reasonable. In complex LV, coordination dramatically shifts the P resonance from 7.6 ppm in the original oxide VI to 94.1 ppm in the complex. The one-bond coupling constant between phosphorus and hydrogen also decreased from 571 Hz to 366 Hz in the complex.

In chelate P-O-P phosphoxane coordinated complexes **XXXVII-XLIV**, chemical shifts of P vary with the different R group of phosphorus. In chromium complexes, this difference is around 8 ppm between complex **XXXVII** with diethylamino groups and complex **XLI** with the piperidino groups. In tungsten complexes, this difference is

111

around 11 ppm between complex **XL** with diethylamino group and complex **XLII** with the piperidino group. In polyphosphoxane ring complexes, the difference of chemical shift caused by different R groups of phosphorus is small, typically around 4 ppm between complex **XLIV** with the dicyclohexylamino group and complex **L** with the dimethyl-piperidino group, both having the same structure of $Cr_2(CO)_7[R_2NPO]_5$.

The large difference of chemical shift in polyphosphoxane ring complexes is mainly caused by different coordination geometries. Comparing the chromium cage **LI** and cage-isomer **L** with the same molecular formula, $Cr_2(CO)_8[DMP \cdot PO]_4$, the difference is around 15 ppm. In the chromium cage complex, a singlet at 171 ppm is close to the 177 ppm and 174 ppm observed for the coordinated P atoms in complexes **XXIV** and **XLIII**, $Cr(CO)_4[R_2NPO]_4$, all of these having 6-membered chelate rings. By contrast, the singlet at 155.4 in the chromium cage-isomer complex is significantly shifted upfield. Both ^1H and ^{13}C NMR spectra of this complex revealed two distinct diastereotopic methine groups. These spectra suggest a lack of symmetry about the cis-CrP_2 chelate plane. A reasonable structure would have a tetradentate P_4O_4 ring in a twist-boat/twist-boat (C_i) conformation 1,3- and 5,7-coordinated to two cis-$Cr(CO)_4$ moieties (Figure 2-11). The resulting four-membered Cr-P-O-P chelate rings can account for the -15 ppm upfield shift (the ring contribution of a four- versus a six-membered chelate ring)[29] of the ^{31}P signal in **L** compared to **LI**. This structural assignment was confirmed by X-ray structural determination (Figure 2-8).

112
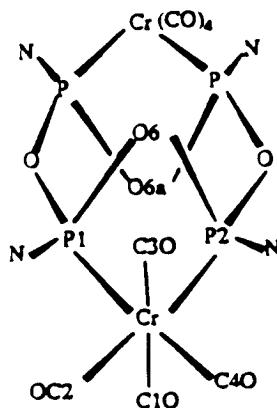
Figure 2-11: Structure of Complex L

The pentaphosphoxane ring complexes **XLVI**, **XLVII**, and **LII** have the typical A_2MX_2 splitting patterns in their proton-decoupled ^{31}P NMR spectra, corresponding to a conformation of the 10-membered pentaphosphoxane ring set up to complex both the cis-$Cr(CO)_4$ and fac-$Cr(CO)_3$ units (Figure 2-12).[9] Assuming that the solid-state structure is retained in solution and that the high-field multiplet is due to the four-membered chelate ring, we can assign the MX_2 portion of spectra to the fac-$M(CO)_3$ (M=Cr, W) P nuclei and the A_2 resonances to the cis-$M(CO)_4$ (M=Cr, W) P nuclei.
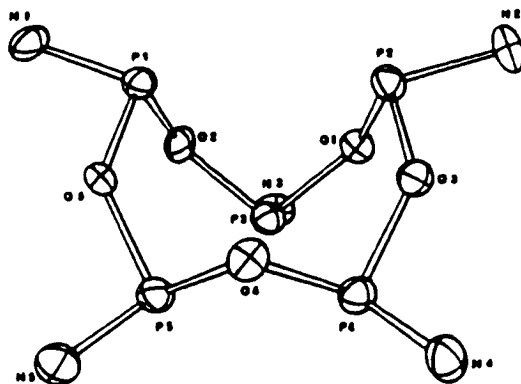
Figure 2-12: Conformation of the P_5O_5 ring in complexes **XLVI**,
XLVII, and **LII**

113

The proton-decoupled ^{31}P NMR spectrum of red tungsten complex **XLVIII** exhibited an AXYZ pattern with the A resonance far downfield at 267.7 ppm. These four separate resonances illustrate significant changes from a symmetrical cage structure. The XYZ resonances at 133.2 ppm, 100.1 ppm, and 84.2 ppm are typically due to coordination with tungsten. The coupling constant of $^1J_{P-W}$=120 ppm between ^{183}W and ^{31}P are observed for all four resonances indicating P-W bonding in all cases. The low-field multiplet at 267.7 ppm is inconsistent with typical W-coordinated tertiary phosphines or phosphites and is instead in the region for phosphenium cations or phosphido ligands.[30,31] The X-ray structure of the molybdenum diisopropylamino analogue[11] explicitly showed the latter to be present. Since the phosphido chemical shift is known to be quite sensitive to the extent of metal-metal interaction,[32] the same trend of shift value at 306.3 ppm from molybdenum and 267.7 ppm to tungsten implies that this complex **L** can have a structure similar to its molybdenum analogue (Figure 2-13).
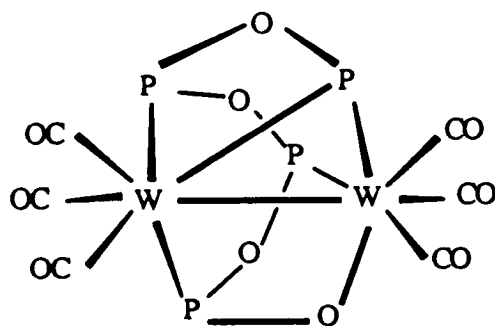
Figure 2-13: Proposed structure of complex **L**

The four CO stretching bands of chelating phosphoxane complexes in their Infrared spectra are consistent with the C_{2v} symmetry around a single metal center, suggesting the cis-M(CO)$_4$P$_2$ coordination sphere. The CO stretching bands are also useful in

114

structural assignment of polyphosphoxane complexes. Three CO stretching bands appeared in the Cr cube complex which has near C_{3v} symmetry around each metal center with fac-$Cr(CO)_3P_3$ coordination sphere. The number of V_{CO}'s expected for this compound should be two (a_1 + e) according to C_{3v} symmetry. The CO fine-structure in the 1876-1893 cm^{-1} region can be explained as discussed in Chapter 1.

c) Structure Comparisons:

The P-N and P-O bond lengths in all metal polyphosphoxane complexes are very close in the range of 1.61-1.63 Å and 1.61-1.68 Å respectively. The P-O-P bond angles are in the range of 121.3°-129.6° except in complexes XXX and L which have two sets of P-O-P bond angles. In bimetallic XXX (Figure 1-19), three phosphoruses coordinate to two metals. The P-O-P bond angles between these P's are only 117.7°, smaller than average bond angles in other metal polyphosphoxane complexes, because formation of the metal-metal bond (Fe-Mo) forces the three P's to bent toward each other in order to bridge two metals. Second set of P-O-P bond angles at 127.4° is in the normal range because one P remains uncoordinated. Electron counting on both metals are of interest. Mo with 16 e's would be electon-dificient but for the lone pair donation from the 18 e's electron-precise Fe center. In complex L (Figure 2-8), due to small chelate ring size the P-O-P bond angle in the four-membered Cr-P-O-P chelate rings are at 100.9°, smallest among the polyphosphoxane ring values. By contrast, other P-O-P bond angles in the P_4O_4 ring are at 134.5°, large compared to other rings. P-O bond lengths in such Cr-P-O-P chelate rings are 1.66 Å, about 0.3 Å longer than other P-O bond length (1.63 Å) in this P_4O_4 ring. It keep to maintain the four-membered Cr-P-O-P rings. The smaller P-O-P bond angles and longer P-O bond length.

Generally, P-M-P bond angles in square-planar and octahedral geometries with

115

monodentate phosphines are at around 95°. In metal polyphosphoxane complexes, the P-M-P bond angles in such geometries are smaller due to the chelating nature of the ligands. In complexes VII (Figure 1-8) and XVII (Figure 1-10) with square-planar geometries at metal centers, the angles are 84.4° and 85.7°, or about 15° smaller than typical values. In bimetallic complex XXX and Cr-cage LI (Figure 2-9) with octahedral geometries at their metal centers, these values are 83.0° and 80.0° respectively. Complexes L and LIII (Figure 2-10) with octahedral geometries at their metal centers show different values each other and from the other four complexes. The compressed P-M-P bond angle of 66.5° in complex L is certainly due to the smaller chelate ring. While the value of 93.0° in complex LIII with three six-membered chelate rings is close to the idealized value. The discussed bond lengths and bond angles are summarized in Table 2-7.

Table 2-7: Summary of Bond Lengths and Bond Angles

Compound		P-O (Å)	P-O-P (°)	P-M-P (°)
$PdCl_2[^iPr_2NPO]_4$	VII	1.61-1.68	128.4	84.4
$PtCl_2[Cy_2NPO]_4$	XVII	1.61-1.68	121.3	85.7
$Fe(CO)_3[^iPr_2NPO]_4Mo(CO)_4$	XXX	1.62-1.67	117.7(127.4)	83.0
$Cr_2(CO)_8[DMP-PO]_4$	L	1.63-1.66	100.9(134.5)	66.5
$Cr_2(CO)_8[DMP-PO]_4$	LI cage	1.63-1.66	127.6	80.0
$Cr_2(CO)_6[DMP-PO]_6$	LIII	1.62-1.65	123.3	92.7

116

Conclusions and Suggestions for Future work

The thermal reaction of phosphine oxide, $(R_2N)_2P(O)H$, with Group VI metal carbonyls and direct substitution of $[R_2NPO]_3$ at metal complexes of labile ligands provide two approaches to the synthesis of polyphosphoxane complexes. The formation of a novel P_6O_6 complex from the direct thermal reaction of phosphine oxide with a P_5O_5 phosphoxane complex provides insight into the production of polyphosphoxane ring complexes. Polyphosphoxane complexes with even larger rings may be synthesized by the methods developed here.

X-ray structural data and solution NMR spectra show that the tetraphosphoxane rings are unusually versatile in their coordinative and conformational flexibility (Scheme 12). They can be 1,3,5,7-tetradentate ligands adopting the boat-boat conformation in bimetallic Mo, Cr, and Ni cage complexes or the isomeric 'open' structure with the P_4O_4 ring in a C_i twist-boat geometry. They can also function as a 1,5-bidentate donor toward a single metal center, adopting either chair-boat or chair-chair forms. Additionally, a 1,3-chelating mode is also feasible for smaller metals like Ni(II). Even a 1,3,5-tridentate mode bridging two different metals has been conformed.

SCHEME 12:

1,3-chelating mode   1,5-chelating chair-chair mode   1,5-chelating boat-chair mode

117

| cage, boat-boat mode | twist-boat mode | 1,3,5-metal bridging mode |
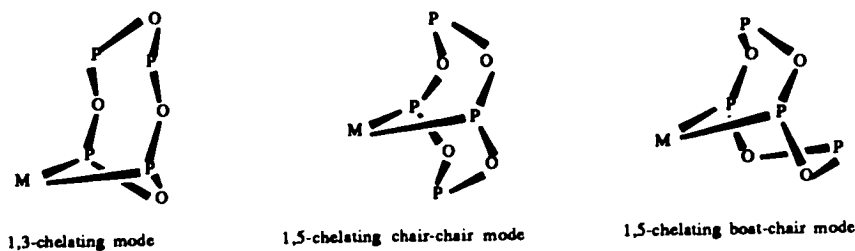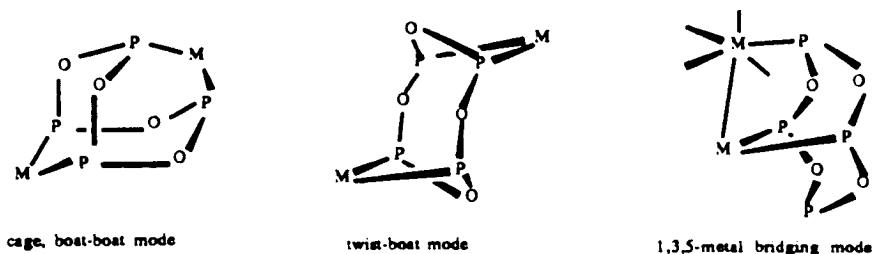
The triphosphoxanes, $[R_2NPO]_3$, behave as bidentate ligands (Scheme 13), yielding significantly less robust products that readily transform into tetraphosphoxane cage complexes. They can be suitable starting materials to build up to tetra- or pentaphosphoxane rings around metal (II) ion centers. By contrast, as a free ligand, the tetraphosphoxane ring is unstable relative to the triphosphoxane ring, reverting to it under ambient conditions.

SCHEME 13:
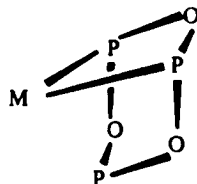
The formation of pentaphosphoxane $[R_2NPO]_5$ rings was achieved by choosing appropriate R groups on the dialkylamino P-substituent. The P_5O_5 rings can serve as the pentadentate ligands bridging one cis-coordinated M (0) or M (II) and one fac-coordinated M (0). They also can function as 1,5-bidentate donors toward a single metal center (Scheme 14).

SCHEME 14:

118
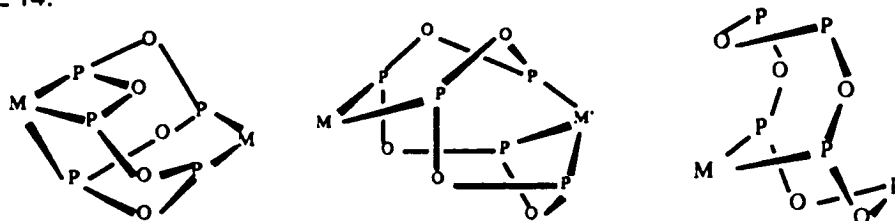
The novel hexaphosphoxane [DMP-PO]$_6$ ring was formed around two chromium centers. Structural characterization confirmed that it can serve as a hexadentate ligand simultaneously toward two fac-coordinated metals. Formation of this complex illustrates that P_nO_n (n > 5) rings can be built up by stepwise addition of R-P=O units from the thermal reaction of M-P$_5$O$_5$ complex with excess $(R_2N)_2P(O)H$.

Monometallic polyphosphoxane ring complexes can be suitable precursors to new heterobimetallic complexes in which tetra- and pentaphosphoxane rings can be tri-, tetra-, or pentadentate ligands coordinating two different metals. New heterobimetallic or even trimetallic complexes can be formed by choosing suitable monometallic precursors. Furthermore, the polyphosphoxane ring can transfer between metals dependent upon metal affinity toward such rings. Some metal polyphosphoxane complexes could be produced from this ring transfer reaction which cannot be formed directly from substitution and thermal reactions.

A Ni(0)-cage complex may be accessible in high yield by choosing zero-valent Ni starting complexes. Its chemistry and potential catalytic properties can then be investigated.

119

EXPERIMENTAL

All experiments were carried out using standard Schlenk techniques under a dry nitrogen atmosphere. Hexane was distilled from CaH_2 and toluene from sodium, while THF was distilled from sodium benzophenone ketyl. Triethylamine was distilled from KOH before use. Phosphorus trichloride, diisopropylamine, dicyclohexylamine, piperidine, and dimethylpiperidine were reagent grade chemicals obtained from Aldrich Chemicals. Molybdenum hexacarbonyl, chromium hexacarbonyl, and tungsten hexacarbonyl were purchased from Pressure Chemicals, Inc.

^{1}H, ^{13}C and ^{31}P NMR spectra were recorded on both the JEOL FX90Q and the Bruker AM 360 spectrometers using an internal deuterium lock. ^{1}H and ^{13}C shifts were referenced to internal TMS, while ^{31}P shifts were referenced to external 85% phosphoric acid. Infrared spectra were recorded on a Perkin-Elmer 283B instrument. Elemental analyses were performed at the University of New Hampshire Instrumentation Center using a Perkin-Elmer 240B Elemental Analyser.

(Norbornadiene)chromium tetracarbonyl,[33] (norbornadiene)molybdenum tetracarbonyl,[34] (norbornadiene)tungsten tetracarbonyl,[35] (cycloheptatriene)molybdenum tricarbonyl,[36] nickel dichloride dimethoxyethane,[37] nickel dibromide dimethoxyethane,[38] nickel diiodide ditetrahydrofuran,[39] bis-(benzonitrile)palladium dichloride,[40] bis-(benzonitrile)palladium dibromide,[41] (norbornadiene)platinum dichloride,[42] bis-(diisopropylamino)phosphine oxide, bis-(dicyclohexylamino)-phosphine oxide VI,[7] bis-(diethylamino)phosphine oxide VI, bis-(piperidino)-phosphine oxide V,[43] were prepared according to the literature.

120

[iPr2NPO]3 Tris-[(diisopropylamino)phosphoxane] **Ring 1**. An amount of 6.4 ml (8.1 g, 40 mmol) of (iPr2N)PCl2 and 11.2 ml (8.1 g, 80 mmol) of triethylamine in 60 ml of THF was chilled in an ice bath. From a dropping funnel, 0.61 ml (30 mmol) of distilled water in 30 ml of THF was added dropwise with rigorous stirring over 2 h. After addition was completed, the reaction mixture was allowed to warm to room temperature and refluxed an additional 1 h. After cooling, the white precipitate of amine hydro-chloride was filtered off and the THF filtrate was evaporated and extracted by hot hexane. After evaporation of hexane, the residue was 4.7 g (80%) of the white solid **Ring 1**.

[Cy2NPO]3 Tris-[(dicyclohexylamino)phosphoxane] **Ring 2**. An amount of 27.5 g (97 mmol) of (Cy2N)PCl2 and 11.2 ml (19.7 g, 194 mmol) of triethylamine in 100 ml of THF was chilled in an ice bath. From a dropping funnel, 1.70 ml (94 mmol) of distilled water in 30 ml of THF was added dropwise with rigorous stirring over 2 h. After addition was completed, the reaction mixture was allowed to warm to room temperature and refluxed an additional 1 h. The white precipitate of amine hydro-chloride was filtered off and the THF filtrate was evaporated and extracted by hot hexane. After cooling of the hexane solution, the white precipitate was filtered and dried under vacuum to give 33 g (50%) of the white solid **Ring 2**. Anal. Calcd for $C_{36}H_{66}N_3OP_3$: N, 6.16; C, 63.43; H, 9.69; Found: N, 6.29; C, 63.23; H, 9.75.

[sBu2NPO]3 **Ring 3**, [Ph2NPO]3 **Ring 4**, [iPrCyNPO]3 **Ring 5**, and [iPrPhNPO]3 **Ring 6**. An amount of 29 mmol of phosphine dichloride and 58 mmol of triethylamine in 100 ml of THF was chilled in an ice bath. From a dropping funnel, 27 mmol of distilled water in 30 ml of THF was added dropwise with rigorous stirring over 2 h. After addition was completed, the reaction mixture was allowed to warm to room temperature and refluxed an additional 1 h. The white precipitate of amine hydro-

121

chloride was filtered off and the THF filtrate was evaporated and extracted by hot hexane. After evaporation of hexane, the residue of thick liquids were crude products and were used without further purification. Rings were checked for purity by ^{31}P NMR spectroscopy before use in subsequent reactions.

(^{i}Pr$_2$N)(BHT)P(O)H (Oxide I): An amount of 0.2 mole of PCl$_3$ was added dropwise into a mixture of 0.2 mol of BHT and 0.6 mole of triethylamine at room temperature. The suspension was refluxed for 20 min. and cooled down to room temperature. The 200 ml of CH$_2$Cl$_2$ was added and the suspension was cooled down to -78°C. The 0.2 mol of ^{i}Pr$_2$NH was added dropwise with vigorously stirring. The suspension warmed to room temperature for 2 h. After filtration, an amount of 0.2 mol of water was added dropwise with vigorous stirring into the filtrate at 0°C over 3 h. Then the suspension was filtered to remove large amounts of white solid amine hydrochloride. The filtrate was washed three times with water and dried with anhydrous CaCl$_2$. After filtration, the filtrate was evaporated and the residue reprecipitated from cold hexane to give white solid product.

(^{i}Pr$_2$N)(DIPP)P(O)H (Oxide II): An amount of 0.2 mole of PCl$_3$ was added dropwise into the mixture of 0.2 mole of BHT and 0.6 mole of triethylamine at 0°C. The 200 ml of CH$_2$Cl$_2$ was added and the suspension was cooled down to -78°C. The 0.2 mol of ^{i}Pr$_2$NH was added dropwise with vigorous stirring. The suspension was warmed to room temperature for 2 h. After filtration, an amount of 0.2 mol of water was added dropwise with vigorous stirring to the filtrate at 0°C over 3 h. The suspension was then filtered to remove large amounts of a white solid amine hydrochloride. The filtrate was washed three times with water and dried with anhydrous CaCl$_2$. After filtration, the filtrate was evaporated to give crude product as a very thick liquid.

122

(iPr$_2$N)(tBuO)P(O)H (Oxide III): The mixture of 0.2 mol of tBuOH and 0.4 mol of triethylamine was added dropwise with vigorous stirring into the solution of 0.2 mol of PCl$_3$ in 150 ml of petroleum ether at 0°C. After warming to room temperature and filtration, an amount of 0.2 mol of iPr$_2$NH was added dropwise with vigorous stirring to the filtrate at 0°C. The suspension was allowed to warm to room temperature and stirred for an hour. A mixture of 0.2 mol of water and 0.2 mol of triethylamine was added slowly into the suspension at 0°C. Then the suspension was warmed to room temperature for 2 h. and filtered to remove large amounts of white solid amine hydrochloride. The filtrate was washed three times with water and dried with anhydrous MgSO$_4$. After filtration, the filtrate was evaporated to give the crude product as a colorless liquid.

(DMP)$_2$P(O)H (Oxide VII): An amount of 24 ml (20 g, 176 mmol) of DMP was added dropwise with vigorous stirring into the solution of 4.5 ml (6.1 g, 44 mmol) of PCl$_3$ and 100 ml of CH$_2$Cl$_2$ at -78°C. The suspension was then warmed to room temperature for 2 h. After filtration to remove white precipitate of salt, filtrate was mixed with 6 ml (4.1 g, 40 mmol) of triethylamine. Then 0.7 ml (1.2 g, 40 mmol) of H$_2$O was added slowly with vigorous stirring into the solution at 0°C. After warming to room temperature and filtration, the filtrate was washed three times with water and dried with anhydrous MgSO$_4$. After filtration, the filtrate was evaporated and residue reprecipitated from cold hexane to give 4 g (33%) of white solid product.

(iPrCyN)$_2$P(O)H (Oxide VIII): An amount of 66 ml (56 g, 398 mmol) of iPrCyNH was added dropwise with vigorous stirring into the solution of 10 ml (13.6 g, 99 mmol) of PCl$_3$ and 150 ml of CH$_2$Cl$_2$ at -78°C. The suspension was then warmed to room temperature for 2 h. After filtration to remove a white salt precipitate, the filtrate was mixed with 14 ml (10.1 g, 100 mmol) of triethylamine. Then 1.8 ml (1.8 g, 100

123

mmol) of H_2O was added slowly with vigorous stirring into the solution at 0°C. After warming to room temperature and filtration, the filtrate was washed three times with water and dried with anhydrous $MgSO_4$. After filtration, the filtrate was evaporated to give a very thick liquid of crude product.

$NiCl_2[^iPr_2NPO]_4$ (I). An amount of 2.0 g (4.5 mmol) of triphosphoxane $[^iPr_2NPO]_3$ and 0.6 g (2.7 mmol) of $NiCl_2$·DME was stirred in 30 ml of hexane. The yellow suspension turned to brown after 24 h. After filtration and hexane washing, the residue was dissolved in methylene chloride and filtered through Celite to remove any unreacted $NiBr_2$·DME. The filtrate was evaporated to give 0.8 g (41% based on Ni) of crude complex I as a brown solid.

$NiBr_2[^iPr_2NPO]_4$ (II). An amount of 0.70 g (1.6 mmol) of triphosphoxane $[^iPr_2NPO]_3$ and 0.37 g (1.2 mmol) of $NiBr_2$·DME were stirred in 20 ml of hexane. The orange-red suspension turned to brown after 24 h. After filtration and hexane washing, the residue was dissolved in methylene chloride and filtered through Celite to remove any unreacted $NiBr_2$·DME. The filtrate was evaporated to give 0.5 g (60% based on Ni) of complex II as an orange-red solid. Anal. Calcd for $Br_2C_{24}H_{56}N_4NiO_4P_4$: N, 6.94; C, 35.93; H, 6.94; Found: N, 6.94; C, 35.68; H, 6.94.

$NiCl_2[Cy_2NPO]_4$ (III). An amount of 6.2 g (9.1 mmol) of triphosphoxane $[Cy_2NPO]_3$ and 1.0 g (4.6 mmol) of $NiCl_2$·DME was stirred in 30 ml of hot toluene at 90°C in oil bath. The yellow suspension turned red after 5 h. After cooling down to room temperature and filtration through Celite, filtrate was evaporated to dryness and washed by hexane to give 2.4 g (50 % based on Ni) of unstable crude complex III as a red solid.

124

<u>NiBr$_2$[Cy$_2$NPO]$_4$ (IV).</u> An amount of 1.7 g (2.4 mmol) of triphosphoxane [Cy$_2$NPO]$_3$ and 0.6 g (1.8 mmol) of NiBr$_2$·DME was stirred in 30 ml of hexane. The orange-red suspension turned to brown after 24 h. After filtration and hexane washing, the residue was dissolved in methylene chloride and filtered through Celite to remove any unreacted NiBr$_2$·DME. The filtrate was evaporated to give 1.21 g (60% based on Ni) of complex IV as an orange-red solid. Anal. Calcd for Br$_2$C$_{48}$H$_{88}$N$_4$NiO$_4$P$_4$: N, 4.96; C, 51.12; H, 7.86; Found: N, 4.75; C, 50.93; H, 8.18.

<u>NiI$_2$[Cy$_2$NPO]$_4$ (V).</u> An amount of 0.6 g (0.9 mmol) of triphosphoxane [Cy$_2$NPO]$_3$ and 0.18 g (0.56 mmol) of NiI$_2$·2THF was stirred in 30 ml of THF. The purple suspension turned to red-purple after 3 h. After filtration through Celite, filtrate was evaporated to dryness and washed by hexane and dried to give 0.48 g (70 % based on Ni) of the crude unstable complex V as a purple solid.

<u>NiCl$_2$[Cy$_2$NPO]$_5$ (VI).</u> An amount of 2.6 g (3.8 mmol) of triphosphoxane [Cy$_2$NPO]$_3$ and 0.6 g (2.7 mmol) of NiCl$_2$·DME was stirred in 40 ml of hexane. The yellow suspension turned darker after 24 h. After filtration and hexane washing, the residue was dissolved in methylene chloride and filtered through Celite to remove any unreacted NiCl$_2$·DME. The filtrate was evaporated to give 1.65 g (48 % based on Ni) of complex VI as a yellow solid. Anal. Calcd for C$_{60}$Cl$_2$H$_{110}$N$_5$NiO$_5$P$_5$·[C$_6$H$_5$CH$_3$]: N, 5.15; C, 59.24; H, 8.75; Found: N, 5.13; C, 59.26; H, 8.96.

<u>PdCl$_2$[^{i}Pr$_2$NPO]$_4$ (VII).</u> Triphosphoxane [^{i}Pr$_2$NPO]$_3$ (1.5 g, 3.4 mmol) and 1.0 g (2.6 mmol) of PdCl$_2$·2PhCN were stirred in 30 ml of hexane at room temperature. After 24 h, the orange suspension turned to a yellow color. After filtration, the light yellow residue was washed with hexane and dried under reduced pressure to give 0.8 g (40% based on Pd) of complex VII. Crystals of X-ray quality were obtained by re-

125

crystallization from chloroform/hexane layerring. Anal. Calcd for $C_{24}Cl_2H_{56}N_4O_4P_4Pd$: N, 7.31; C, 37.61; H, 7.31; Found: N, 7.24; C, 37.94; H, 7.58.

PdBr$_2$[^{i}Pr$_2$NPO]$_4$ (VIII). Triphosphoxane [^{i}Pr$_2$NPO]$_3$ (0.3 g, 0.7 mmol) and 0.2 g (0.4 mmol) of PdBr$_2$·2PhCN were refluxed in 30 ml of hexane. After 6 h, the orange suspension turned to a yellow color. After cooling down to room temperature and filtration, the light yellow residue was washed with hexane and dried under reduced pressure to give 0.8 g (40% based on Pd) of complex VIII. Anal. Calcd for Br$_2$C$_{24}$H$_{56}$N$_4$O$_4$P$_4$Pd: N, 6.60; C, 33.71; H, 6.60; Found: N, 6.46; C, 34.12; H, 6.77.

PdCl$_2$[Cy$_2$NPO]$_4$ (IX). Triphosphoxane [Cy$_2$NPO]$_3$ (1.1 g, 1.6 mmol) and 0.46 g (1.2 mmol) of PdCl$_2$·2PhCN were stirred in 30 ml of hexane at 4°C. After 72 h, the orange suspension turned to a yellow color. After filtration, the light yellow residue was washed with hexane and dried under reduced pressure to give 1.0 g (80% based on Pd) of complex IX.

PdBr$_2$[Cy$_2$NPO]$_4$ (X). Triphosphoxane [Cy$_2$NPO]$_3$ (1.1 g, 1.5 mmol) and 0.5 g (1.1 mmol) of PdBr$_2$·2PhCN were stirred in 30 ml of hexane at 4°C. After 72 h, the orange suspension turned to a yellow color. After filtration, the light yellow residue was washed with hexane and dried under reduced pressure to give 0.9 g (70% based on Pd) of complex X. Anal. Calcd for Br$_2$C$_{48}$H$_{88}$N$_4$O$_4$P$_4$Pd: N, 4.77; C, 49.05; H, 7.55; Found: N, 4.61; C, 49.34; H, 7.70.

PdCl$_2$[Cy$_2$NPO]$_5$ (XI). Triphosphoxane [Cy$_2$NPO]$_3$ (1.98 g, 2.9 mmol) and 0.6 g (1.5 mmol) of PdCl$_2$·2PhCN were refluxed in 40 ml of hexane. After 12 h, the orange suspension turned to a yellow color. After cooling down to room temperature and filtration, the light yellow residue was washed with hexane and dried under reduced

126

pressure to give 1.6 g (81% based on Pd) of complex **XI**. Anal. Calcd for $C_{60}Cl_2H_{110}N_5O_5P_5Pd$: N, 5.33; C, 54.85; H, 8.44; Found: N, 5.29; C, 54.49; H, 8.69.

PdBr2[Cy2NPO]5 (XII, A). Triphosphoxane [$Cy_2NPO]_3$ (0.9 g, 1.2 mmol) and 0.3 g (0.6 mmol) of $PdBr_2\cdot2PhCN$ were refluxed in 40 ml of hexane. After 12 h, the orange suspension turned to a yellow color. After cooling down to room temperature and filtration, the light yellow residue was washed with hexane and dried under reduced pressure to give 0.6 g (75% based on Pd) of complex **XII**. Anal. Calcd for $Br_2C_{60}H_{110}N_5O_5P_5Pd$: N, 4.99; C, 51.38; H, 7.85; Found: N, 4.83; C, 51.45; H, 8.18.

PdBr2[Cy2NPO]5 (XIII, B). An amount of 0.1 g $PdBr_2[Cy_2NPO]_5$ (A, **XII**) was refluxed in 20 ml of toluene for 6 h. After cooling down to room temperature and evaporation, the light yellow residue was washed with cold toluene and dried under reduced pressure to give 0.07 g (70%) of the complex **XIII**. Anal. Calcd for $Br_2C_{60}H_{110}N_5O_5P_5Pd$ [$C_6H_5CH_3$]: N, 4.69; C, 53.84; H, 7.96; Found: N, 4.74; C, 54.16; H, 8.13.

PtCl2[iPr2NPO]4 (XIV). Triphosphoxane [$^iPr_2NPO]_3$ (0.3 g, 0.64 mmol) and 0.15 g (0.4 mmol) of $PtCl_2\cdot NBD$ were refluxed in 20 ml of hexane for 6 h. After cooling down to room temperature and filtration, the white precipitate was washed with hexane and dried under reduced pressure to give 0.25 g (75% based on Pt) of complex **XIV** .

PtCl2[iPr2NPO]5 (XV). Triphosphoxane [$^iPr_2NPO]_3$ (0.3 g, 0.64 mmol) and 0.15 g (0.4 mmol) of $PtCl_2\cdot NBD$ were refluxed in 20 ml of hexane for 16 h. After cooling down to room temperature and filtration, the white precipitate was washed with hexane and dried under reduced pressure to give 0.4 g (80% based on Pt) of complex **XV**. Anal. Calcd for $C_{60}Cl_2H_{110}N_5O_5P_5Pt\cdot[C_6H_5CH_3]$: N, 4.69; C, 53.84; H, 7.96; Found: N,

127

4.67; C, 53.31; H, 8.42.

PtCl₂[Cy₂NPO]₄ (XVI, XVII). Triphosphoxane [Cy₂NPO]₃ (0.3 g, 0.64 mmol) and 0.15 g (0.4 mmol) of PtCl₂·NBD were stirred in 20 ml of hexane at room temperature for 10 h. After filtration, the white precipitate was washed with hexane and dried under reduced pressure to give the mixture of complex **XVI** and complex **XVII**.

Mo(CO)₄[ⁱPr₂NPO]₃ (XVIII). The triphosphoxane [ⁱPr₂NPO]₃ (0.7 g, 1.6 mmol) and 0.48 g (1.6 mmol) of Mo(CO)₄NBD were dissolved in 15 ml of hexane to gave a yellow solution, which was stirred at 29° C for 12 h. The resulting very pale yellow suspension was filtered and the solid washed with cold hexane and dried under reduced pressure to give 410 mg (41%) of analytically pure **XVIII**. Anal. Calcd for $C_{22}H_{42}MoN_3O_7P_3$: N, 6.47; C, 40.69; H, 6.47; Found: N, 6.47; C, 40.77; H, 6.79.

Mo(CO)₄[Cy₂NPO]₃ (XIX). The triphosphoxane [Cy₂NPO]₃ (1.0 g, 1.3 mmol) and 0.4 g (1.3 mmol) of Mo(CO)₄NBD were dissolved in 30 ml of hexane to gave a yellow solution, which was stirred at 25° C for 2 h. The resulting very pale yellow suspension was filtered and the solid washed with cold hexane and dried under reduced pressure to give 1.1 g (91%) of analytically pure **XIX**. Anal. Calcd for $C_{40}H_{66}MoN_3O_7P_3$: N, 4.72; C, 53.99; H, 7.48; Found: N, 4.78; C, 53.66; H, 7.57.

Mo(CO)₄[ⁱPr₂NPO]₄ (XX). The triphosphoxane [ⁱPr₂NPO]₃ (0.7 g, 1.6 mmol) and 0.48 g (1.6 mmol) of Mo(CO)₄NBD were refluxed in 20 ml of hexane to gave a yellow solution for 10 h. After cooling down to room temperature, the micro-crystalline precipitate was filtered off. The solid was washed with cold hexane and dried under reduced pressure to give the cage complex **XX**.

128

$\underline{Mo(CO)_4[Cy_2NPO]_4}$ $\underline{(XXI)}$. The triphosphoxane $[Cy_2NPO]_3$ (1.0 g, 1.3 mmol) and 0.4 g (1.3 mmol) of $Mo(CO)_4NBD$ were refluxed in 20 ml of hexane for 10 h to gave a yellow solution. After cooling down to room temperature and standing for 10 h, the crystalline precipitate was filtered off and washed with cold hexane and dried under reduced pressure to give the cage complex **XXI**.

$\underline{Mo(CO)_4[^iPr_2NPO]_4}$ $\underline{(XXII)}$. The triphosphoxane $[^iPr_2NPO]_3$ (0.7 g, 1.6 mmol) and 0.48 g (1.6 mmol) of $Mo(CO)_4NBD$ were dissolved in 30 ml of hexane to gave a yellow solution which was stirred at 40° C for 12 h. After cooling down to room temperature and standing for 10 h, the crystalline precipitate was filtered off and washed with cold hexane and dried under reduced pressure to give 0.31 g (25%) of cage isomer complex **XXII**.

$\underline{Mo(CO)_4[Cy_2NPO]_4}$ $\underline{(XXIII)}$. The triphosphoxane $[Cy_2NPO]_3$ (1.0 g, 1.3 mmol) and 0.4 g (1.3 mmol) of $Mo(CO)_4NBD$ were dissolved in 30 ml of hexane to gave a yellow solution, which was stirred at 40° C for 8 h. After cooling down to room temperature and standing for 10 h, the crystalline precipitate was filtered off and washed with cold hexane and dried under reduced pressure to give 0.12 g (10%) of cage isomer complex **XXIII**.

$\underline{Cr(CO)_4[Cy_2NPO]_4}$ $\underline{(XXIV)}$. The triphosphoxane $[Cy_2NPO]_3$ (1.6 g, 2.3 mmol) and 0.2 g (0.78 mmol) of $Cr(CO)_4NBD$ were refluxed in 50 ml of hexane for 40 h. After cooling down to room temperature and standing for 10 h, some crystalline precipitate of $Cr(CO)_6$ formed and was removed by filtration. The solution was decolorized by adding a small amount of Al_2O_3 and filtering through Celite. The filtrate was evaporated and recrystallized from hexane to give 0.8 g (30% based on Cr) of complex **XXIV** upon cooling. Anal. Calcd for $C_{52}CrH_{88}N_4O_8P_4$: N, 5.22; C, 58.24; H, 8.21; Found: N, 5.12;

129

C, 58.21; H, 8.35.

Fe(CO)₃[Cy₂NPO]₄ (XXV). The triphosphoxane [Cy₂NPO]₃ (0.6 g, 0.8 mmol) and 0.3 g (0.8 mmol) of Fe₂(CO)₉ were refluxed in 20 ml of hexane for 10 h. After cooling down to room temperature and filtration through Celite, the filtrate was evaporated and the residue chromatographed on an alumina column using 2.5% EtOAc/hexane as the eluent. The eluate was evaporated to dryness and recrystallized by dissolving in hot hexane and then cooling to room temperature to give about 0.2 g (12% based on Fe) of complex **XXV**. Anal. Calcd for C₅₁H₈₈FeN₄O₇P₄: N, 5.34; C, 58.43; H, 8.39. Found: N, 5.11; C, 58.77; H, 8.82.

Fe(CO)₄[ⁱPr₂NPO]₄ (XXVI, XXVII). The triphosphoxane [ⁱPr₂NPO]₃ (3.4 g, 7.3 mmol) and 2 g (5.4 mmol) of Fe₂(CO)₉ were refluxed in 60 ml of toluene for 18 h. After cooling down to room temperature and filtration through Celite, the filtrate was evaporated and residue extracted by 120 ml of hot hexane. After filtration, the filtrate was evaporated and the residue chromatographed on an alumina column using 2.5% EtOAc/hexane as the eluent. The eluate was evaporated to dryness and residue recrystallized by dissolving in hot hexane and then cooling to room temperature to give about 0.8 g (20% based on Fe) of a mixture of **XXVI** and **XXVII**. The yellow large cube crystals of **XXVII** and pale-yellow small prisms of **XXVI** were readily separated manually to give pure products. Anal. Calcd for C₂₇H₅₆FeN₄O₇P₄: N, 7.69; C, 44.54; H, 7.69. Found: N, 7.57; C, 44.32; H, 7.91. Anal. Calcd for C₂₈H₅₆FeN₄O₇P₄: N, 7.41; C, 44.48; H, 7.41. Found: N, 7.38; C, 43.81; H, 7.57.

Mo(CO)₄[Cy₂NPO]₄·NiBr₂ (XXVIII). The NiBr₂[Cy₂NPO]₄ (0.45 g, 0.4 mmol) and 0.12 g (0.4 mmol) of Mo(CO)₄NBD were stirred in 25 ml of toluene at 90°C for 3 h. The red clear solution turned to pale brown. After cooling down to room temperature

130

and filtration through Celite, the filtrate was evaporated and residue chromatographed on an alumina column using 2.5% of EtOAc/hexane as the eluent. The eluate was concentrated to form a precipitate. After filtration, the red-brown solid was dried under reduced pressure to give about 0.25 g (50% based on Mo) of complex **XXVIII**. Anal. Calcd for $Br_2C_{52}H_{88}MoN_4NiO_8P_4$: N, 4.19; C, 46.76; H, 6.64. Found: N, 4.10; C, 46.76; H, 6.87.

$\underline{Mo(CO)_4 \cdot [Cy_2NPO]_5 \cdot PdCl_2 (XXIX)}$. The $PdCl_2[Cy_2NPO]_5$ (0.26 g, 0.2 mmol) and 0.06 g (0.2 mmol) of $Mo(CO)_4NBD$ were stirred in 30 ml of toluene at 90°C for 5 h. After cooling down to room temperature and filtration through Celite, the filtrate was evaporated and residue chromatographed on an alumina column using 5% EtOAc/hexane as the eluent. The eluate was concentrated to form a precipitate. After filtration, the pale-yellow solid was dried under reduced pressure to give about 0.1 g (40% based on Mo) of complex **XXIX**. Anal. Calcd for $C_{64}Cl_2H_{110}MoN_5O_8P_5Pd$: N, 4.69; C, 50.66; H, 7.42. Found: N, 4.36; C, 50.41; H, 7.78.

$\underline{Mo(CO)_4 \cdot [^iPr_2NPO]_4 \cdot Fe(CO)_3 (XXX)}$. The $Fe(CO)_3[^iPr_2NPO]_4$ (0.2 g, 0.27 mmol) and 0.18 g (0.33 mmol) of $Mo(CO)_4NBD$ were refluxed in 20 ml of hexane for 5 h. After cooling down to room temperature, the solution was evaporated and residue chromatographed on an alumina column using 0.5% of EtOAc/hexane as the eluent. The eluate was evaporated to dryness and residue recrystallized from cold hexane. The large pale-yellow crystals were dried under reduced pressure to give about 0.19 g (80% based on Fe) of complex **XXX**. Anal. Calcd for $C_{31}H_{56}FeMoN_4O_{11}P_4$: N, 5.98; C, 39.78; H, 5.98. Found: N, 6.03; C, 39.83; H, 5.98.

$\underline{Ni_2(CO)_4 \cdot [Cy_2NPO]_4 (XXXI)}$. The $NiBr_2[Cy_2NPO]_4$ (1.5 g, 1.3 mmol) and 0.48 g (1.3 mmol) of $Fe_2(CO)_9$ were stirred in 40 ml of toluene at 90°C for 2 h. The clear

131

red solution turned to a golden-brown suspension. After cooling down to room temperature and filtration through Celite, the filtrate was evaporated and residue extracted by hexane. After filtration, the filtrate was evaporated to dryness and the residue chromatographed on an alumina column using 2.5% of EtOAc/hexane as the eluent. The eluate was evaporated to give about 0.27 g (17% based on Ni) of white solid of complex **XXXI**. Anal. Calcd for $C_{52}H_{88}N_4Ni_2O_8P_4$: N, 4.92; C, 54.89; H, 7.73. Found: N, 4.71; C, 54.87; H, 8.11.

PdClBr·[Cy2NPO]5 (XXXII). The triphosphoxane $[Cy_2NPO]_3$ (1.2 g, 1.75 mmol), 0.34 g (0.87 mmol) of $PdCl_2·2PhCN$ and 0.27 g (0.87 mmol) of $NiBr_2DME$ were refluxed in 40 ml of hexane for 14 h. After cooling to room temperature and filtration, the solid was washed by hexane and extracted by 40 ml of chloroform. After filtration through Celite, the filtrate was evaporated to dryness and residue was dried under reduced pressure to give about 0.6 g (52% based on Pd) of white solid complex **XXXII**.

PdBr2·[sBu2NPO]4 (XXXIII). The triphosphoxane $[^sBu_2NPO]_3$ (0.5 g, 1.0 mmol) and 0.15 g (0.3 mmol) of $PdBr_2·2PhCN$ were refluxed in 15 ml of hexane for 8 h. The brown suspension turned yellow. After cooling down to room temperature and filtration, the solid was washed by hexane and extracted by 20 ml of chloroform. After filtration through Celite, the filtrate was evaporated to dryness and residue was dried under reduced pressure to give about 0.15 g (51% based on Pd) of white solid of complex **XXXIII**.

PdBr2·[iPrCyNPO]4 (XXXIV). The triphosphoxane $[^iPrCyNPO]_3$ (0.3 g, 0.4 mmol) and 0.1 g (0.2 mmol) of $PdBr_2·2PhCN$ were refluxed in 20 ml of hexane for 8 h. The brown suspension turned yellow. After cooling down to room temperature and filtration, the solid was washed by hexane and extracted by 20 ml of chloroform. After filtration

132

through Celite, the filtrate was evaporated to dryness and residue was dried under reduced pressure to give about 0.06 g (35% based on Pd) of white solid complex **XXXIV**.

NiBr$_2$·[Ph$_2$NPO]$_5$ (**XXXV**). The triphosphoxane [Ph$_2$NPO]$_3$ (0.3 g, 1.2 mmol) and 0.2 g (0.65 mmol) of NiBr$_2$·DME were refluxed in 15 ml mixture of hexane and toluene for 2 h. The orange suspension turned red. After cooling down to room temperature and filtration, the red solid was washed by hexane and dried under reduced pressure to give about 0.11 g (40% based on Ni) of crude red complex **XXXV**.

[Cy$_2$NPO]$_3$S$_2$ (**XXXVI**). The triphosphoxane [Cy$_2$NPO]$_3$ (0.3 g, 0.4 mmol) and 0.3 g of sulfur were stirred in 30 ml of hexane at room temperature for 4 h. The suspension was filtered. The filtrate was evaporated to dryness and residue was dried under reduced pressure to give a white solid of crude compound **XXXVI**.

Cr(CO)$_4$(Et$_2$N)$_2$POP(Et$_2$N)$_2$ (**XXXVII**). An amount of 1.6 g (7.1 mmol) of Cr(CO)$_6$ and 3 g (14 mmol) of phosphine oxide (Et$_2$N)$_2$P(O)H were refluxed in 25 ml of xylene for 8 h. The pale-yellow solution changed to a black suspension. After cooling, the black suspension was filtered through Celite. The filtrate was evaporated and residue chromatographed on an alumina column using 2.5% EtOAc/hexane as the eluent. The eluate was evaporated to dryness and recrystallized from cold hexane to give about 0.6 g (16% based on Cr) of complex **XXXVII**. Anal. Calcd for C$_{20}$CrH$_{40}$N$_4$O$_5$P$_2$: N, 10.56; C, 45.28; H, 7.55. Found: N, 10.30; C, 44.34; H, 7.71.

Mo$_2$(CO)$_8$[Et$_2$NPO]$_4$ (**XXXVIII**) and Mo(CO)$_4$(Et$_2$N)$_2$POP(Et$_2$N)$_2$ (**XXXIX**). An amount of 1.9 g (7.1 mmol) of Mo(CO)$_6$ and 3 g (14 mmol) of phosphine oxide (Et$_2$N)$_2$P(O)H were refluxed in 20 ml of xylene for 3 h. The pale-yellow solution changed to a black suspension. After cooling, the black suspension was filtered through

133

Celite. The filtrate was evaporated and residue chromatographed on an alumina column using 2.5% EtOAc/hexane as the eluent. The eluate was evaporated to dryness and recrystallized from cold hexane to give about 0.1 g (4.6% based on Mo) of cage complex **XXXVIII** and about 0.4 g (30%) of complex **XXXIX**.

W(CO)$_4$(Et$_2$N)$_2$POP(Et$_2$N)$_2$ (XL). An amount of 2.5 g (7.1 mmol) of W(CO)$_6$ and 3 g (14 mmol) of phosphine oxide (Et$_2$N)$_2$P(O)H were refluxed in 25 ml of xylene for 3 h. The pale-yellow solution changed to a black suspension. After cooling, the black suspension was filtered through Celite. The filtrate was evaporated and residue chromatographed on an alumina column using 2.5% EtOAc/hexane as the eluent. The eluate was evaporated to dryness and recrystallized from cold hexane to give about 0.9 g (19% based on W) of complex **XL**. Anal. Calcd for C$_{20}$H$_{40}$N$_4$O$_5$P$_2$W: N, 8.46; C, 36.26; H, 6.05. Found: N, 8.43; C, 36.12; H, 6.32.

Cr(CO)$_4$(PIP)$_2$POP(PIP)$_2$ (XLI). The phosphine oxide (PIP)$_2$P(O)H (2 g, 9 mmol) and 1 g (4.6 mmol) of Cr(CO)$_6$ were refluxed in 20 ml of xylene for 8 h. The pale-yellow solution changed to a black suspension. After cooling, the black suspension was filtered through Celite. The filtrate was evaporated and extracted with 30 ml of acetone. The acetone solution was decolorized by adding a small amount of Al$_2$O$_3$ and filtering through Celite. The filtrate was evaporated to dryness and recrystallized from cold hexane to give about 0.4 g (10% based on Cr) of complex **XLI**.

W(CO)$_4$(PIP)$_2$POP(PIP)$_2$ (XLII). The phosphine oxide (PIP)$_2$P(O)H (2 g, 9 mmol) and 1.6 g (4.6 mmol) of W(CO)$_6$ were refluxed in 25 ml of xylene for 12 h. The pale-yellow solution changed to a black suspension. After cooling, the black suspension was filtered through Celite. The filtrate was evaporated and extracted with 30 ml acetone. The acetone solution was decolorized by adding a small amount of Al$_2$O$_3$ and

134

filtering through Celite. The filtrate was evaporated to dryness and recrystallized from cold hexane to give about 0.3 g (6% based on Cr) of complex **XLII**.

$Cr(CO)_4[Cy_2NPO]_4$ **(XXVII, XLIII)** and $Cr_2(CO)_8[Cy_2NPO]_4$ **(XLIV)**. The phosphine oxide $(Cy_2N)_2P(O)H$ (4.5 g, 11 mmol) and 0.8 g (3.6 mmol) of $Cr(CO)_6$ were refluxed in 20 ml of toluene for 36 h. The clear colorless solution changed to a dark-brown suspension. After cooling, the suspension was filtered through Celite. The filtrate was evaporated and residue was dissolved with 30 ml hot hexane after washing by acetone. The hexane solution was cooled down and concentrated to precipitate about 0.2 g (32% based on Cr) of complex **XXVII**. Anal. Calcd for $C_{52}CrH_{88}N_4O_8P_4$: N, 5.22; C, 58.24; H, 8.21. Found: N, 5.12; C, 58.21; H, 8.35. After filtration, the solution contained a mixture of complex **XLIII** and complex **XLIV** (1:4).

$Cr(CO)_5\text{-}(Cy_2N)_2P(O)H$ **(XLV)** and $Cr_2(CO)_7[Cy_2NPO]_5$ **(XLVI)**. Method A: The phosphine oxide $(Cy_2N)_2P(O)H$ (4.5 g, 11 mmol) and 0.8 g (3.6 mmol) of $Cr(CO)_6$ were refluxed in 20 ml of toluene for 36 h. The clean colorless solution changed to a dark brown suspension. After cooling, the suspension was filtered through Celite. The filtrate was evaporated and extracted with 30 ml of acetone. The acetone solution was evaporated to dryness and chromatographed on an alumina column using 0.5% of EtOAc/hexane as eluent. The first fraction to elute was a tiny amount of unstable complex **XLV**. The second fraction to elute gave about 0.12 g (20% based on Cr) of complex **XLVI**. Anal. Calcd for $C_{60}CrH_{110}N_5O_{12}P_5$: N, 4.88; C, 56.05; H, 7.72. Found: N, 4.43; C, 56.14; H, 8.22.

Method B: The phosphine oxide $(Cy_2N)_2P(O)H$ (4.5 g, 11 mmol) and 0.8 g (3.6 mmol) of $Cr(CO)_6$ were refluxed in 25 ml of xylene for 36 h. The clean colorless solution changed to a dark brown slight suspension. After cooling, the suspension was

135

filtered through Celite. The filtrate was evaporated and extracted with 30 ml of acetone. The acetone solution was evaporated to dryness and chromatographed on an alumina column using 0.5% of EtOAc/hexane as eluant. The eluate gave about 1.4 g (65% based on Cr) of complex **XLVI**.

$W_2(CO)_7[Cy_2NPO]_5$ **(XLVII) and** $W_2(CO)_6[Cy_2NPO]_4$ **(XLVIII).** The phosphine oxide $(Cy_2N)_2P(O)H$ (3.5 g, 8.5 mmol) and 1 g (2.8 mmol) of $W(CO)_6$ were refluxed in 20 ml of toluene for 48 h. The clear colorless solution changed to a dark brown suspension. After cooling, the suspension was filtered through Celite. The filtrate was evaporated and chromatographed on an alumina column using hexane as eluent. The first fraction to elute gave crude unstable complex **XLVII**. The second fraction to elute was a red mixture. After standing 4 days, red crystals of complex **XLVIII** were deposited. Anal. Calcd for $C_{54}H_{88}N_4O_8P_4W \cdot (1.5C_6H_{14})$: N, 3.56; C, 48.09; H, 6.90. Found: N, 3.59; C, 47.94; H, 7.20.

$W(CO)_4[Cy_2NPO]_3$ **(XLIX).** The hexane solution of complex $W_2(CO)_7[Cy_2NPO]_5$ **(XLVII)** after standing for 2 days gave a large amount of white precipitate. The major portion of this precipitate was the complex $W(CO)_4[Cy_2NPO]_3$ **(XLIX)**.

$Cr_2(CO)_8[DMP-PO]_4$ **(L, LI) and** $Cr_2(CO)_7[DM-PPO]_5$ **(LII).** The phosphine oxide $(DMP)_2P(O)H$ (3.0 g, 11.0 mmol) and 0.9 g (4.0 mmol) of $Cr(CO)_6$ were refluxed in 20 ml of toluene for 48 h. The clear colorless solution changed to a dark brown suspension. After cooling, the suspension was filtered through Celite. The filtrate was evaporated and chromatographed on an alumina column using hexane as eluent. The eluate was a mixture. This mixture was recrystallized from cold toluene to give a major product of complex **LII** of about 0.28 g (18% based on Cr). Anal. Calcd for $C_{54}Cr_2H_{88}N_4O_8P_4 \cdot (1.5C_6H_{14})$: N, 5.90; C, 49.57; H, 6.57. Found: N, 5.96; C, 49.35;

136

H, 6.72. The filtrate was concentrated and X-ray quality crystals of complex **L** was grew and separated out, 0.06 g (4.6% based on Cr). Subsequently, large crystal of cage complex **LI** were obtained (0.03 g, 2.3% based on Cr). Anal. Calcd for $C_{54}Cr_2H_{88}N_4O_8P_4 \cdot (1.5C_6H_{14})$: N, 5.80; C, 44.80; H, 5.80. Found: N, 5.78; C, 45.11; H, 5.93.

<u>$Cr_2(CO)_6[DMP-PO]_6$ (LIII)</u>. The phosphine oxide $(DMP)_2P(O)H$ (0.1g, 1 mmol) and 0.1 g (0.1 mmol) of $Cr_2(CO)_7[DMPPO]_5$ were refluxed in 20 ml of xylene for 6 h. After cooling down to room temperature and filtration, the precipitate was recrystallized from cold toluene to give 0.1 g (90% based on **LII**). X-ray quality crystals were obtained by gradually cooling down a hot toluene solution over 5 days. Anal. Calcd for $C_{54}Cr_2H_{88}N_4O_8P_4 \cdot (2C_6H_5CH_3)$: N, 5.95; C, 52.79; H, 7.08. Found: N, 5.82; C, 52.21; H, 7.14.

<u>$Mo_2(CO)_8[DMP-PO]_4$ (LIV)</u>. The phosphine oxide $(DMP)_2P(O)H$ (1 g, 3.6 mmol) and 0.5 g (1.8 mmol) of $Mo(CO)_6$ were refluxed in 20 ml of toluene for 48 h. The clear colorless solution changed to a dark brown suspension. After cooling, the suspension was filtered through Celite. The filtrate was evaporated and chromatographed on an alumina column using hexane as eluent. The eluate was evaporated and recrystallized from cold toluene to give about 0.3 g (32% based on Mo) of complex **LIV**. Anal. Calcd for $C_{54}H_{88}Mo_2N_4O_8P_4 \cdot (1.5C_6H_{14})$: N, 5.32; C, 41.09; H, 5.32. Found: N, 5.28; C, 41.19; H, 5.50.

137

REFERENCES

[1] Kraihanzel, G.S.; Bartish, C.M.; *J. Am. Chem. Soc.* 1972, **94**, 3572.

du Preez, A.L.; Marais, I.L.; Haines, R.J.; Pidcock, A.; Safari, M.; *J. Chem. Soc., Dalton Trans.* 1981, 1918.

Che, C.M.; Schaefer, W.P.; Gray, H.B.; Dickson, M.K.; Stein, P.B.; Roundhill, D.M. *J. Am. Chem. Soc.* 1982, **104**, 4253.

Wong, E.H.; Prasad, L.; Gabe, E.J.; Bradley, F.C.; *J. Organomet. Chem.* 1982, **236** 321.

Wong, E.H.; Valdez, C.; Gabe, E.J.; Lee, F.L.; *Polyhedron*, **8**(19), 1989, 2339

[2] Niecke, E.; Zorn, H.; Krebs, B.; Henkel, G.; *Angew. Chem. Int. Ed. Engl.* 1980, **19** 709-710.

[3] Chasar, D.W.; Fackler, J.P.; Mazany, A.M.; Komoroski, R.A.; Kroenke, W.J.; *J. Am. Chem. Soc.* 1986, **108**, 5956-5962.

Chasar, D.W.; Fackler, J.P.; Komoroski, R.A.; Kroenke, W.J.; Mazany, A.M.; *J. Am. Chem. Soc.* 1987, **109**, 5690-5693.

[4] Nifant'en, E.E.; Koroteev, M.P.; Ivanov, N.L.; Gudkova, I.P.; Predvoditelev, D.A.; *Dokl. Chem. (Engl. Transl.)* 1967, **173**, 398-401.

[5] Wong, E.H.; Turnbull, M.M.; Gabe, E.; Lee, F.L.; Lepage, Y.; *J. Chem. Soc., Chem. Commun.* 1983, 776.

[6] Wong, E.H.; Gabe, E.J.; Charland, J.; *J. Chem. Soc., Chem. Commun.* 1988, 1632

[7] Wong, E.H.; Turnbull, M.M.; Hutchinson, K.D.; Valelez, C.; Gabe, E.J.; Lee, F.L.; Page, Y.L.; *J. Am. Chem. Soc.,* 1988, **110**(25), 8422

[8] Wong, E.H.; Gabe, E.J.; Lee, F.L.; *J. Chem. Soc., Chem. Commun.*, 1989, 1236

[9] Wong, E.H.; Sun, X.; Gabe, E.J.; Lee, F.L.; Charland, J.; *Organometallics*, 1991, **10**, 3010-3020

[10] Turnbull, M.M.; Valdez, C.; Wong, E.H.; Gabe, E.J.; Lee, F.L.; *Inorg. Chem.* **31**(2), 1992, 208-214

[11] Yang, H.; Wong, E.H.; Jasinski, J.P.; Pozdniakov, R.Y.; Woudenberg, R.; *Organometallics*, 1992, **11**, 1579

[12] Yang, H.; Wong, E.H.; Rheingold, A.L.; Owens Watermire, B.E.; *J. Chem. Soc., Chem. Commun.*, 1993, 35

[13] Nieche, E.; Englemann, M.; Zorn, H.; Krebs, B.; Henkel, G.; *Angew. Chem., Int. Ed. Engl.* 1980, **19**, 710-712

[14] King, R.B.; Sadanani, N.D.; *J. Org. Chem.* 1985, **50**, 1719-1722.

138

[15] Allcock, H.R.; *Chem. Rev.*, 1972, **72**, 315-356

A. Durif; <u>The chemistry of Inorganic Homo and Heterocycles</u>, Vol. 2, I. Haiduc and D.B. Sowerby, Eds. Academic Press, 1987

John C. van de Grampel; *Coord. Chem. Rev.*, 1992, **112**, 247-271

[16] Glonek, T.; Van Wazer, J.R.; Kleps, R.A.; Meyers, T.C.; *Inorg. Chem.*, 1974, **13**, 2337-2345

Ogata, N.; Sanui, K.; Harada, M.J.; *Polym. Sci., Polym. Chem. Educ.*, 1979, **17**, 2401-2411

Durif, A.; <u>The Chemistry of Inorganic Homo- and Heterocycles;</u> Haiduc, I.; Sowerby, D.B., Eds.; Academic Press: New York, 1987; Vol. 2, Chapter 22

[17] Zeiss, W.; Schwartz, W.; Hess, H.; *Angew. Chem., Int. Ed. Engl.* 1977, **16**, 407.

Gallicano, K.D.; Rettig, S.J.; Trotter, J.; *Can. J. Chem.* 1982, **60**, 3415-2419.

Gallicano, K.D.; Rettig, S.J.; Trotter, J.; *Can. J. Chem.* 1984, **62**, 1869-1873.

Malavaud, C.; N'Gando M'Pondo, T.; Lopez, L.; Barrans, J.; Legros, J-P.; *Can. J. Chem.* 1984, **62**, 43-50.

Barent, J.M.; Bent, E.G.; Haltiwanger, R.C.; Norman, A.D.; *J. Am. Chem. Soc.* 1980 **111**, 6883-6884.

[18] Driess, M.; Reisgys, M.; Pritzkow, H.; *Angew. Chem., Int. Ed. Engl.* 1992, **31**, 1510-1513.

[19] Huheey, J.E.; *Inorganic Chemistry,* Harper & Row, Publishers, New York, 1983 Chapter 11

[20] Baker, R.T.; Calabrese, J.C.; Krusic, P.J.; Therien, M.J.; Trogler, W.C.; *J. Am. Chem. Soc.* 1988, **110**(25), 8392-412

Casey, C.P.; Whiteker, G.T.; Campana, C.F.; Powell, D.R.; *Inorg. Chem.*, 1990, **29**(8), 3376-81

Liu, H.; Eriks, K.; Prock, A.; Giering, W.P.; *Organometallics*, 1990, **9**, 1758

[21] D.E.C. Corbridge; <u>Phosphorus-an outline of its chemistry, biochemistry and technology,</u> Elsevier Science Publishers B.V. 1985

[22] Tofke, S.; Behrens, U.; *J. Organomet. Chem.*, 1988, **338**(1), 29-45

Ziegler, M.L.; Blechmitt, K.; Nuber, B.; Zahn, T.; *Chem. Ber.*, 1988, **121**(1) 159-71

[23] Pregosin, P.s.; Kunz, R.W.; <u>^{31}P and ^{13}C NMR of Transition Metal Phosphine Complexes;</u> Sprineger-Verlag, Berlin, 1979;

139

[24] Verkade, G, Quin, L.D.;   P-31 NMR spectroscopy in Stereochemical Analysis, VCH, New York, 1987, chapter1

[25] Garrou, P.E.,   *Chem. Rev.*, 1981, **81**, 229-266

[26] Tolman, C.A.;   *J. Am. Chem. Soc.*; 1970, **92**, 2956

[27] Rahman, M.M.; Liu, H.; Eriks, K.;   *Organometallics*, 1989, **8(1)**, 4

[28] Zwierzak, A.; Koziara, A.;   *Tetrahedron*, 1967, **(23)**, 2243-2252

[29] Garrou, P.E.;   *Chem, Rev.*, 1981, **81**, 229-266

[30] Verkade, G, Quin, L.D.;   P-31 NMR spectroscopy in Stereochemical Analysis, VCH, New York, 1987, chapter16

[31] Verkade, G, Quin, L.D.;   P-31 NMR spectroscopy in Stereochemical Analysis, VCH, New York, 1987, chapter17

[32] Petersen, J.L.; Steeart, R.P.;   *Inorg. Chem.*, 1980, **19**, 186;

   Carly, A.J.; Maclaughlin, S.A.; Taylor, N.J.,   *J. Organomet. Chem.* 1981, **204**, C27

[33] Bennett, M.A.; Pratt, L.; Wilkinson, G.;   *J.Chem. Soc.*, 1961, 2037

[34] King, R.B.; Ed.   Organometallic Synthesis; Academic Press, New York, 1965, p124

[35] King, R.B.; Fronzaglia, A.;   *Inorg. Chem.* 1966, **5**, 1837-45

[36] Abel, E.W.; Bennett, M.A.; Burton, R.; Wilkinson, G.;   *J. Chem. Soc.* 1958, 4559

[37] Ward, L.G.L.;   *Inorg. Synth.*, 1972, **13**, 154

[38] Diel, B.N.; Haltiwanger, R.C.; Norman, A.D.;   *J. Am. Chem. Soc.*, 1982, **104**, 4700

   Diel, B.N.; Brandt, P.F.; Haltiwanger, R.C.; Hackney, M.L.J.; Norman, A.D.; *Inorg. Chem.* 1989, **26**, 2871

[39] McMullen, A.K.; Tilley, T.D.; Rheingold, A.L.; Geib, S.J.;   *Inorg. Chem.*, 1990, **29**, 2231

[40] Doyle, J.R.; Slade, P.E.; Jonassen, H.B.;   *Inorg. Synth.*, 1960, **6**, 218

[41] McGindle, R.; Alyea, E.C.; Ferguson, G.; Dias, S.A.; McAlees, J.;   *J. Chem. Soc.; Delton Trans.*, 1980, **1**, 137

[42] Angelici, R.J.;   *Inorg. Sunth.*, 1990, **28**, 346-348

[43] CA 63: 13310;   CA 64: 9576

APPENDICES

APPENDIX A

Crystal Data for Complexes VII, L, LI, and LIII:

For complex VII, $PdCl_2[{}^iPr_2NPO]_4$: $PdCl_2P_4O_4N_4C_{24}H_{56}$, monoclinic, $C2/c$, $a=19.985(5)$, $b=11.0945(10)$, $c=17.934(9)$ Å, $\beta=112.04(3)°$, $Z=4$, no. of unique reflections=3500, no. of observed reflections=3246, $R(F)=0.051$, $R(wF)=0.060$.

For complex L, cage isomer $Cr_2(CO)_8[DMP-PO]_4$: yellow block, $C_{36}H_{56}Cr_2N_4O_{12}P_4$, triclinic, $P1$, $a=9.905(3)$, $b=11.668(4)$, $c=12.189(4)$ Å, $\alpha=96.62(2)$, $\beta=110.81$ (2), $\gamma=112.59(2)°$, $V=1162.95(5)$ Å^3, $Z=1$, $D_x=1.378$ g cm^{-3}, $T=296$ K. Of 4799 data collected (Siemens P4, MoKα, $2\theta_{max}=52°$), 4571 were independent and 3489 were observed ($4\sigma F_o$). At convergence: $R(F)=4.81\%$, $R(wF)=6.99\%$.

For complex LI, cage $Cr_2(CO)_8[DMP-PO]_4$: colorless block, $C_{36}H_{56}Cr_2N_4O_{12}P_4$, monoclinic, $I2/a$, $a=27.593(8)$, $b=18.105(7)$, $c=18.648(5)$ Å, $\beta=91.45(2)°$, $V=9313(5)$ Å^3, $Z=8$, $D_x=1.376$ g cm^{-3}, $T=296$ K. Of 9464 data collected, 9164 were independent and 5611 were observed. At convergence: $R(F)=5.89\%$, $R(wF)=6.95\%$.

For complex LIII, cubane $Cr_2(CO)_6[DMP-PO]_6$: colorless block, $C_{48}H_{84}Cr_2N_6O_{12}P_6$, triclinic, $P1$, $a=11.882(4)$, $b=12.112(4)$, $c=13.219(4)$ Å, $\alpha=62.28(2)$, $\beta=66.18$ (2), $\gamma=67.54(2)°$, $V=1494.95(5)$ Å^3, $Z=1$, $D_x=1.36$ g cm^{-3}, $T=296$ K. Of 4122 data collected, 3916 were independent and 2910 were observed ($4\sigma F_o$). At convergence: $R(F)=4.01\%$, $R(wF)=4.42\%$.

142

Crystals of complex LIII, cubane $Cr_2(CO)_6[DMP-PO]_6$, were also obtained as a xylene solvated; the structures of the dichromium complex are chemically identical in these two forms with Cr--Cr seperations of 4.700(1) Å and 4.692(2) Å respectively. Crystal data for this complex (xylene): colorless block, $C_{48}H_{84}Cr_2N_6O_{12}P_6$, triclinic, P1, a=10.650(2), b=12.407(3), c=13.064(3) Å, α=106.64(3), β=93.60(2), γ=95.92(2)°, V=1637.3(6) Å^3, Z=1, D_x=1.352 g cm^{-3}, T=237 K. Of 6055 data collected, 5778 were independent and 4515 were observed. At convergence: R(F)=4.66%, R(wF)=5.19%.

143

APPENDIX B

COMPOUND NUMBER ASSIGNMENTS

I	$NiCl_2 \cdot [^iPr_2NPO]_4$
II	$NiBr_2 \cdot [^iPr_2NPO]_4$
III	$NiCl_2 \cdot [Cy_2NPO]_4$
IV	$NiBr_2 \cdot [Cy_2NPO]_4$
V	$NiI_2 \cdot [Cy_2NPO]_4$
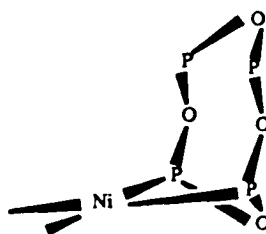
VI	$NiCl_2 \cdot [Cy_2NPO]_5$
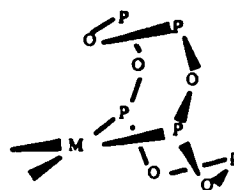
VII	$PdCl_2 \cdot [^iPr_2NPO]_4$
VIII	$PdBr_2 \cdot [^iPr_2NPO]_4$
IX	$PdCl_2 \cdot [Cy_2NPO]_4$
X	$PdBr_2 \cdot [Cy_2NPO]_4$

144

XI $PdCl_2 \cdot [Cy_2NPO]_5$

XII $PdBr_2 \cdot [Cy_2NPO]_5$ isomer A

XIII $PdBr_2 \cdot [Cy_2NPO]_5$ isomer B

XIV $PtCl_2 \cdot [^iPr_2NPO]_4$

XV $PtCl_2 \cdot [Cy_2NPO]_5$

145
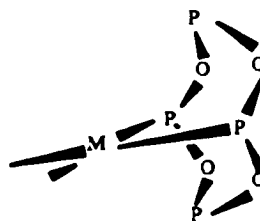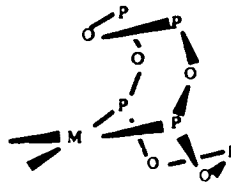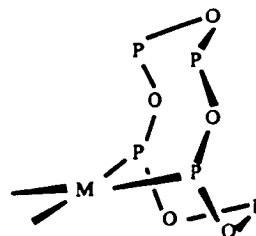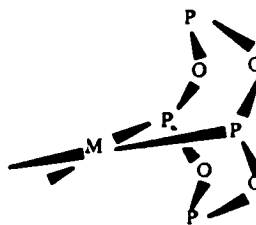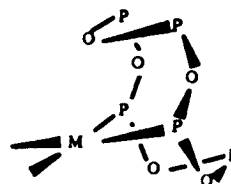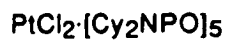
XVI $PtCl_2 \cdot [Cy_2NPO]_4$ isomer A
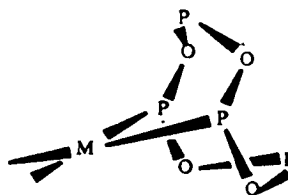
XVII $PtCl_2 \cdot [Cy_2NPO]_4$ isomer B
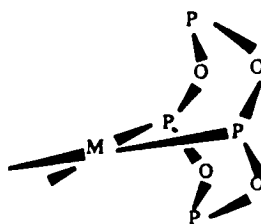
XVIII $Mo(CO)_4 \cdot [^iPr_2NPO]_3$

XIX $Mo(CO)_4 \cdot [Cy_2NPO]_3$
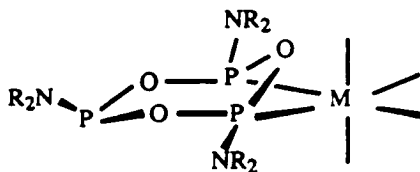
XX $Mo_2(CO)_8 \cdot [^iPr_2NPO]_4$ cage

XXI $Mo_2(CO)_8 \cdot [Cy_2NPO]_4$ cage

146
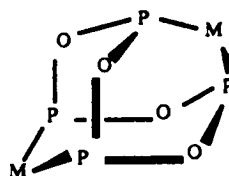
XXII $Mo_2(CO)_8 \cdot [^iPr_2NPO]_4$ cage isomer

XXIII $Mo_2(CO)_8 \cdot [Cy_2NPO]_4$ cage isomer
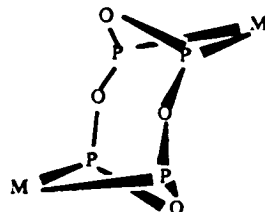
XXIV $Cr(CO)_4 \cdot [Cy_2NPO]_4$
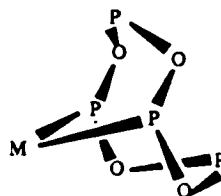
XXV $Fe(CO)_3 \cdot [Cy_2NPO]_4$
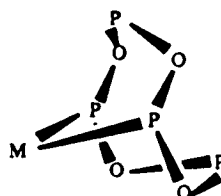
XXVI $Fe(CO)_3 \cdot [^iPr_2NPO]_4$

147

XXVII $Fe(CO)_4 \cdot \{^iPr_2NP[OP(O)^iPr_2N]_2PN^iPr_2\}$

XXVIII $Mo(CO)_4 \cdot [Cy_2NPO]_4 \cdot NiBr_2$

XXIX $Mo(CO)_3 \cdot [Cy_2NPO]_5 \cdot PdCl_2$

XXX $Mo(CO)_4 \cdot [^iPr_2NPO]_4 \cdot Fe(CO)_3$

(F)

XXXI $Ni_2(CO)_4 \cdot [Cy_2NPO]_4$ cage

148

XXXII   PdClBr·[Cy$_2$NPO]$_5$

XXXIII   PdBr$_2$·[^{s}Bu$_2$NPO]$_4$
XXXIV   PdBr$_2$·[^{i}PrCyNPO]$_4$

XXXV   NiBr$_2$·[Ph$_2$NPO]$_5$

XXXVI   [Cy$_2$NPO]$_3$S$_2$

149
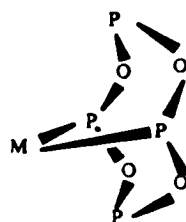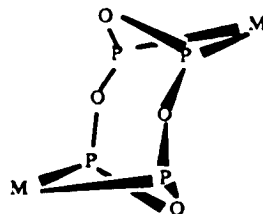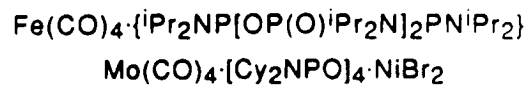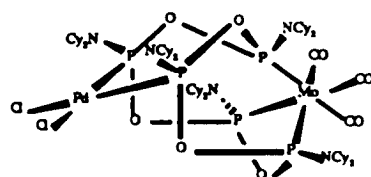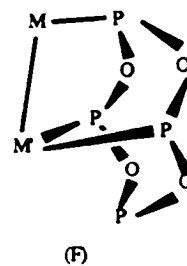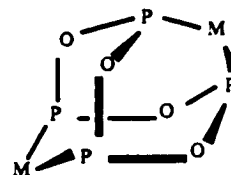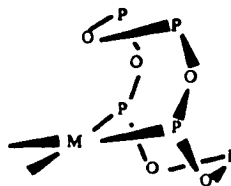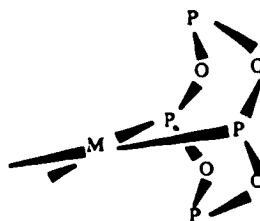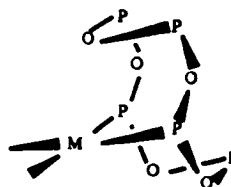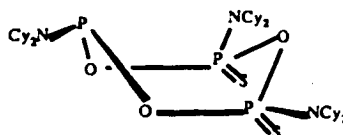
XXXVII	$Cr(CO)_4 \cdot (Et_2N)_2POP(Et_2N)_2$
XXXVIII	$Mo(CO)_4 \cdot (Et_2N)_2POP(Et_2N)_2$
XXXIX	$Mo_2(CO)_4 \cdot [Et_2NPO]_4$
XL	$W(CO)_4 \cdot (Et_2N)_2POP(Et_2N)_2$
XLI	$Cr(CO)_4 \cdot (PIP)_2POP(PIP)_2$
XLII	$W(CO)_4 \cdot (PIP)_2POP(PIP)_2$
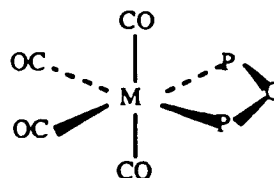
XLIII $\qquad$ $Cr(CO)_4 \cdot [Cy_2NPO]_4$ isomer
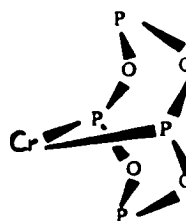
XLIV $\qquad$ $Cr_2(CO)_8 \cdot [Cy_2NPO]_4$ cage isomer

XLV $\qquad$ $Cr(CO)_5 \cdot (Cy_2N)_2P(O)H$

150

XLVI $Cr_2(CO)_7 \cdot [Cy_2NPO]_5$

XLVII $W_2(CO)_7 \cdot [Cy_2NPO]_5$

XLVIII $W_2(CO)_6 \cdot [Cy_2NPO]_4$

XLIX $W(CO)_4 \cdot [Cy_2NPO]_3$

L $Cr_2(CO)_8 \cdot [DMP\text{-}PO]_4$ cage isomer

151

LI   Cr₂(CO)₈·[DMP-PO]₄ cage

$Cr_2(CO)_8 \cdot [DMP\text{-}PO]_4$ cage

LII $Cr_2(CO)_7 \cdot [DMP\text{-}PO]_5$

LIII $Cr_2(CO)_6 \cdot [DMP\text{-}PO]_6$

LIV $Mo_2(CO)_8 \cdot [DMP\text{-}PO]_4$ cage

152
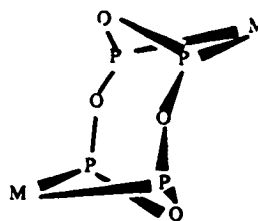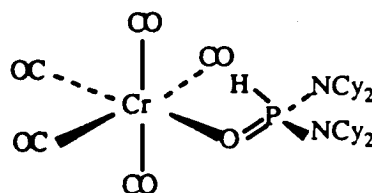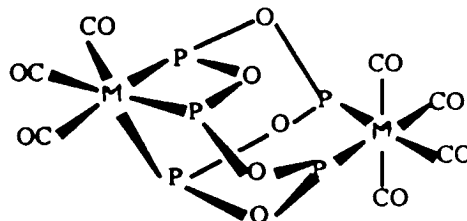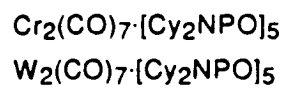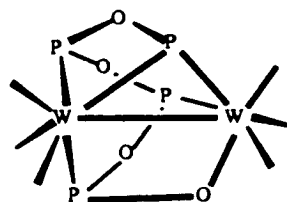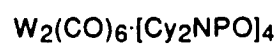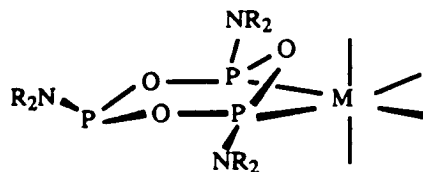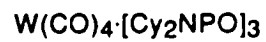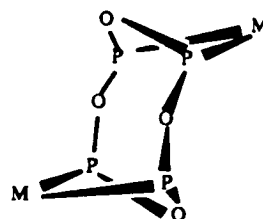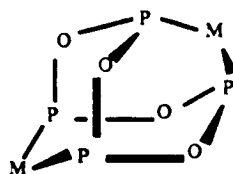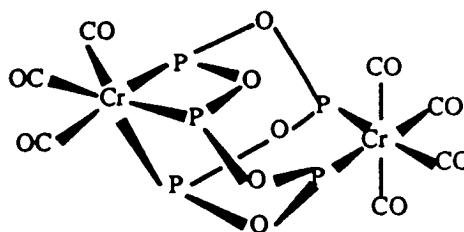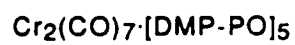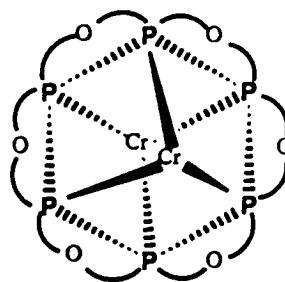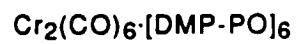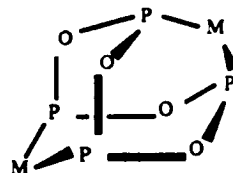
APPENDIX C

^{1}H, ^{13}C NMR SPECTRA AND IR SPECTRA OF SELECTED COMPLEXES

NiBr$_2$[Cy$_2$NPO]$_4$ (IV) ^{1}H NMR spectrum in CDCl$_3$

154

NiBr$_2$[Cy$_2$NPO]$_4$ (IV) ^{13}C {^{1}H} NMR spectrum in CDCl$_3$

155
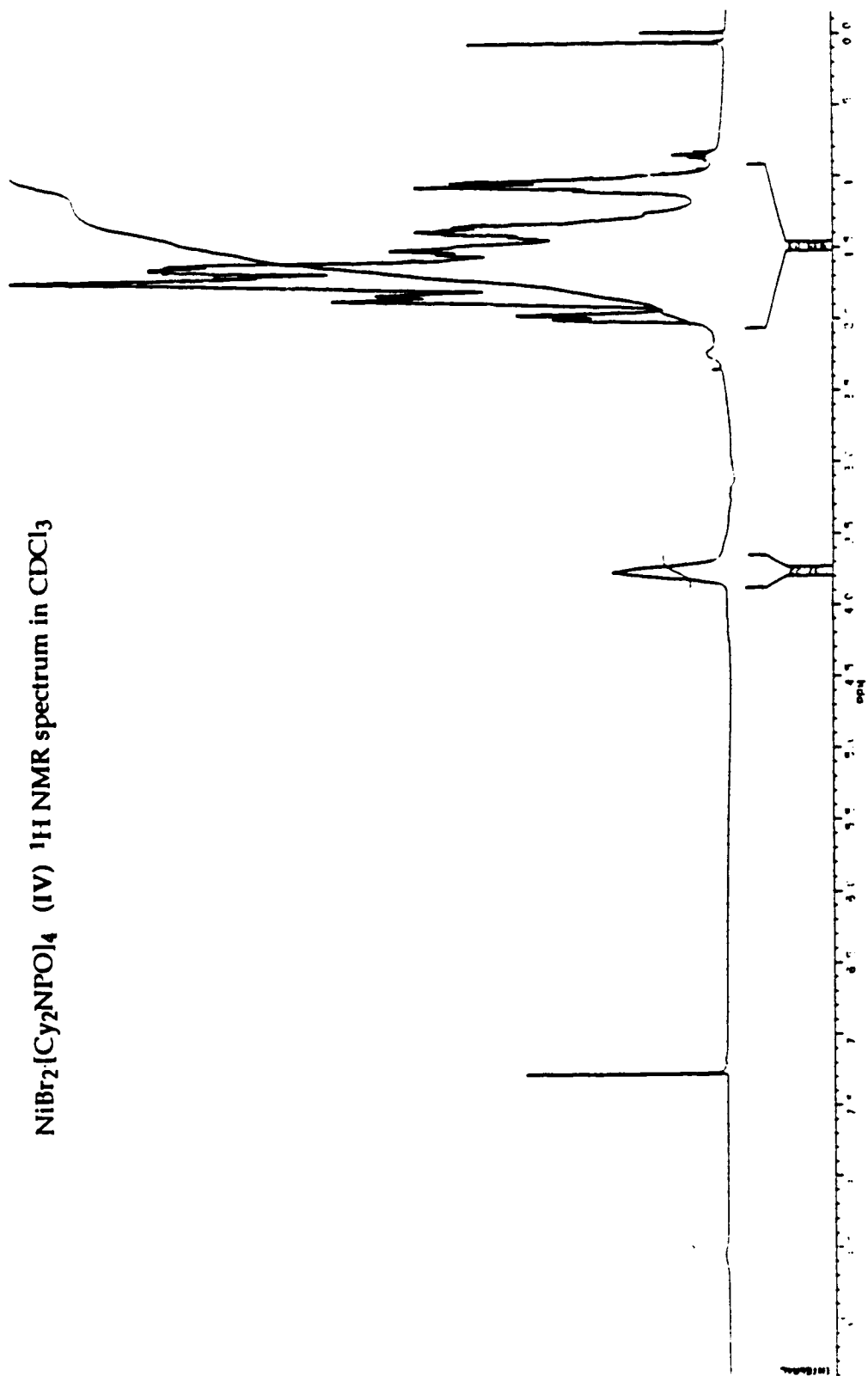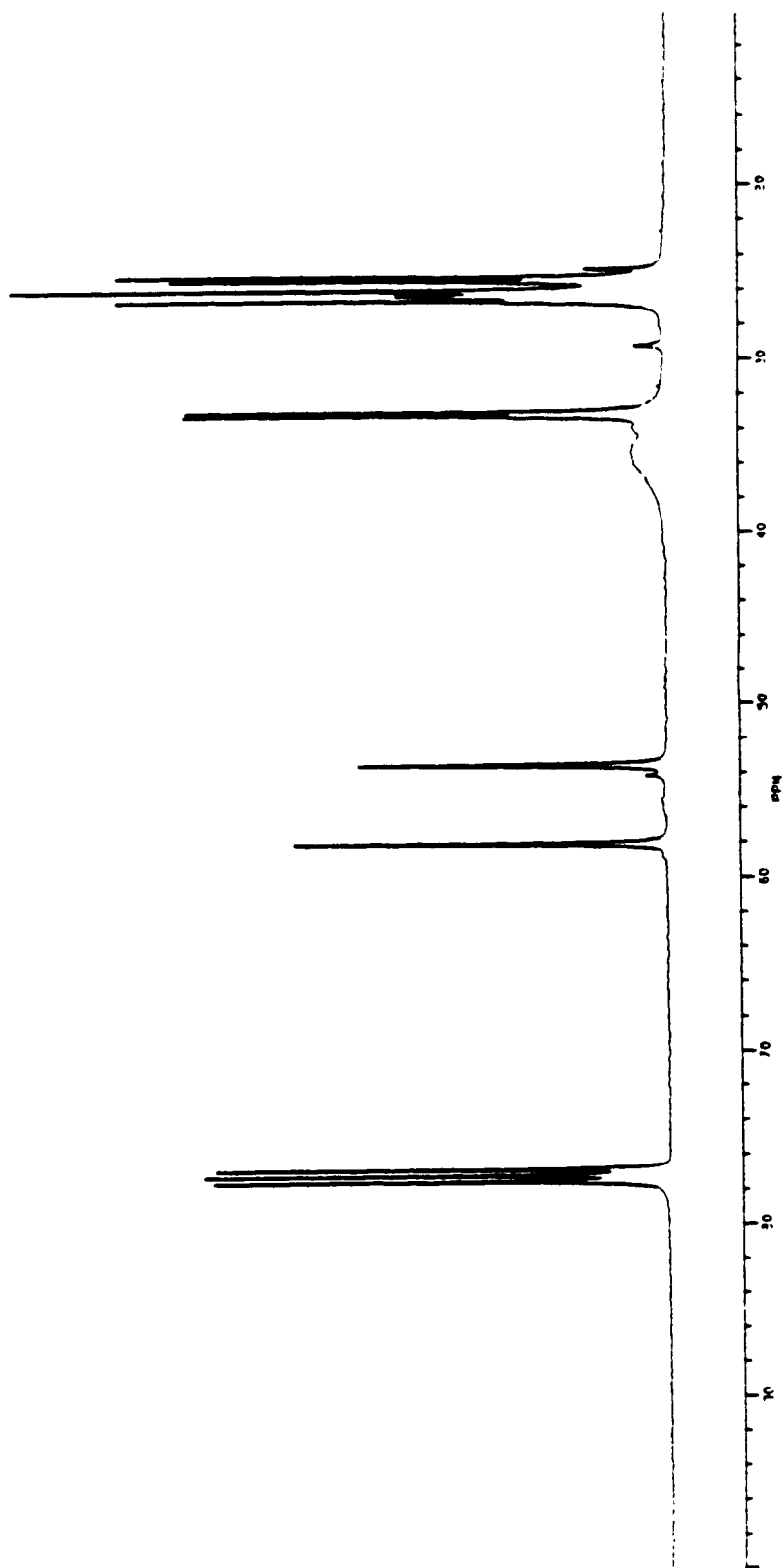
PdCl$_2$[Cy$_2$NPO]$_5$ (XI) IR spectrum (KBr)

156
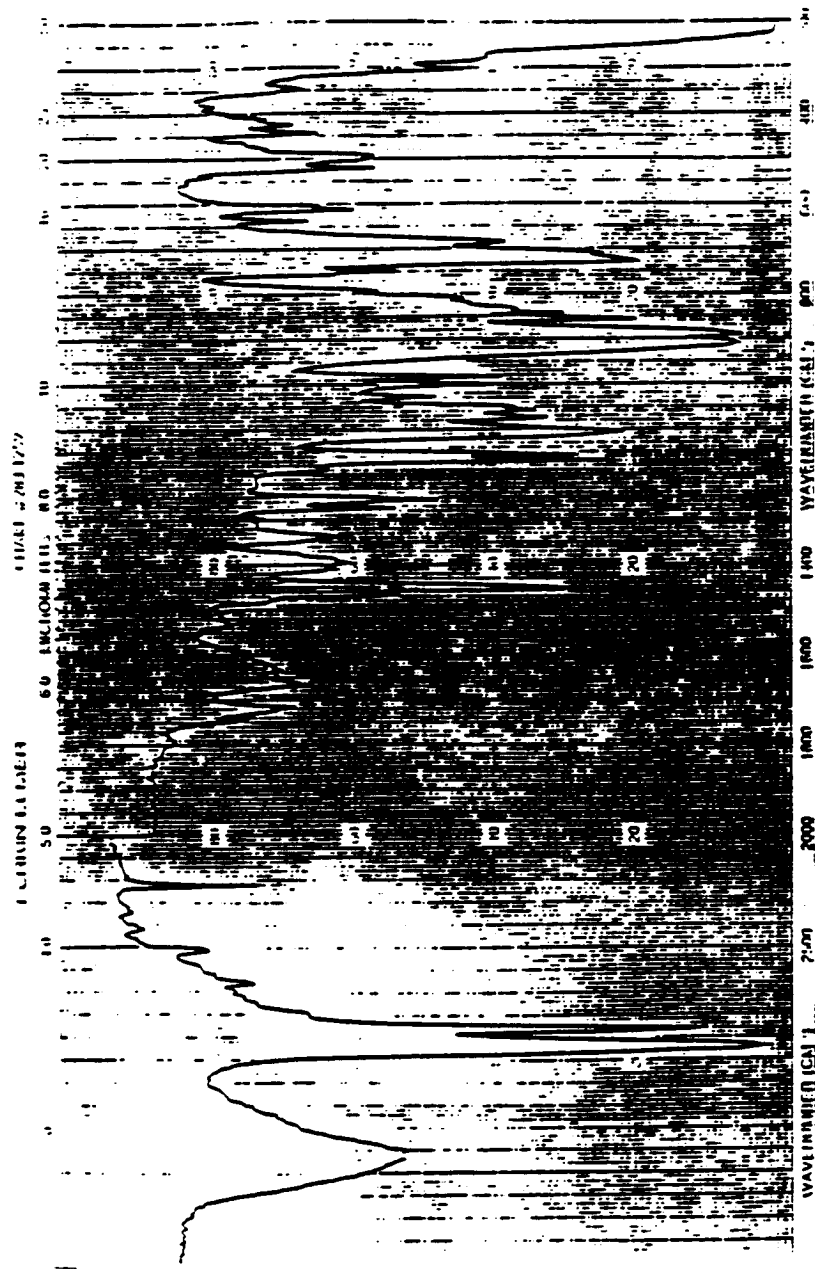
PdCl$_2$[Cy$_2$NPO]$_5$ (XI) ^{13}C {^{1}H} NMR spectrum in CDCl$_3$

157
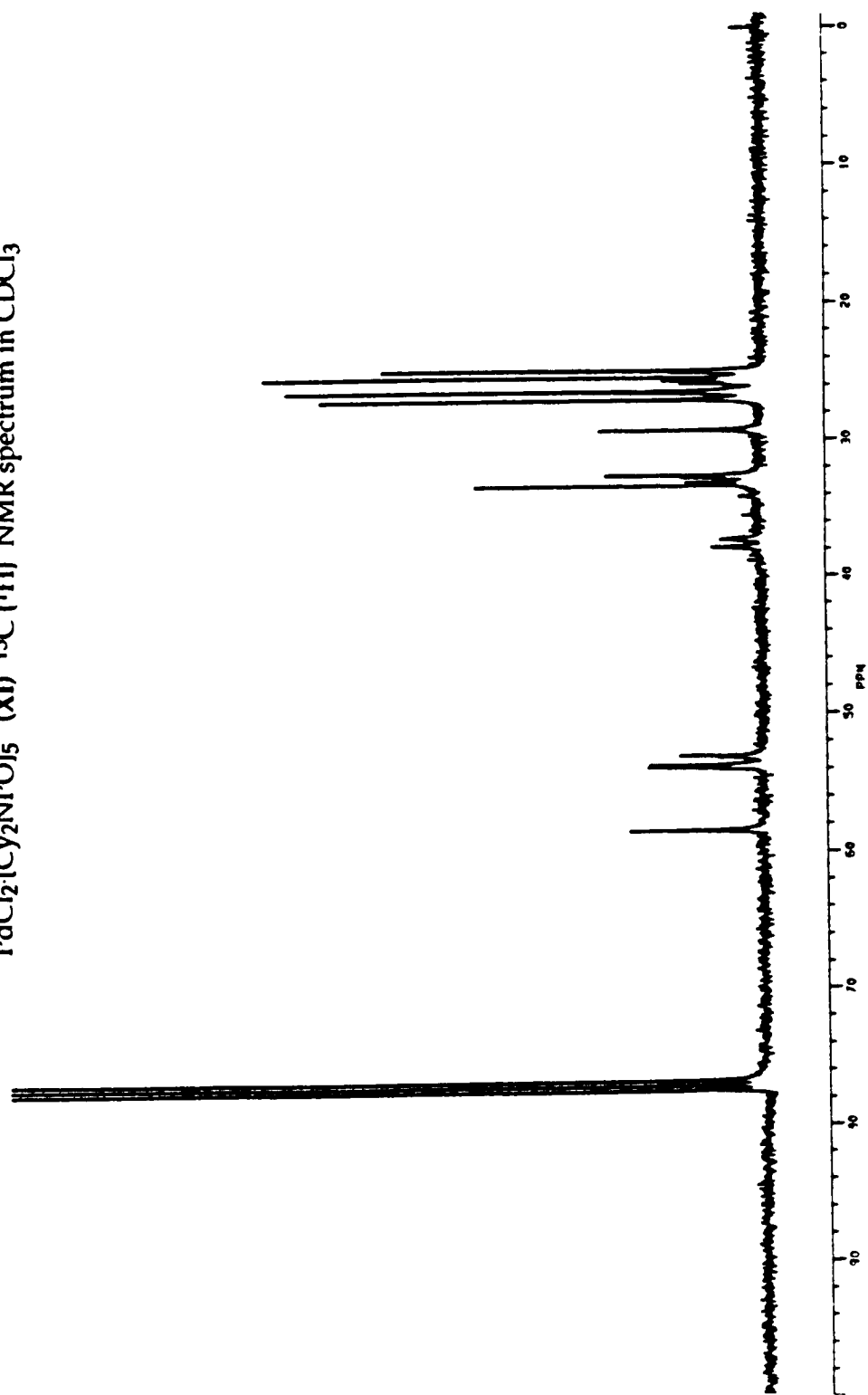
PdCl$_2$·[Cy$_2$NPO]$_5$ (XI) ^{1}H NMR spectrum in CDCl$_3$

158
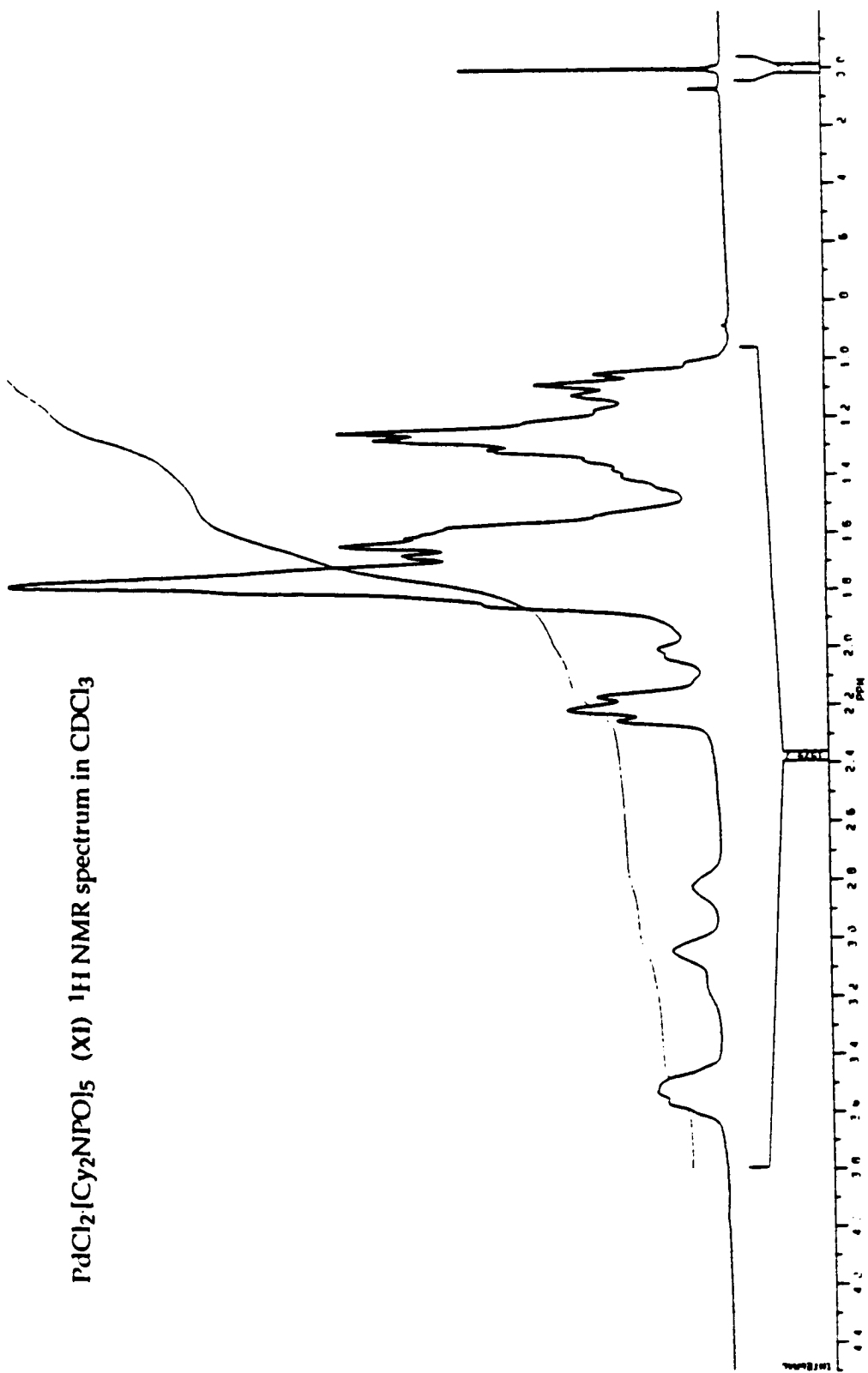
NiBr₂·[Cy₂NPO]₄·Mo(CO)₄ (XXVIII) ¹H NMR spectrum in CDCl₃

159
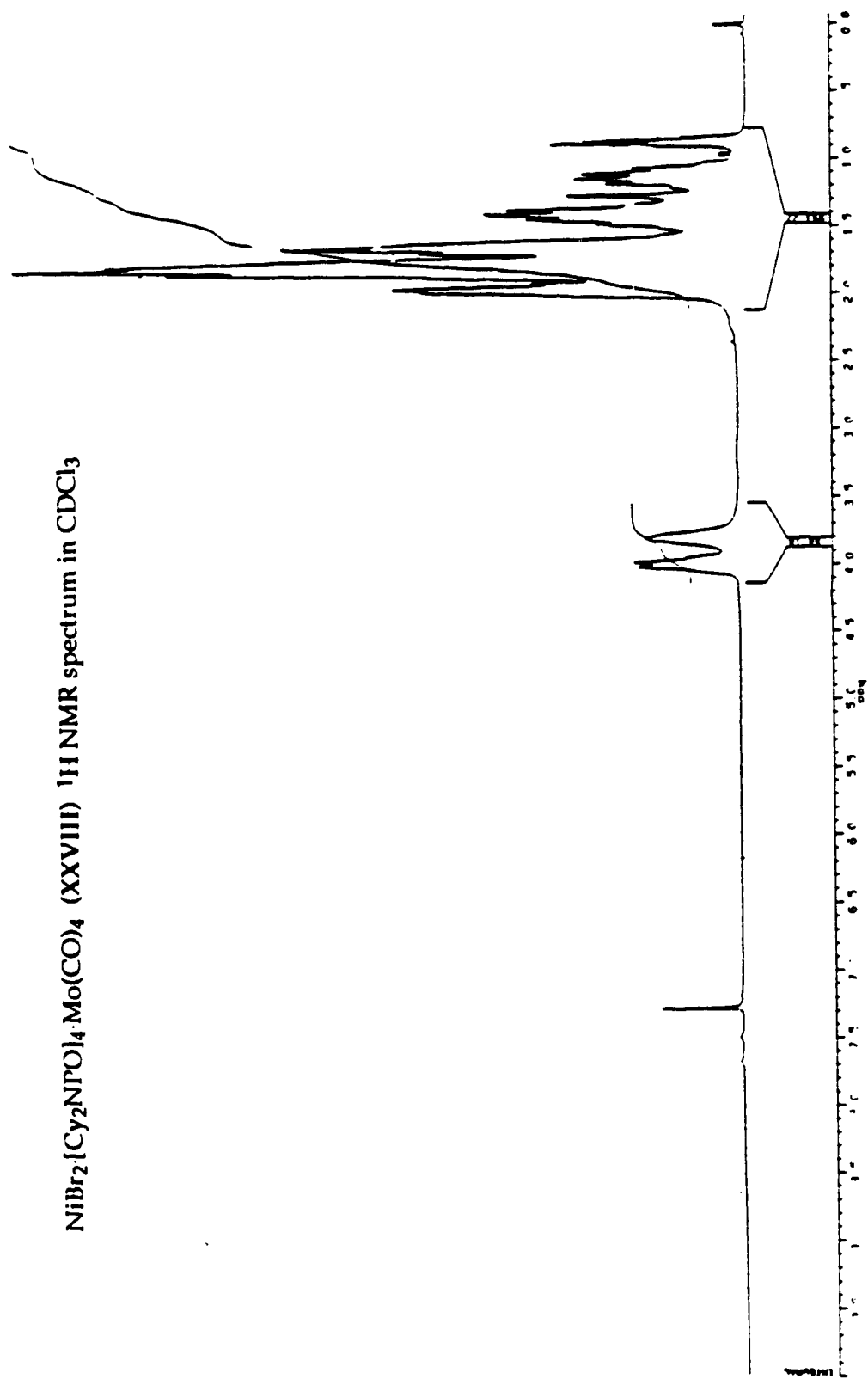
$NiBr_2[Cy_2NPO]_4 \cdot Mo(CO)_4$ (XXVIII) ^{13}C {^{1}H} NMR spectrum in $CDCl_3$

160
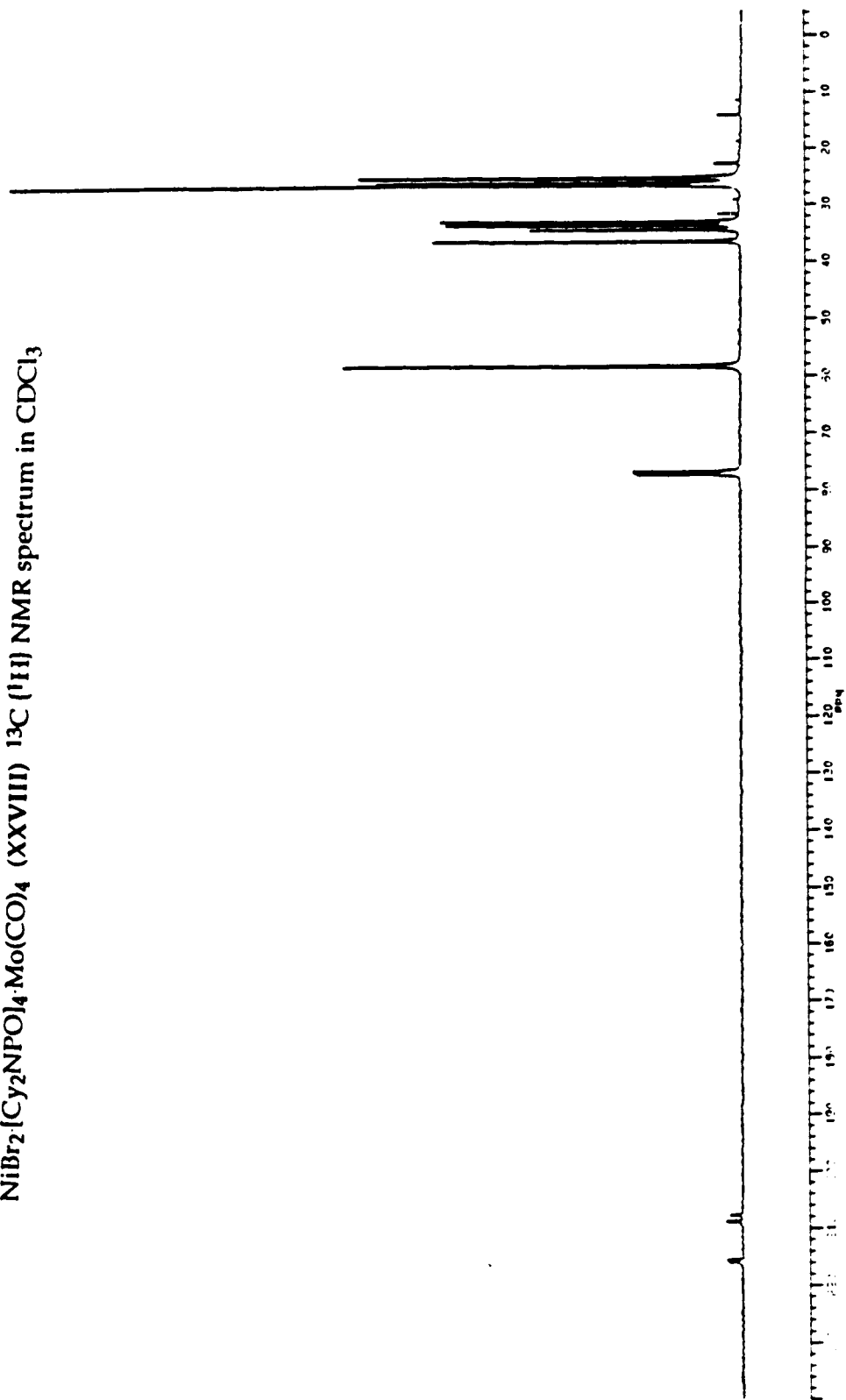
PdCl$_2$·[Cy$_2$NPO]$_5$·Mo(CO)$_3$ (XXIX) ^{1}H NMR spectrum in CDCl$_3$

161
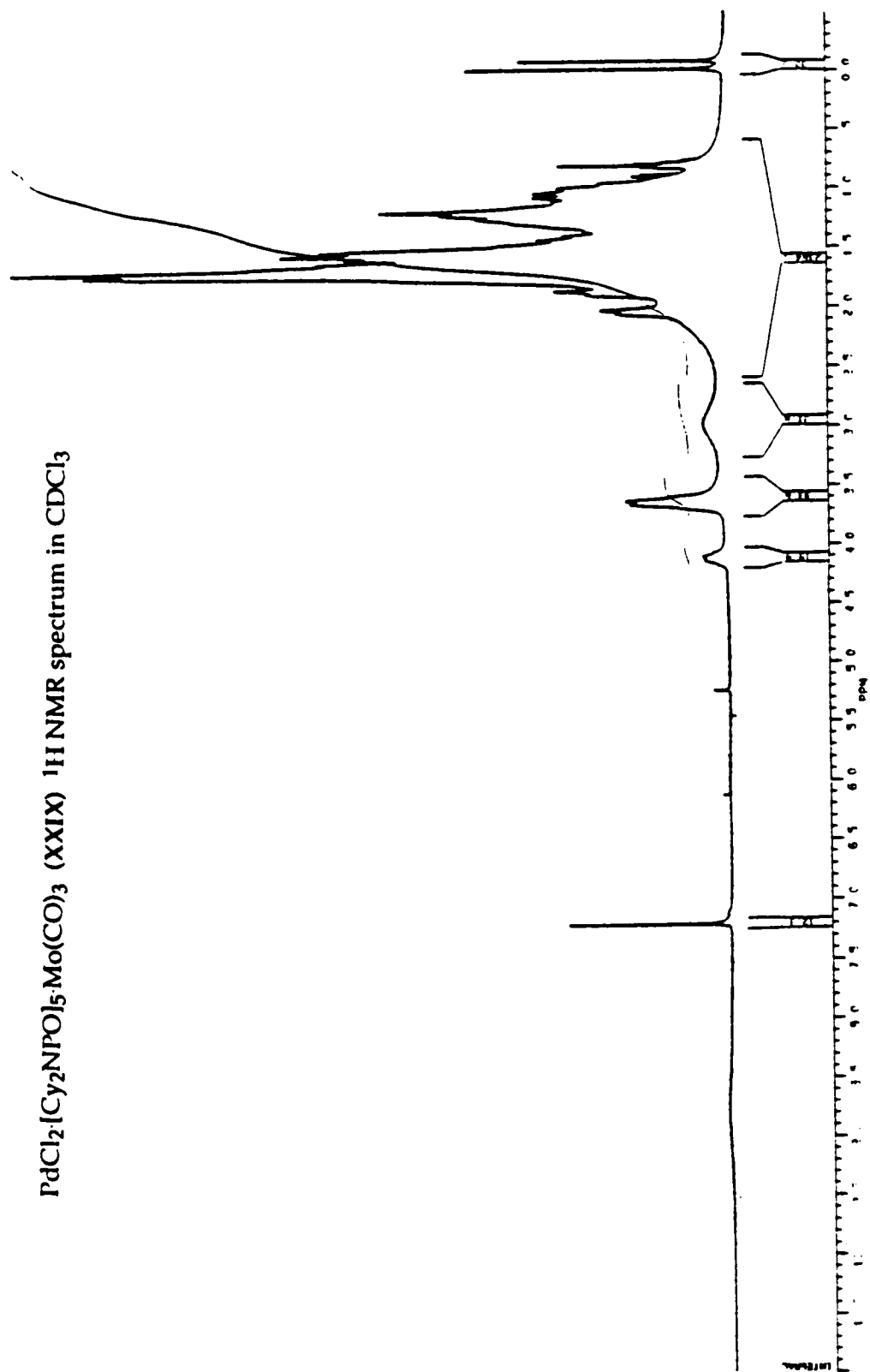
PdCl$_2$·[Cy$_2$NPO]$_5$·Mo(CO)$_3$ (XXIX) ^{13}C {^{1}H} NMR spectrum in CDCl$_3$

162
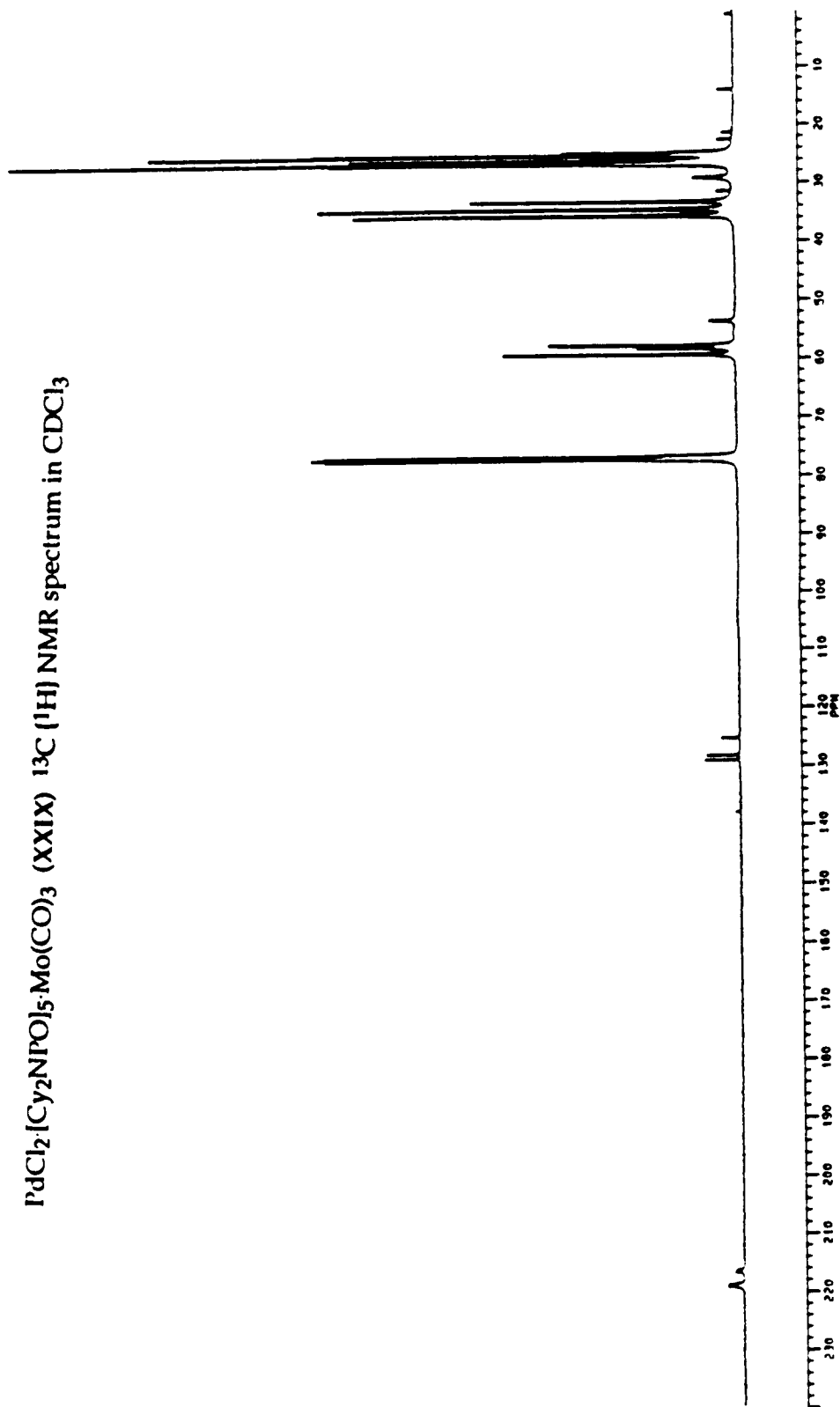
Ni$_2$(CO)$_4$·[Cy$_2$NPO]$_4$ (XXXI) cage IR spectrum (KBr)

163
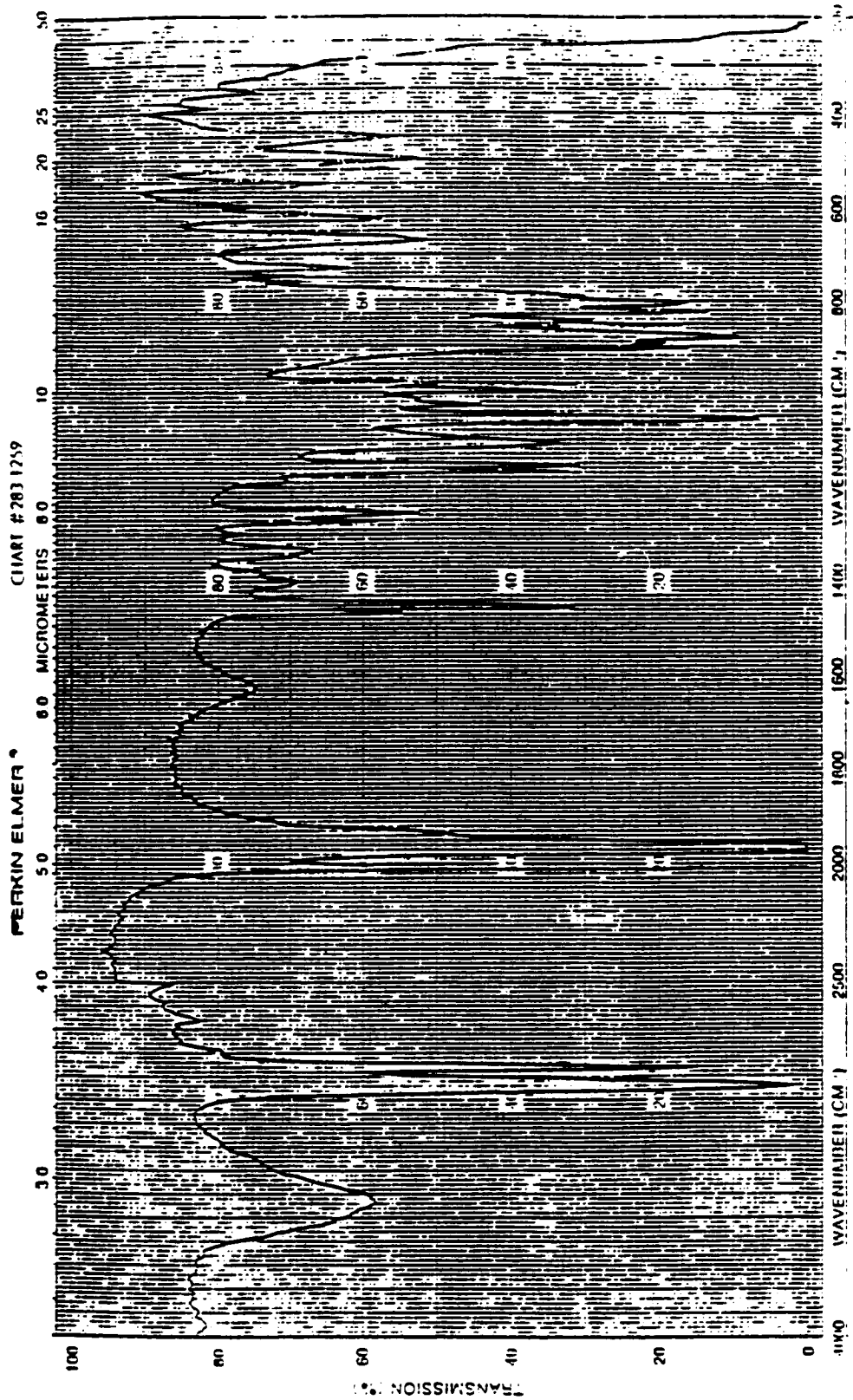
Ni$_2$(CO)$_4$·[Cy$_2$NPO]$_4$ (XXXI) cage ^{13}C {^{1}H} NMR spectrum in CDCl$_3$

164
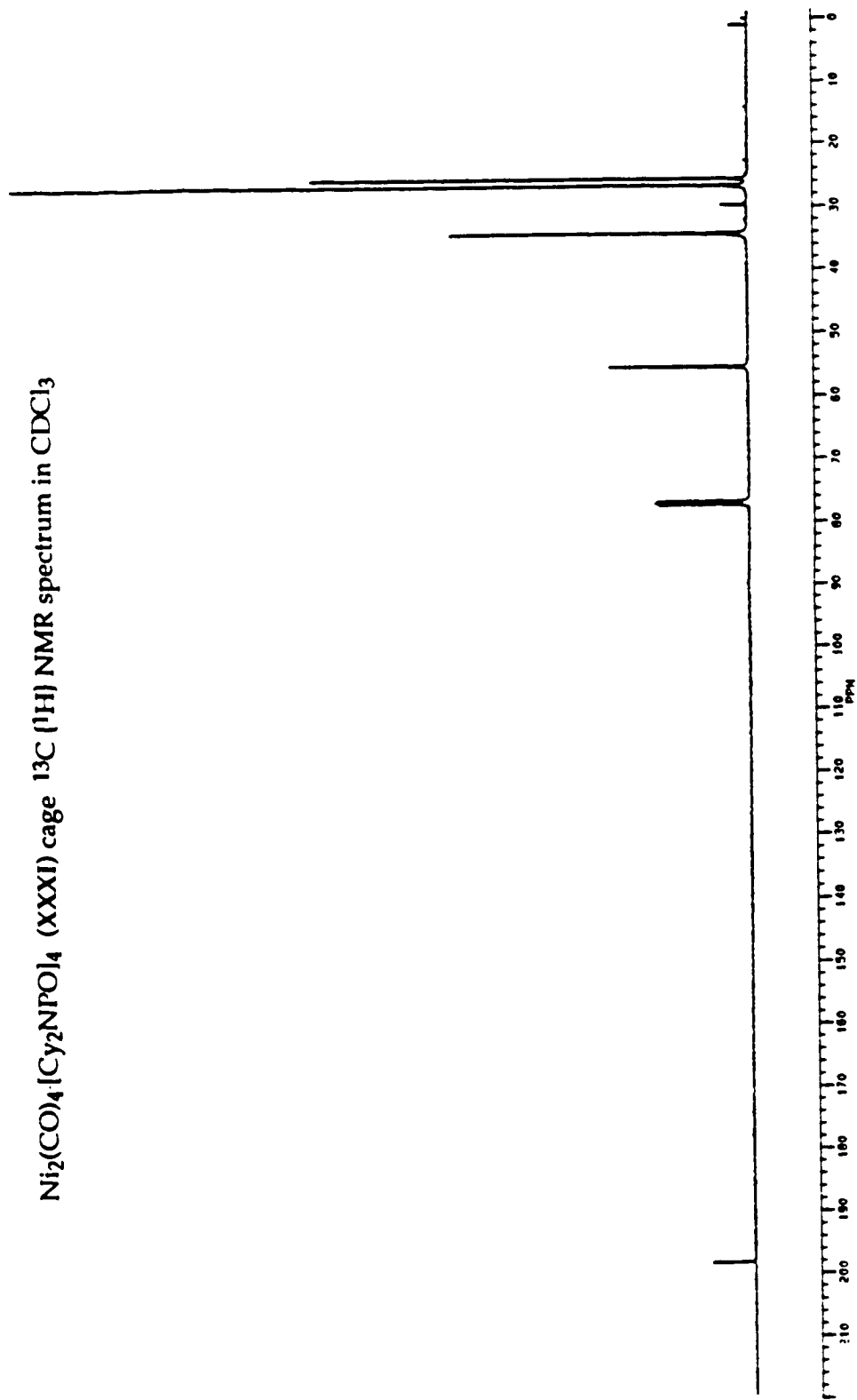
$Ni_2(CO)_4[Cy_2NPO]_4$ (XXXI) cage ^1H NMR spectrum in $CDCl_3$

165
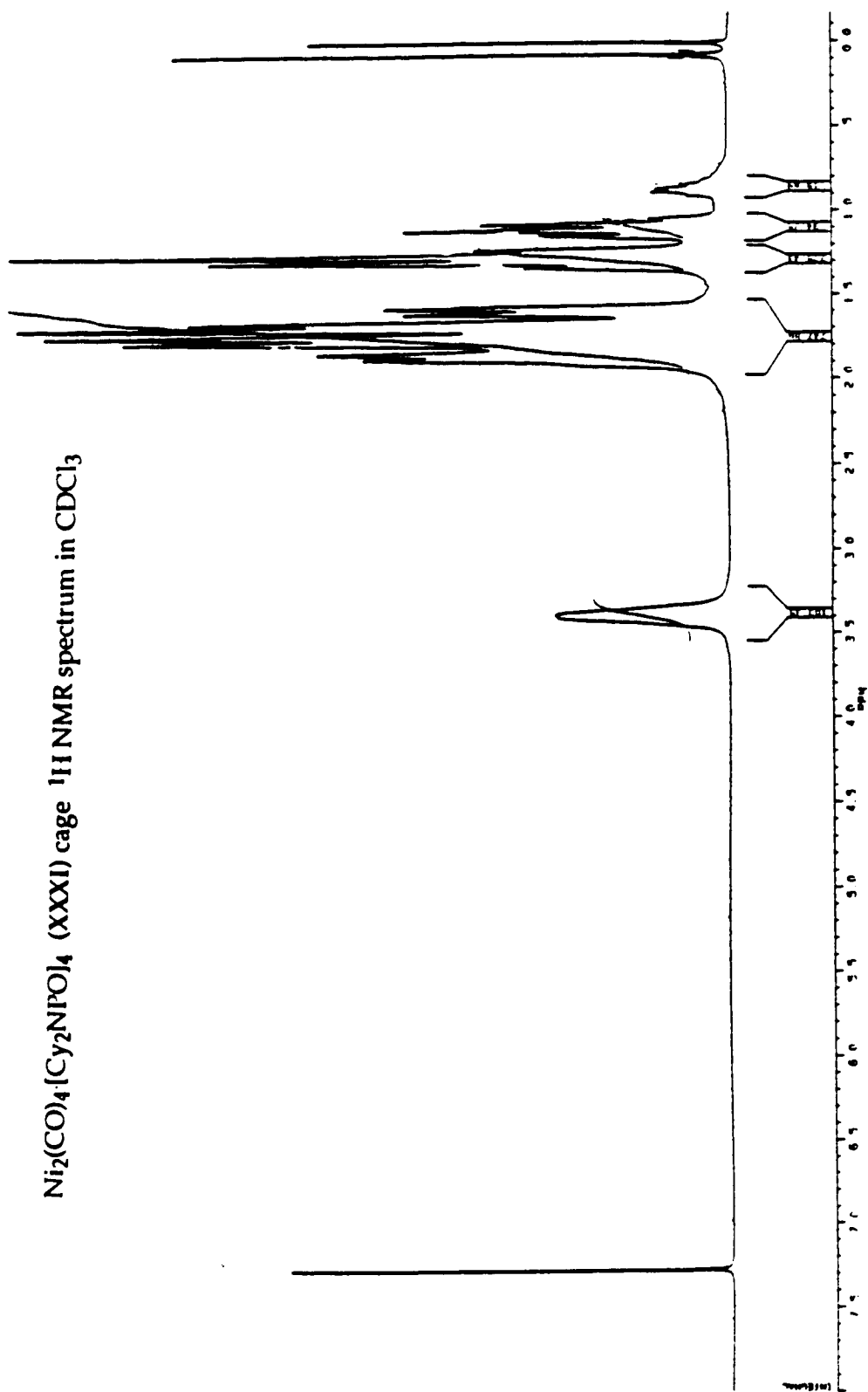
Cr(CO)$_4$[PIP]$_2$POP[PIP]$_2$ (XXXVII) IR spectrum (KBr)

166
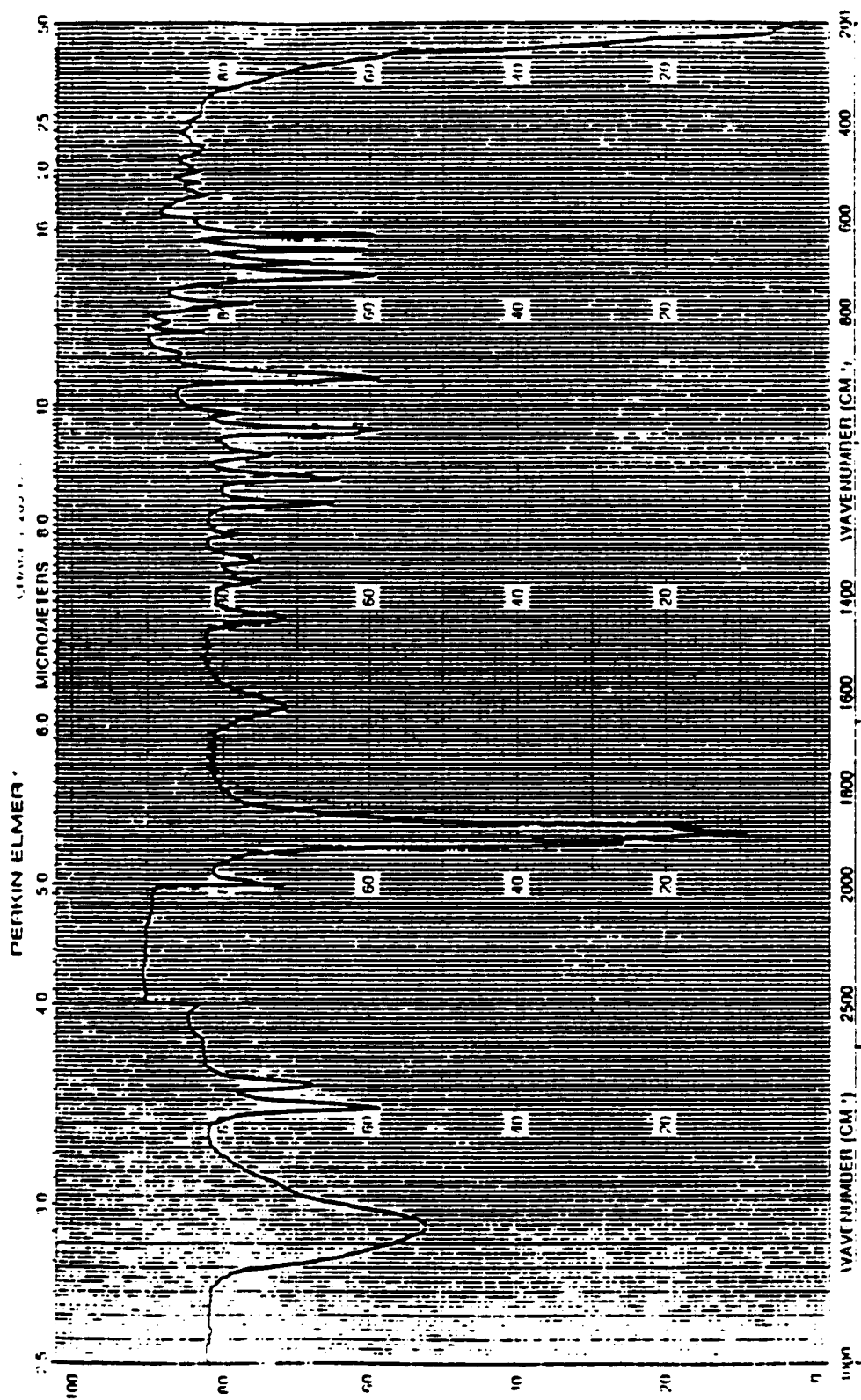
Mo(CO)$_4$·[Et$_2$N]$_2$POP[Et$_2$N]$_2$ (XXXVIII) ^{1}H NMR spectrum in CDCl$_3$

167
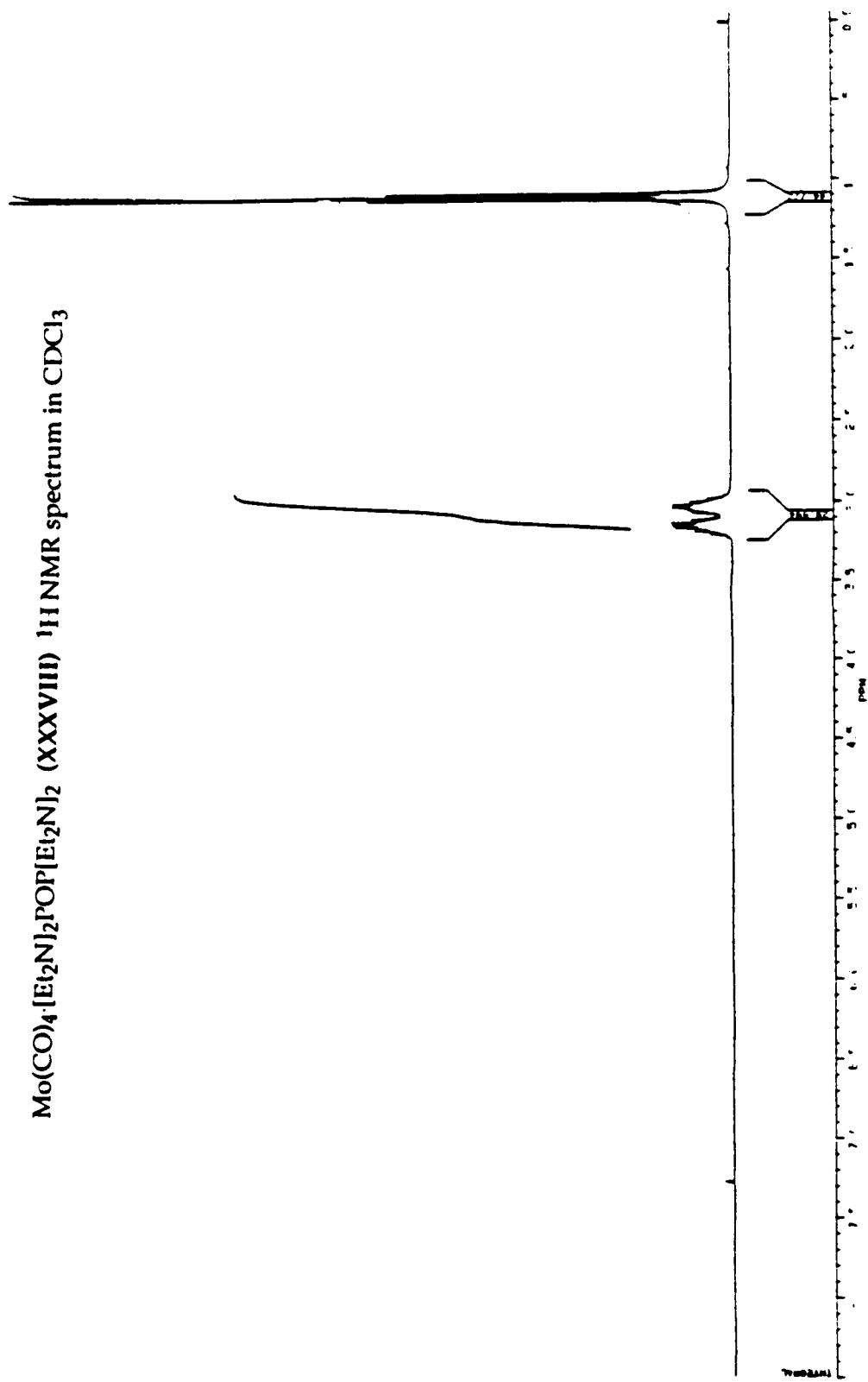
Mo(CO)₄[Et₂N]₂POP[Et₂N]₂ (XXXVIII) ¹³C {¹H} NMR spectrum in CDCl₃

168
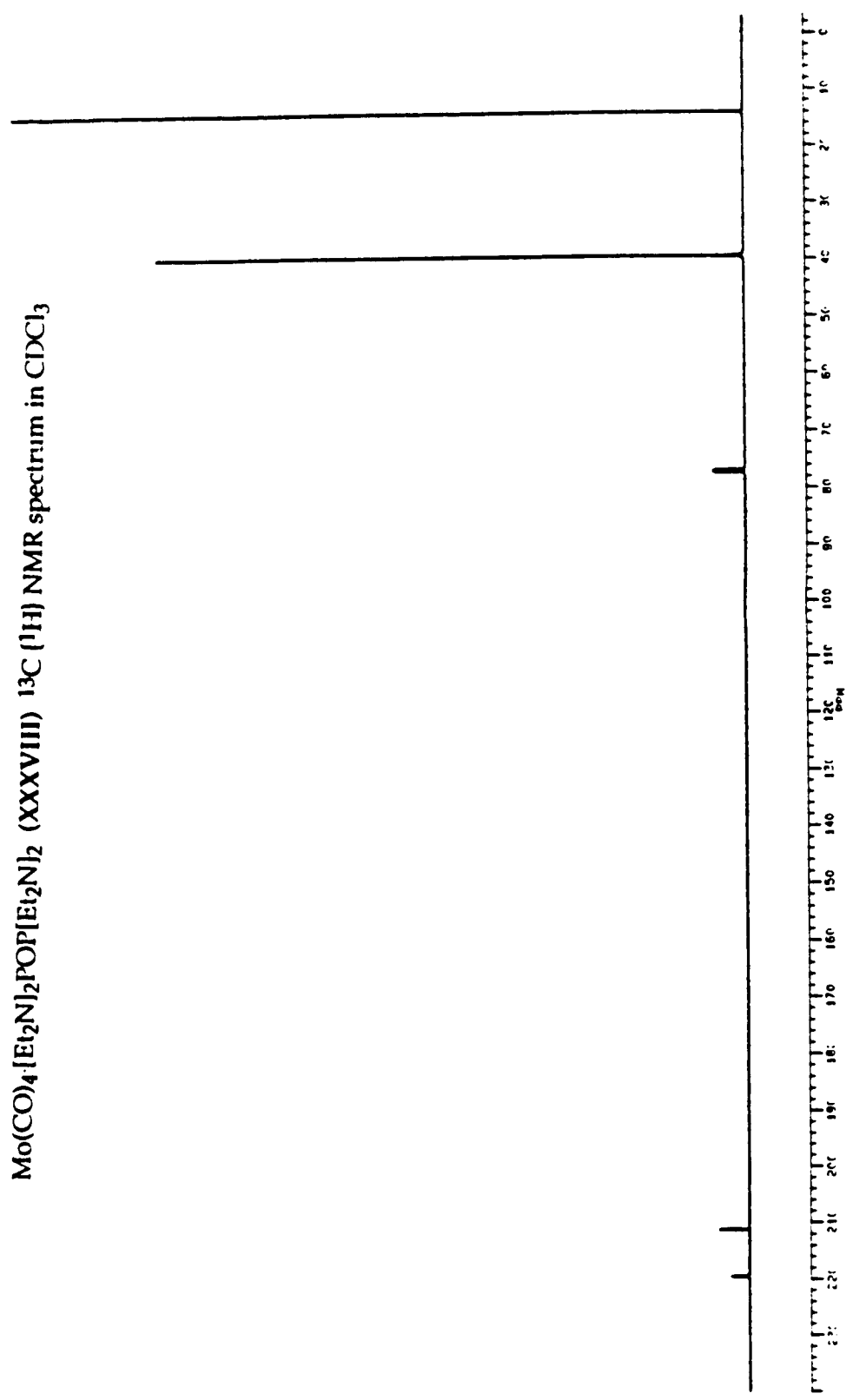
Cr(CO)₅[Cy₂N]₂P(O)H (XLV) IR spectrum (KBr)

169

Cr(CO)$_5$·[Cy$_2$N]$_2$P(O)H (XLV) ^{31}P {^{1}H} NMR spectrum in CDCl$_3$

170

Cr(CO)₅·[Cy₂N]₂P(O)H (XLV) ¹H NMR spectrum in CDCl₃

171
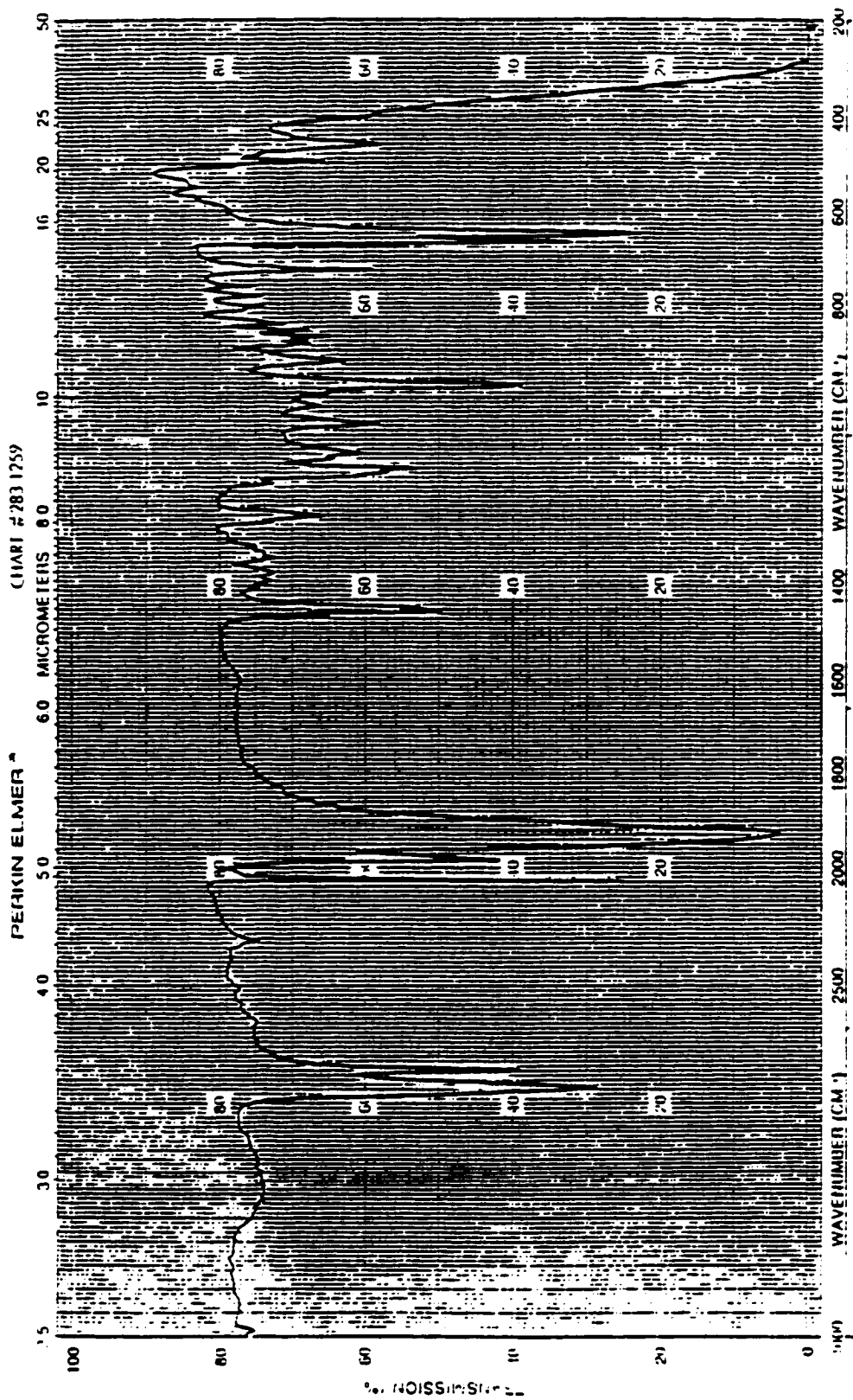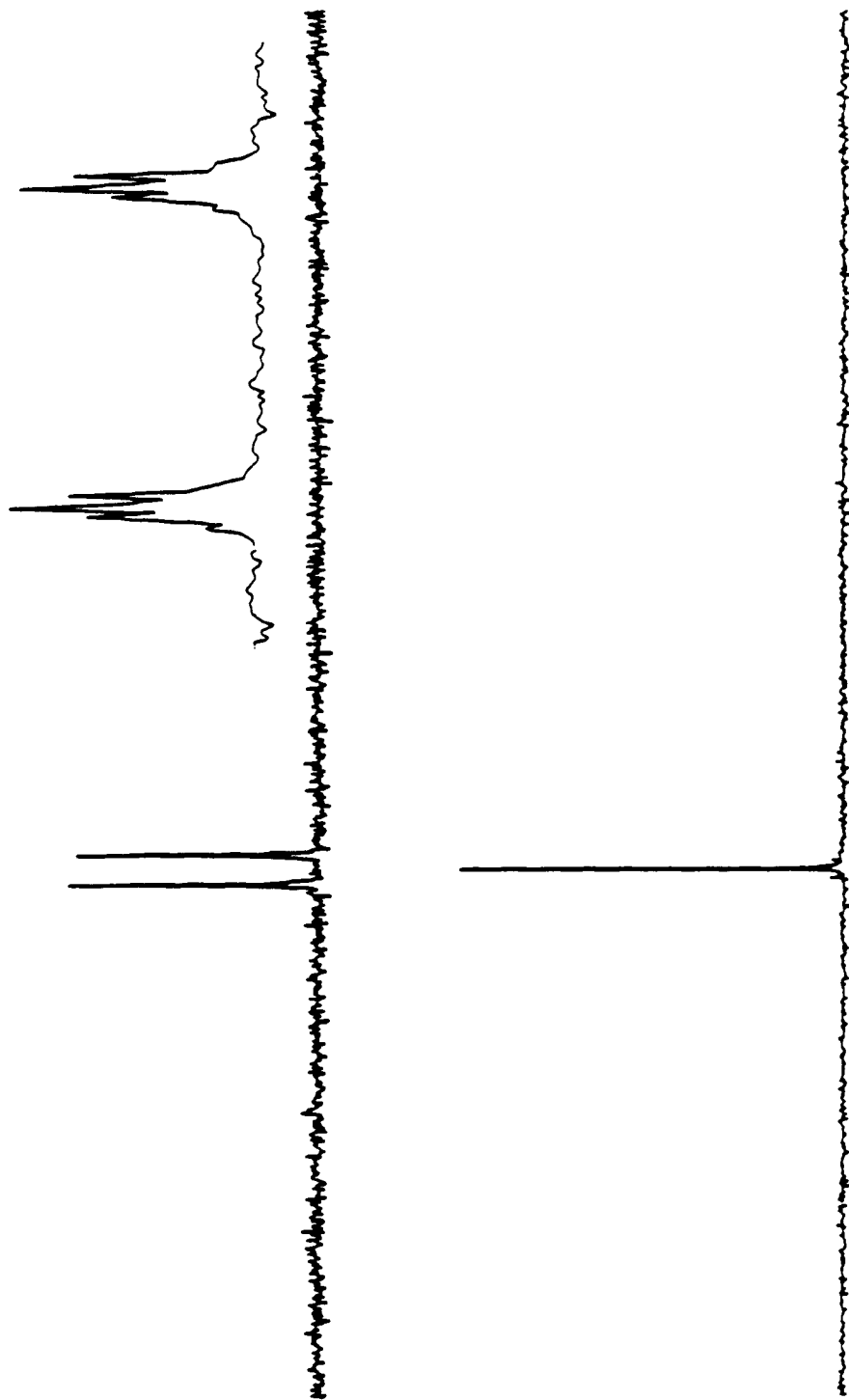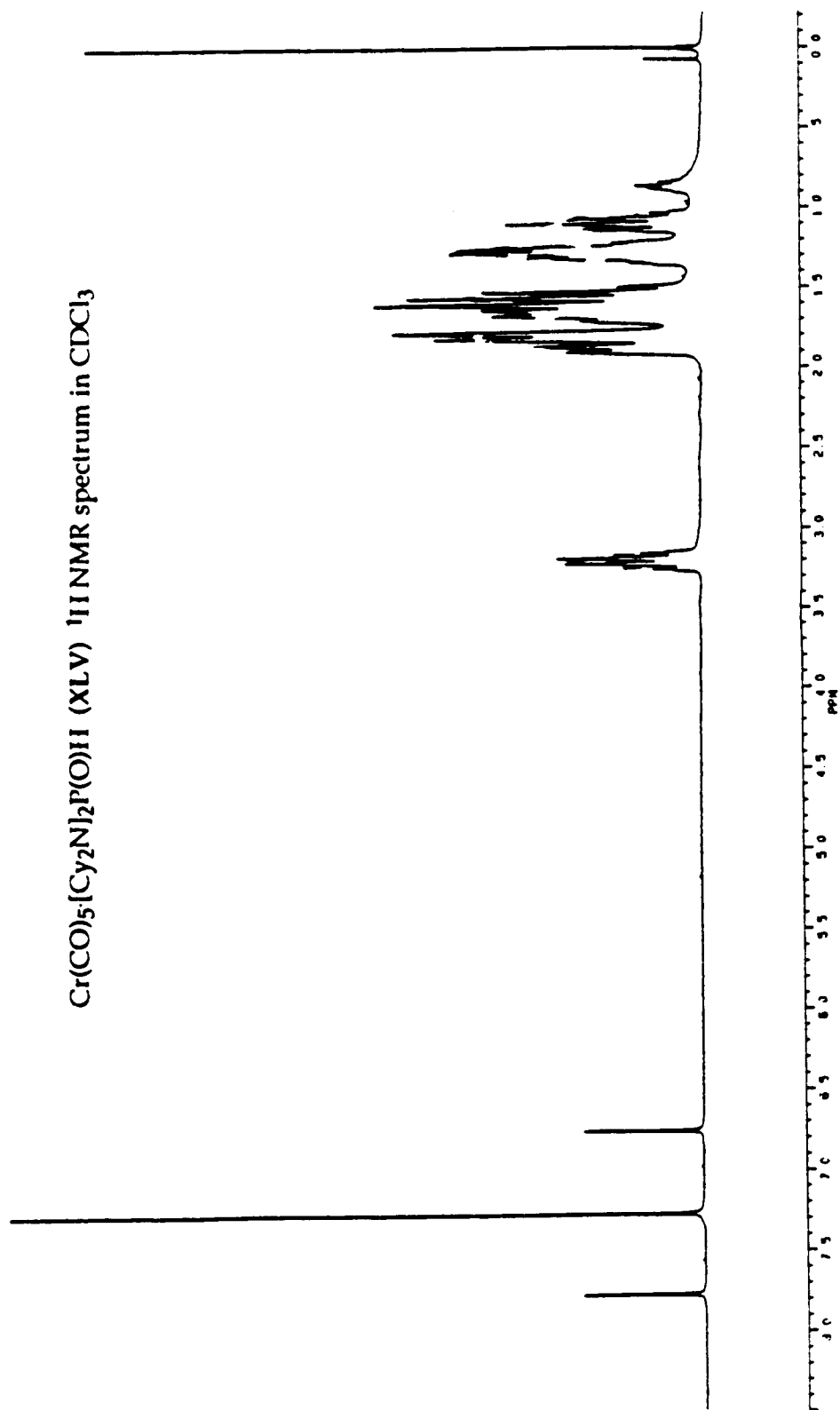
Cr(CO)₅[Cy₂N]₂P(O)H (XLV) ¹³C [¹H] NMR spectrum in CDCl₃

172
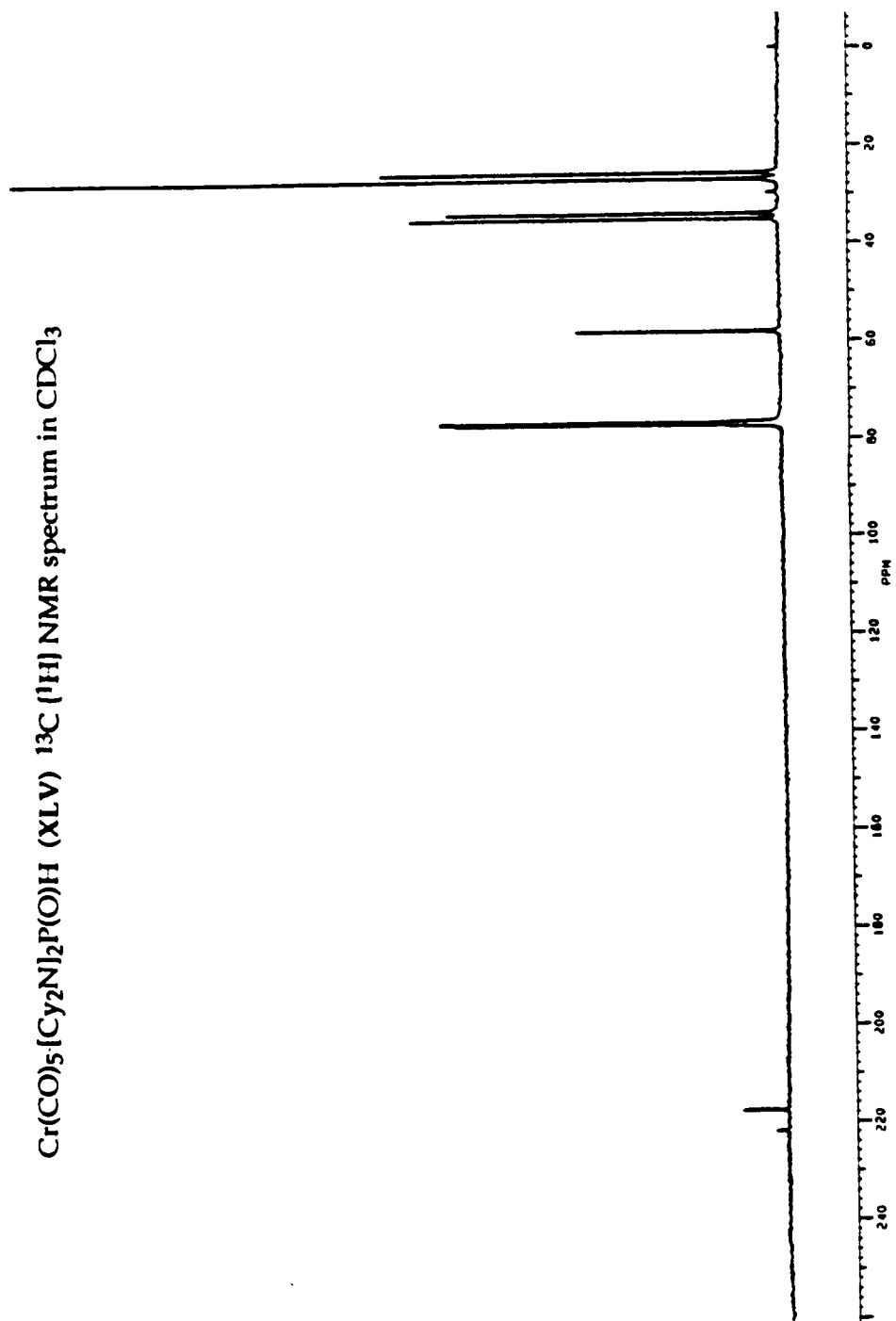
Cr$_2$(CO)$_6$[DMP-PO]$_6$ (LIII) cubane IR spectrum (KBr)

173
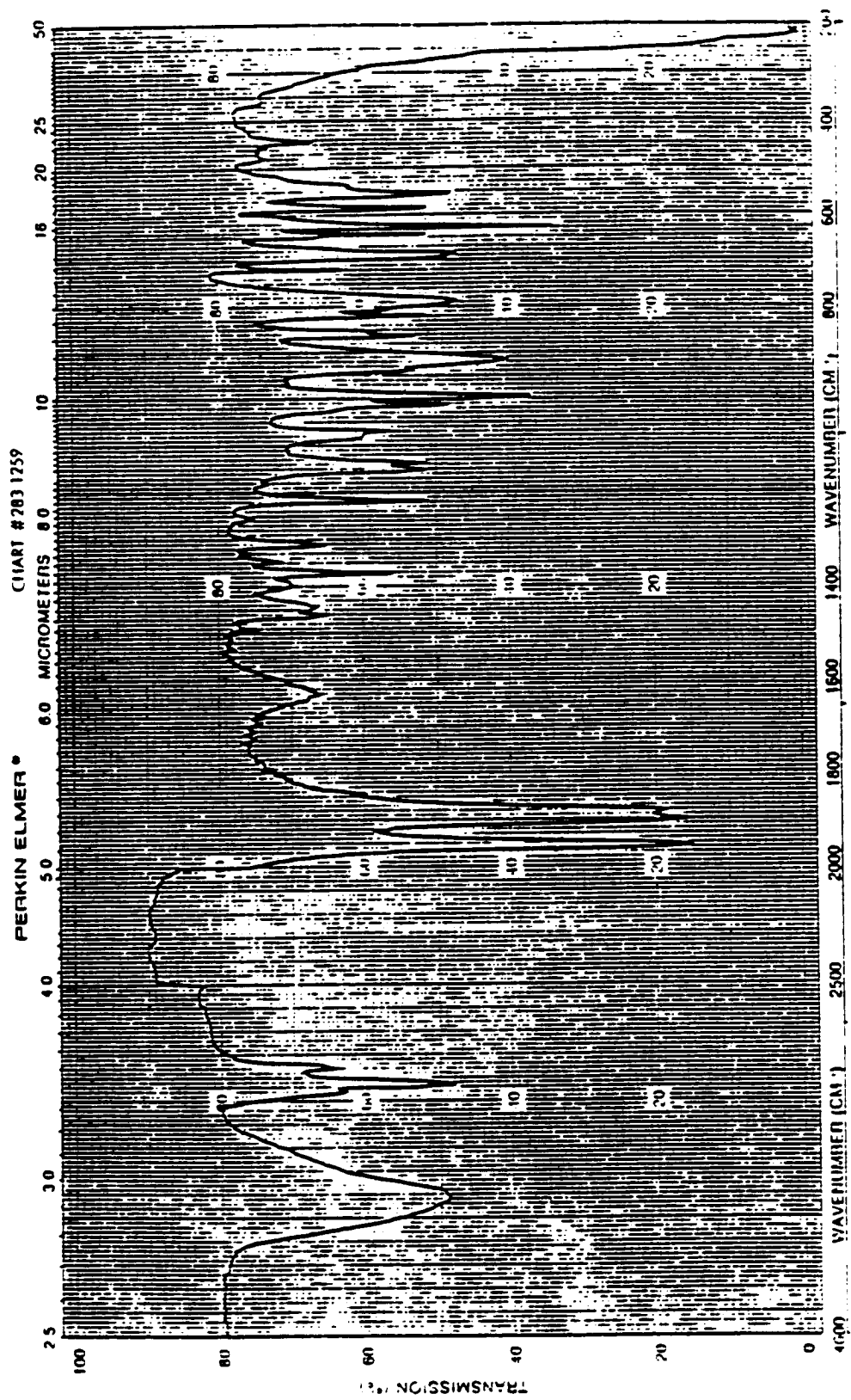
Cr$_2$(CO)$_6$[DMP-PO]$_6$ (LIII) cubane ^{1}H NMR spectrum in CDCl$_3$

174